**Facoltà di Scienze Matematiche Fisiche e Naturali**
**Dipartimento di Scienze della Terra**

**DOTTORATO DI RICERCA IN SCIENZE DELLA TERRA**

**CICLO XXVI**

**Progetto di Ricerca**

# Processing and interpretation of new multichannel seismic profiles. The Central-Eastern margin of the Tyrrhenian basin.

**Dottoranda: Alessia Conti**

**Docente guida: Dott.ssa S. Bigi**

# CONTENTS

# CHAPTER 1

# Introduction

Extensional forces in the continental lithosphere lead to the formation of rifted areas, a zone where the crust is pulled apart; if a continental rift is extended far enough, full continental break-up may occur and a passive margin is established on each side of the rift. Eventually, an active spreading center may develop and oceanic crust is emplaced.

There can be different factors that can lead to the formation of a rift, and two end-members models have been defined: the "active rifting model", in which extension is generated by the rising of hot material within the lithopshere or by the interaction of mantle plumes; the "passive rifting model", in which the rift forms because of far-field stresses related to plate tectonics. In nature, both components of these models can be found simultaneously in the same rifted area.

Others models attempt to explain the crustal stretching occurring in rifted areas in terms of pure shear (McKenzie, 1978) and simple shear (Wernicke, 1985) models. The first model predicts a symmetric thinning of the crust, with opposing major listric faults that sole out at the brittle-ductile transition zone; lower crust is thinned by plastic deformation, while the upper crust deforms by brittle faulting, and horizontal extension is balanced by vertical thinning. The simple shear model results in an asymmetric rift, controlled by a dipping detachment fault or shear zone, which crosscut the crust and eventually the entire lithosphere. The hangingwall and footwall are characterized by different geometry and thermal conditions. Also in this case, observations demonstrate that both the models can be valid in different areas and even in some zones elements from both can be present.

Passive rifted margins are further classified in volcanic rifted margins and magma-poor rifted margins; the differentiation is mainly based on the volumes of magmas generated as a response to the extension, but the classification is not always straightforward.

A basic conceptual model (Boillot et al., 1980) proposes that magma-poor rifted margins are formed by a proximal part, characterized by high-angle listric faults bounding continental blocks and rift basins, and a distal part, characterized by thinned crust, possibly separated from the oceanic crust by a domain of exhumed sub-continental mantle (Fig. 1.1). The deep-reaching listric faults of the proximal part may sole out on a common detachment surface, while in the distal margin the listric faults may cut across the entire crust leading to a detachment at the Moho discontinuity. This can lead to the exhumation of the mantle further seaward, before the oceanic crust is actually reached; sampling and drilling of the continent-ocean-transition zone, for example at the Iberian Margin, show in fact partially serpentinized mantle peridotites (Whitmarsh et al., 2001).

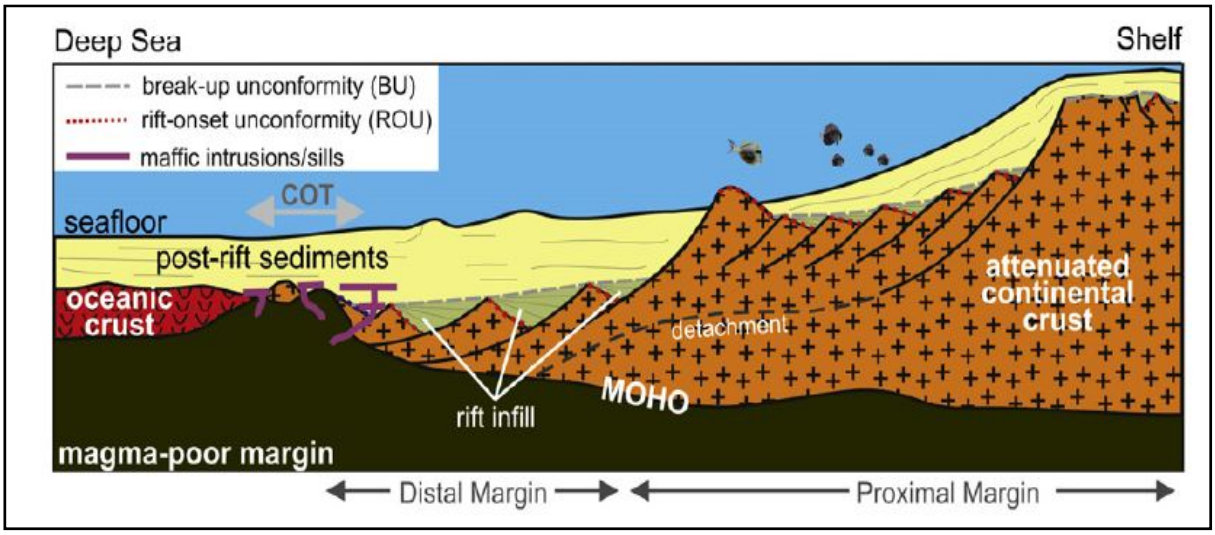


Fig. 1.1- Characteristics of a magma-poor margin (Franke, 2013).

Two key unconformity surfaces are generally recognized at passive rifted margins (Fig. 1.2): the rift-onset unconformity, which separate the pre- and syn-rift strata and in seismic data is generally recognized as an angular unconformity with top-lap truncations of seismic reflectors. The other surface is the breakup unconformity, which divides the syn- from the post-rift sediments: it truncates the wedge-shaped syn-rift deposits of the rift basins, separating them from the drape of post-rift sediments. This unconformity merges seaward with the top of the igneous oceanic crust, whereas it can be present at the unstretched edge of a continental margin as an erosional unconformity, merged with the rift-onset unconformity to form a composite unconformity.

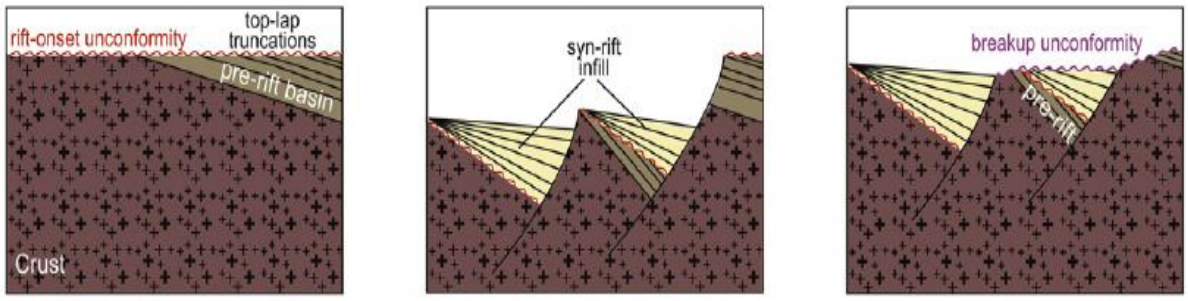


Fig. 1.2 - Key unconformities on rifted margins (Franke, 2013).

Despite of the extensive studies and the several models proposed regarding the rift areas, the processes involved in their formation and evolution are still not completely understood and different topics are debated, such as for example the asymmetry of the conjugate margins, the horizontal extension by faulting and crustal thinning, or the width and nature of the continent-ocean transition zone. Natural hazards commonly occur in rifted margin areas and

geological resources are often located on these zones, where traps for oil and gas can form due to the faulting processes; thus, understanding the evolution of these margins could be very useful.

The Tyrrhenian Sea margin, object of this research, can be considered a passive rifted margin of magma-poor type; according to some authors, its origin is linked to the eastward rollback of the subducting Adria plate under the European plate, and the extension on the overriding lithosphere lead to the formation of the back-arc basin (Malinverno and Ryan, 1986; Doglioni, 1991). The Tyrrhenian basin is the youngest basin of the western Mediterranean Sea, formed since Tortonian to present day. Asymmetric passive margins, thinning toward the ocean, surround the triangular shaped basin; they determine the transition to the bathyal plain, where zones floored with oceanic crust are present in the Vavilov and Marsili basins.

Conditions to study the extensional processes of rifted margins are ideal in the Tyrrhenian Sea: this is a young, tectonically active basin, and post rift sedimentary cover did not cancel the previous signature and passive margins; moreover, in a relative small area (conjugate passive margins are not so far from each other) a great variety of different processes is displayed.

This research work is focused on the central-eastern margin of the Tyrrhenian basin, in particular on the Pontine Islands sector. This is an area where the continental shelf is connected with the Vavilov abyssal plain through one of the steepest escarpment of the whole Mediterranean Sea, being narrow (up to 20 Km) and steep (5°-10°, locally up to 30°) and whose geometry and kinematics still need to be investigated.

Aim of the research is to propose a reconstruction of the central-eastern Tyrrhenian margin in terms of tectonic (geometry, kinematics and timing of the deformation) and seismostratigraphic setting, in order to contribute to the knowledge of the processes involved in the evolution of the passive margins of peninsular Italy. It is worth to notice that the whole passive margin is taken into account in the research, from the continental shelf to the abyssal plain, passing through the continental slope; this allow to highlight the possible relationships between the deformation affecting in the different sectors, which are still poorly constrained, and to establish a link between the Latium-Campania margin and the Vavilov basin. Within the general context of the Mediterranean geodynamics, the results obtained can lead to a better understanding of the development and evolution of structures observed in the early stages of rifted continental margins and back-arc basins.

The area is essentially investigated by means of multichannel seismic reflection profiles, collected during the oceanographic cruise Tir 2010 on the R/V Urania research vessel, funded by CNR of Italy and carried in October 2010. The set of multichannel seismic lines investigating the Pontine Archipelago sector have been processed and interpreted; they have the advantage to provide a complete overview of the investigated area, given that they cover the margin from the continental shelf sector to the bathyal area. In addition, part of the lines acquired in 1986 by Western Geophysical Co. for oil exploration purposes have been analyzed to better define the shallower continental shelf sector; two CROP profiles complete the seismic dataset utilized. To constrain from a chronostratigraphic point of view the main unconformities interpreted and so unravel the main tectonic phases, well data were used for

chronostratigraphic calibration of the seismic lines, and to infer the age of major unconformities that could be related to main tectonic phases; outcrop information, geological maps and sections already published also have been taken into account to integrate the dataset.

In the first part of this work (Chapter 2 and 3), the Tyrrhenian area is presented in all its aspects (geodynamic, geophysical, structural and stratigraphic), with a particular focus on the Latium-Campania margin; a summary and review of the main previous studies is also provided. In Chapter 4 the data analyzed are presented and an overview of the processing of the Tir data, which was a fundamental part of the research project, is provided. Chapter 5 is devoted to the seismic-stratigraphic interpretation and calibration of the main seismic units and surfaces using well data; Chapter 6 illustrates the main tectonic structures and deformative features interpreted along the continental shelf, slope and abyssal plain. In Chapter 7 an interpretation of the tectonic-stratigraphic evolution of the margin is proposed, in the light of the new data here analyzed, and integrated with the already published results. Finally, Chapter 8 is a summary of the main results and conclusions, including some broader implications.

# CHAPTER 2

# Geological background of the Tyrrhenian area

The Tyrrhenian basin has a roughly triangular shape, bordered by the continental rifted margins of Corsica-Sardinia block to the west, Sicily to the south and peninsular Italy to the east. The focus of this thesis lies on the central-eastern Tyrrhenian sector, in an area comprising the Latium-Campania rifted margin, precisely the Pontine archipelago sector, and the northern apex of the Vavilov abyssal plain (Fig. 2.1).

In order to provide a general overview of the Tyrrhenian Basin, in this chapter the geophysical characters of the area are described, together with a brief discussion of its geodynamic setting. It follows a particular focus on the deep central Tyrrhenian basins and the surrounding passive margins, with a description of the main structural and stratigraphic features and the main events that led to the formation of the basin.

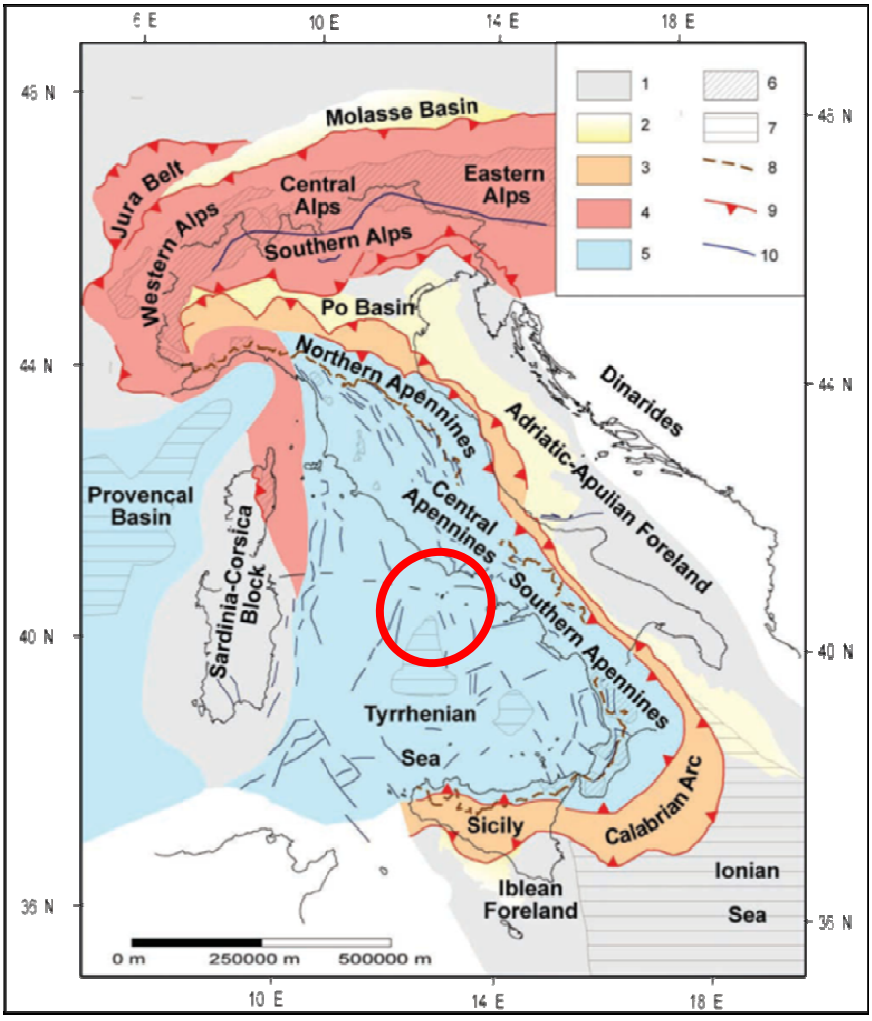


Fig. 2.1 - Synthetic tectonic map of Italy and surrounding seas: 1) Foreland areas; 2) foredeep deposits; 3) Apennines domains (compressional); 4) Alpine orogenesis; 5) back-arc basin system (affected by extensional tectonics); 6) outcrops of crystalline basement; 7) regions characterized by oceanic crust; 8) Apenninic water divide; 9) main thrusts; 10) faults. In the red circle, localization of the investigated area of the thesis (Scrocca et al., 2003).

## 2.1 The geodynamic setting

The Tyrrhenian Sea is the youngest active basin located in the western Mediterranean Sea. The geodynamic evolution of this area is commonly ascribed to the interaction of two plates, the European and the Adria plates.

Since the Eocene-Oligocene, the subduction of the Adria plate underneath the European plate led to the consumption of the previously formed Tethyan oceanic lithosphere and its corresponding passive margins (Carminati et al., 2012). The resulting overthrusting and uplifting of the Apennines–Maghrebides chain was associated with the stretching of continental crust, which led to the formation of several extensional basins superimposed on the orogen, coeval with roll-back of the Apennines–Maghrebides subduction system. The back-arc extension started in the central-northern area of the western Mediterranean basin with the opening of the Ligurian-Provencal basin (~30-20 My), and migrated towards southwest (Valencia Trough, ~30–20 My; Alborán basin, ~20–0 My), south (Algerian basin, ~25–20 My) and finally to the southeast, with the opening of the Tyrrhenian Sea (~12–0 Ma) (Lustrino et al., 2011 and reference therein) (Fig. 2.2).

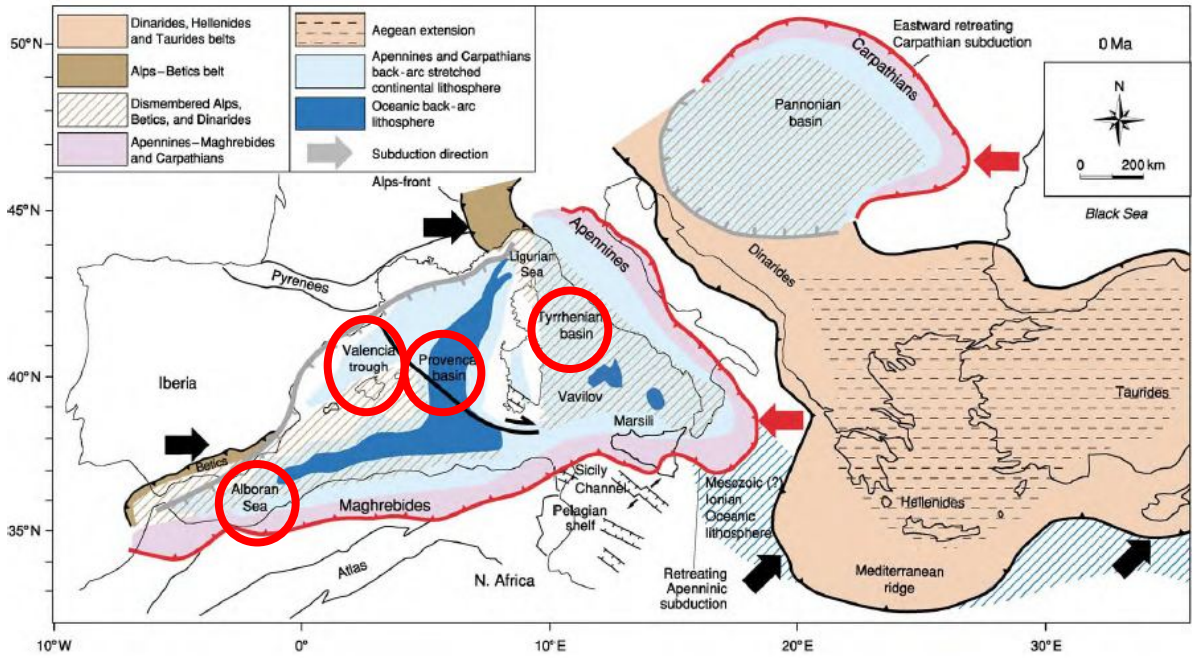


Fig. 2.2 - Present geodynamic framework of the Mediterranean area. Extensional basins related to the Apennines-Maghrebides subduction are superimposed on the orogenic belt; they are the Valencia, Provencal, Alboran, Algerian, and Tyrrhenian basins (red circles). (Carminati & Doglioni, 2005).

The coeval evolution of Apennine subduction and back-arc extension, and the eastward migration of both, provides a link between these two processes. The progressive migration of the accretionary prism - foredeep system is connected to an underlying mantle flow pushing eastward against the subduction plate; the shear between the down-going and retreating

lithosphere and the eastward compensating mantle is transferred upward, generating the shortening within the accretionary wedge and extension in the back-arc (Scrocca et al., 2007) (Fig. 2.3).

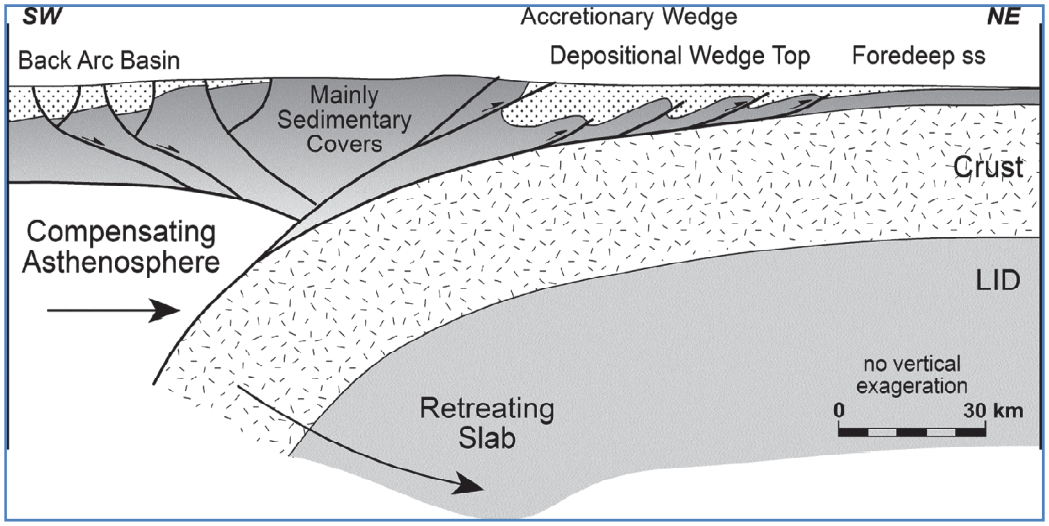


Fig. 2.3 - Schematic cross-section of an orogen due to a W-directed retreating subduction zone, showing the generation of the shortening within the accretionary wedge and the extension in the back-arc basin (Scrocca et al., 2007).

Rifting in the Tyrrhenian basin started in the northern-central portion and rate and direction of opening were not homogeneous; the opening process started in a W-E direction but, according to Doglioni (1991) and Carminati et al. (1998), the direction of extension in the northern Tyrrhenian Sea changed progressively from east to northeast, whereas in the southern sector it changed from east to southeast. Furthermore, the opening rate was higher in this latter sector, with an average of 5-6 cm/y according to Patacca et al. (1997), in contrast with the average of 1.5-2 cm/y in the northern part. This difference is caused by the nature of the subducting lithosphere, formed by the old oceanic Ionian crust under the Calabrian arc, and by continental crust in the remaining parts (Doglioni et al., 2004). The existence of a subducting slab is inferred by a narrow but well defined Wadati–Benioff seismic zone and by the volcanic arc of the Aeolian Islands in the Ionian region (Faccenna et al., 2001)

## 2.2 Geophysical characters of the Tyrrhenian area

The Tyrrhenian area has been the subject of several studies which contributed to reveal its geophysical and geological features.

In foreland areas lithospheric thickness (Fig. 2.4) varies from 70 Km in the Adriatic Sea to around 110 km in the southeast in Puglia region, whereas it shows the highest values along

the Alps chain, up to 130 km; in the Tyrrhenian basin, lithospheric thickness thins to 20-30 km, being this the new lithosphere formed in the back-arc basin.

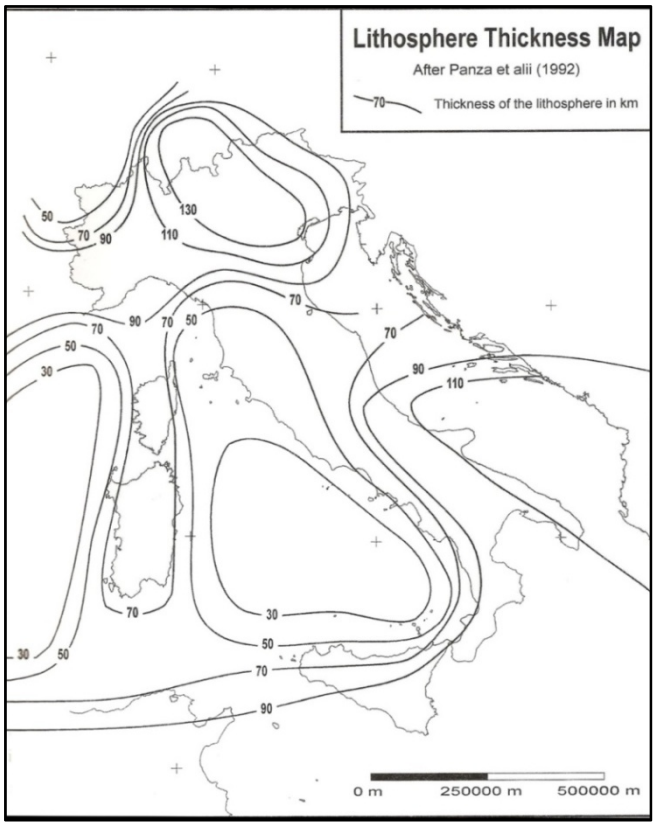


Fig. 2.4 - Lithospheric thickness (after Panza et al, 1992).

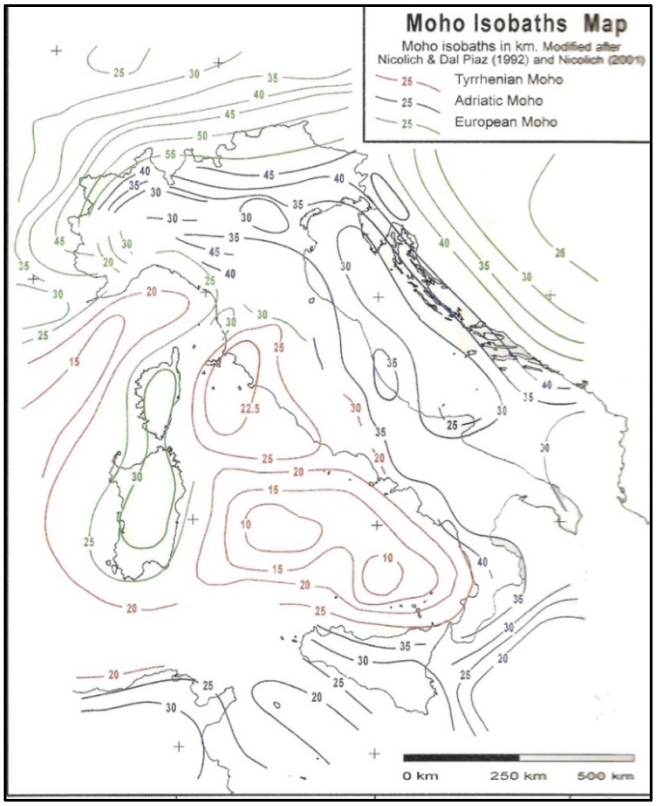


Fig. 2.5 - Moho isobaths map; green lines correspond to European Moho, blue lines to Adriatic Moho, red lines to Tyrrhenian Moho (modified after Nicolich & Dal Piaz (1992) and Nicolich (2001)).

Three different Moho discontinuities are distinguished (Fig. 2.5): below the back-arc basin there is a Moho of neogenic formation characterized by low velocities (Tyrrhenian Moho); an old Mesozoic Moho is present in the Padano-Adriatic-Iblean foreland areas (Adriatic Moho); another old Mesozoic Moho is also highlighted below the Alpine thrust belt and the Sardinia-Corsica block (European Moho). Oceanic crust is present in the Tyrrhenian basin with a thickness of about 10 km and in the Ionian Sea where a Mesozoic oceanic crust is buried underneath a thick pile of sediments; the remaining crust is generally continental.

Gravimetric field data (Fig. 2.6) show the density variation of the crustal portion; the Tyrrhenian area is dominated by a high gravity anomaly field, increasing from north to south. Maximum positive values are located in the two sub-basins, the Vavilov and Marsili, with values around 240-250 mGal, according to the map shown in Fig. 2.6. In the southern basin the anomalies resemble the bathymetric feature of the central basins and they run NE-SW, whereas in the northern part they show an N-S pattern.

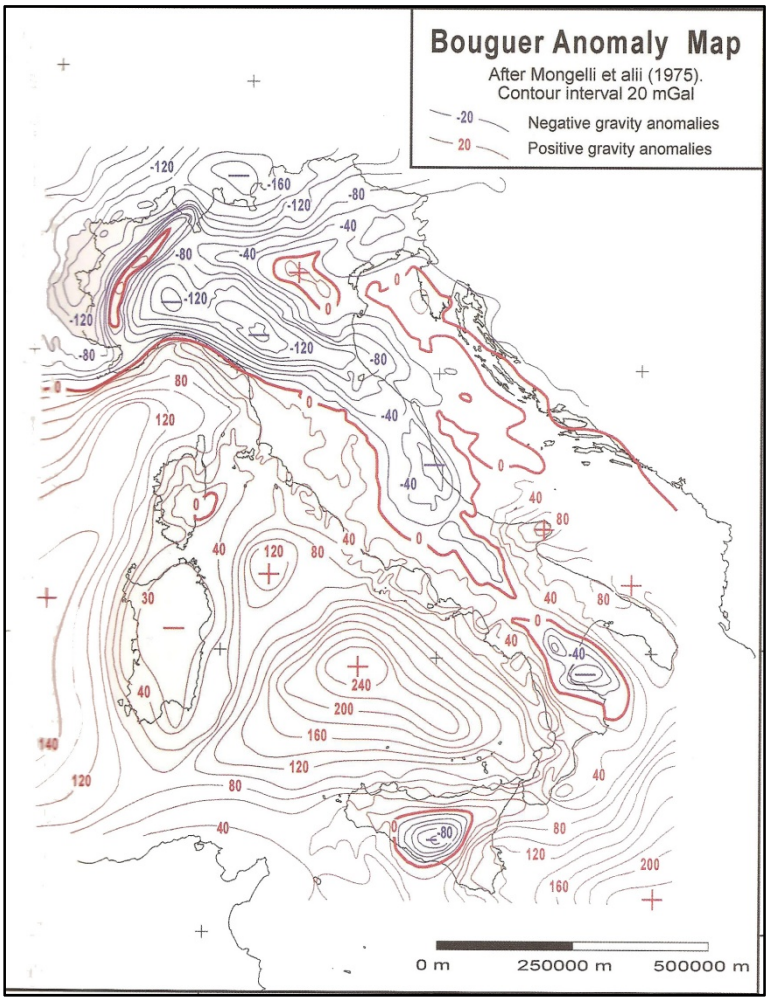


Fig. 2.6 – Bouger gravity anomaly map (after Mongelli et al., 1975).

Different regional maps have been produced regarding the heat flow values (Fig. 2.7) in the Tyrrhenian area (Mongelli et al., 1991; Cataldi et al., 1995; Della Vedova, 2001, among the others); as can be seen in Fig. 2.7, the onshore part of the Italia Peninsula shows low heat flow values (generally less than 100 mW/m$^2$, 30-40 mW/m$^2$ in the foreland domain), except for the Tuscan-Latium area, where high values are reached due to the volcanic setting. In the northern domain of the Tyrrhenian Sea, the heat flow field displays a regular pattern, with values ranging from 80 to 120 mW/m$^2$; in the southern domain instead, generally the heat flow field is characterized by high values, with a maximum located in the Marsili basin (250 mW/m$^2$). In this sector, the extension of the crust and the resulting upwelling of the astenospheric mantle is a crucial factor determining these high values (Zito et al., 2003).

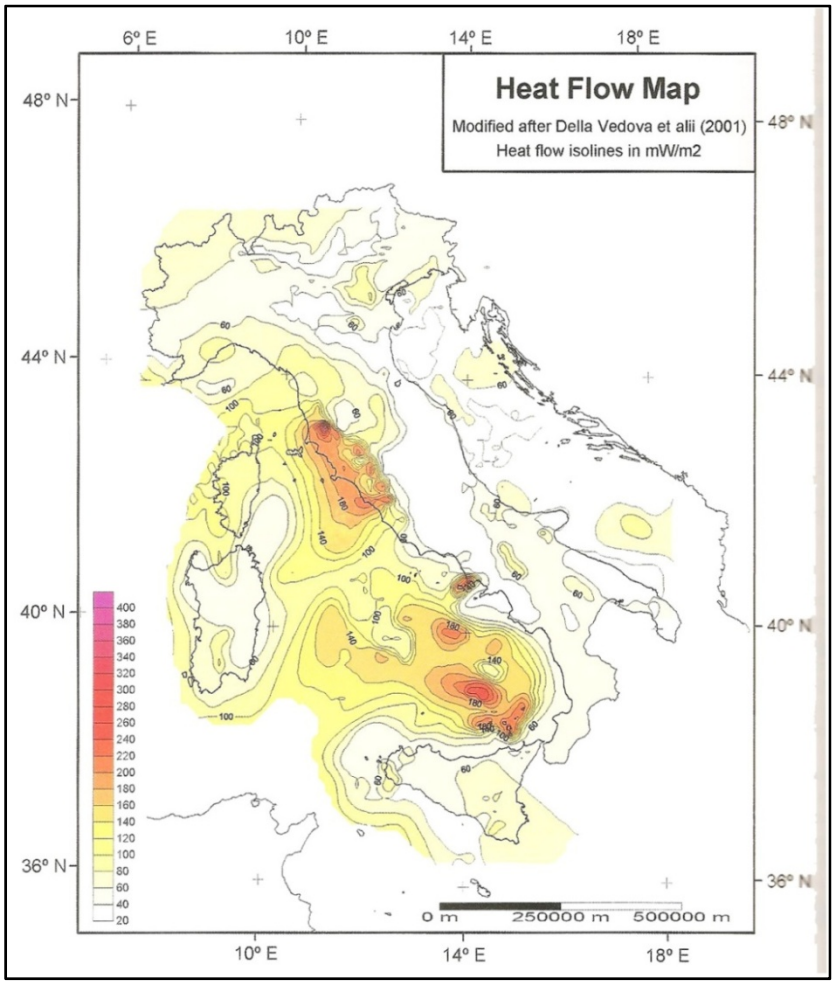


Fig. 2.7 - Heat flow map (modified after Mongelli et al. (1991), Cataldi et al. (1995), Della Vedova et al. (2001).

Regarding the magnetic anomalies, several studies tried to reveal the occurrence of magnetic anomalies with a striped pattern in the central plains of the Tyrrhenian Sea where oceanic crust is present. In Nicolosi et al. (2006) seven magnetic anomaly stripes were

identified in the Marsili basin, with an alternation of normal and reverse polarity, similar to those observed in mature oceanic environments. However, Florio et al. (2011) indicate that the filtering processes applied by the previous researchers are not appropriated and affirm that this pattern of magnetic anomaly does not fit with an ocean-like central expansion model; according to this work, the distribution of magnetic sources may suggest that the crustal tearing induced by extensional processes is not concentrated solely beneath the seamounts, but has involved different areas in different times.

Seismicity distribution can be observed in Fig. 2.8; earthquakes are distributed all around the Alps and the Apennines and in the south Tyrrhenian Sea several intermediate and deep earthquakes occurred; depth distribution of these earthquakes define a Wadati-Benioff zone down to 500 km that can be correlated with the subduction of the Ionian oceanic lithosphere; the subducting slab is quite steep and has a thickness of about 80 Km (Selvaggi & Chiarabba, 1995).

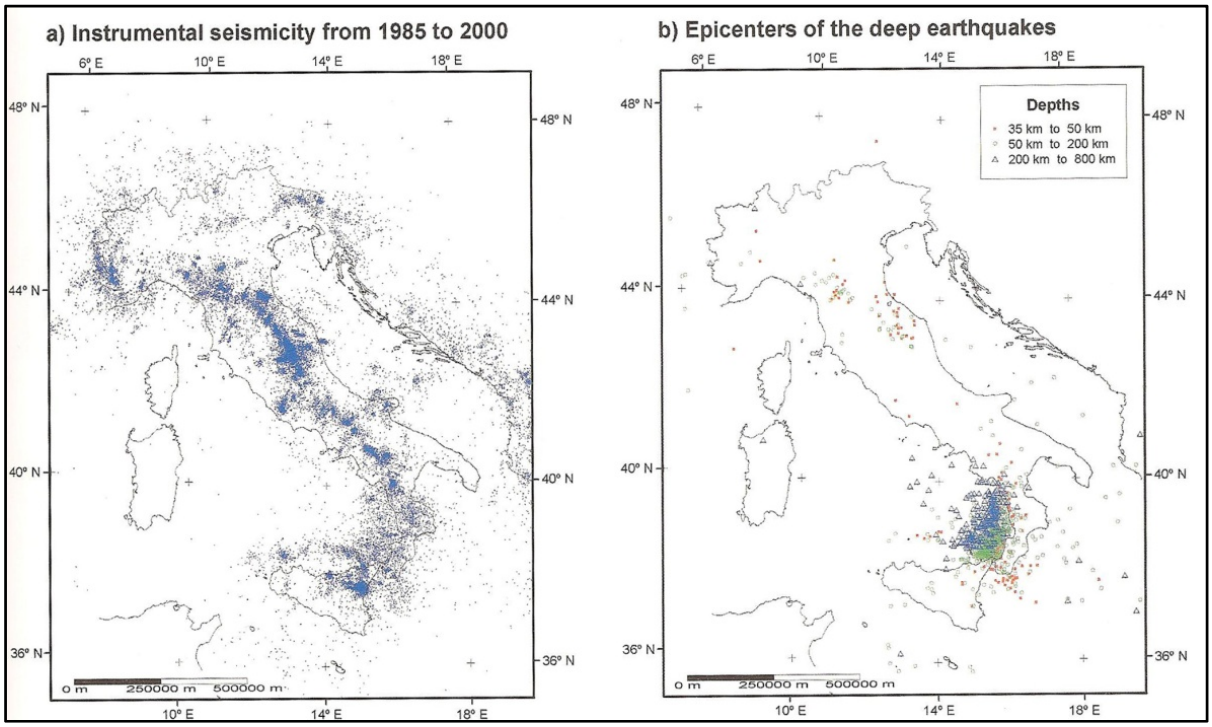


Fig. 2.8 - a) epicentral map of the instrumental seismicity recorded between 1985 and 2000. b) epicenters of the deep earthquakes (depth > 35 Km) (Valensise & Pantosti, 2001).

Based on the variability of lithosphere properties, thermal regime and the chemical composition of magma, the Tyrrhenian basin is commonly subdivided in two domains, the northern and the southern domain; they are separated by an east-west trending magnetic anomaly alignment called 41$^{st}$ Parallel line (Spadini & Wezel, 1994; Bruno et al., 2000). The northern Tyrrhenian domain is characterized by a maximum depth of 2000-2200 m and a 20 km thick continental crust; seafloor shows a smooth topography in the area of the Tuscan archipelago and east of Corsica (Corsica basin), with depth generally less than 1000 m.

Slightly to the south, depth increase up to 2000 m and seafloor is generally rugged, showing roughly parallel N-S striking horst and graben structures. Heat flow values range from 50 $mW/m^2$, at the Sardinia and Corsica margin, to 150 $Mw/m^2$, toward the peninsular margin (Della Vedova, 1984; Wang et al., 1989). In correspondence of the above mentioned 41$^{st}$ Parallel Line, the main geophysical characters change and water depth abruptly increases, reaching its maximum in the Vavilov basin (3600 m); the southern domain of the Tyrrhenian basins display a less rugged morphology, with deep central bathyal plains, thinner crust of about 10 km, and higher values of heat flow (more than 250 $mW/m^2$) measured in the Vavilov and Marsili basins (Della Vedova et al., 1984; Zito et al., 2003).

The 41$^{st}$ parallel Line represents the conventional separation line between the two domains of the Tyrrhenian Sea; this feature is well known for its magnetic patterns related to different geologic structures, such as intrusive submerged bodies, volcanic islands and fault systems. There are different hypothesis concerning this area: Spadini and Wazel (1994) correlate the magnetic and free air gravity alignment to the opening of the basin and Quaternary vertical sinking due to post rift cooling and intraplate compression. According to other authors (Boccaletti et al., 1990; Carminati et al., 1998, among many others) this feature could be interpreted as an E-W left lateral shear zone induced by the asymmetric opening of the basin, whereas Mantovani et al. (1996) and Mascle & Chaumillon (1997) consider this zone as narrow N-S trending basins and tilted fault bounded blocks, with no evidence of strike slip movements. Other authors consider this lineament as a lithospheric discontinuity: Patacca et al. (1990) affirmed that the two areas separated by the 41$^{st}$ Parallel Line have different lithospheric retreats, so that this lineament must be considered as a major discontinuity; Serri (1990) also considered the lineament as a lithospheric feature, separating two distinct mantle domains and two different magma sources, probably derived from different subducting slabs, one made of continental lithosphere in the northern domain and one made of oceanic lithosphere in the southern domain.

## 2.3 Structural - stratigraphic setting of the Tyrrhenian area

### 2.3.1 The Central deep Basins

The central bathyal area of the Tyrrhenian Sea can be divided into two sub-basins: the Vavilov basin to the northwest and the Marsili basin to the southeast.

The deep plains of the Vavilov basin (Fig. 2.9) are delimited to the west by the Selli Line and to the east by the lower slope of the southeastern Tyrrhenian active margin and the Marsili Basin. The morphology of the sea floor is mostly flat, only complicated by large seamounts, seamount chains and fault scarps. The Selli line is a NE-SW trending fault-scarp, connecting the Sardinia passive margin to the Tyrrhenian ocean domain, forming a morphological scarp extending ca. 80 km and with an average offset of 250/300 m.

To the west, the area is occupied by the Magnaghi basin, separated from the Gortani basin by the D'Ancona Ridge and the Vavilov volcanic seamount (Gamberi & Marani, 2004). In the Magnaghi basin average values of the depth are 3300-3400 m and the seafloor is slightly irregular; according to Mascle and Rehault (1990), this sector is part of the lower Sardinia continental margin, rifted from intra-Messinian to intra-Pliocene times. The Magnaghi volcano lies at the base of the Sardinia continental margin west of the Selli Line, with a length of about 25 km and an elevation of 1470 m above the surrounding seafloor; it is made up of tholeiitic to alkali basalts (Robin et al., 1987; Savelli, 1988) of Late Pliocene age (Kastens et al., 1990; Savelli, 1988).

The northern apex of the Vavilov basin closes against the steep continental slope of the Latium-Campania margin. Here two seamounts are present, the De Marchi and the Flavio Gioia Smts., 80 km apart, both N-S trending and rising about 1200 m above the abyssal plain; they are both characterized by asymmetric flanks, with the fault scarp dipping toward the basin steeper than the other. Between this two seamounts is localized the Gortani Ridge, a 40 km linear morphological high with an average elevation of 300-400 m, made up of T-MORB basalt flows. A major feature localized in the central part of the basin is the Vavilov volcano, standing 2800 m above the seafloor and elongated in a NNE-SSW direction; it shows a steep, smooth western flank and a gentler eastern flank, and it is formed by tholeiitic to alkali basalts (Robin et al., 1987; Savelli, 1988) of Late Pliocene age (Kastens et al., 1990; Savelli, 1988). Another relevant morphological feature is the D'Ancona Ridge, made up of several highs arranged in an arcuate shape.

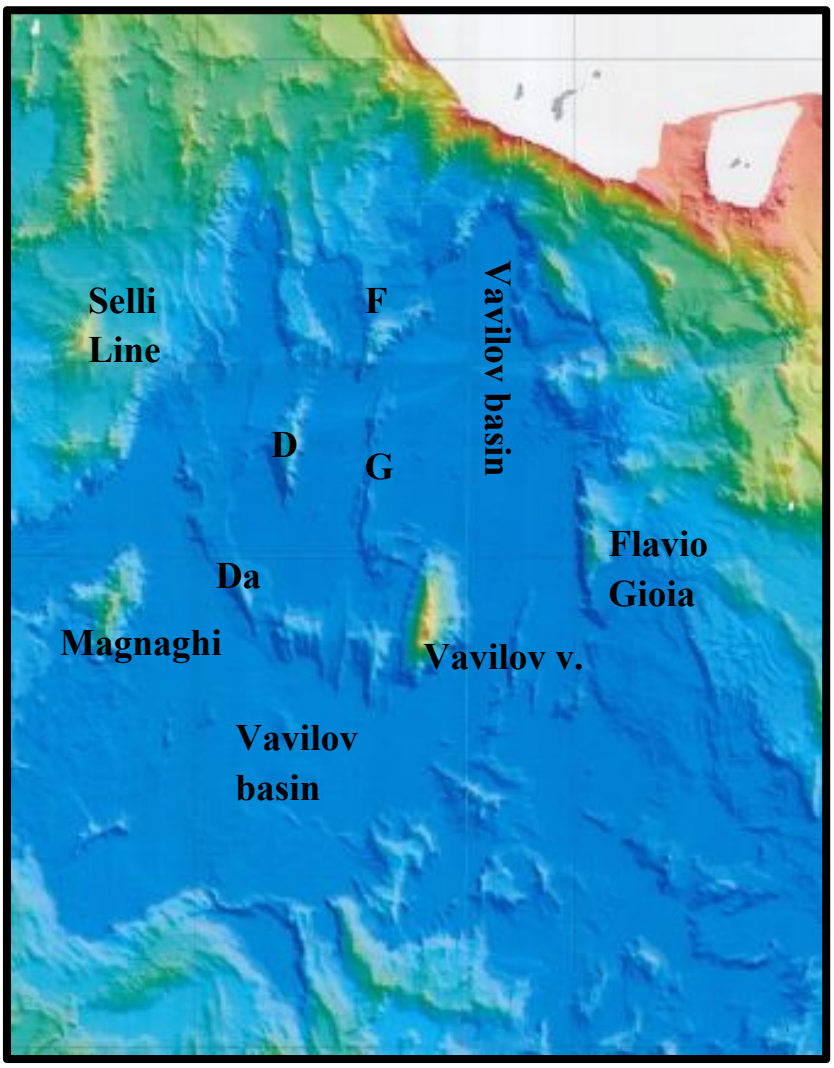


Fig. 2.9 - Vavilov basin and some of its morphological elements: D, De Marchi Smt; F, Farfalla Smt; G, Gortani ridge; Da, D'Ancona ridge. Bathymetric map after Marani & Gamberi (2004).

To the southeast, the Vavilov basin passes to the more recent Marsili basin (Fig. 2.10), through a subdued sill characterized by a thicker crust (15 km instead of the 10 km of the Marsili basin); the Marsili basin displays a rhombohedral shape, with a depth of 3500 m. It is bounded to the south and to the east by the Aeolian volcanic arc located on the upper slope, cut by the Stromboli canyon and by the Palinuro volcanic complex to the north; the basin is dominated by the large Marsili volcano, with an elevation of 3000 m above the seafloor, elongated NNE-SSW. A series of linear fault scarps that form symmetrical horst and graben structures flanks each side of the volcano, characterized at its summit by an alignment of elongated cones. Data show a different composition for the volcanic products, tholeiitic near the base and calc-alkaline toward the summit (Selli et al., 1977); the age is estimated around 0.7 My based on magnetic anomalies (Faggioni et al., 1995) and about 0.1 My based on

radiometric dating (Selli et al., 1977). Islands and submarine volcanoes associated to the Marsili back-arc occupy the upper slope of the southeastern Tyrrhenian Sea.

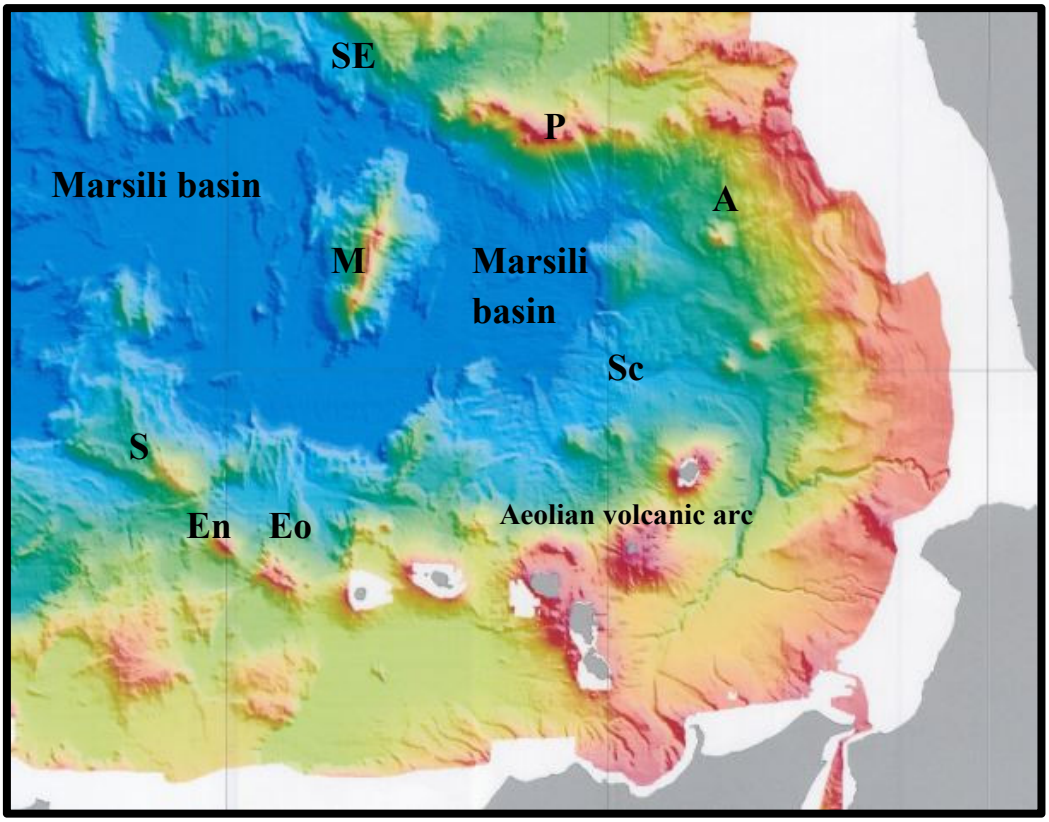


Fig. 2.10 - Marsili basin and some of its morphological elements: SE, Sartori escarpment; P, Palinuro volcanic complex; A, Alcione volcano; Sc, Stromboli canyon; S, Sisifo volcanic ridge; En, Enarete volcano; Eo, Eolo volcano; M, Marsili volcano. Bathymetric map after Marani & Gamberi (2004).

### 2.3.2 The passive margins of the Tyrrhenian area

The bathyal plain of the Tyrrhenian basin is surrounded by the rifted margins of Corsica-Sardinia block, Sicily and Peninsular Italy; the margin is wider off Sardinia-Corsica than along the Apennines and Sicily, giving a broadly asymmetric shape to the whole basin. Whereas the Sardo-Corso margin represents a typical passive continental margin, the eastern and southern one are associated with high seismicity, active volcanism and elevated rates of uplift of land areas, represented by the Apennine mountain chain (Marani & Gamberi, 2004). In this paragraph some characteristics of these margins will be briefly described.

The Sardinia-Corsica margin (Fig. 2.11) includes two major domains (Mascle & Rehault 1990; Rehault et al., 1987; Marani & Gamberi, 2004), each showing a different seismic-stratigraphy setting. From west to east, the margin is composed by the upper slope area, about

50 km wide; it contains two large north to south elongated sediment-filled basins, the Sardinia and the Corsica basin, with the seafloor lying at about 1000 m of depth. This domain is bounded eastward by sublinear basement highs, north-south trending, such as the Pianosa-Elba Ridge or the Monte Baronie Ridge, the largest structural high in the Tyrrhenian Sea, with a length of more than 120 km. Numerous canyons dissect the outer continental shelf of Corsica and Sardinia, which contribute to the basin filling; two large canyon systems, the Sarrabus and the Orosei Canyons, merge to form the Valley of Sardinia. This latter feature extends within the second domain, the middle slope, formed by a relatively flat area extending about 70 km seawards at 2500-2800 m water depth, and named the Cornaglia Terrace. The so called Central Fault System or R. Selli Line interrupts this area toward the east; it is delineated by a series of north-northeast trending scarps, relatively linear, and it separates the Sardinia-Corsica margin from the Vavilov abyssal plain. The group of faults that form the Selli Line lowered the edge of the Sardinia margin of 500-1000 m respect to the central domain and have a extensional pattern, although this fracture zone could have had a dextral strike-slip motion during Lower Miocene time (Rehault et al.,1985), linked to drifting of the Sardinia block.

Samples dredged on this fault scarp have given indications on the extent of the Hercynian basement and sedimentary cover of Sardinia and some Jurassic formations (Selli and Fabbri, 1971; Selli, 1974; Fabbri and Curzi, 1979; Colantoni et al., 1981; Gennesseaux et al., 1985); Messinian and lower Pliocene formations overlie this basement. The several seamounts present in these domains are linked to large tilted blocks formed by the development of rotational faults generally dipping eastward. The half graben formed by tilting are actually filled by the Sardinia basin sediments; also in the Cornaglia Terrace similar structures are present, although a thinner sediment cover is observed. Thus, the Sardinia-Corsica margin records the rifting episode that resulted in the formation of the Tyrrhenian Sea and it represents the passive margin geodynamic province of the basin.

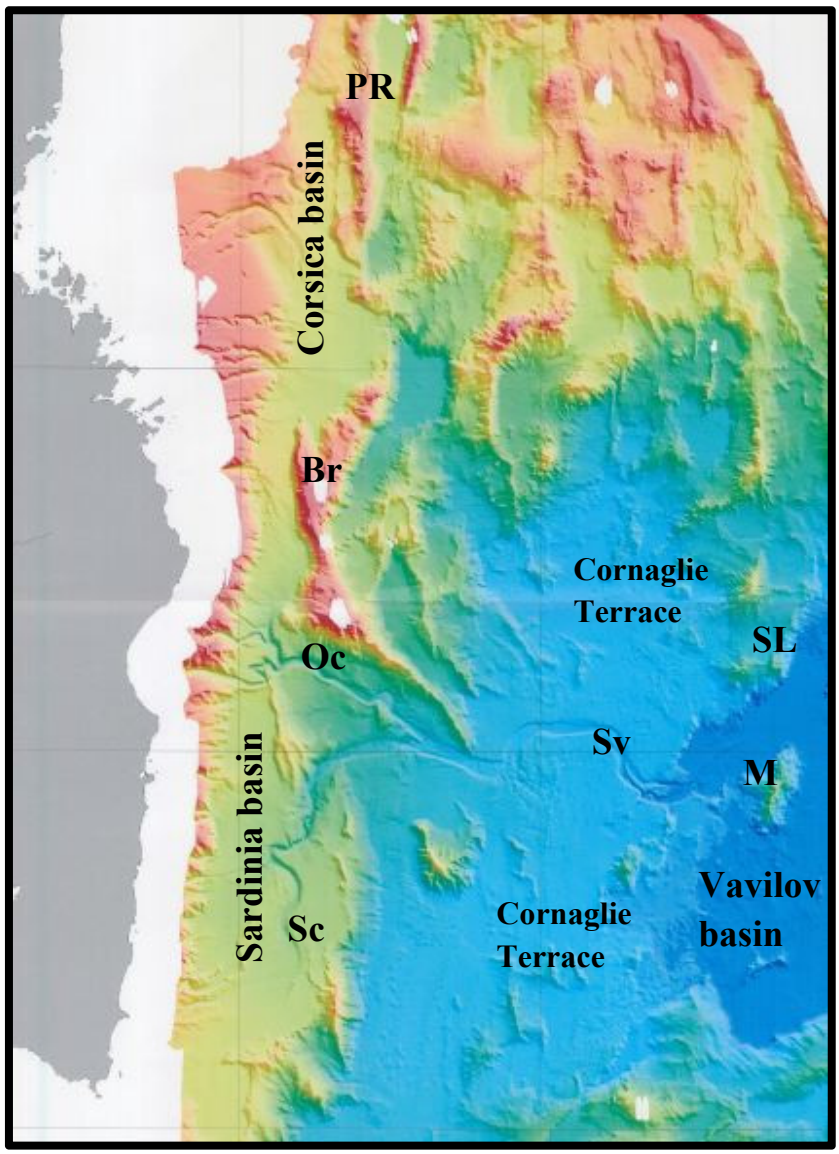


Fig. 2.11 – The Sardinia-Corsica margin. Br, Baronie Ridge; Pr, Pianosa Ridge; Oc, Orosei Canyon; Sc, Sarrabus canyon; Sv, Sardinia valley; SL, Selli Line; M, Magnaghi volcano. Bathymetric map after Marani & Gamberi (2004).

The peninsular Italy and the Sicily Tyrrhenian margins are narrow and characterized by rough reliefs. The Sicilian margin (Fig. 2.12) presents a barely east-west trend, delimited northward by the lower slope which connects the margin with the Marsili bathyal plain. The area is morphologically articulated in horst and graben structures and in particularly the western part presents a rough and irregular morphology; several intraslope basins related to the extensional Tyrrhenian tectonics are found along the upper margin (Fig. 2.12). Enclosed between Sicily and Calabria the main Cefalù, Gioia and Paola basins are flanked offshore by the islands and seamounts of the active Aeolian volcanic arc, positioned on the upper slope, southeastward of the Marsili back-arc basin. A narrow continental shelf is present along the Sicilian margin in this sector, whereas the Calabrian margin, from Capo Vaticano to the

northern Messina Strait, is characterized by a ramp morphology, without any evident shelf-slope break (Fabbri et al,. 1980). The Stromboli valley is one of the principal morphological features: it runs in the central portion of the Gioia basin and along its course it receives numerous tributaries from the Sicilian (Milazzo and Niceto channels) and Calabrian margin (the Gioia-Mesima channel-canyon system) and from the Aeolian volcanic slope; it is thus the main trunk of a submarine sedimentary pathway that feeds a deep-sea fan in the Marsili basin (Gamberi & Marani, 2006). The northern Calabrian margin, between the Palinuro volcanic complex and the submarine extension of Capo Vaticano, consists of the upper slope, the Paola intraslope basin, an intermediate slope, the Lametini flat and a further slope that marks the transition to the Marsili basin.

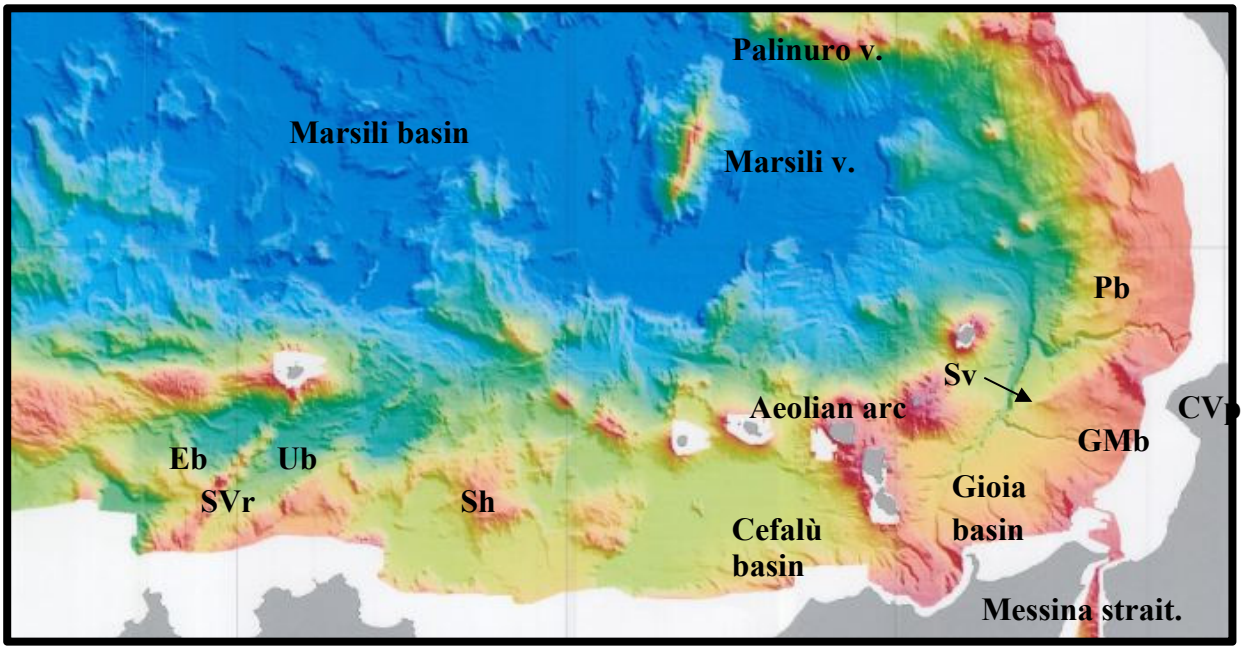


Fig. 2.12 – Calabria-Sicilian margin. Pb, Paola basin; Sv, Stromboli valley; GMb, Mesima-Gioia channel-canyon system; CVp, Capo Vaticano promontory; Sh, Solunto high; SVr, San Vito ridge; E, Erice basin; Ub, Ustica basin. Bathymetric map after Marani & Gamberi (2004).

The northern sector of the eastern peninsular margin (Tuscania and northern Latium regions), delimited by the Tuscan archipelago and the Pontine islands, is characterized by mostly N-S trending structural highs and adjacent, relatively flat-lying, basins. Major structures are the Civitavecchia Valley and the Tiberino seamount, among others. The Latium–Campania margin (Fig. 2.13) extends from the area of the Pontine Island to the Palinuro volcanic complex; this sector is characterized by a complex slope that flanks to the east the Vavilov abyssal plain and constantly widens southward reaching a width of 150 km in the Palinuro area. The margin displays a NW-SE direction and the southern Apennine chain represents the emergent area to the east of the margin. It has a general down to-the-west stepping morphology, with intraslope basins mainly narrow (except for the Palmarola, Ventotene and Capri basins) and basement highs sometimes not overlay by sediments, due to

the recent age of tectonics. Some portions of the intra-slope basins are completely separated from the upslope sectors; other portions are, on the contrary, characterized by complex submarine drainage networks that connect successive deeper intra-slope basins (like Ischia and Magnaghi valley and the Dohrn canyon) (Marani & Gamberi 2004). A major distinctive feature of this sector is the Sartori Escarpment, a fault system NNW-SSE trending, 80 km long, interpreted as left lateral transtensive system (Musacchio et al., 1999).

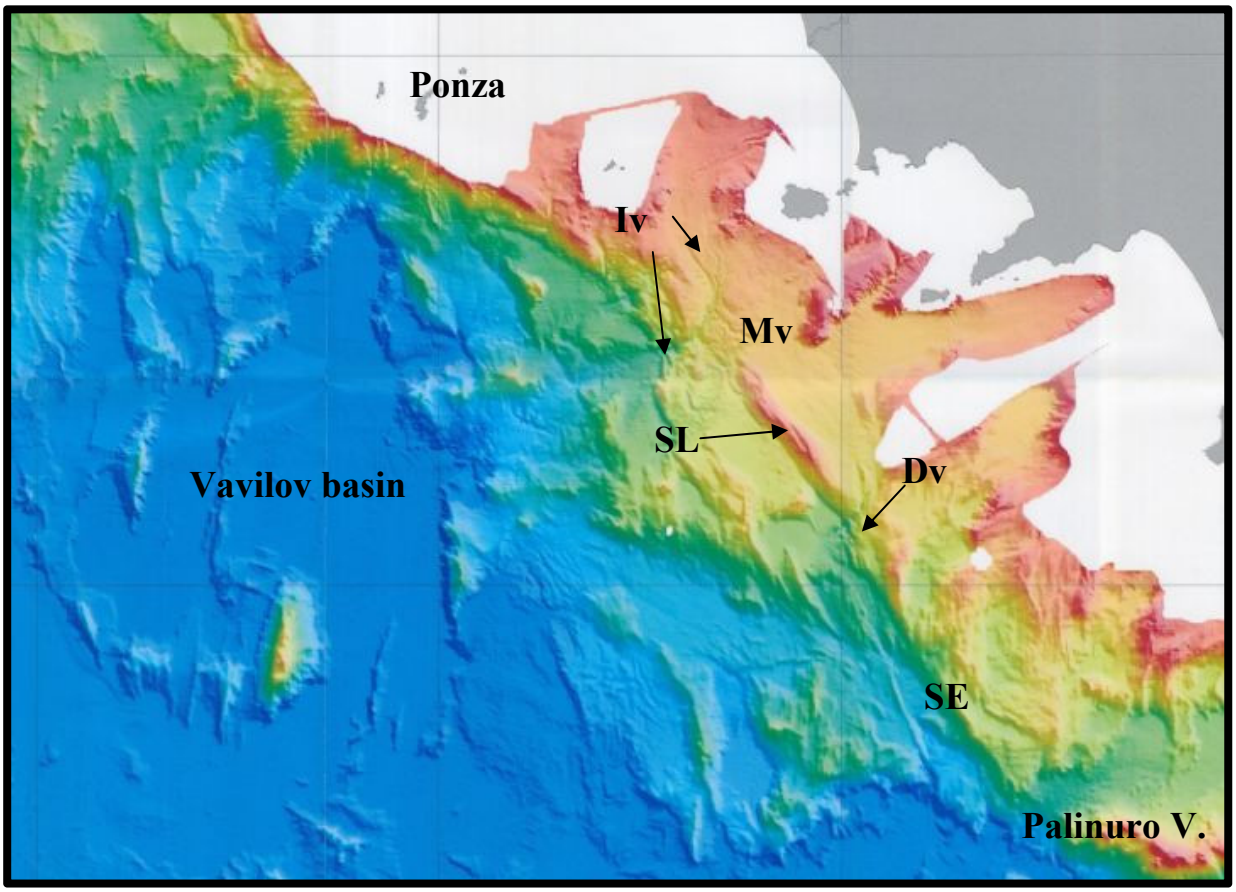


Fig. 2.13 - Peninsular eastern margin of the Tyrrhenian Sea. Iv, Ischia valley; Mv, Magnaghi valley; SL, Sirene lineament; Dv, Dhorn valley; SE, Sartori escarpment. Bathymetric map after Marani & Gamberi (2004).

### 2.3.3 The stratigraphic setting of the Tyrrhenian area

The Tyrrhenian basin is superposed on several different geological and structural domains: a segment of Hercynian chain bounds the basin to the west; to the north and to the SE (Calabria) Alpine units deformed in pre-neogene times are present; along the Italian peninsula and Sicily neogene Apenninc units show deformations coeval to the development of the basin (Sartori, 1986).

Segre (1958) and Selli (1974) first dealt with the characterization of the geology of the Tyrrhenian basement rocks, based on morphostructural elements of bathymetric maps and direct seafloor sampling respectively; all basement rocks were attributed to Hercynian domain, except for tertiary igneous and sedimentary rocks dredge along the Campania and Sicilian margin. Later, Calcagnile et al. (1981) and Selli (1981) reported also the presence of Alpine type rocks, while the work of Heezen et al., (1971) and Colantoni et al., (1981) increased the information about basement rocks. Furthermore, Sartori (1986) analyzed samples collected by the Istituto per la Geologia Marina of Bologna (now ISMAR-CNR) and by the ODP Leg 107. According to this author the acoustic basement can be subdivided in two groups: the pre-Tortonian igneous, metamorphic and sedimentary rocks, deformed by stretching of the basin; the second group is formed by Tortonian to recent igneous rocks, synchronous to the formation of the Tyrrhenian basin. In the pre-Tortonian rocks are included lithotypes derived from the European crust of the Alpine foreland and from the European continental margin deformed by the Alpine orogenesis; lithotypes belonging to this domain are localized on the Baronie Smt., the Cornaglia Smt., at the base of the site 654 and appear to reach the area of the Selli Line. Tethyan ophiolites seem to occur only in the area ideally connecting east Corsica with the Catanzaro isthmus in Calabria (for example they were recovered at the ODP site 656, on the De Marchi Seamount); fragments of the Calabride-Kabilide complexes are found quite internally to the their present land position, suggesting that the Calabrian arc is both the most bent and the most stretched structural domain. The carbonate platforms and basins of mainly Mesozoic age belonging to the African-Apulian continental margin deformed by Alpine-Apenninic orogenesis occur along the margins of the basin off Campania and Sicilia, and also at the center of the basin till the Selli Line. The Tortonian to Recent igneous rocks are divided in three cycles: upper Tortonian-Messinian, Pliocene and Pleistocene, each characterized by the occurrence of different magmatic types, alkaliolivinic+tholeiitic vs. calcalkaline+shoshonitic. The Upper Tortonian-Messinian cycle correspond to the initial phase of stretching of the basin and its products are found off Corsica and northern Sardinia; the Pliocene cycle products are arranged in a belt extending from Sardinia to the Vavilov basin and include magmatic products related to stretching and oceanic crust emplacement. The Pleistocene cycle products are abundant in the SE Tyrrhenian basin, in the Aeolian arc and along the peninsula margin; the latter however mostly display a high K-chemistry and its meaning in terms of extension or subduction processes is debated.

Regarding the sedimentary cover, the stratigraphic knowledge is mainly based on multichannel seismic data acquired during different surveys and especially on the seven sites of the Ocean Drilling Program (ODP), Leg107, drilled across the basin (Fig. 2.14); sites 654, 653, 652 and 656 are localized on the Sardinia passive margin, whereas sites 650, 651, 656 were drilled in the central Vavilov and Marsili basins. The main results of these surveys are extensively exposed in several papers, as Kastens et al. (1988), Kastens & Mascle (1990), Sartori (1990), among the others, and hereafter the main characteristics of each site is exposed.

Site 654 is located on a fault-bounded tilted block on the upper continental Sardinian margin; the seismic profile MS-4 crossing the site shows four major seismic units which reflect pre-, syn- and post-rift geometric arrangement. The lowermost 140 m of Site 654

represent a transgressive sequence: at the base there are 60 m of conglomerate, gravel and gravelly mudstone, probably of subaerial deposition. These sediments are overlain by oyster-bearing glauconitic sands, presumably of near shore environment; these two units (not directly dated) are overlain by nannofossil ooze of uppermost Tortonian and lowermost Messinian age, indicating a change from restricted marine to open marine environments. This change is attributed to subsidence of the continental crust during the rifting of the Tyrrhenian Sea. A 36 m thick unit of organic carbon rich claystones and dolomitic/ calcareous siltstones register the onset of a marine environment characterized by restricted water circulation, linked to the general Messinian desiccation of the Mediterranean Sea. This event is recorded by 70 m of gypsum interbedded with calcareous clay, mudstone, sandstone and dolostone at site 654. The final 243 m thick Plio-Pleistocene unit consists of nannofossil ooze and calcareous mud, with occasional volcanic ash, and it correspond on the seismic line to the post-rift stage, with the synrift-postrift transition occurring near the end of the Messinian.

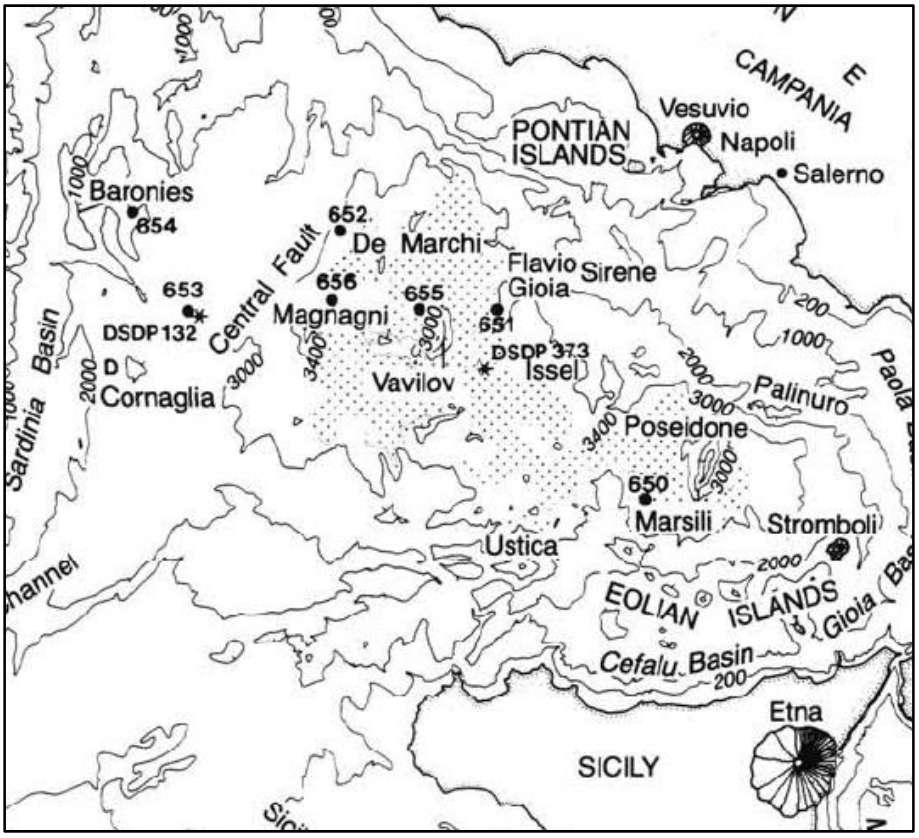


Fig. 2.14 - Simplified bathymetry of the Tyrrhenian area with ODP Leg 107 sites locations indicated (Mascle & Rehault, 1990).

Site 653 is located on the Cornaglia Terrace, near the previous DSDP site 132; it penetrated several tens of meters into restricted marine and evaporitic Messinian sediments and 220 m of hemipelagic Plio-Pleistocene sequence similar to that recovered at DSDP 132 (Hsu et al., 1973).

Site 562 is located on the lower Sardinia continental margin; the bottom 533 m consist of monotonous, barren, gypsiferous, calcareous sandy and silty mud and mudstone. A Messinian age is assumed for these deposits, with depositional environment compatible with a closed lake in which salinity fluctuated widely. Plio-Quaternary sediments are composed by hemipelagic marine sediments with minor volcanic glass; comparison with seismic reflection data indicates the prerift/synrift contact in correspondence of the basal 40 m barren Messinian interval; the synrift/postrift falls within the lower Pliocene of the drilled sequence.

Site 656 is located on the western flank of the De Marchi Seamount; dredging on the steeper eastern flank of the seamount have revealed Paleozoic and Mesozoic sedimentary and low grade metamorphic rocks (Heezen et al., 1971; Colantoni et al., 1981). At the bottom site 656 shows a conglomerate with an oxide rich, barren matrix, derived from Alpine type basement; a 10 m thick layer of calcareous dolomitic mudstone overlain the conglomerate, probably Messinian in age. The contact between these two units is gradational and seems to represent a change from subaerial to subaqueous environment, derived from tectonic subsidence or flooding near the end of Messinian desiccation. The drilled lower Pliocene to middle Pleistocene sections are characterized by nannofossils ooze, overlain by upper Pleistocene detrital and volcanogenic sediments; numerous hiatuses and slumps are present, which may indicate sedimentary instabilities and/or tectonic activities.

Site 655 is located on the crest of the north-south trending Gortani ridge; at the bottom 120 m of tholeiitic basalts were drilled, comparable to the basement previously drilled at DSDP Site 373 on a similarly trending ridge lying just at the base of the Campania margin; they are overlain by 80 m of upper Pliocene to Pleistocene marly nannofossil ooze with occasional volcanoclastic layers and sapropels. Several observations suggest that the basalt erupt 3.4-3.6 Ma ago.

Site 651 (Fig. 2.15) is located on the eastern flank of a broad basement north-south trending swell in the center of the basin; this swell lies along strike from the Vavilov volcano and the seismic section shot across the site shows a strong diffractive basement covered by well layered reflectors, presumably turbiditic. The basement stratigraphy revealed by site 651 is complex: a unit of dolerites, metasediments, metadolerites and altered peridotite fragments, sandwiched between two layers of basalt and basalt breccias, all underlain by serpentinized peridotite. The oldest sedimentary unit is a 40 m thick dolostones, lacking of fossils, overlain by calcareous ooze and calcareous claystone dated as late Pliocene; up section volcanogenic sediments becomes more important and much of the Pleistocene sequence is reworked volcanogenic debris.

Site 650 is located near the western edge of the Marsili basin; the basement here is formed by vesicular basalt, emplace as flows. The sediment immediately above is dated 1.67-1.87 Ma and consist of nannofossil ooze, dolomitized near the basement. The Pliocene and lower Pleistocene sequences consists generally of occasional volcanoclastic layers interbedded with calcareous muds and ooze, and a pumice layer is present which can be traced throughout the entire Marsili basin. Upper Pleistocene is dominated by gravitationally redeposited volcanogenic sediments.

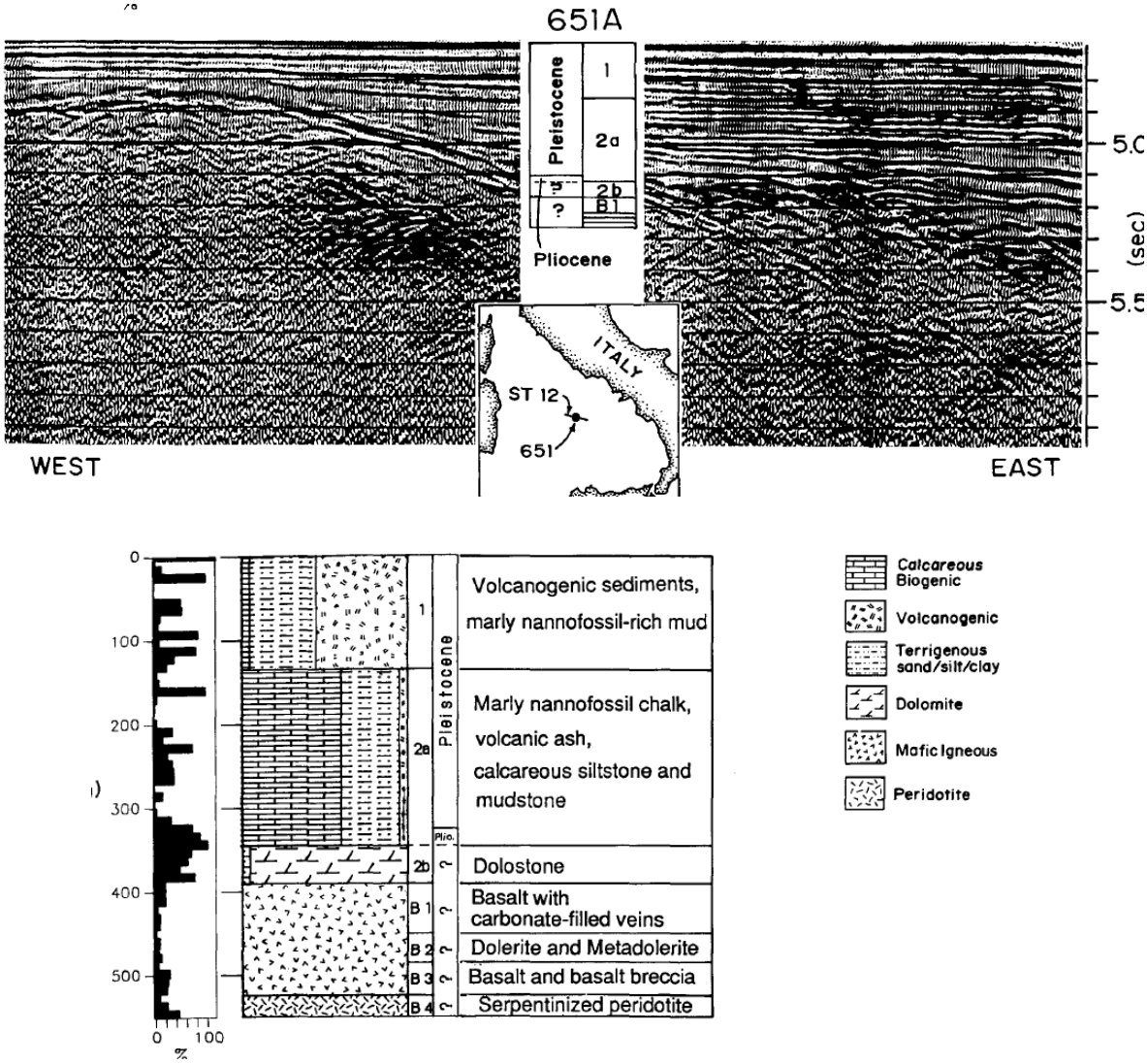


Fig. 2.15 - ODP site 651. In the upper part the seismic reflection profile showing the location of site 651 on the flank of a basement swell in the Vavilov basin; above, core log indicating the lithologic units identified at the site location (Kastes & Mascle, 1990).

## 2.4 Evolution of the Tyrrhenian Sea

The pre-rifting events that shaped the Tyrrhenian basement have been inferred by examination of rocks sampled, which resulted to belong to different geological and structural domains.

Evidence at site 654 and 653 suggests that the area which now constitutes the upper Sardinia margin was part of the Hercynian belt during late Paleozoic; during Mesozoic the present day Sardinia margin was part of the Pangea supercontinent and observations at site 654 suggest a shelf carbonate environment, which in fact characterized Sardinia, Corsica and a broad belt of the perimeter around the Paleotethys. During middle to late Triassic rifting began to split Europe from Africa in the region south and east of Corsica-Sardinia (no trace of Triassic rift facies has been identified in samples of Leg 107), and during Jurassic and early Cretaceous seafloor spreading occurred. Remnants of this Mesozoic ocean, the so called "Piemont Ligurian Ocean" are testified by the metagabbro, metadolerite ad greenstone clasts at site 656; radiolarian-bearing biomicrites at site 652 were probably deposited in an open marine setting during late Jurassic-mid Cretaceous. Tethys Ocean begun to be subducted in mid Cretaceous, which lead to the suturing between Calabria and Sardinia; at Site 652 a recovered pebble containing benthic foraminifera, bryozoans, red algae, testifies a shallow carbonate bearing sea, probably will local emerged areas. Consumption of ocean crust was completed by the end of Eocene. During the early to middle Oligocene started the Apennine–Maghrebide subduction and several 'V-shaped' basins (Provencal basin, Valencia Trough, Alborán basin, Algerian basin) opened in response to back-arc extension in the overriding plate, coeval with roll-back of the Apennine–Maghrebide subduction system.

There are few evidence that the onset of the rifting processes in the Tyrrhenian area can be referred to the late Burdigalian (Sartori, 1990; Gueguen et al., 1998); the syn-rift evolution is generally ascribed to the Upper Tortonian-Messinian (e.g., Mascle and Rehault, 1990; Moussat et al., 1986), or Serravallian–Early Tortonian as proposed by Malinverno and Ryan (1986). The Tyrrhenian rifting proceeded through steps; the first phase affected the Cornaglia terrace west of the Selli Line, characterized by north trending extensional faults. This phase spans from upper Tortonian to intra-Messinian times like testified by ODP Sites 654, 653 and DSDP site 132 and leads to the generation of a deep Messinian basin in the Cornaglia Terrace. A second rifting cycle was active east of the Selli Line from upper (?) Messinian to lower Pliocene (probably including *G. margaritae* zone); during this period the region presently occupied by the Vavilov basin turned from an emerged and eroded chain into a rifted margin; oceanic crust was emplaced in the Vavilov basin just after this phase, around 4.3 My ago, at the base of the *G. puncticulata* zone, and proceed until 2,6 My (end of *G. aemiliana*). In Upper Pliocene a new rifting phase affected the area, but mostly confined to the southeast Tyrrhenian Sea; in the Marsili basin started emplacement of oceanic crust and extensional stresses affected the entire region. Calcalkaline, shoshonitic and high K volcanism become important (Roman, Campania, Aeolian provinces) and produce huge amounts of volcanoclastic material discharged into the deep basins. Pleistocene subsidence also was very strong and affected not only the Marsili basin but the entire area east of the Selli Line.

Extension and subsidence began and ended earlier on what is now the upper Sardinian continental margin than on the actual lower margin; evidence of this is supported by the age of synrift sediments: at site 654, localized on the upper margin, sediments drilled from upper Tortonian to middle Messinian are considered synrift; on the other hand, at site 652, localized on the lower continental margin, the synrift/postrift transition is placed at early Pliocene, whereas onset of the rift is dated within the Messinian, again after the event on the upper margin. No early Tortonian or pre-Tortonian sediments were recovered, so it is possible that western Tyrrhenian experience an earlier phase of rifting and subsidence.

Regarding the Messinian deposits during the desiccation event, the only area where seismic reflection profiles clearly indicate a thick evaporitic sequence is the deep structural basin under Cornaglia terrace (ODP Site 653) and several small basins near Sardinia. So it was inferred that western Tyrrhenian was the deepest part of the basin during Messinian. Instead, the present lower Sardinia margin was relatively high standing in this time, as testified by Sites 652 and 656.

According to the inferred age of the basalts, first eruption was at 7.5 My; this implies an overlap in time between stretching on the Sardinia margin and the basalt injection at the centre of the basin. In addition, the rifting and related magmatism migrated in time from west to east. According to several evidences it seems correct to say that the oldest basaltic basement in the Marsili basin is probably uppermost Pliocene in age, whereas the oldest basaltic basement at the Vavilov basin is not younger than early Pliocene and may be as old as Late Miocene. This is compatible with the hypothesis of growth of a back arc basin through migration of the hinge zone of the subducting slab (Malinverno & Ryan, 1986). Several researchers suggested a constant extension direction in the Tyrrhenian Sea in the last 10 Ma: NW–SE, according to Rehault et al. (1987) and Faccenna et al. (1997, 2004); E–W according to Trincardi and Zitellini (1987), Gueguen et al. (1997), Faccenna et al (2007). Other works propose a change of extension direction in the Tyrrhenian basin from E–W to NW–SE in the Quaternary (Sartori, 2003), or Doglioni (1991) and Carminati et al. (2008), which proposed a change from E to NE in the northern domain and from E to SE in the southern domain. In the south-eastern part, it has deviated to the SE since the late Pliocene (e.g., Doglioni, 1991; Kastens et al., 1988; Sartori, 1989; Savelli, 2002).

# CHAPTER 3

# The Latium-Campania margin: structural-stratigraphic setting and previous studies

In the first part of this chapter is briefly illustrated the geological-structural setting of the Latium-Campania passive margin and of the overlooking Vavilov basin; since in this sector the transition from a continental passive margin to an oceanic basin occurs, the evaluation of the structural and stratigraphic features could provide key data for the interpretation of the evolution and the processes involved in basin extension and formation of its continental margins.

In the second part of the Chapter, the main published studies regarding this sector are discussed. The architecture of the Sardinian and the North Sicily Tyrrhenian margin are relatively well resolved (Mauffret & Contrucci, 1999; Pepe et al., 2000; Sartori et al., 2004; Trincardi and Zitellini, 1987, among the others); in contrast, the tectonic architecture of peninsular Italy is less constrained and is less known about its evolution. During the 80's, the firsts structural and seismostratigraphic studies were carried out, based on different seismic surveys that investigated this sector of the Tyrrhenian Sea; more recent investigation has also focused on submarine instability of the continental slope, evolution of the volcanism and its implications and stratigraphy of the last glacio-eustatich cycle.

## 3.1 The Latium-Campania passive margin

In the study area the continental shelf (delimited by the -200 m isobath) is around 25 km wide; it reaches its maximum extension offshore Circeo Promontory (more than 40 km) determining a structural high between the onshore sector and the western Pontine archipelago (Ponza, Zannone and Palmarola islands) (Fig. 3.1).

Two main peri-Tyrrhenian basins (Fabbri et al., 1981; Malinverno & Ryan, 1986; Trincardi & Zitellini, 1987; Oldow et al., 1993) are enclosed in this shelf sector, the Terracina and the Gaeta basins (Aiello et al., 2000), located in waters down to the -150 m isobath. They form the seaward prolongation of the coastal plains localized on the Latium-Campania onshore: the Terracina basin represents the seaward extension of the Piana Pontina, bounded to NE and SE by the Ausoni and Aurunci carbonate massifs. The Gaeta basin instead represents the seaward prolongation of the alluvial plain of the Garigliano River, bounded to the north by the Aurunci range, to northeast by the Roccamonfina volcano and to the southeast by the elongated NE-SW Mt. Massico horst; the latter consists of Trias to Early Miocene carbonates and minor late Miocene terrigenous sediments (Bruno et al., 2000). Plio-Pleistocene siliciclastic deposits of marine, coastal and deltaic environment (conglomerates, sands and shales) fill the basins, sometimes with intercalation of volcanoclastic levels. This sediments overlie tectonic structures of the Apenninic chain which usually form the acoustic basement of the coastal basins; the basement is composed of terrigenous-shaly basinal sequences («Flysch di Frosinone», «Flysch del Cilento»; D'Argenio et al.,1973; Parotto and Praturlon, 1975) and of thick platform and basinal Meso-Cenozoic carbonates (Latium-Abruzzi platform) as documented by offshore well stratigraphy of Mara 1 and Michela1); these sequences are exposed in the adjacent mainland (Bartole et al., 1983; Bartole, 1984).

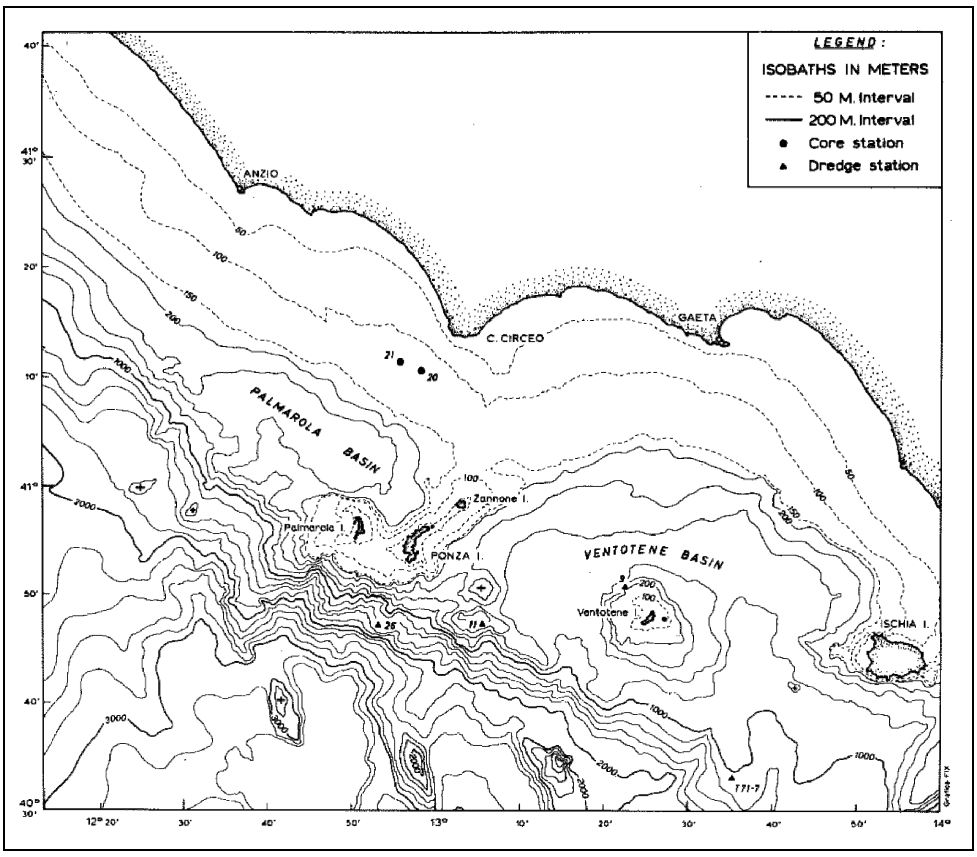


Fig. 3.1 - Bathymetry of the Pontine archipelago area. Continental platform is delimited by the -200 isobath; the Ponza-Zannone high divided the Palmarola basin (to the NW) from the Ventotene basin (to the SE) (Zitellini et al., 1984).

The Capo Circeo-Zannone alignment divides two major intraslope basins which are the principal areas of sedimentary deposition in this sector: the Palmarola basin, localized to the NW of the alignment, has a maximum depth of 570 m and a thickness of the Plio-Quaternary sedimentary infill of 1200 m (Zitellini et al., 1984); the Ventotene basin, localized to the SE, reaches a maximum depth of 860 m with an infill of 1000 m of thickness (Zitellini et al., 1984) (Fig. 3.1).

Volcanic activity was very strong in the Latium- Campania margin during Plio-Quaternary time and is generally ascribed to the Roman province (Lustrino, 2011 and references therein), which includes the volcanoes of Vulsini Mountains, Cimini Mountains-Vico, Sabatini Mountains, Alban Hills, Ernici Mountains, Mount Roccamonfina, Pontine islands, Procida, Vivara and Ischia islands, Mount Vesuvius, and Phlegrean Fields. In particular, the western islands of the Pontine archipelago, i.e. Ponza, Palmarola and Zannone islands, developed during two main volcanic cycles of early Pliocene and Pleistocene age, and they are located on the structural high that divides the Ventotene and Palmarola basins, representing in fact an emerged part of the Tyrrhenian continental shelf. The eastern group of Pontine islands, Ventotene and Santo Stefano, are more recent in age and represent the

subaerial portion of a large submerged strato-volcano emplaced at the center of the Ventotene basin.

The volcanic products lie on a complex substratum cropping out at Zannone island; this island is composed by several tectono-stratigraphic units having different lithological nature and thickness: crystalline basement, Meso-Cenozoic sequences possibly deformed, uplifted and eroded during the Alpine subduction and later by the Apennines tectonics, overlaid by Plio-Pleistocene volcanic and sedimentary sequences (De Rita et al., 1986, Zitellini et al., 1984).

The shelf break is well defined and articulated, with a variable depth between 95 and 160 m, deeper in the sector between Ponza and Palmarola islands. Beyond the shelf break a complex slope sector, NW-SE oriented, connects the continental shelf to the abyssal plain at 3550 m of depth. The escarpment connecting the Latium-Campania margin is a very complex feature, tectonically controlled, displaying different characteristics along its path: in the northern sector, in proximity of the western Pontine archipelago, a single slope sector is responsible for the deepening of the margin toward Vavilov plain. In this portion it is the steepest continental slope of the eastern Tyrrhenian continental margin, with inclination locally up to 30° (Chiocci et al., 1996). Moving to the southern sectors it constantly widens and a set of closely spaced fault scarps develops in a NNW-SSE direction, resulting in a downthrown stepping margin morphology; they follow the trend of the so called Sartori Escarpment, a major fault system (Curzi et al., 2003) 80 km long, interpreted as a left lateral transtensive system (Musacchio et al., 1999). Due to the recent age of tectonic events that originated this setting, the basement highs are not yet mantled by slope sediments; so, the main loci for sediment accumulation are the intraslope basins formed on top of the basement depressions, generally NNW-SSE trending. These basins are mainly narrow and isolated from the upslope sectors, with a predominance of hemipelagite cover and mounded bodies resulting from mass wasting processes. Nevertheless, some major intraslope basin develops, like the Capri basin or the Paestum basin; some portions of the intraslope basins are also characterized by drainage systems that connect successive deeper basins, until the bathyal plain, like the Ischia valley or the Dorhn canyon. The upper sector of the continental slope (< 2000m depth) is interested by numerous, relatively short, fault scarps, which dissect the region into different small horsts and grabens, trending N-S and NE-SW.

Morphologically the slope sector developed in front of the Pontine archipelago has a very irregular shape and morphology, due to erosive/instability phenomena affecting almost all of the continental slope seafloor and causing the slope retreat (Chiocci et al., 2003). This variable physiographic setting of the escarpment is strictly linked to the tectonic activity, which is both responsible for the formation of the slope itself and of the high gradients, than for the development of the submarine instability processes. The extensional regime took place since lower Pliocene up to the Quaternary as a consequence of the Tyrrhenian basin opening.

At the base of the escarpment is localized the northern apex of the Vavilov abyssal plain, also called Gortani basin: this sector is part of the area surveyed during Tir 2010 cruise and it is delimited to the south by the Vavilov seamount and the arcuate shaped D'Ancona Ridge, to the east by the lower slope of the Campania continental slope, with the prominent Flavio

Gioia seamount and to the west by the De Marchi and the Farfalla seamounts. The latter two features, the Flavio Gioia and De Marchi Smts., are 80 km apart, both N-S trending and rising about 1200 m above the surrounding seafloor, both characterized by steep fault scarps dipping toward the basin.

The flat Vavilov plain more than 3000 m deep is filled with distal turbidites deposits with a basin-wide areal extent; the large seamounts and seamount chains that occupy its central parts can be related both to basement crustal blocks than to submarine volcanoes (Structural model of Italy, 1991, Gamberi & Marani, 2004). The above mentioned Flavio Gioia and De Marchi Smts. represent, according to Marani & Gamberi (2004), the final trace of rotational crustal blocks within the Vavilov basin, so probably they identify the boundary between the oceanic crust of the basin and the surrounding thinned crustal blocks in this sector.

According to the results of the ODP Leg 107 (Mascle & Rehault 1990, Sartori 1990), some portions of the Tyrrhenian Sea are floored with oceanic crust, emplaced during two distinct episodes; the oldest one is dated between 4.6-2.3 My and it refers to the Vavilov back arc basin. The younger is dated less than 2 My and occurs in the Marsili back arc basin, toward the south eastern sector of the Tyrrhenian Sea.

Regarding the seismicity, this sector is characterized by a weak activity, even if earthquakes with small values are more frequent here than in the onshore sector (Favali et al., 2004).

## 3.2 Previous studies

### 3.2.1 Structural and seismostratigraphic setting of the Latium-Campania passive margin

This paragraph provides a synthetic overview of the principal studies about the structural setting of different portions of the Latium-Campania passive margin and about the seismostratigraphic characters that different authors described in this sector.

Zitellini et al. (1984) analyzed several seismic lines and sampling stations in the area around the Pontine islands, trying to define the tectonic evolution of Palmarola and Ventotene basins. According to the authors, the main extensional tectonic phase shaping the two basins started in the lower Pliocene resulting in areas of major sedimentary accumulations; the same tectonic phase was also responsible for the formation of the continental slope and was linked with the beginning of the volcanic evolution of Ponza island. The authors recognized that, to the west of the Zannone-Capo Circeo alignment, the main fault directions are NW-SE; instead, to the east of the same alignment, structures are predominantly E-W oriented. Deposition of the Plio-Quaternary infill started in lower Pliocene, but in this work it is also suggested the occurrence of an earlier N-S post-orogenic extensional event probably Messinian in age, responsible of the so called "Terracina basin".

Regarding the sedimentary infill, showed in Fig. 3.2, the authors recognized three different seismic units, in agreement with other works (Fabbri et al., 1981; Trincardi and Zitellini, 1987; Zitellini et al., 1986) which analyzed others sectors of the Tyrrhenian basins.

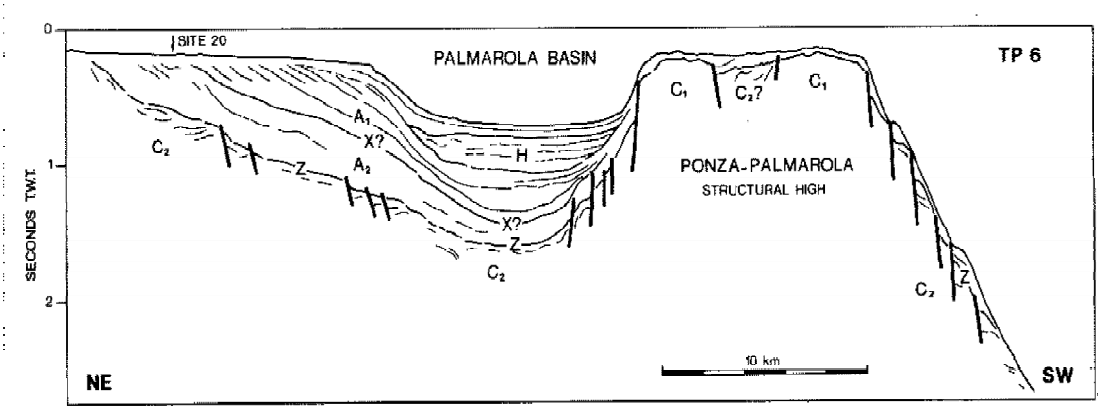


Fig. 3.2 - Line drawing of a seismic section across the Palmarola basin (Zitellini et al., 1984).

The seismic unit C identifies the acoustic substratum, divided in C1, non reflective, and C2 reflective; the seismic unit B is the post-orogenic sequence of upper Miocene (Messinian, basal limit undefined); the seismic sequence A is Plio-Quaternary in age, divided by the mid-

Pliocene unconformity X in A1, from the mid Pliocene p.p. to the present, and A2, from lower Pliocene to mid Pliocene p.p. (Fig. 3.2).
On the continental platform area, according to Zitellini et al. (1984) and De Rita et al. (1986) (Fig. 3.3), the Ponza-Zannone structural high is bounded by a system of normal faults trending NE-SW which produced the lowering down toward the Ventotene (southeast) and toward the Palmarola basins (northwest, less abruptly). To the north and to the south the shelf is cut by en-echelon faults striking E-W, which offset the structure down toward the Tyrrhenian basin. The lower Pliocene extensional tectonics with Apenninic direction and the "Sicilide" type substratum recognized in the western Pontine sector allow the correlation with the tectonic evolution and deformation of the Umbria-Marche domain. For this reason, the Pontine archipelago structure can be considered similar to those buried along the Tyrrhenian coast, between Anzio and Circeo Mt., interpreted as fragments of the inner (Umbro-Tuscan) basins thrusted onto the Latium-Campania Meso-Cenozoic carbonate platforms (Parotto, 1980). The E-W deformation links instead the eastern sector of this area to the southern Apennines, where similar direction of deformation can be found.

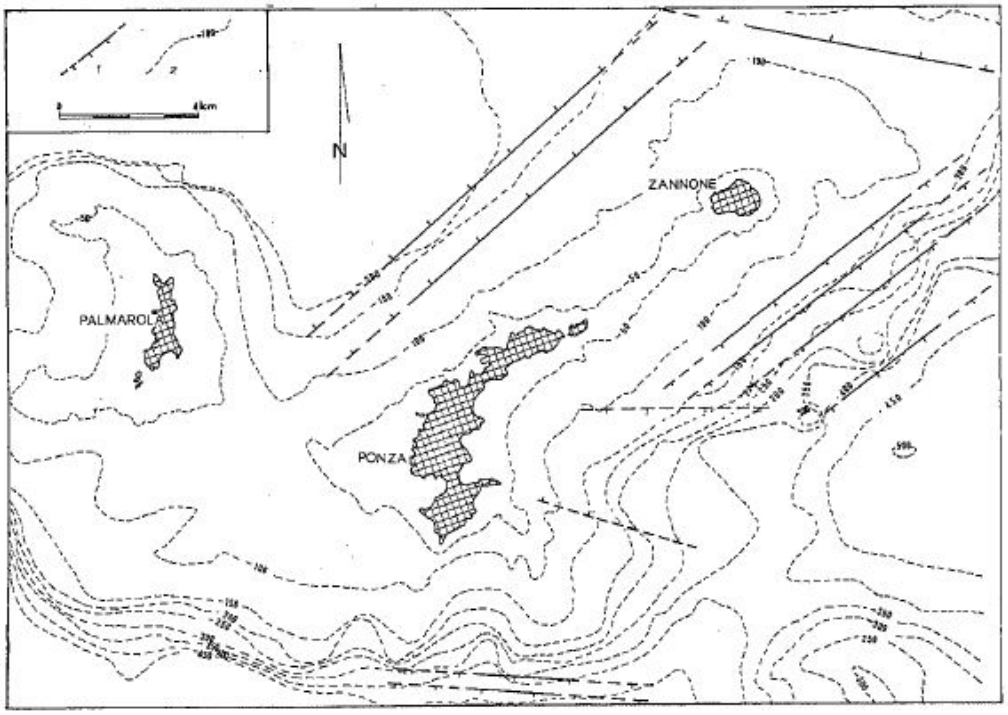


Fig. 3.3 – Main structural trends along the Ponza-Zannone structural high (Pantosti & Velona, 1986).

The continental margin between Civitavecchia and Capo Circeo has been analyzed by Marani and Zitellini (1986), using seismic reflection profiles. They recognized two distinct tectonic episodes: the first one is characterized by an elongated system of rotated blocks, N-S trending, which originated the Civitavecchia Valley half graben system, 140 km long (Fig. 3.4

A); this phase has a Late Miocene - Early Pliocene age and it is probably linked to the Tyrrhenian rift.

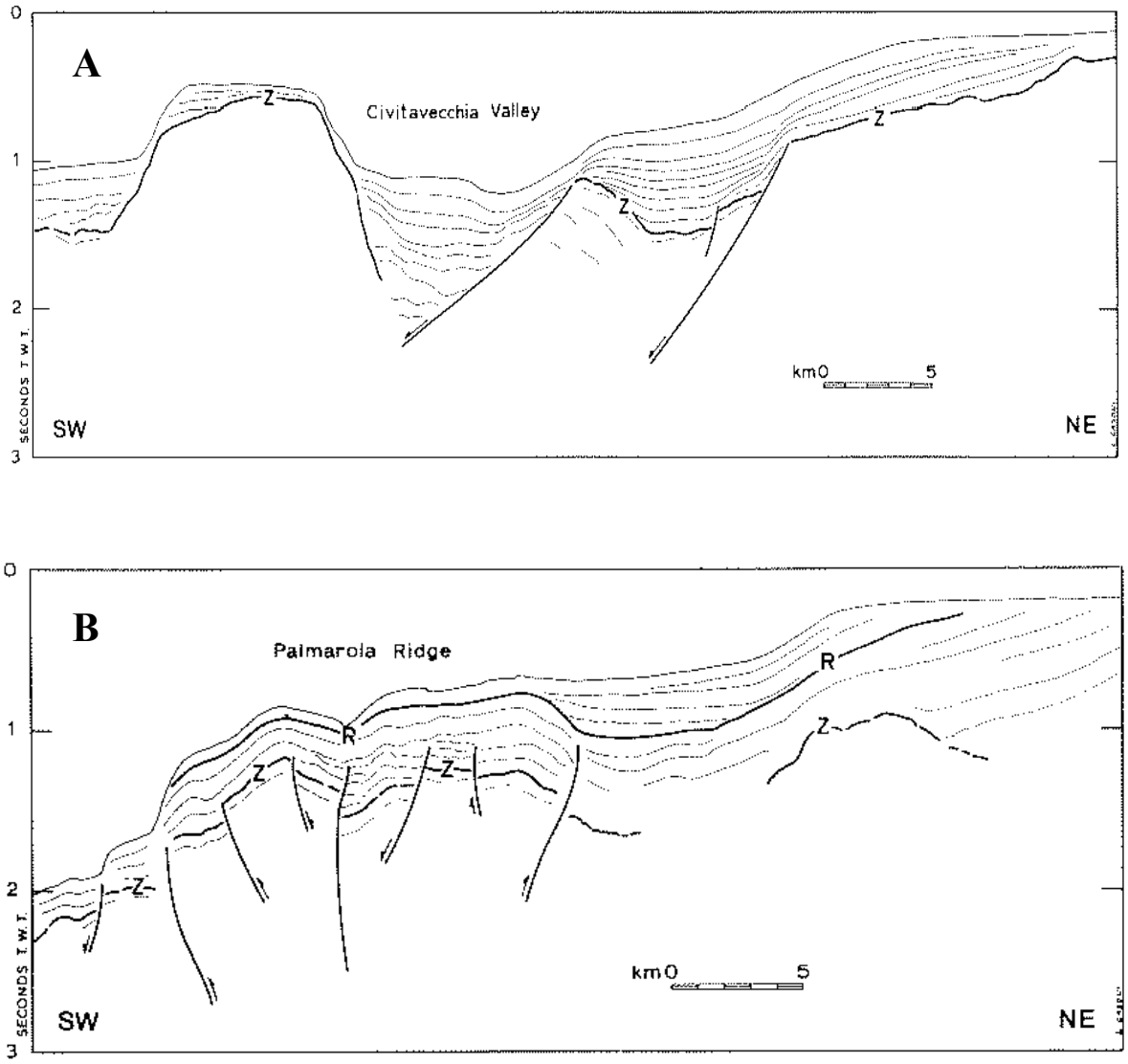


Fig. 3.4 –Line drawing of seismic lines showing the structures characterizing the Civitavecchia Valley half graben system (A) and the Palmarola fold system (B). Z represents the acoustic substratum, R the end of folding (Marani and Zitellini, 1986).

The second tectonic episode is more evident along the upper slope south of Anzio and it consisted in localized folding and uplift, generating structures NW-SE striking, bounding seaward the Palmarola basin (Fig. 3.4 B). Here the authors described a wide anticline developed above already faulted and uplifted sediments, corresponding to the distal, upper slope portions of prograding units that constituted the continental shelf. Since progradation began about 1.5 Ma ago, the age of this deformation is Pleistocene and it is, according to the

authors, linked to the transpression resulting from the strike slip movements affecting the basement blocks. So, according to these authors, some of the basins along the Tyrrhenian margin can be ascribed to rift-related block rotation, whereas others are related to the Pleistocene episodes of uplift and folding.

In Bartole et al. (1984), the authors investigated the portion of the Tyrrhenian margin between Ventotene island and Policastro, highlighting both orogenic and post-orogenic features. The main orogenic features (Fig. 3.5 A), occurring in the Gaeta area, are the NE trending, Palmarola-Terracina overthrust, characterized by a right lateral strike slip kinematics. The northern portion of this thrust crops out in the Circeo Promontory. The authors inferred a Messinian age for the main thrust activity and an Early Pliocene age for the strike slip activity. Another important orogenic feature is the "Zannone-Volturno overthrust" which consists of an approximately E-W trending lineament, verging toward the north; on the basis of seismic studies (Bartole, 1983) a middle Miocene age can be postulated to the overthrusting activity, with minor movements till Early Pliocene.

Regarding the post-orogenic features (Fig. 3.5 B), the authors reveal three principal directions: a) apenninic, mostly shown on the main slope and escarpment systems; b) anti-Apenninic, which is a common orientation of the numerous canyons cutting the upper slope; c) an E-W trend, characteristic of the slope system which limits the Palinuro basin and the Policastro and Gaeta Gulfs, positioned eastward of the important regional lineament called the 41$^{st}$ Parallel Line. The NE–SW direction also prevails in the southern sector of the margin, characterized by a horst-and-graben northeast trending submarine topography.

Summarizing, the authors highlighted a Miocenic deformation linked to the orogenesis, as demonstrated by the thrust fronts and by the distribution of the allochthonous thrusted units. The post-orogenic extensional tectonics took place from the Early Pliocene to the present day; the shelf is characterized by a weak post-orogenic tectonics, whereas the slope was affected by intense differential movements which completely masked the previous compressive structures. Accumulation of Plio-Quaternary sediments occurred in depocenters which represented the seaward extension of the coastal plain grabens.

In Bartole (1984) four seismostratigraphic units, characterizing the Campania shelf, are recognized by means of calibration of wells and correlation with land. The bottom unit is referred to Mesozoic carbonate platforms, which commonly constitutes the local acoustic basement; the upper sequence is a chaotic sequence made up of tectonically deformed sediments of Cenozoic age, mainly attributable to the Ligurian and Sicilian allochthonous complexes and to associated flysch units. Up section, two post orogenic sequences are described: the lower is constituted by Upper Miocene-Lower Pliocene sediments and it is separated, by a regional unconformity of Early Pliocene age, from the upper post-orogenic unit, which is made up of Lower-Middle Pliocene to Quaternary sediments. Such seismostratigraphic units appear also to be widely extended throughout the studied region down to the lower slope.

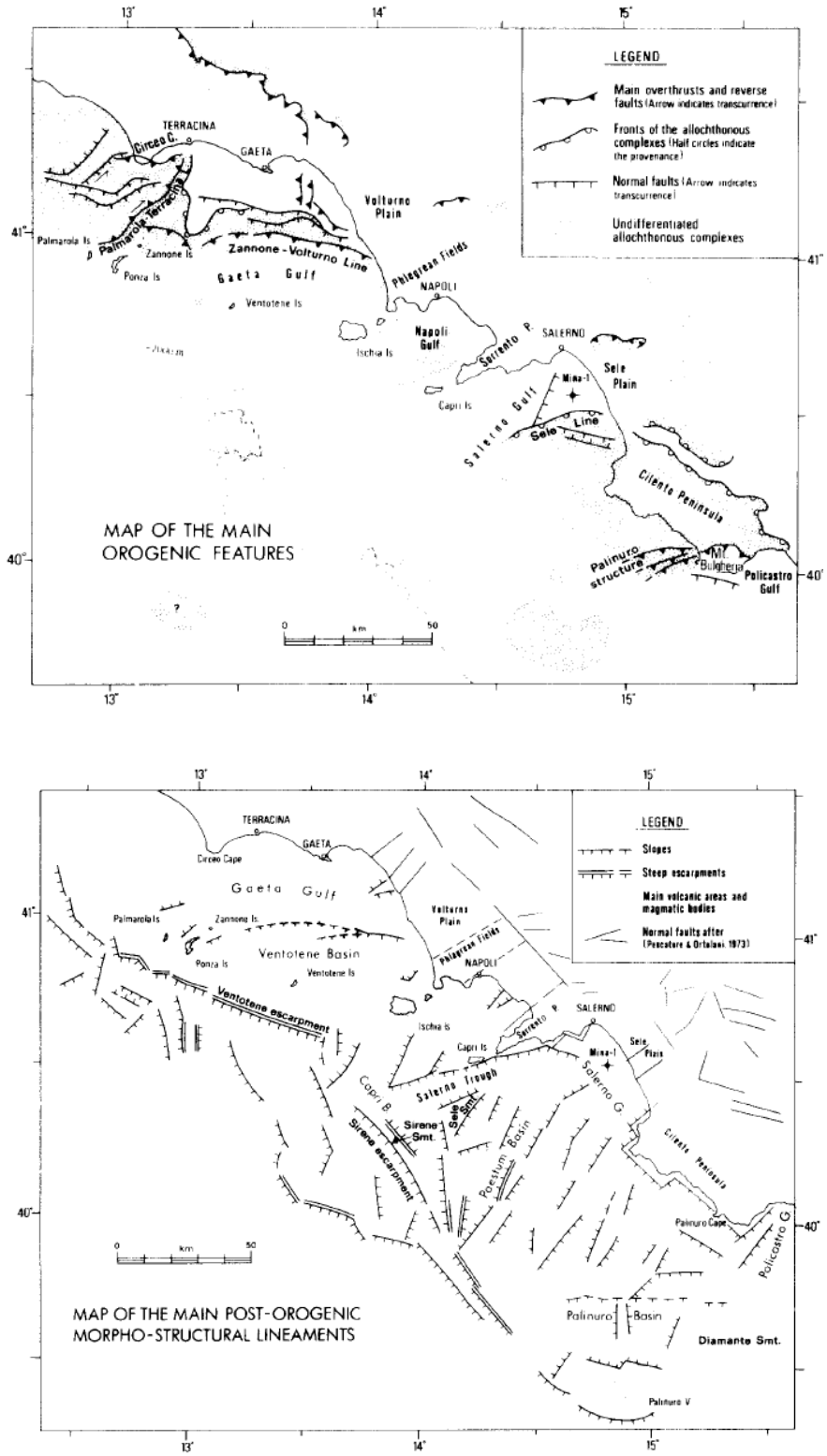


Fig. 3.5 - Maps of the main orogenic (A) and post-orogenic features along the Campania margin (Bartole et al., 1984).

### 3.2.2 The peri-Tyrrhenian basins

The Tyrrhenian margins encompass a number of structurally-confined basins, generally called peri-Tyrrhenian basins (Fabbri et al., 1981; Malinverno and Ryan, 1986; Trincardi and Zitellini, 1987; Oldow et al., 1993) which from a morphological point of view correspond to overall sub-planar areas within the continental shelf.

Mariani & Prato (1988) investigated the main neogenic coastal basins along the Tyrrhenian margin, grouped them into three groups (Tuscan, Tuscan-Latium and Campania), and, for each basin, described the thickness, the structural setting and the seismic sequences. They concluded that these basins present the typical character of continental passive margins and they are mainly formed by fault bounded half grabens. According to the authors, the basins are probably linked to anti Apennines, strike slips faults, trending NE-SW. The maximum subsidence is Pliocene in age in the Tuscan basins, whereas in the Latium and in the Campania basins, the maximum thickness corresponds with Pleistocene. In addition, the volcanic facies thickness increased from north to south.

Aiello et al. (2000) investigated the Terracina and Gaeta extensional basins and recognized several main seismostratigraphic units and fault systems. The Gaeta basin is E-W oriented and shows two main depocenters. It is bounded to the north and to the south by E-W trending normal faults and to the east by a NW-SE trending normal fault. In the Terracina basin, roughly N-S oriented, half-graben structures are downthrown seaward through normal faults. The extensional tectonic controlled not only the Plio-Quaternary sedimentation but involved also the Meso-Cenozoic tectonic units of the acoustic basement; in the Terracina basin deformation involved mainly the acoustic basement, whereas in the Gaeta basin the basal Plio-Quaternary group is strongly affected by wedging and growth processes, controlled both by Plio-Quaternary extensional tectonics phases and tectonic inversion.

The same authors divided the Plio-Quaternary infill of the pery-Tyrrhenian Campania basins into 10 sequences, bounded by unconformities corresponding to regional onlap, downlap or erosional surfaces (Fig. 3.6).

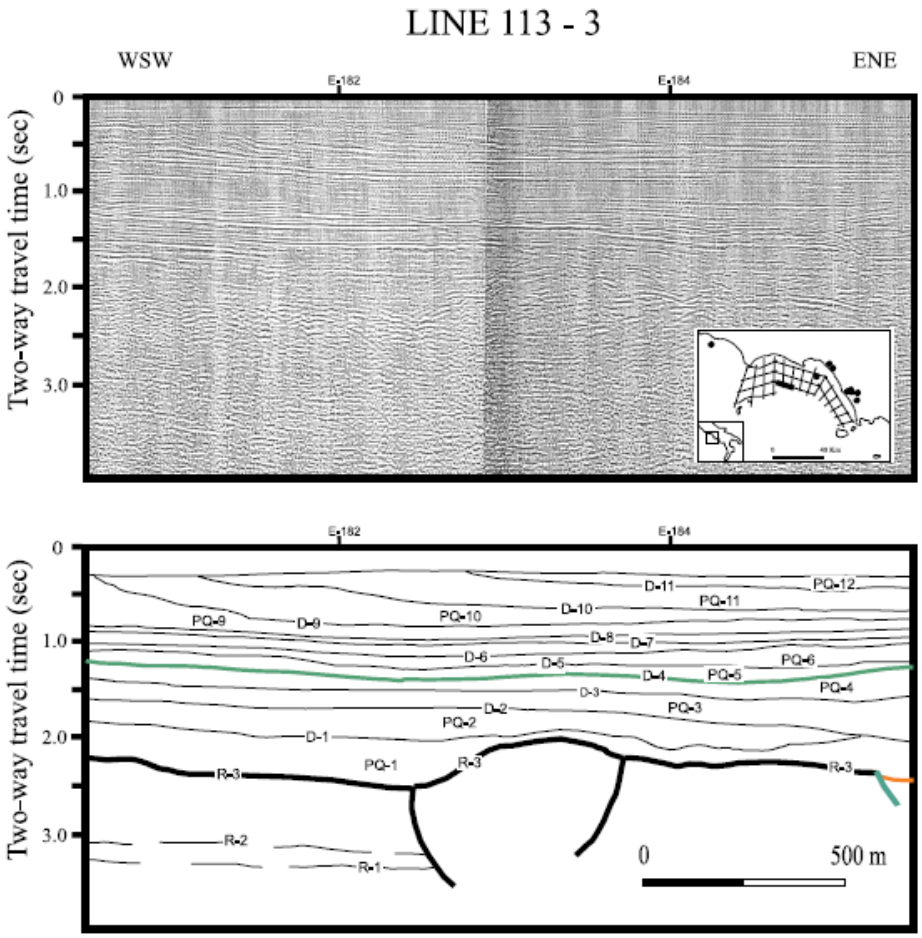


Fig. 3.6 - Main seismic units interpreted by Aiello et al., 2000.

The lower group of seismic sequences (called PQ1-PQ4) shows seismic facies with parallel reflectors onlapping the top of the acoustic basement and the presence of normal faulting. The "D4" reflector represents, according to the authors, an important tectonic unconformity, associated to a regional downlap surface probably of Early Pleistocene in age; the above sequences (PQ5-PQ10) have a prograding pattern and are formed by sandy and shaly sediments essentially undeformed.

Several other studies (Aiello et al. 2011, 2011b, 2010) are focused on the Campania sector of the margin, immediately southward of the area object of the present thesis. Aiello et al. (2011) analyzed some seismic lines of the SISTER survey in the zone of the Naples Gulf and Ischia island and recognized the main regional morpho-structures (Fig. 3.7): the Banco di Fuori, a morpho-structure high of Meso-Cenozoic carbonates, bounding southwards the Naples Bay; the Dohrn canyon, which separate the eastern side of the Bay from the western one, characterized by sedimentary sequences and volcanic units respectively; the Capri structural high, a sedimentary high related to regional uplift of Meso-Cenozoic carbonates; the Magnaghi canyon; the Capri basin, filled by Pleistocene–Holocene sediments overlying Meso-Cenozoic carbonatic unit; the Salerno Valley, a half-graben filled by three seismic units

corresponding to Quaternary marine deposits, overlying chaotic sequences related to the ‘‘Flysch del Cilento’’ Auct.; the Volturno basin, filled by four marine to deltaic seismic sequences, frequently alternating with volcanoclastic levels, overlying deep seismic units, correlated with Miocene flysch deposits (sands and shales) and Meso-Cenozoic carbonates.

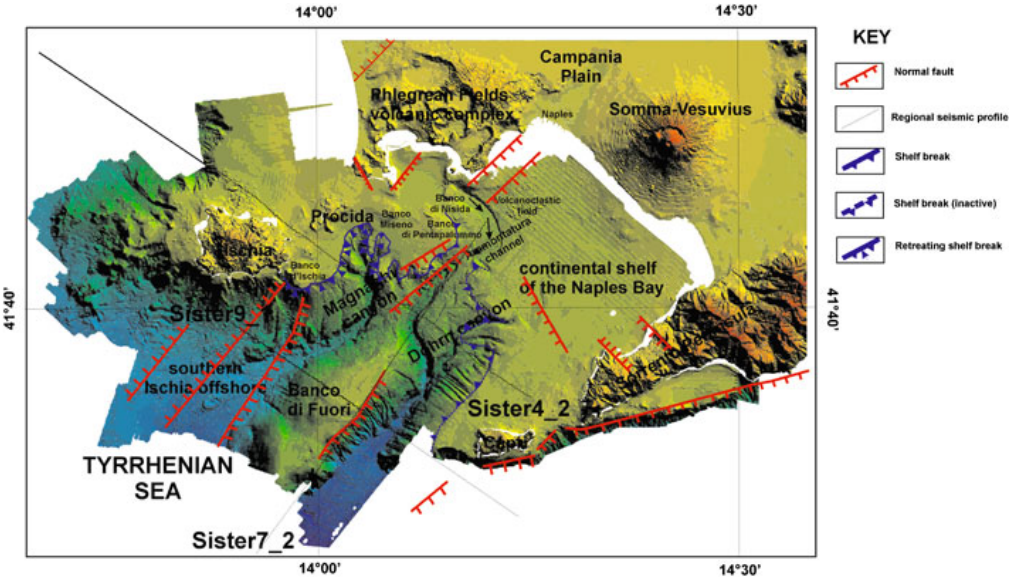


Fig. 3.7 - Interpretation of regional morpho-structures on Digital Elevation Model of Naples bay (Aiello et al., 2100).

The Volturno basin (Fig. 3.8) has been extensively analyzed in another paper by Aiello et al. (2011) with the aim to show the stratigraphic relationships between the filling in the Quaternary basin and the Meso-Cenozoic acoustic basement, and the relationships with the Gaeta and Terracina basin. The authors recognized four main seismic sequences in the basin and assigned a Pleistocene age to them; the Volturno basin is described as a half-graben structure, characterized by down-thrown blocks along normal faults affecting mainly the top of the Miocene acoustic basement. They also describe an older extensional phase Pliocene in age, NW-SE oriented, whereas the Pleistocene phase, which acted through high-angle normal faults, has a NE-SW and E-W direction. According to the authors, the structure of the continental margin is controlled by asymmetric-linked fault systems, which are characterized by a main detachment level, listric normal faults and rollover anticlines. The different trends of extension are related to two distinct kinematic elements, the Northern Apennine Arc and the Southern Apennine Arc. The N-S extension is a consequence of the motion of the Northern Apennine Arc during the first stage of rotation, between 3.5 My and 0.78 My. The NW-SE extension is related to the migration of the Southern Apennines to the south-east, when the Northern Apennines rotation was already stopped.

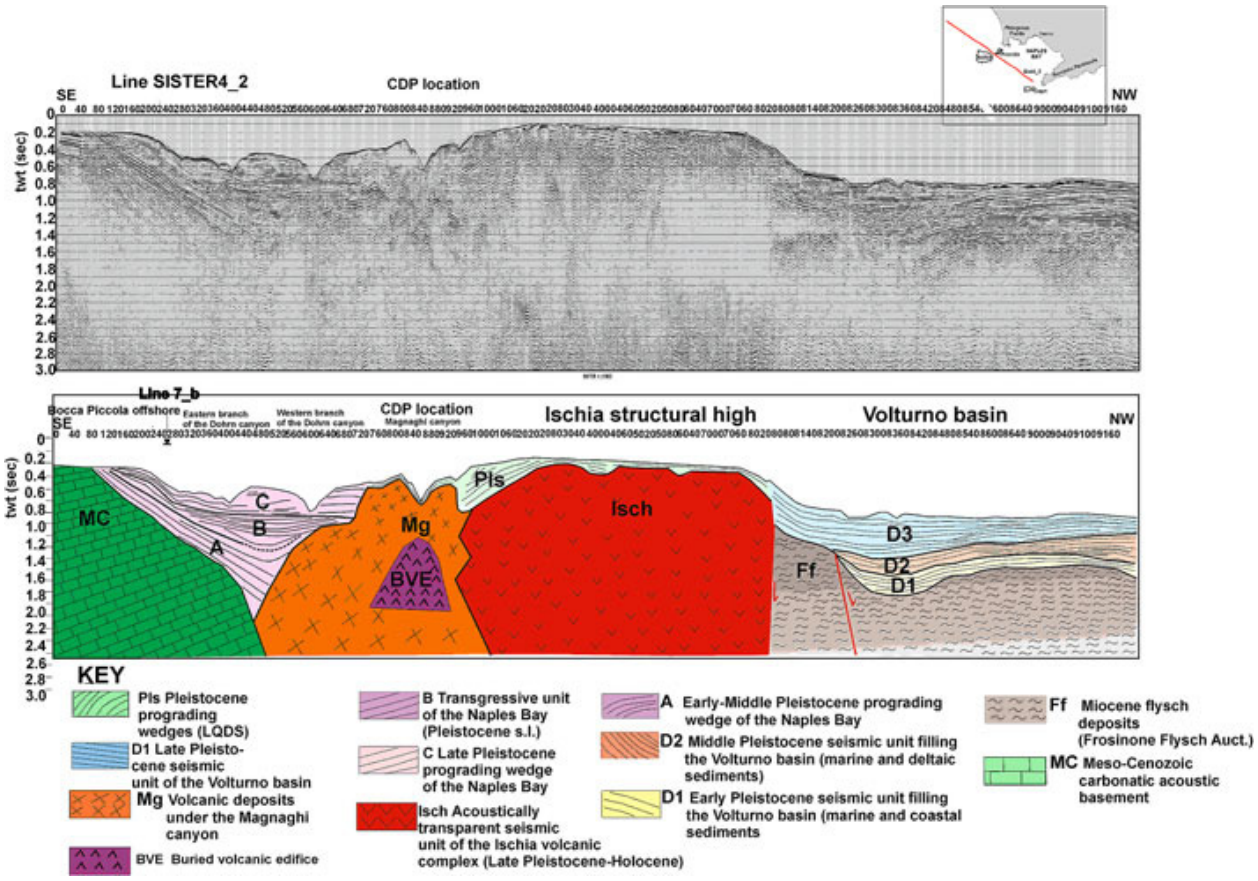


Fig. 3.8 - Seismic profile Sister4_2 and corresponding interpretation, showing the Volturno basin to the NW, and its relationships with the acoustic basement and the Ischia high.

A recent work by Milia et al. (2013) analyzes in detail the Gaeta basin in order to link the geologic evolution of the Campania margin with the Tyrrhenian central plain. In this study the Gaeta basin is divided into three sub-basins (northern, central and southern basins) where the authors describe four seismic unconformity-bounded units (PP, A, B, C) overlying the acoustic substratum. PP unit is Pliocene –Lower Pleistocene in age, A, B, C units are from Pleistocene to recent; thirteen depositional sequences of the 4th order (100 ka) are identified above an older unconformity bounded unit (Pliocene-early Pleistocene in age) and a poly-phased evolution in the basin is recognized. The link to the Tyrrhenian plain is based on the analysis of the CROP line M-29B, where the authors identified a detachment fault in the subsurface of the Vavilov basin, which separates footwall mantle rocks (serpentinized peridotites, drilled at Gortani Ridge, ODP Site 651, 655) from hanging wall Alpine ophiolites, both stratigraphically covered by Mid-Oceanic Ridge basalts. According to this study, along the Campania margin, coeval structures occur, corresponding to the crustal part of the detachment fault system that developed in the Vavilov basin; other faults are instead active later, during the Plio-Pleistocene, and disrupt the detachment fault. The authors concludes that rifting was polyphasic in the Tyrrhenian basin and they propose a kinematic evolution for the last 10 Ma, consisting of an older extensional event (stages 1–2) off Sardinia and in the

Vavilov basin (leaving the Eastern Tyrrhenian margin unaffected), and younger ones (stages 3–5) developed in the whole Tyrrhenian region; in particular they document a Pliocene–Quaternary change of the extension direction along the Campania continental margin (Fig. 3.9).

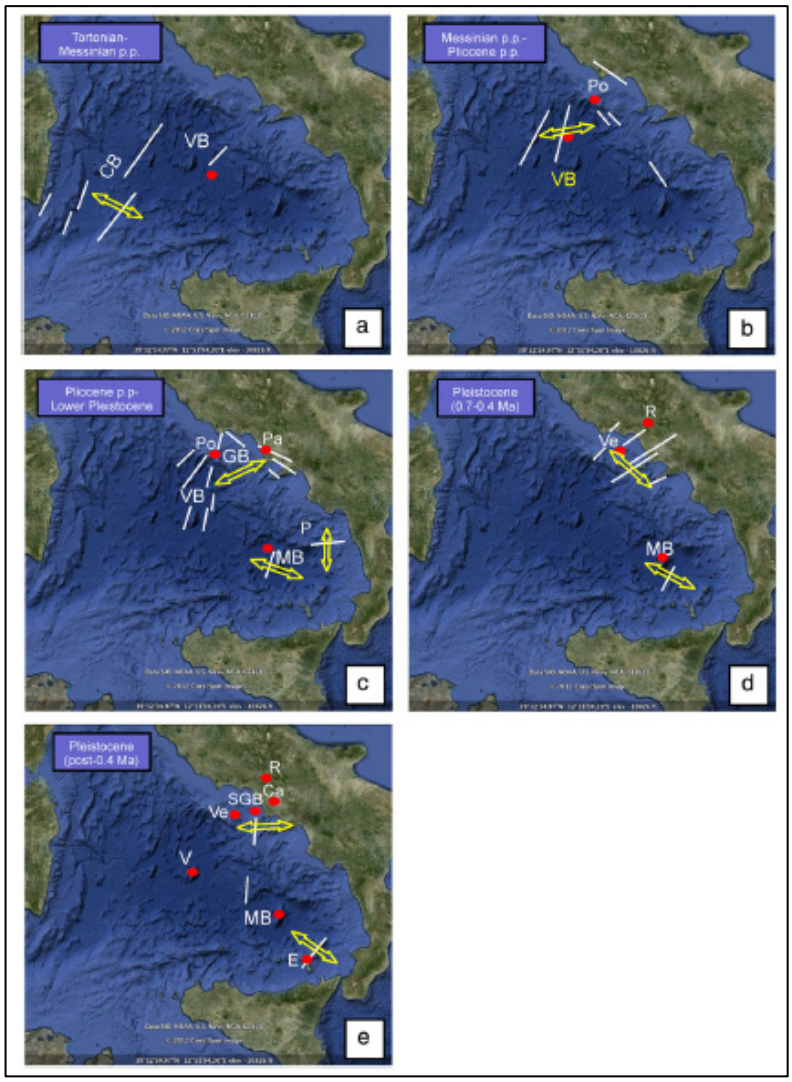


Fig. 3.9 - Sketch of the different kinematic phases in Tyrrhenian basin over the last 10 My (Milia et al., 2013).

### 3.2.3 The slope area

In the Latium-Campania margin the continental slope connecting the Vavilov abyssal plain with the continental platform is one of the steepest escarpment of the whole Mediterranean Sea, being narrow up to 20 Km and steep 5°-10°, locally up to 30°.

Chiocci et al. (1998 and 2003) investigated on the morpho-stratigraphic setting of the area in front of the Pontine archipelago, extending from the shelf break down to the abyssal plain. The authors analyzed side scan sonar data acquired during two cruises in 1998 and 2001 and pointed out several instability processes affecting almost all (98%) the continental slope seafloor and causing the slope retreat. Instability features are variable in extension and typology, but the authors found a relationship between slope gradient and distribution of the different processes: steepest areas with mean value of 6°-10° (max. value 30°) are characterized by pervasive sliding and punctual mass transport processes, developed mainly by linear scar-channel systems, dendritic gullies networks, canyons, simple and complex slides. More gently sloping areas (3°- 4°) are characterized by amalgamation of the debris transfer features and deposition of such debris; in areas with slope gradient lower than 3° the mass movements develop mainly as debris flow deposits (Fig. 3.10).

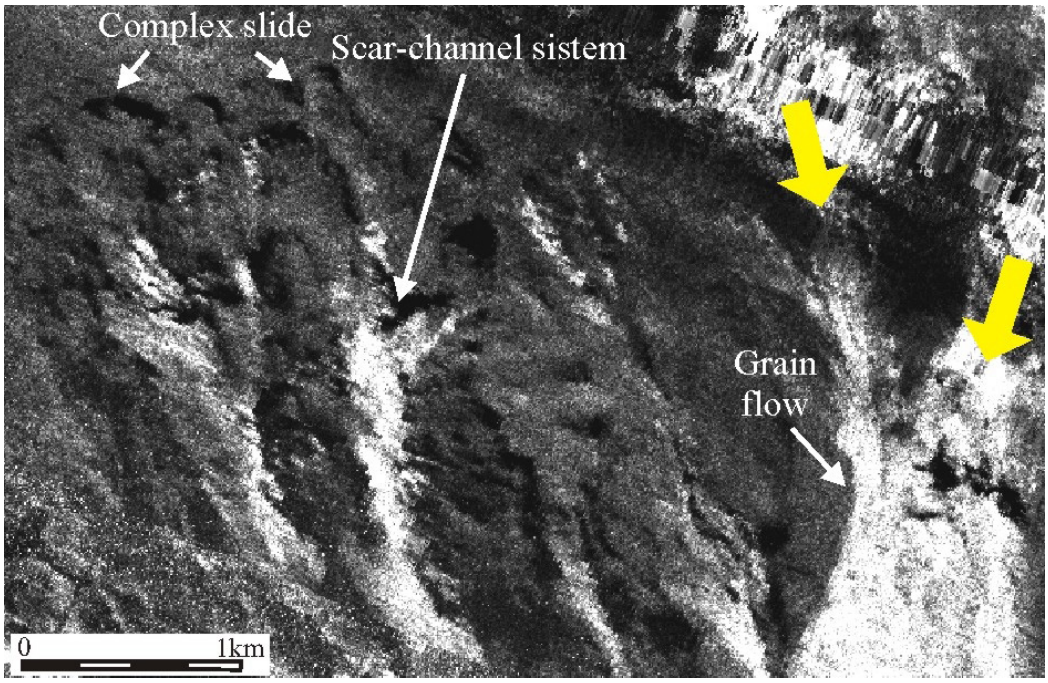


Fig. 3.10 - Upper continental slope sonar image, showing linear scar-channel systems, complex slides and grain flows (Chiocci et al., 2003).

The continental slope sector has been studied also by Conti et al. (2013) from a depositional point of view; in this work the authors analyzed planktic foraminifera and endo-epilithozoan faunas colonising Fe–Mn crusts and volcanic samples dredged along the slope between 400 and 2000 m of depth. Results from this study show that sectors of the upper Pontine slope experienced, during the Plio-Pleistocene, periods of emplacement of volcanic products and/or sediment deposition, alternate with periods of sediment starvation and

hardground formation. The sediment starved seafloor is found on morphological highs characterized by steep flanks, unsuitable for sediment deposition, whereas sediment gravity flows that could contribute to sediment deposition are confined to topographic lows. According to the authors, the interplay among volcanism, tectonically induced topography, mass wasting, distance from the mainland and activity of bottom currents, led to sediment-starved and morphologically complex setting; this significantly differs from most of the well-fed, constructional margins of the Mediterranean Sea, characterized by the stacking of shelf/slope deposits.

According to the analysis carried by Brandano and Civitelli (2007) on 33 sediment samples collected in the range from -15 to -250 m, the western Pontine archipelago is characterized by siliciclastic-carbonate mixed sedimentation: in the infralittoral zone, erosional processes on the rocky shoreline produce reworked volcaniclastic deposits, reworked by wave-induced near-shore currents. In the upper circalittoral zone, sediments are principally biogenous, consisting of coralline algae, foraminifera, bryozoans, mollusks and echinoderms; finally, in the lower circalittoral zone, the sediment is composed of skeletal grains and planktic foraminifera. The recent sediments blanket the rocky substrate and the last-glacial lowstand deposits, with sand that is the dominant grain-size class, except in water depths greater than 200 m where silt size predominates (up to 80%).

Lowstand depositional terraces are identified in Chiocci and Orlando (1996, 2004). The depositional bodies exhibit a wedge shape with an internal prograding configuration and limited thickness, superimposed on the regular sloping morphology of the continental slope. According to this studies, the terraces formed during sea level still stands lower than present, corresponding to the Last Glacial Maximum. This terrace shows a gradual variation in depth with a difference of about 50 m between the eastern end (island of Zannone, terrace edge at -140 m) and the western end (island of Palmarola, terrace edge at - 90 m) probably due to different rate of uplift along the archipelago. Post glacial deposits (formed from the last 18.000 years) are instead poor and discontinuous due to the distance from the provenance area, to the high hydrodynamic conditions and low sedimentation rate; at east of Palmarola a terrace with an edge about 20 m is found, which can probably be related to present depositional processes. Terraces referred to previous glacio-eustatic are rare and occur only in the area of external platform and edge, where in some cases it is possible to observe several terraces at different levels.

### 3.2.4 The Quaternary volcanism

The Pontine archipelago is formed by five volcanic islands: the western group is formed by Ponza, Zannone and Palmarola islands, and they represent an emergent part of the Tyrrhenian continental shelf; the eastern group, Ventotene and Santo Stefano, instead were emplaced in a sedimentary basin on the continental shelf.

Several works investigated the nature and timing of the volcanism in the area: Barberi et al. (1967), De Rita et al. (1986, 2001), Conte and Savelli (1994), Scutter et al. (1998) Conte and Dolfi (2002), Cadeaux et al. (2005), Fedele et al. (2003), Bellucci et al. (1997), among the others.

According to all these studies, the western islands developed during two main volcanic cycles that produced submarine and subaerial acidic products. In particular, at Ponza island the older unit occurs in the northern and central part of the island; it is composed by dikes and hyaloclastites of submarine origin, variable in composition from rhyolite to rhyodacite. In the northernmost part of the island this unit was affected by an extensive hydrothermal alteration event, which caused deep kaolinitization and the formation of bentonite deposits.

Several works concerned the genetic interpretation of the rhyolite dykes and hyaloclastites: in Barberi et al. (1967) and Scutter et al. (1998) the hyaloclastite is supposed to be the quenched facies of an extensive lava flows, later cut by dykes during and after emplacement. On the contrary Carmassi et al. (1983) and De Rita et al. (1986), do not consider the emplacement of the dykes and the surrounding hyaloclastites in two different times, but as different aspects of the same emplacement process; they suggested that dykes where emplaced when the outer layers of hyaloclastites became thick enough to protect the melt from direct contact with sea water. De Rita et al. (2001), refine the interpretation of these deposits as feeder dyke-hyaloclastite complexes (Fig. 3.11). According to these authors, hyaloclastite and dikes are contemporaneous and locally grade from one to another; they are explained by the presence at Ponza of three lava domes coinciding with Mt. Pagliaro, Cala dell'Acqua and Cala Fontana localities, all align along a NE trend. The lava of the domes was emplaced in pulses which, when lava was extruded onto the seafloor, produce a thick carapace of fragmented hyaloclastite; further pulses of magma intrusion produce the concentric fractures and faults observed on the island. Dikes intruded along these fracture systems and invaded previously emplaced hyaloclastite. The annular arrangement of the deformation is related to the local stress pattern, due to a combination of gravity and stresses produced by rising magma; the influence of the regional tectonic stress field can be identified at a greater scale, with NE alignment of the domes parallel to one of the regional extensional fault system characteristic of the area.

The final phase of volcanic activity at Ponza occurred entirely in a subaerial environment and is composed by trachytic deposits occurring in the southern part of the island and forming pyroclastic sequences, local scoria cones and lava flows in the Mt. La Guardia area; an erosional surface, overlain by marine terrace deposits, divides the pyroclastic sequence.

Also Palmarola island is composed by rhyolitic products; they were emplaced during two different phases: the first one produced a large hyaloclastite unit formed by juvenile blocks, which mainly crops out in the southern end of Palmarola. The second volcanic phase is characterized by the extrusion of rhyolitic domes into the hyaloclastites at the center and the northern part of the island (Vezzoli, 1999).

The volcanic products of Zannone can be correlated to the oldest episode of Ponza; they derive from a single eruptive cycle linked to a center located northwest from the actual island. According to De Rita et al. (1986), the beginning of the activity is marked by an explosion

breccia; this deposit is covered by a pyroclastic surge and an overlying sequence of alternating pyroclastic and lava flows.

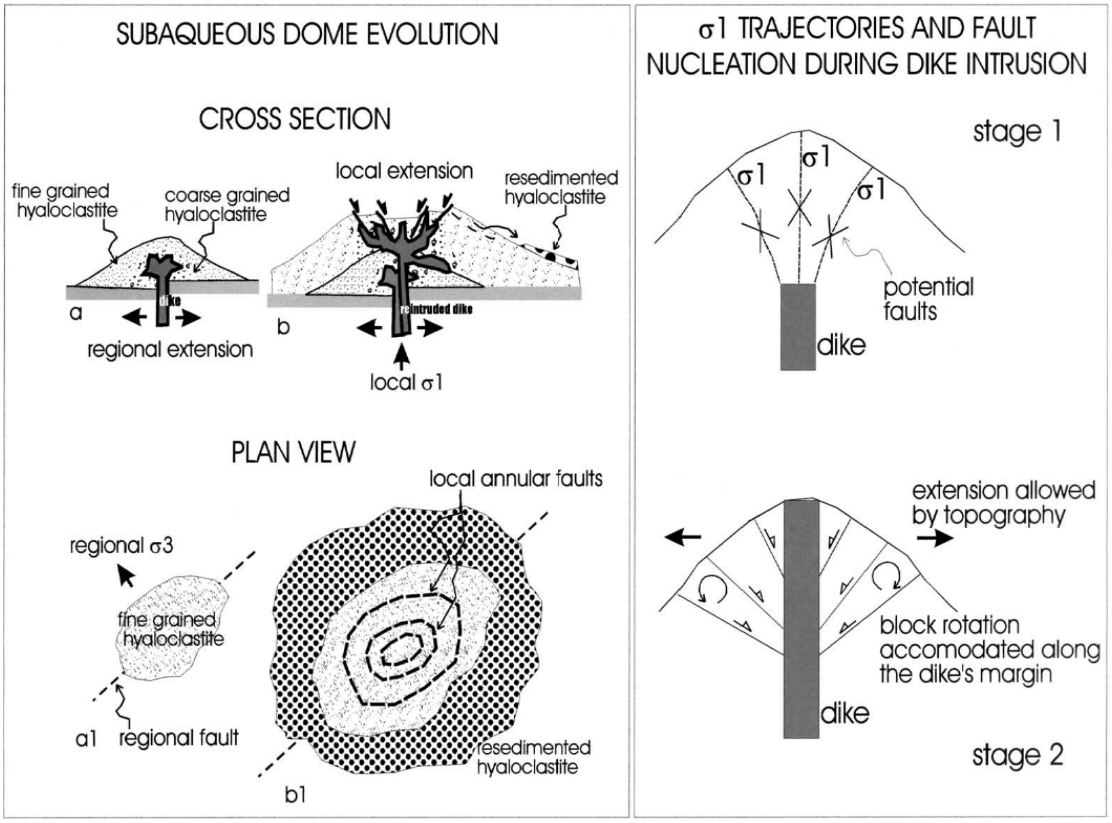


Fig. 3.11– Model for the emplacement of submarine domes (De Rita et al., 2001).

Ventotene and Santo Stefano represent the subaerial portion of a large submerged strato-volcano emplaced at the centre of the Ventotene basin and rising about 700 m from the sea bottom; they are composed of basaltic to trachytic effusive and pyroclastic products (Metrich et al., 1988). The same authors identified a possible caldera collapse, 2-3 km off the western coast of Ventotene, where it is supposed the eruptive center was located. De Vivo et al. (1995) indicate that the volcanic products were deposited through a number of eruptions that formed different units; starting at the bottom there is: a basal complex of lavas and associated cones of scoriae; fall and surge deposits and interbedded palaeosoils; the Parata Grande Ignimbrite; finally, aeolian deposits.

Volcanism took place in this area during late Pliocene: according to Barberi et al. (1967) and Savelli (1984, 1987) Ponza volcanism started at 5 My; Cadeaux et al. (1995) indicated instead a starting date at 4.4 My, with the rhyolitic dykes and hyaloclastite deposit erupted in less than 500 ka. The trachytic bodies were emplaced between 1.3 and 1 My depending on the authors (Cadeaux et al., 2005; Barberi et al.,1967; Bellucci et al., 1997) and they represent the end of the activity in this portion of the Pontine archipelago. The island of Palmarola was entirely built during Early Pleistocene, with K–Ar ages ranging from 1.64 to 1.52 My,

whereas volcanism at Ventotene and Santo Stefano erupted in a time span of 0.92-0.33 My (Metrich et al., 1988).

According to Cadeaux et al. (2005), Ponza rhyolites show geochemical similarities with some of the anatectic Tuscan acidic rocks in their major and trace element compositions; however, they do not present all the mineralogical and chemical characteristics of rocks formed by crustal anatexis. Conte and Dolfi (2002) suggest that Ponza rhyolites could represent a differentiated melt derived from a mafic-intermediate calc-alkaline magma, which interacted with sialic crust during ascent. Differently from Ponza, Palmarola rhyolites do not share any geochemical and age similarities with the Tuscan anatectic acidic rocks. Actually, although only 6–8 km apart, the two islands display significantly different geochemical signatures: Cadeaux et al. (2005) claim that geochemical modeling shows that Ponza Pliocene calc-alkaline rhyolites are representative for orogenic magmas emplaced in a syn- to late-collisional context, whereas the younger Pleistocene products (Palmarola peralkaline rhyolites) represent transitional- type magmas emplaced in a late- to post- collisional context (Fig. 3.12).

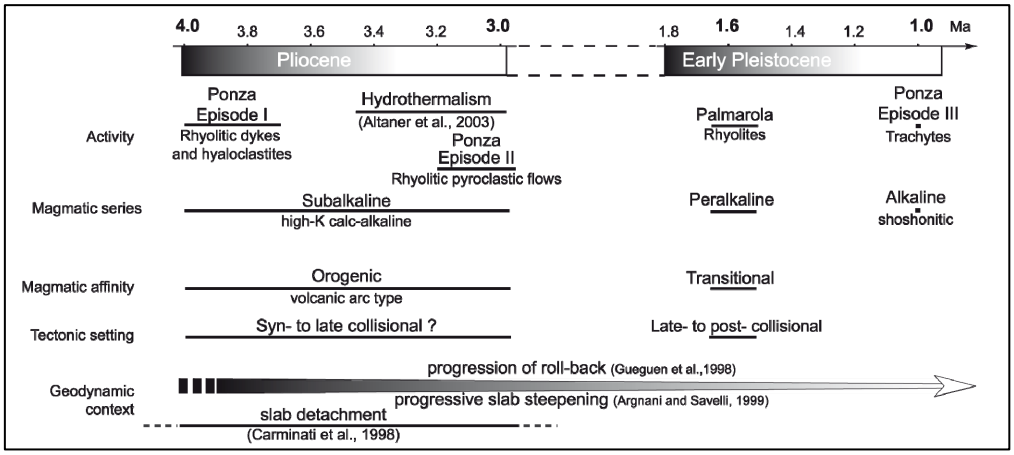


Fig. 3.12 - Comparison between the evolution of the geodynamical context of the Tyrrhenian and the chronological results for Ponza and Palmarola volcanic formations (Cadeaux et al., 2005).

The transition between these two types of magmatism has been estimated to last less than 1.3 My; according to the authors, the transition could be correlated with a change to an extensional tectonic environment or with a process of slab breakoff occurring during Pliocene.

### 3.2.5 The eastern onshore regions

In this last paragraph the focus is on the stratigraphic and structural setting of the substratum covered by the siliciclastic Plio-Quaternary succession, which extensively crops out in the onshore areas of peninsular Italy and (although to minor extent) at Zannone island.

Zannone is the only island of the Pontine archipelago where the pre-volcanic substratum crops out, made up of metamorphic and sedimentary units (Segre, 1954; De Rita et al., 1986; Pantosti & Velona, 1986, among the others). The lower unit is made by quartzite and phillites of low grade metamorphic rocks, generally assumed of Paleozoic age (Segre, 1954; Parotto, 1980). This unit is overthrusted by black clays, limestones and dolomitic limestones cropping out in the northeastern part of the island; they can be probably referred to late Triassic (Noric-Retic) age. Above the Triassic unit, an erosional surface is present, which also constitutes a fault plane. The unit overlapping the tectonic feature is made by limestones and marly limestones of pelagic environment, with planktonic foraminifera ascribed to late Cretaceous-Eocene age. At the top of this unit, terrigenous sediments, marls and sandstones are found, probably of turbiditic origin; Segre (1954) referred these deposits to Messinian age due to the presence of gypsum and gypsiferous clays; De Rita et al. (1986) instead referred the same deposits to Langhian-Serravallian age, relating the presence of gypsum to the circulation of hydrothermal fluids of volcanic origin. On top of the metamorphic and sedimentary units there is the vast volcanic cover already described, with the contact between volcanic unit and the underlying products always hidden by detrital units. Two small outcrops of marls and clays are also present along the western coast of Palmarola island; Carrara et al. (1986) refers these deposits to deep marine sediments of Pliocene age.

The geological and structural setting of Zannone was defined by several deformation events, of both ductile and brittle type (Fig. 3.13). According to De Rita et al. (1986) and Pantosti and Velona (1986), the first tectonic phase occurred in the metamorphic unit and could be connected either with Hercynian cycle or with the Alpine one. This system shows a N75°W strike. After this phase a period of subsidence and deposition of carbonatic sediments occurs. A second phase of deformation occurred probably during Miocene age and it is linked to the folding of the Triassic unit, with axes N60°E. Later, the erosive phase took place and during the late Miocene and beginning of early Pliocene the third deformation phase, with NW-SE strike, caused the overthrust of the Meso-Cenozoic unit; this phase caused mainly ductile deformations like isoclinals folds, and faults in the quartz vein. The final phases, Plio-Pleistocene in time, are clearly extensional and are testified by the brittle deformations that involve volcanic cover; the main extensional systems that have been identified are NE-SW, E-W and NW-SE striking.

These directions are the same as the regional trend of deformation visible on the continental platform, and this lead to link the recent tectonic on the island with the complex geological evolution that interested this sector of Tyrrhenian margin.

The substratum of the Plio-Quaternary sediments that form the marginal Tyrrhenian plains of the Latium and Campania region is composed by the structural and stratigraphic units that crop out in the surrounding apenninic chain. Several orogenetic phases responsible

for the formation of the southern Apennine chain (of which the Latium and Campania sector are part of) have been defined (Zitellini et al. 1984, and reference therein). A compressional activity of Aquitanian-Langhian age affected the Campania-Lucania carbonate platform and the more internal deposits of the Lagonegro basin. During the Tortonian the deformation reaches the Abruzzi-Campania platform and the Molise basin. Both phases are witnessed by E-W deformations, and the Tortonian phase is also associated with NW-SE structures. Another orogenetic activity generated NE-SW fronts during Messinian; this phase affected the external apenninic margin while distensive tectonics begins on the Tyrrhenian border. Lower Pliocene and mid Pliocene compressional deformation acts in the most external sectors of the entire chain, with a NW-SE direction. The extensional tectonic along the Tyrrhenian margin began in mid-upper Miocene along the Tuscan Apennines and continue with a large lower Pliocene phase that affected the rest of the Tyrrhenian border. The subsidence of the Campania–Latium margin started in the Pliocene northwards the Aurunci Range, in the Latium sector, and migrated southeastwards.

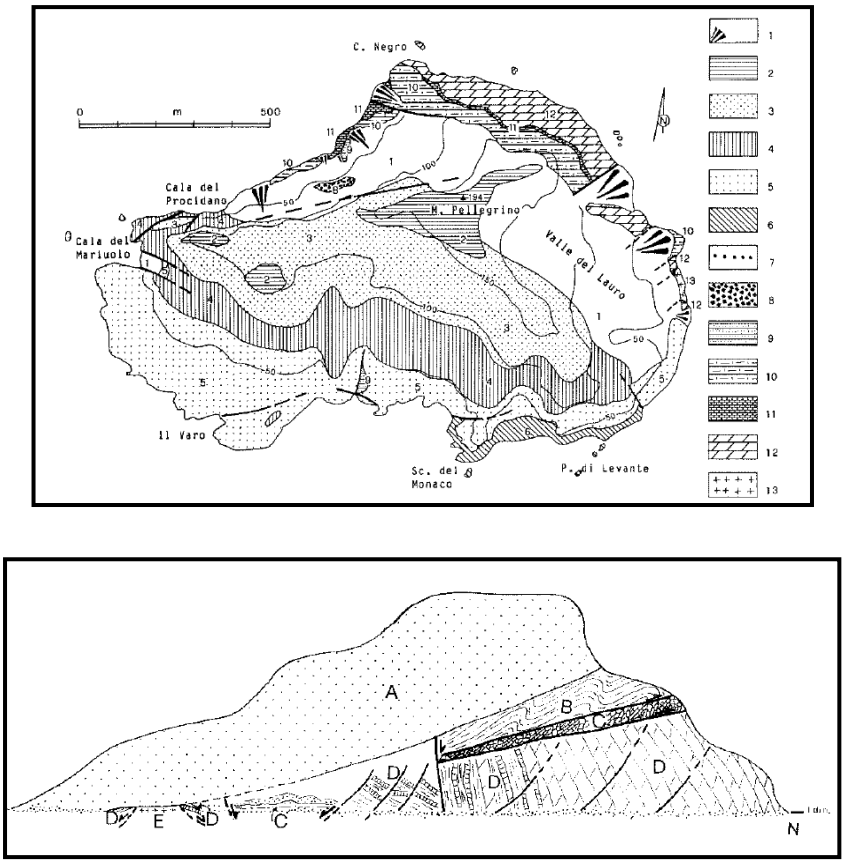


Fig. 3.13 - Geological map (up) and structural sketch of Zannone island. A volcanic units; B Flysch (Miocene); C Scaglia (upper Cretaceous-Paleocene); D dolomites (Rhetian-Norian); E Paleozoic basement (De Rita et al., 1986)

# CHAPTER 4

# Seismic Data and Processing

This thesis is based on the analysis and interpretation of several 2D multichannel seismic reflection profiles, for a total length of 1300 Km (Fig. 4.1).

The dataset investigates the area offshore the Latium and Campania Italian regions, in particularly the sector between the Anzio city and the mouth of Volturno river. It is essentially composed by two different seismic surveys (Fig. 4.1): the survey "E", which is entirely localized on the continental platform area; the survey "TIR 2010", which investigates the edge of the continental platform, the slope sector and part of the bathyal Vavilov plain. The latter are part of a recently acquired (2010) dataset and represent a new set of seismic profiles in this poorly investigated sector. Greater time during the work of this thesis was devoted to the processing and interpretation of these new lines. As it is possible to see in Fig. 4.1, in the same area are present two seismic lines belonging to the CROP seismic dataset (CROP M-29B and M-36), that have been also analyzed. Moreover, all the available and already published seismic lines, geological sections and structural maps integrate and complete the dataset. The available well data are exposed in the chapter dedicated to the seismostratigraphy analysis (Chapter 5).

In the first part of this Chapter the description of the seismic data is provided, whereas in the second part is exposed the processing of the TIR dataset, which was part of the work developed during this thesis.

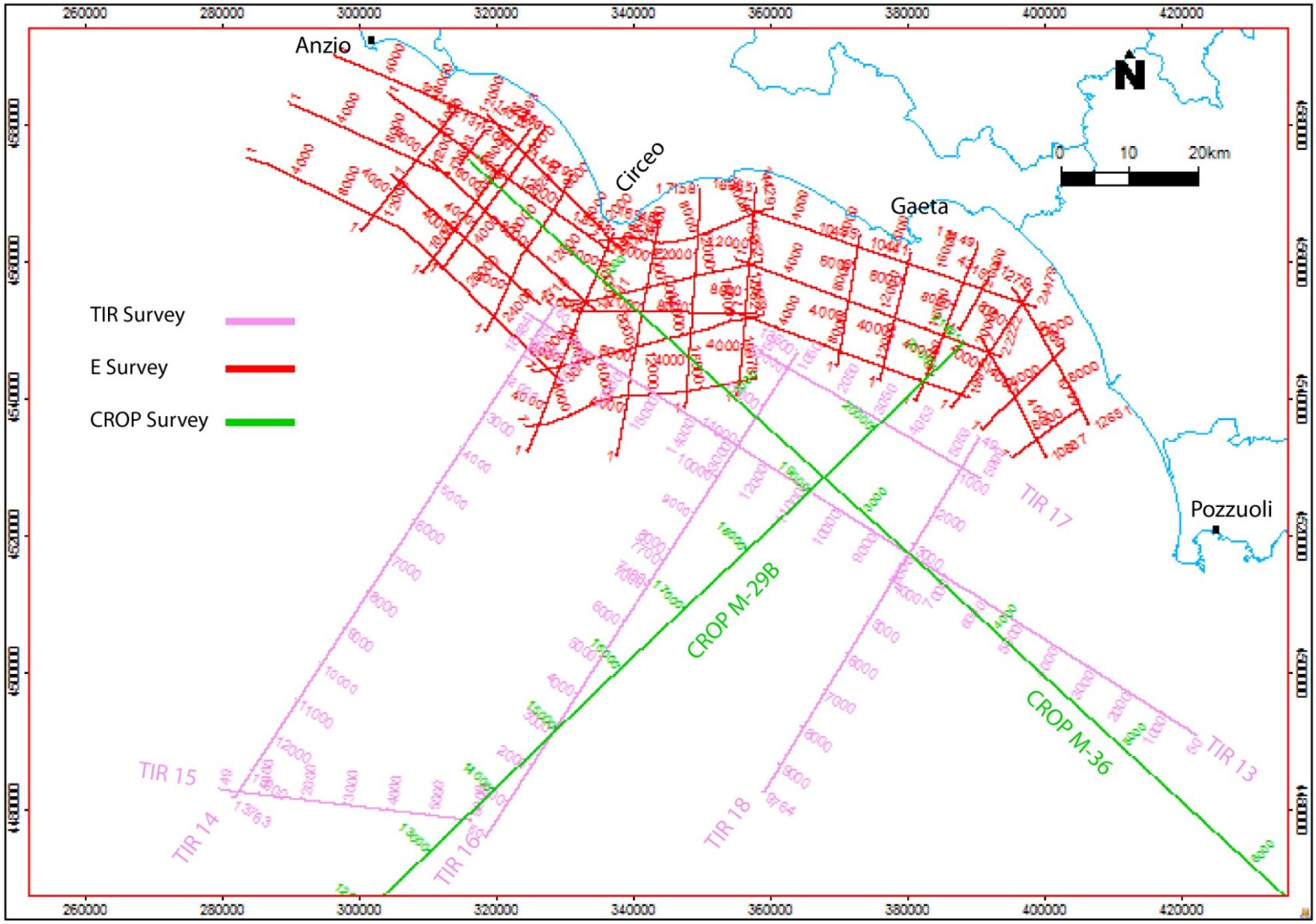


Fig. 4.1- basemap showing all the seismic lines interpreted.

## 4.1 Seismic Data

The following paragraph describes the different seismic datasets analyzed in this study which, as already pointed out, belong to different surveys; particular attention will be provided to the technical information and acquisition parameters of the TIR 2010 survey.

### 4.1.1 "E" Survey

The seismic profiles named "E" analyzed in this work are part of the so called "Reconnaissance Seismic", which is formed by several marine surveys carried on by Agip (now ENI S.p.A.) on behalf of the Italian Ministry of Industry during several years (Fig. 4.2); the campaigns interested different marine sectors (named Zone A, B, C, etc.) along the Italian coasts and this dataset is actually available online thanks to the ViDEPI Project (ww.videpi.com).

The lines considered in this thesis project were acquired in 1968 by Eni-Agip and were processed by Western Geophysical Co.; as it can be observed by the Fig. 4.2 and Fig. 4.3, they form a regular network of inlines and crosslines, which basically investigates the shallow continental platform offshore Latium and Campania regions.

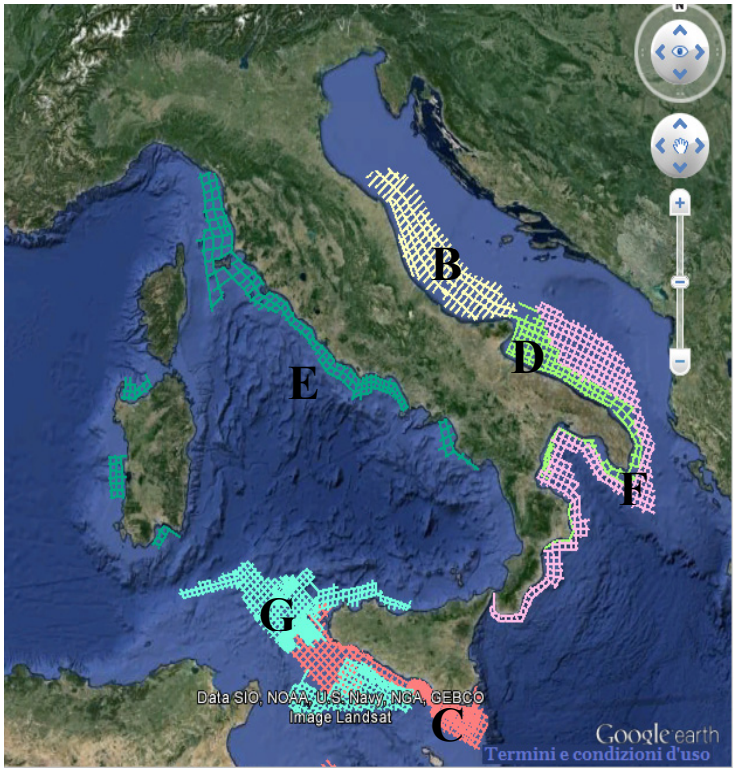


Fig. 4.2 - Reconnaissance seismic campaigns; each color correspond to a different sector (A, B, etc).

In Fig. 4.3 are displayed all the lines interpreted; they belong to the zone E, are all stacked sections, generally between 4 - 5 (twt) seconds deep. They were acquired using an aquapulse energy source and with a cable 1600 m long; the raster files (.jpeg format) have been transformed in .segy files by the use of "image2segy 2.2.6", a free tool developed by the Instituto de Ciencias del Mar (Spain) for Matlab software, in order to be able to import all the dataset into the interpretation software (Petrel).

Despite of their low resolution compared with the newly acquired data, their integration in the seismic dataset allowed a better interpretation particularly on the shelf area, and put some constraints for the new seismic profiles.

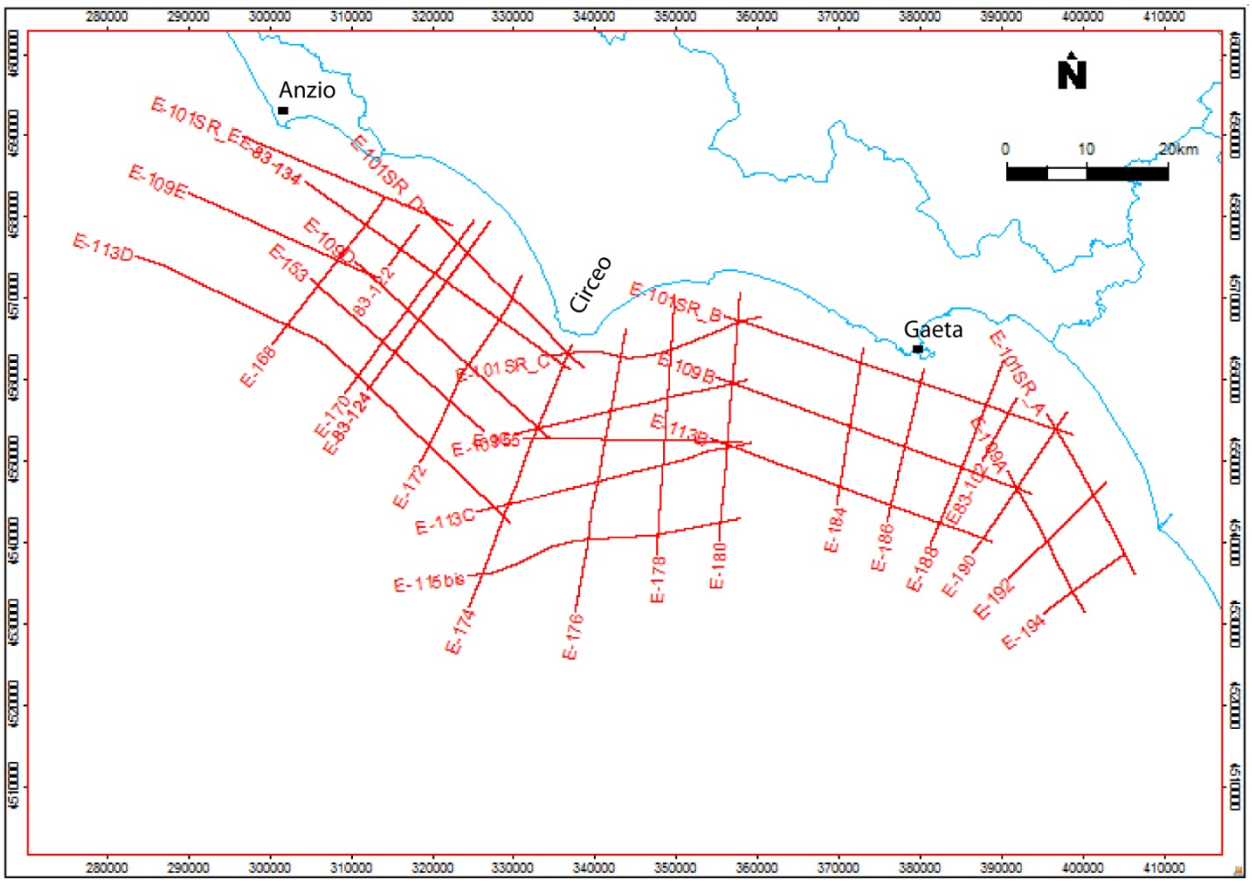


Fig. 4.3 - The Survey E in detail.

### 4.1.2 TIR 2010 Survey

The new multichannel reflection seismic data were acquired in the Tyrrhenian Sea in October 2010, during the oceanographic cruise named TIR 2010 (Fig. 4.4), funded by CNR of Italy (cruise report available at http://www.ismar.cnr.it), in the frame of the Italian CROP Project (http://www.crop.cnr.it). Main purpose of this survey was to study the tectonic setting and the geodynamic evolution of crucial areas of the continental margins of peninsular Italy and the Tyrrhenian bathyal plain.

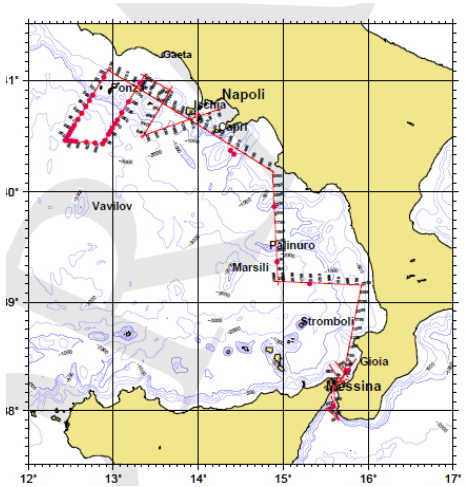


Fig. 4.4 - the R/V Urania and the complete Survey TIR 2010.

The research cruise was carried out with the 61 m R/V Urania (Fig. 4.4), owned and operated by SO.PRO.MAR. and on long-term lease to CNR. The ship is normally used for geological, geophysical and oceanographical work; it is equipped with DGPS and SEAPATH positioning system (satellite link by FUGRO), single-beam and multibeam bathymetry and integrated geophysical and oceanographical data acquisition systems, including ADCP, CHIRP SBP and other Sonar Equipment, other than water and sediment sampling. During the survey, 1006 Km of multichannel reflection seismic lines were acquired, together with 100 $km^2$ of multibeam and 1000 Km of SBP.

The seismic source used was a tuned array of three SERCEL's GI-GUN, configured in harmonic mode (60+60 in3, 60+60 in3, 45+45 in3), with an operative pressure of 2000 psi (140 bar) and towed at 5 m. The cable used in the acquisition was a SERCEL digital streamer, 1225 m long, composed by 97 channels with a group interval of 12.5 m, towed at 4-7 m depth. There were two channel units: a shorter one, composed of one channel group, and lying behind the source, devoted to acquire auxiliary data, such as the signature; a longer one, for seismic data recording, composed by 96 channels. The recording trace length was 12 seconds, shot interval 37.5 m and the seismic sampling rate 0.5 ms.

The TIR 2010 survey is composed by 20 lines; in this thesis, focused on the Latium-Campania margin, lines from TIR-13 to TIR-18 (Fig. 4.5) were processed and interpreted, for a total length of 350 kilometers. Three lines have a NW-SE orientation (parallel to the Italian coast), the others are perpendicular (NE-SW); they investigate part of the continental platform, the continental slope and part of the bathyal Tyrrhenian plain up to 3500 m of depth.

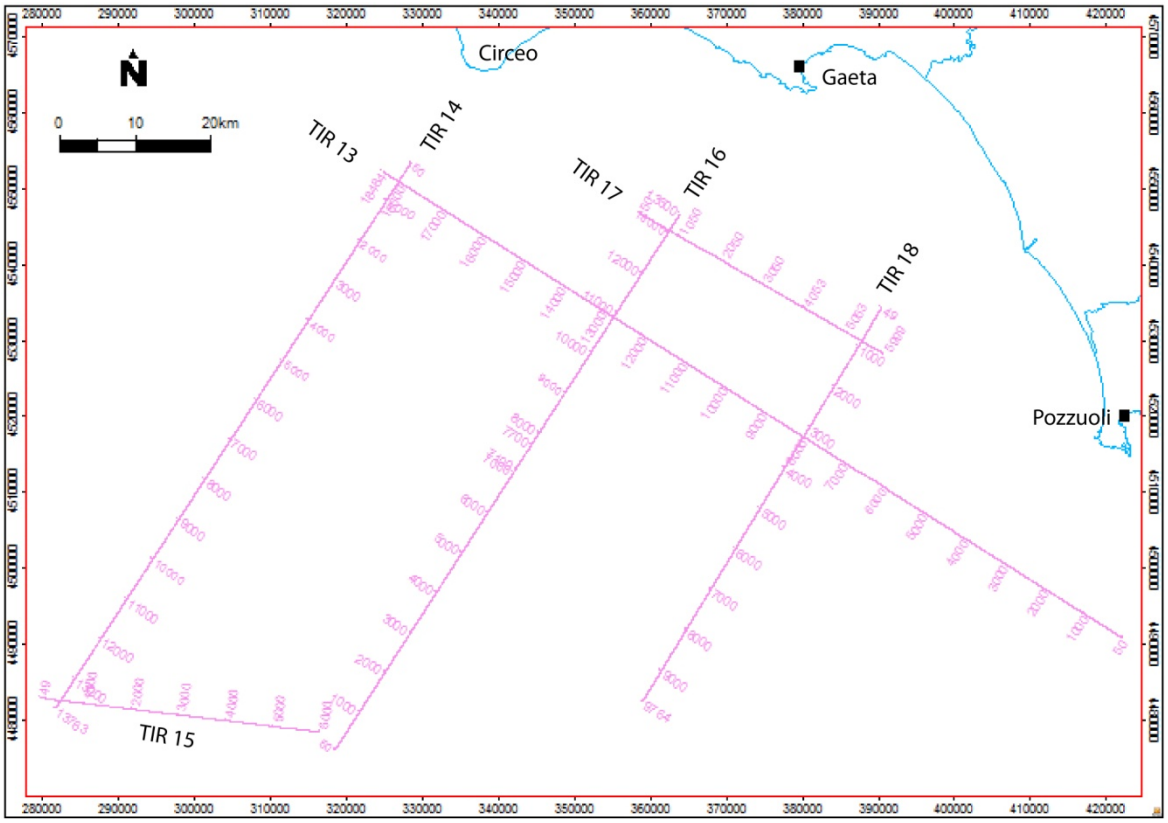


Fig. 4.5 - Survey TIR 2010 in detail.

### 4.1.3 CROP data

Two lines belonging to the CROP project (Fig. 4.6) have been also analyzed in this thesis, as they are localized in the area object of the study. CROP project (Progetto CROsta Profonda, deep Crust project) was a multidisciplinary research project devoted to the study of the Italian lithosphere; it was a cooperation between CNR, ENI (AGIP Division) and ENEL.

Deep reflection seismic profiles were acquired (from about 1989 to 1999), processed and interpreted, both on land (about 1250 Km) and at sea (about 8700 Km). Acquisition and processing were performed mainly by OGS; for the marine lines, recording time is between 17 and 30 seconds, source was an airgun, streamer length was 2000 or 3500 m and number of channels 120 or 180, according to the different cases.

In this work, CROP lines M-29B and M-36 are taken into account (Fig. 4.6, green lines), only in their part in which investigate the study area.

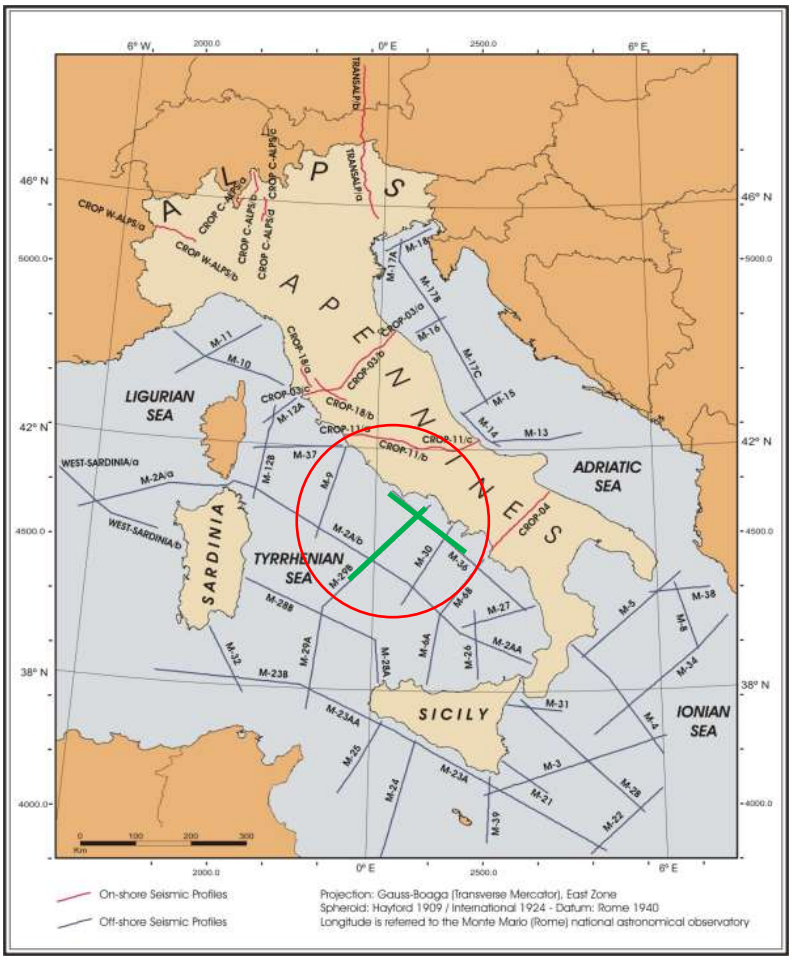


Fig. 4.6 - The CROP survey and in detail the two lines interpreted in this work: M-36 (NW-SE) and M-29B (NE-SW).

## 4.2 Seismic Data Processing

The following part of the chapter describes some theoretical aspects of signal processing (Yilmaz, 2000 is the reference text) and the processing steps applied to the seismic raw data. Data processing consists in a sequence of operations aimed to enhance the signal/noise ratio and to display the results in the form of a seismic section, in order to obtain geological information from it.

The software package "2D Promax" (Hulliburton) was used for the basic processing procedures, aimed at generating post-stack time migrated sections ready for interpretation. A total of six seismic profiles from the TIR 2010 dataset (Pontine Islands sector, Fig. 4.5) were analyzed; a simplified overview of the main processing steps is illustrated in the flowchart in Fig. 4.7.

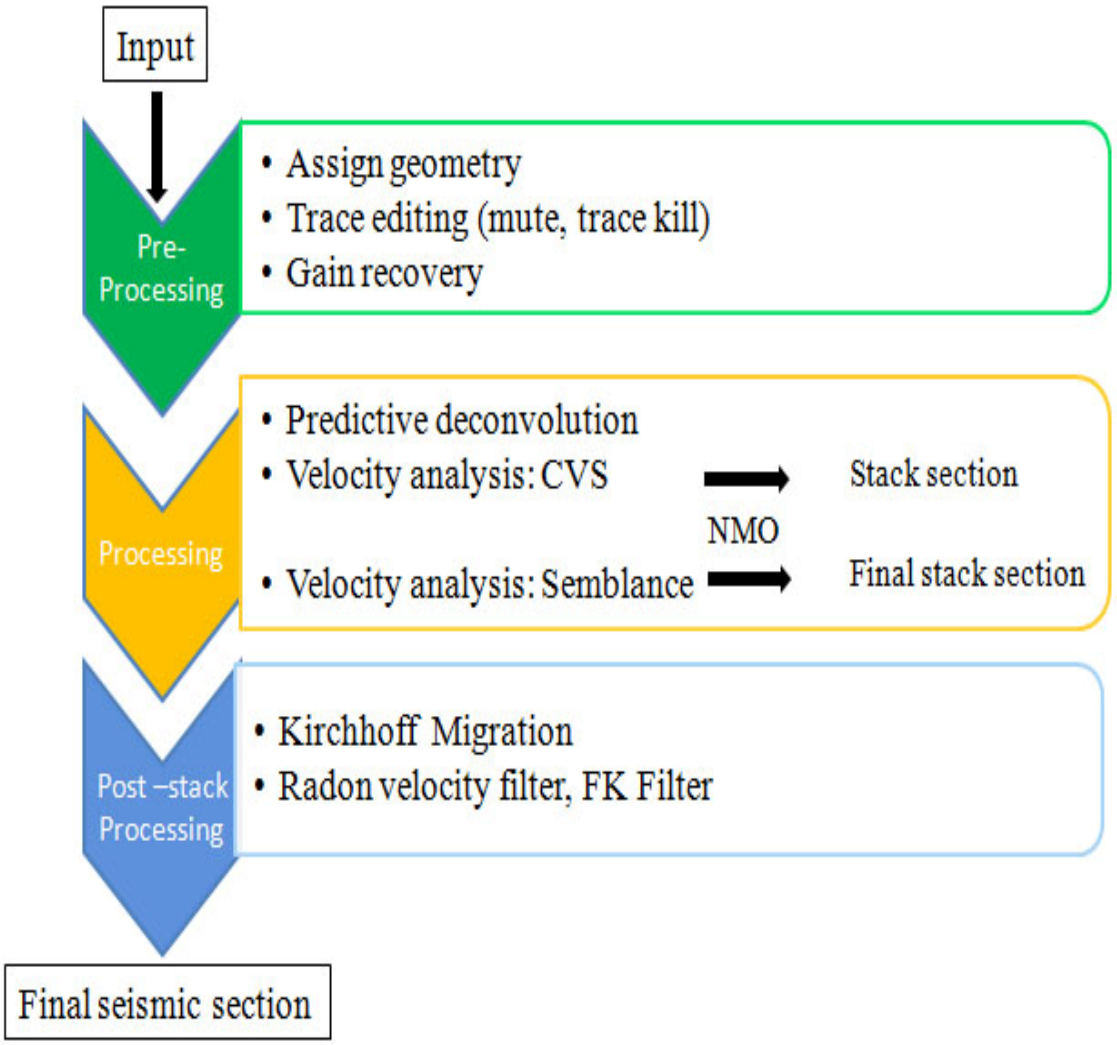


Fig. 4.7 - Flowchart schematically showing the sequence processing applied.

### 4.2.1 Input

Seismic raw data recorded in the field are in SEG-D format, which is a common format for the oil industry; Promax is able to read this kind of data, so no reformatting was needed.

The trace length was reduce from the original 12 seconds recorded in the field to 6 seconds, since the bottom half of the traces contain very little information due to the relatively weak source; furthermore, by reducing the trace length, the volume of data is reduced, so a speed up of later processing sequence is obtained.

Examining the shot gathers, it is evident that they are contaminated by a strong bias effect which means that the mean value of all the traces is not zero. This is likely caused by the very open low-cut acquisition filter in the seismic channels (3Hz/6dB/oct-800Hz/170dB), which allows low frequencies in. In order to eliminate bias effect, the trace DC removal was applied: it removes the DC (or zero frequency) component of the seismic data. This is done by subtracting the average value, called the DC bias, from each seismic trace. It produces a zero-mean seismic trace, but does not affect the frequency content. The program has two possible ways to calculate the level of the DC component in the trace: "(Min+Max)/2" uses the mean of the minimum and maximum sample as the central value to determine DC level; "Mean" uses the arithmetic mean of the samples as the central value. The latter is the more usual approach and the one that was applied to TIR data, and should be zero on a trace with no bias.

The next step was to apply a band pass filter, in order to suppress the strong swell noise affecting the data and the high frequency noise due to cables or machines; a single (i.e. it is applied to all traces at all times) Butterworth filter with minimum phase was designed, with limits having values of 8Hz/18db/160Hz/36db.

A near-trace section was generated by using the nearest trace of each shot gather, to have a first feeling of the seismic profile (Fig. 4.8).

## TIR 17 line

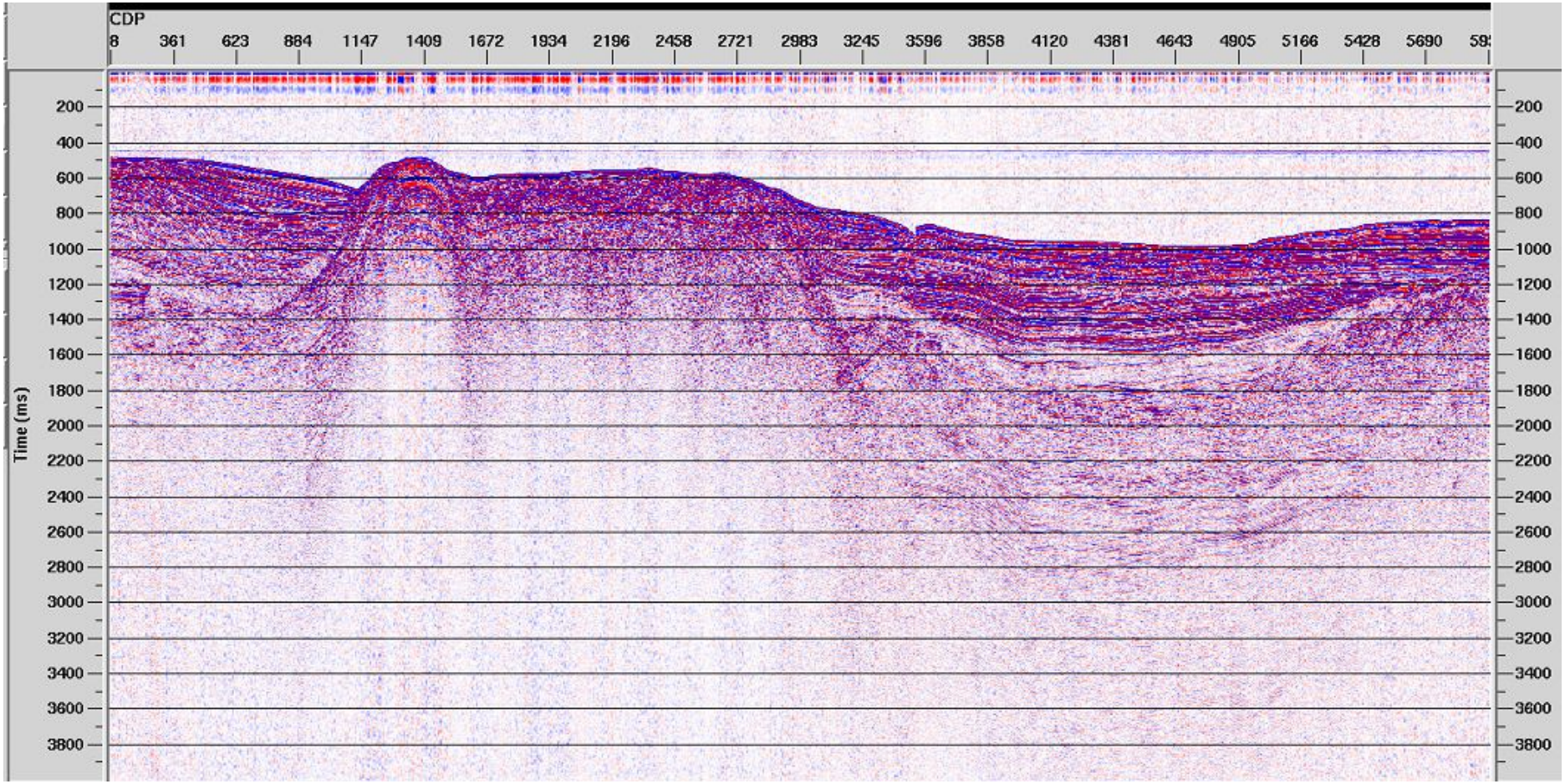


Fig.4.8 - First trace mini section of line TIR 17.

### 4.2.2. Geometry

An accurate information about the acquisition geometry is essential for the processing of multichannel seismic data; seismic data acquisition with multifold coverage is acquired in shot- receiver coordinates, but data can be sorted in different gathers, i.e. Shot Gathers, Common Receiver Gathers, Common Midpoint Gathers (CMP), Common Offset Gathers (Fig. 4.9).

Because seismic data processing is conventionally performed in midpoint-offset coordinates, field geometry information (e.g. location of shots and receivers, shot interval, receiver group interval, trace number, cable geometry, etc., Fig. 4.10) have to be assigned to the dataset in order to sort data into CMP gathers. Some information is imported from SEG-D recorded on the field; other information is merged into the seismic header from an external file. In ProMAX the "Marine Spreadsheet" is used as an editor to add values and automatically enter the information into the database and then the "Inline Geometry Header Load" loads the geometry information from the database to the trace headers of the ProMAX dataset. As in this case the relevant GPS data for receivers were missing, nominal geometries were used, assuming a regular and uniform shot and receiver spacing and a straight cable just behind the source. Nominal CMP and station numbers were computed using regularly incrementing values and all sources and all detectors must be spaced by the exact multiples of the CMP group interval.

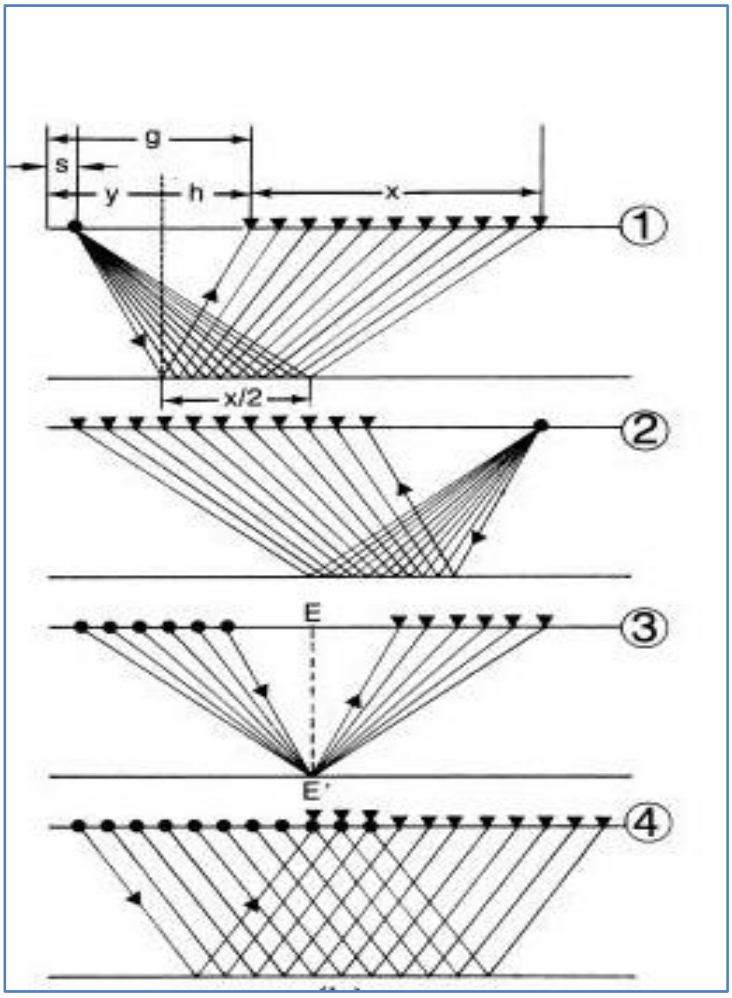


Fig. 4.9 - Different trace gathers (Yilmaz 2001)

1. Common Shot gather
2. Common receiver gather
3. Common CDP gather
4. Common offset gather

s shot coordinate
g receiver coordinate
h (half) offset
y midpoint

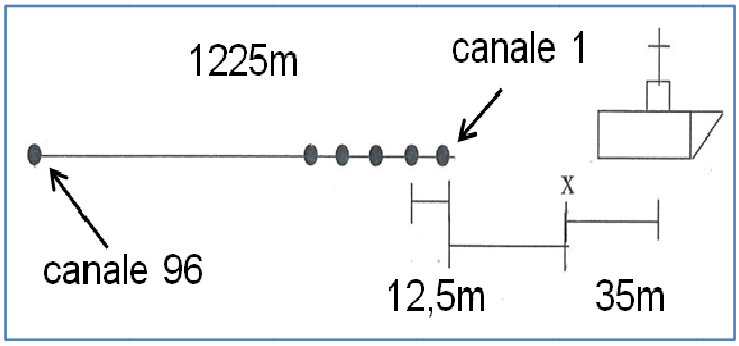


Fig. 4.10 - Part of the field geometry information needed to assign correct geometry to trace headers.

### 4.2.3 Trace editing

In this step the data were checked for quality control: in Fig. 4.11 two shot-gather records are shown; it can be observed:

- Different types of arrivals such as direct arrivals, refracted events and reflected events.
- Different types of noise e.g. multiples, noisy traces.
- The amplitude attenuation at larger travel times due to spherical spreading, transmission losses and internal friction.

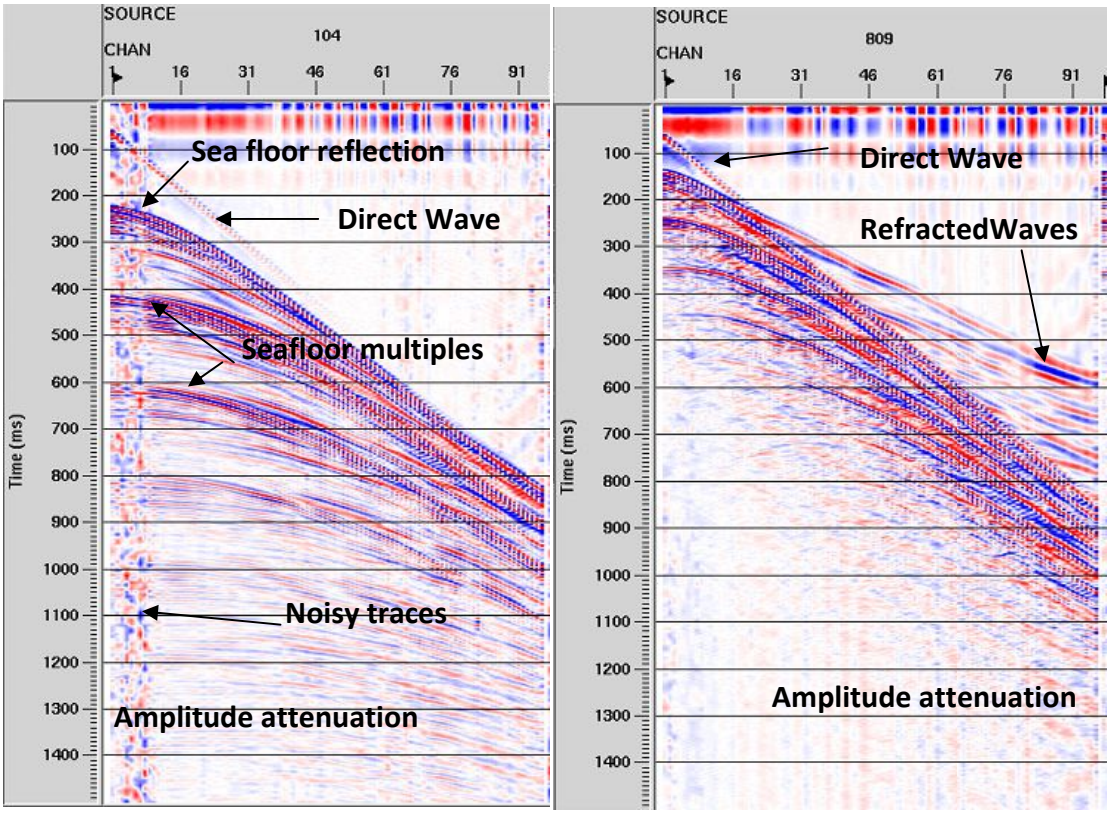


Fig. 4.11 -Two selected shot records showing different arrivals, noise and amplitude attenuation with depth.

Editing involves the removal of traces that are either dead (all samples are zero) or contains too much noise, due for example to technical problems; they are removed as early as possible in the processing sequence and usually replaced with interpolated traces or set to zero. In Fig. 4.12 (top) the trace kill processed is shown; to remove noise above the first arrival and direct waves or refracted arrivals which travel faster than the sea bottom reflection, a top mute was applied (Fig. 4.12, bottom).

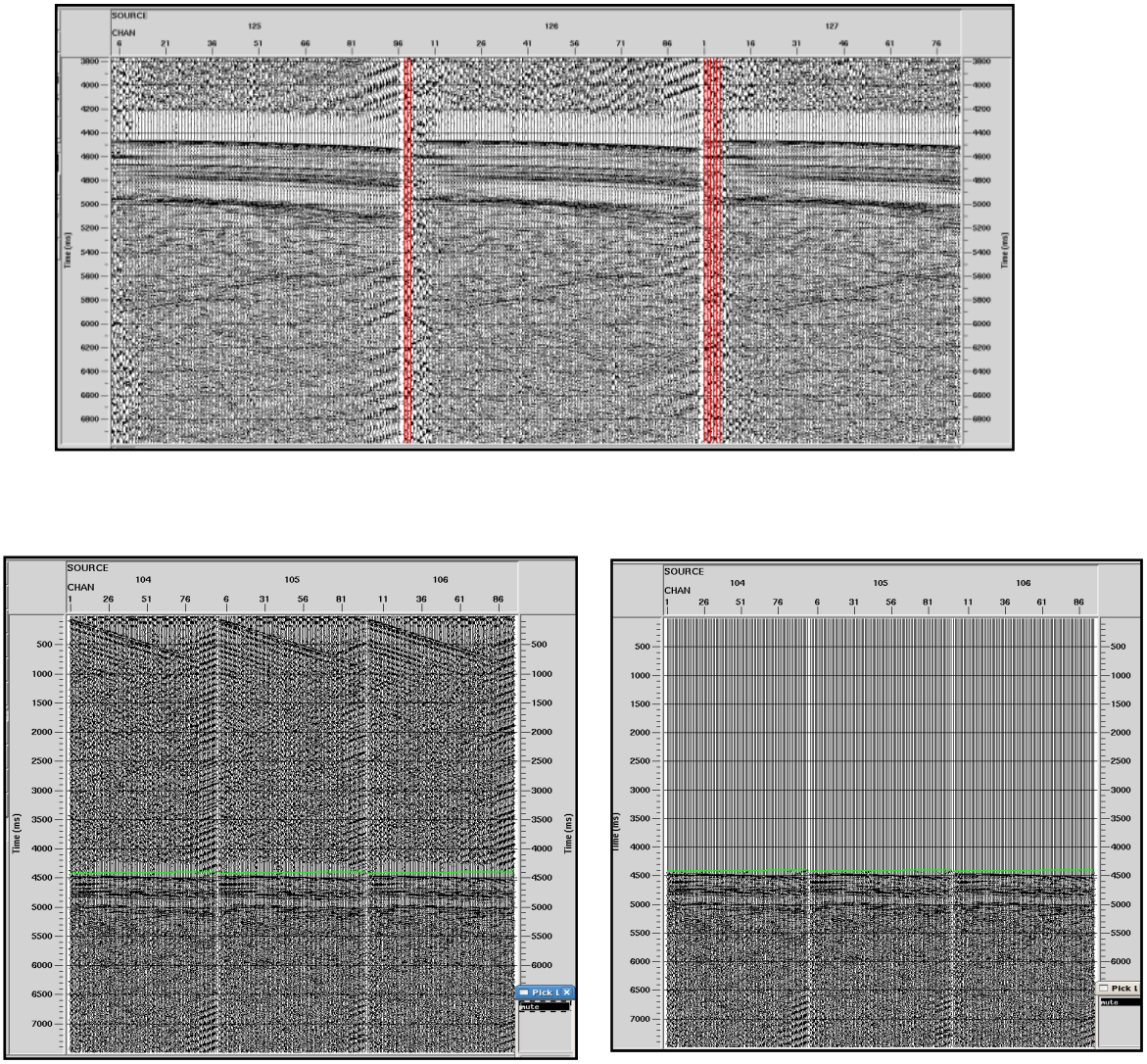


Fig. 4.12 - Top, trace kill operation; bottom, top mute applied.

In order to solve the problem of amplitude attenuation at larger travel times (greater depths), the "true amplitude recovery" was applied. As the seismic wave propagates deeper into the earth, the wavefront covers a larger area: this spreading causes a loss in energy. Given r, the radius of the wavefront, E the energy, from the equation 1 (Eq. 1) it can be seen that the energy decreases as $r^{-2}$ when distance increase, due to this phenomenon called geometrical spreading.

$$\frac{E}{4\pi r^2} \quad \text{Eq. 1}$$

The amplitude is proportional to the square of the energy so it decreases with $r^{-1}$; in addition, the wave is attenuate due to scattering and absorption phenomena. For all these reasons a gain recovery function has to be applied. Amplitude can be enhanced also by applying Automatic Gain Control (AGC); in this case an operator length of 500 ms was used **(**Fig. 4.13).

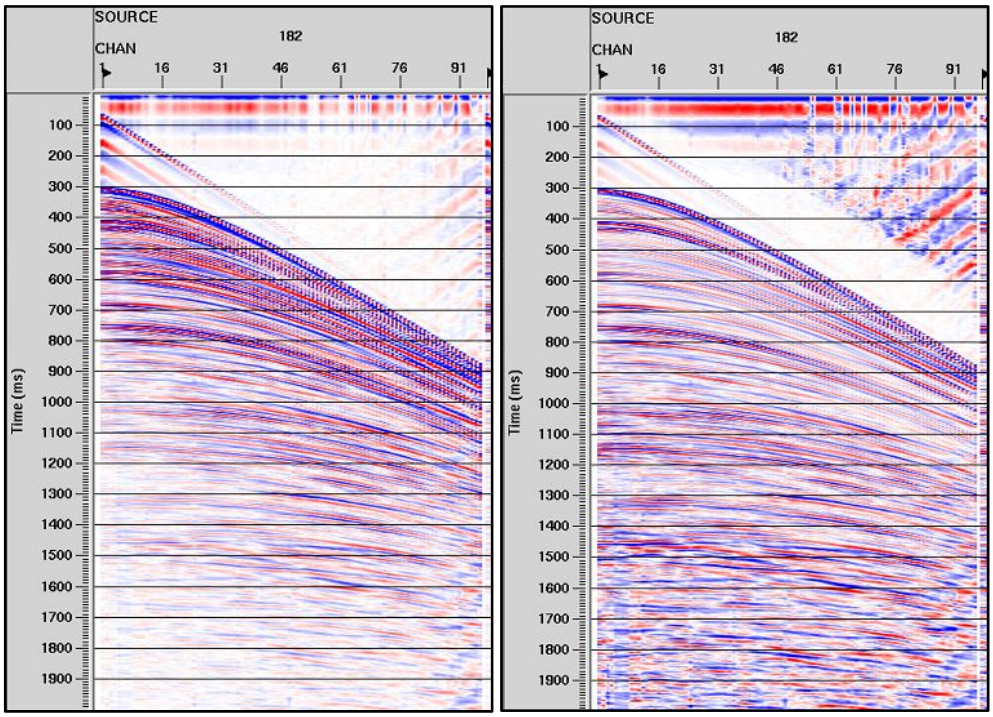


Fig. 4.13 - On the left, shot gather with no AGC applied; on the right, the same shot with AGC applied.

### 4.2.4 Deconvolution

Deconvolution is applied to seismic data in order to improve the temporal resolution of seismic traces and to remove or attenuate multiples and reverberations.

In the convolution model (Fig. 4.14) the recorded seismic trace x(t) is in general the result of the convolved source wavelet w(t) with the earth impulse response (reflectivity) e(t) and additional ambient noise n(t) (* denotes convolution):

$$x(t) = w(t) * e(t) + n(t) \quad \text{Eq. 2}$$

Deconvolution is then the inverse process which tries to recover the reflectivity series (the impulse response e(t)) from the recorded seismogram x(t); in Eq. 2, only x(t), the recorded seismogram is known, whereas w(t), e(t) and n(t) are unknowns: therefore is necessary to do several assumptions to solve the problem. These assumptions are:

1. Earth is made up of horizontal layers of constant velocity.
2. The source generates a compressional plane wave that reflects on layer boundaries at normal incidence, so no shear waves are considered.
3. The source wave is stationary; it does not change as it travels down the subsurface.
4. Noise component is zero.
5. Source waveform is known.
6. Reflectivity is a random process, which means that seismogram has autocorrelation and amplitude spectra similar with the seismic wavelet.
7. Seismic wavelet is a minimum phase and it has a minimum phase inverse.

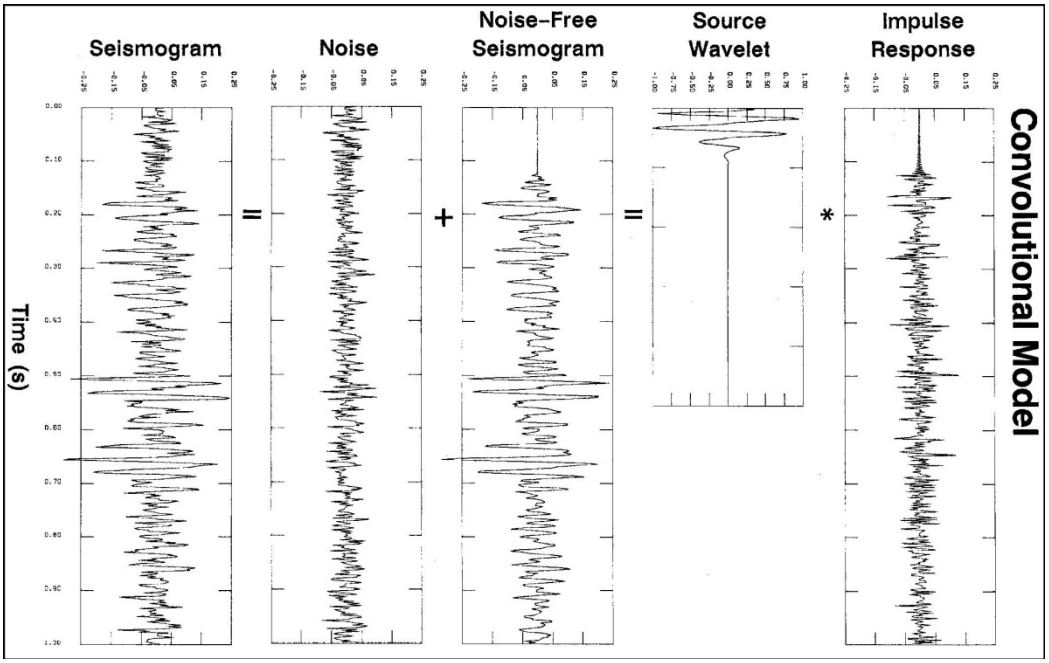


Fig. 4.14 - The convolutional model (Yilmaz, 2001).

A deconvolution operator is in fact an inverse filter (corresponding to the inverse of the seismic wavelet) and in order to apply predictive deconvolution, Wiener filters are designed; this type of deconvolution is the commonest and it tries to estimate and remove the predictable parts of a seismic trace (e.g. multiples) (Fig. 4.15 B) and can also be used to increase resolution by altering wavelet shape and amplitude spectrum (Fig. 4.15 A). Two important parameters have to be specified: the “decon operator length” which determines how much of the correlation to use; the “operator prediction distance”, which is the length of the prediction window (both parameters are expressed in ms).There are no fixed mathematical rules restricting the gap and operator length parameters, they are usually tested extensively, as in fact was done during this work; values between 12 and 25 ms were used on TIR lines for the operator prediction distance, whereas values of decon operator length were chosen between 80-160 ms, depending on the seismic lines. Time gates in which apply the decon operators must be specified, in order to include the target zone and to avoid high amplitudes and extraneous noise; commonly the seabed is omitted, as coherent noise, and first multiple. For example, for a seabed at 80 ms, designed window should start at 200 ms;

also, longer windows are usually better then shorter and windows overlaps can be selected. White noise operator (the percentage of white noise to add to the original spike response) is set at 0.1% and a bandpass filter is applied after decon with 14Hz/26db/200Hz/400db values.

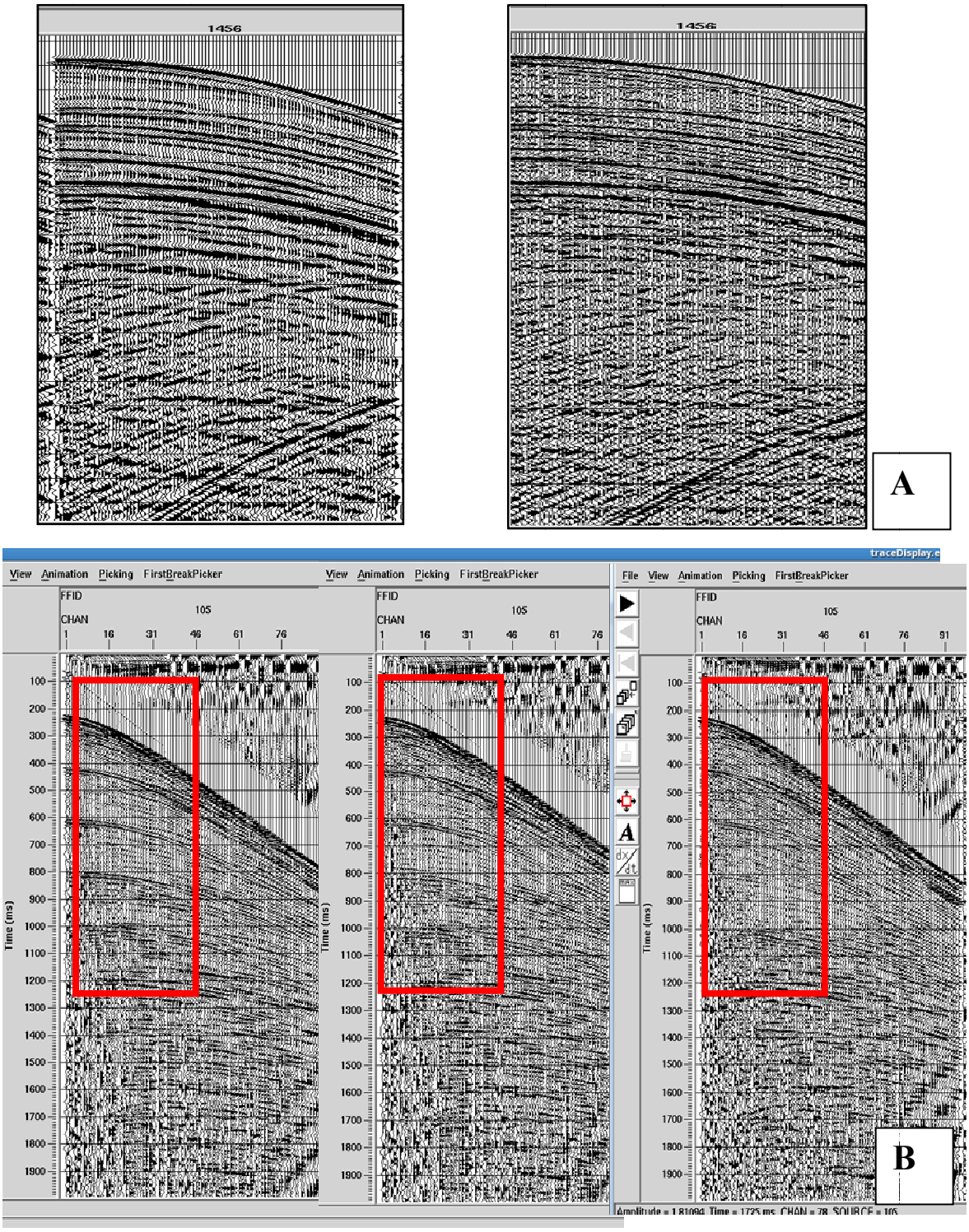


Fig. 4.15 - A) the same shot gather without (left) and with (right) deconvolution applied: an increase in temporal resolution can be notice. B) effects of deconvolution on multiple reflections: attenuation of multiple can be observed from the left figure (no deconvolution) to the central image (operator length 150 ms, prediction distance 20 ms) and to the right image (operator length 300 ms, prediction distance 15). The values chosen are 150/20 ms, which attenuate multiples without affecting also primary reflections.

### 4.2.5 CMP gathers

In this step data are sorted from common shot point to common midpoints (CMP), which are the usual coordinates to perform seismic data processing, after the several operations done on CSP gathers in order to "clean" the data. In CMP sorting the traces that sampled the same midpoint, between shot and receiver, are group together (CMP gather); this provides redundancy of information that enhances S/N ratio and also amplitude is improvement. The terms common midpoint and common depth point are often used interchangeably, but it should be notice that CMP and CDP are equivalent only if reflectors are horizontal and velocities do not vary horizontally; in the case of dipping reflectors the two gathers are not equivalent and only the term CMP gather should be used (Fig. 4.16).

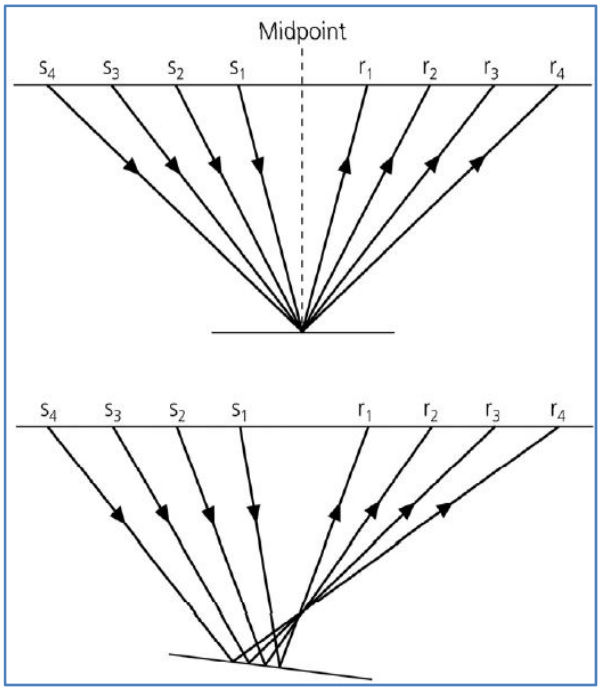


Fig. 4.16 - The difference between CMP and CDP. Stein &Wysession (2003).

### 4.2.6 Velocity analysis

Velocity analysis is one of the most important steps in seismic processing and the velocity model picked is used essentially for two important processes: the Normal Moveout (NMO, see section 4.2.7) correction and migration (see section 4.2.9).Velocity analysis is performed in CMP domain and there exist different ways to perform it; in order to obtain a progressive refinement of the velocity field, the velocity analysis was carried out on all the dataset with two different techniques, the Constant Velocity Analysis (CVS) and the Spectrum Analysis, described in this same section; first the CVS was applied and a first stacked section was obtained; later the spectral analysis was performed and a second and definitive stacked section was obtained. In the text both the velocity analysis techniques are described in this section.

In the CVS technique a portion of line (usually several CDPs) is selected from time to time, and several stacked panels are formed; each panel is formed by a range of CDPs normal moveout corrected and stacked with a range of constant velocities, which vary from the lowest to the highest velocity value expected on the basis of a first data analysis. In this case, velocities ranging from 1500 m/s to 5000 m/s were chosen; on each panel the velocity which yields the best stack response (in terms of amplitude and continuity) at a selected event time is picked (Fig. 4.17); the process is iterated at each CMP location through time

and in this way the velocity function with depth can be reconstruct. The CVS method is especially useful in areas with complex structures, as it allows the interpreter to choose directly the stack with the best continuity.

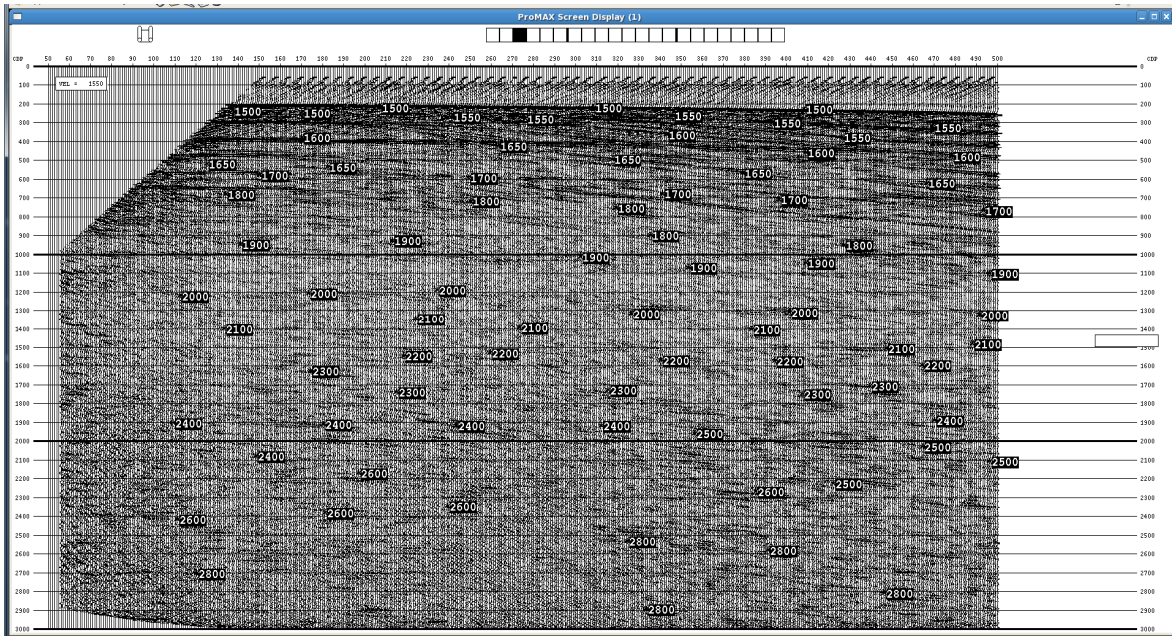


Fig. 4.17 - the picked velocities on a CVS analysis panel.

The second velocity analysis method used is the Spectrum Analysis; this technique is based on the crosscorrelation of the traces and not on the stacked continuity of the stacked events as in the CVS analysis; this method is more suitable for data with multiple reflection problem.

Also in this case the analysis are done on a selected number of CMP and then interpolated to all the other CMPs to create a laterally continuous velocity field. The aim of the velocity spectrum analysis is to obtain picks that correspond to the best coherency of the signal along an hyperbolic trajectory over the entire length of the CMP gather; there are different types of coherency that can be used in computing this process, and in this case the semblance is used, which is the normalized input-to-output energy ratio: the areas of maximum energy are associated to the velocity that better align the reflections. In Fig. 4.18 the technique is better explained: the first panel (A) is the semblance panel, which displays the stack response as a function of time and velocity in a contour plot; velocities are picked on maximum semblance peaks (red color), which have to be picked with a logical method, avoiding alias or multiples. So each pick corresponds to a time velocity pair that will be interpolated to create a continuous velocity function in time. The next Gather panel (B) displays a common offset stacked supergather of a specified number of CMPs; if the picked velocity is correct, the events on the supergather appear flat in time. This panel is used to help in the analysis procedure and for quality control the NMO. The Velocity Function Stacks panel (E) displays a series of side-by-side stacked traces for a set of CDPs. These traces are corrected for NMO with a series of different velocities and it is used to pick velocities by visually locating the maximum stacked response. In the middle there are the flip panel (D), which display the same stacked trace of E, but one panel at time: the display animates when a velocity function is picked on the A or E panels. The dynamic stack panel

(C) displays an approximation of a stack generated with the current velocity pick. This stack is an interpolation of the existing VFS panel. This panel is used as a quality control of the picked function.

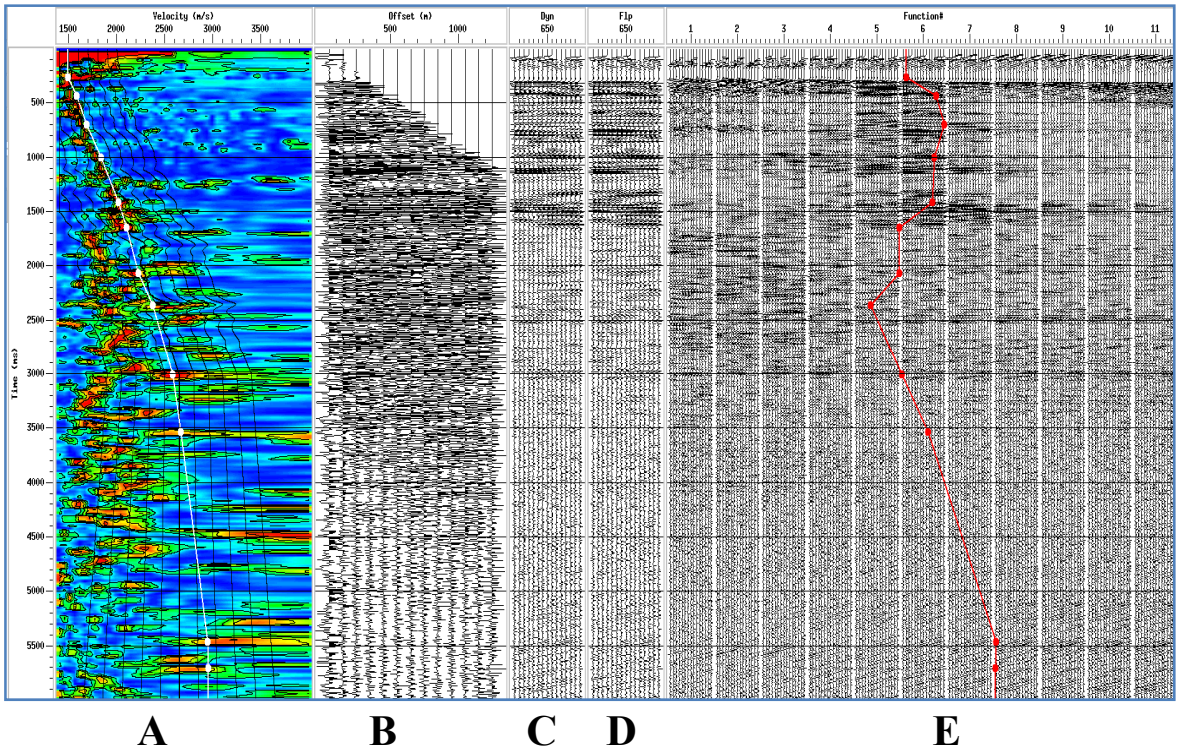


Fig. 4.18 - The panels used in Spectral velocity analysis.

This type of velocity picking is an interactive process, since in any time a velocity pair is picked, NMO correction and stack are automatically adjusted; besides, velocity spectrum not only provide a velocity function, but it can also help in discriminating between primary and multiple reflections. In Fig. 4.19 the final velocity model is display for the line TIR 17.

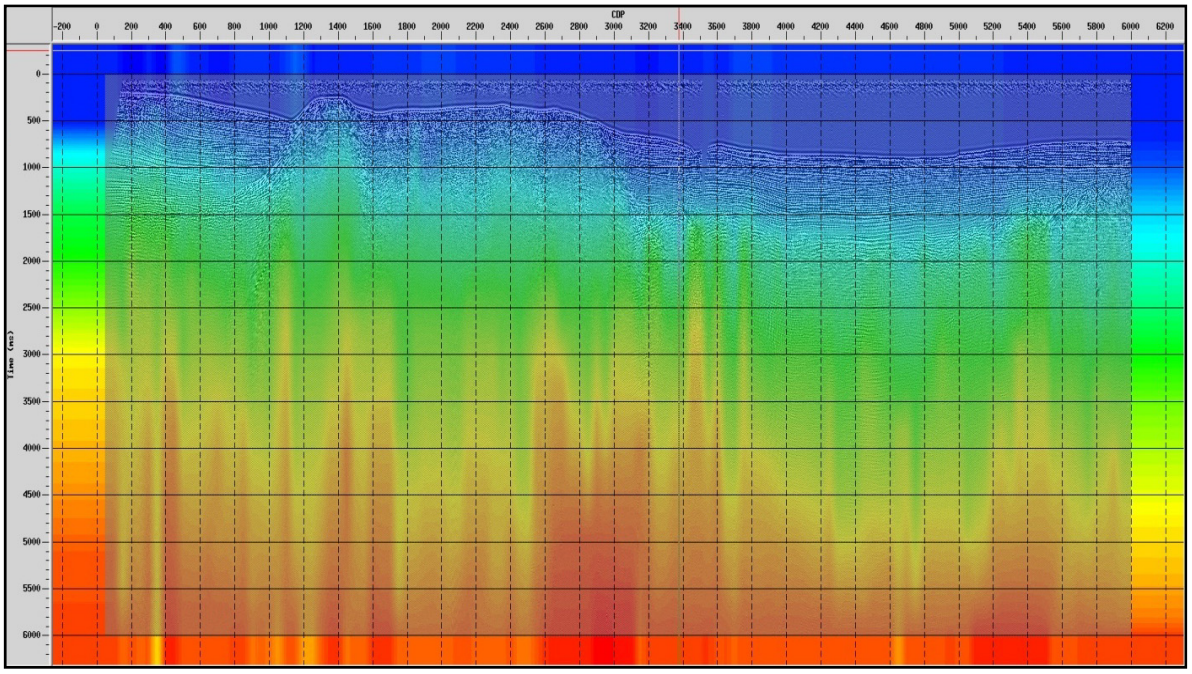


Fig. 4.19 - The final velocity model picked for TIR 17 section

### 4.2.7 Normal Moveout correction

After that velocity analysis is accomplished, Normal Moveout (NMO) corrections can be applied. The travel time curve from source to receiver for a flat reflector is a hyperbola (Fig. 4.20) described by the formula:

$$t^2 = {t_0}^2 + \frac{x^2}{v_{stack}^2} \qquad \text{Eq. 3}$$

NMO ($\Delta t$) is defined as the difference in two-way travel time t(x) for a receiver at a distance x from the source and the two-way travel time at zero offset t(x); in other words, it is the delay of the wavefront in reaching receivers at progressively more distance. Mathematically NMO is given by the formula:

$$\Delta t = t_0 - t(x) \quad with \quad t(x) = \sqrt{t_0^2 + \frac{x^2}{v_{stack}^2}} \qquad \text{Eq. 4}$$

Also in a common midpoint gather moveout is hyperbolic; when NMO-correction is applied all the two way time delays of various offset are transformed into a zero offset equivalent and all reflections are aligned (horizontal) (Fig. 4.20) and stacking can be performed. In order to have the correct alignment of the reflectors, the correct velocity in the Eq. 4 should be used, which is obtained by the velocity analysis (Section 4.2.5). If the velocity applied for correction is too high, and therefore the correction is too small, the reflection hyperbola results under corrected (Fig. 4.20 b); if velocity applied is instead too low, the correction is too large, and the hyperbola results overcorrected (Fig. 4.20 c).
In Fig. 4.21 NMO corrected CDPs are displays; the reflectors which still display an hyperbolic trend are probably multiple reflections.

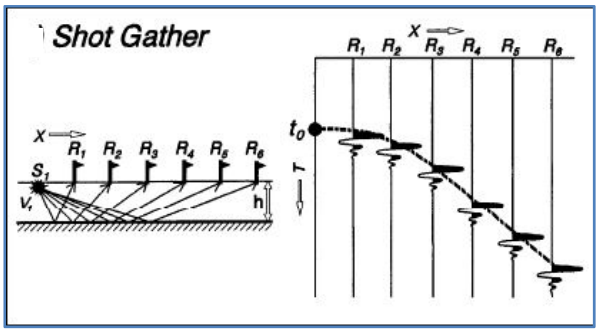


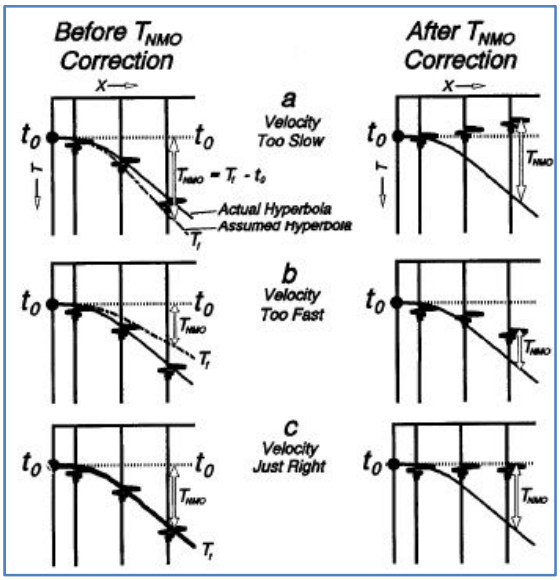


Fig. 1 - Top, the hyperbolic trend of the travel time curve from source to receiver for an horizontal reflector; right, the different cases of NMO corrections.

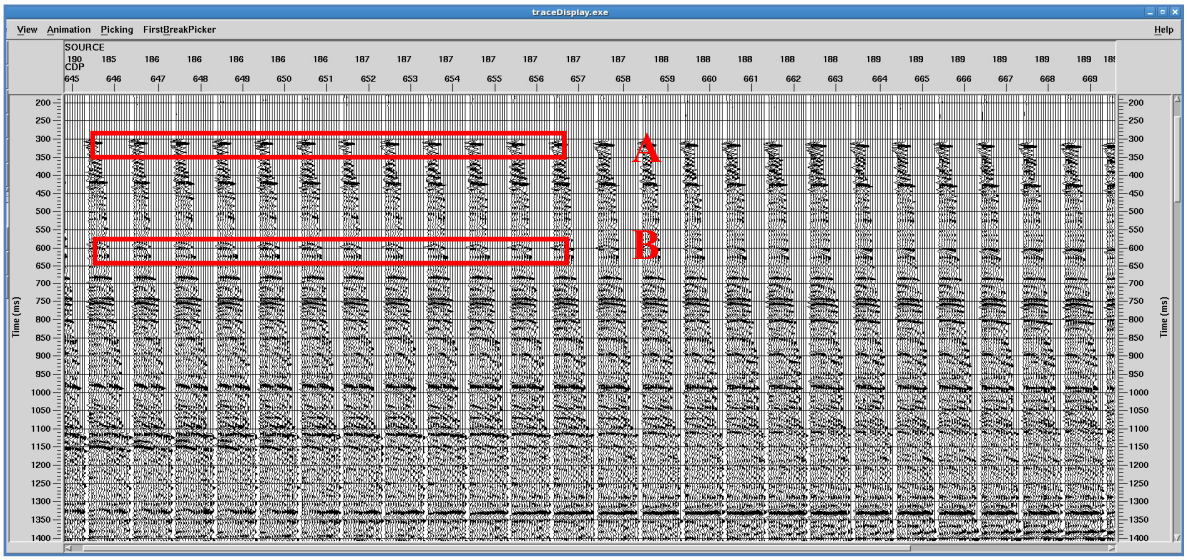


Fig. 4.21- NMO applied on CDP gathers: primary reflections result horizontal (A), hyperbolic trends should be associated to multiple reflections (B).

### 4.2.8 Stacking

The stacked section is formed by the traces that represent the sum of all the traces inside a CDP gather, NMO corrected and then summed, to get one single trace concerning the investigated depth (mid) point; stacking is a powerful tool that allows to increase the signal/noise ratio: the coherent signal will increase due to constructive interference, whereas random noise will be reduced.

Prior to stack, a stretch mute is necessary: stretching of waveforms is an artifact of the NMO application process, and it is essentially a frequency distortion in which the events are shifted to lower frequencies. This phenomenon is particularly evident at shallow times and at the far offsets and it degrades the stacked section; by means of the stretch mutes the program automatically mutes data when stretch caused by NMO correction exceeds a specified limit; in this case a 30% of stretch is allowed in the output traces after the velocity correction.

In Fig. 4.22 and 4.23 improvements can be observed from a first stacked section (A) to the second one (B).

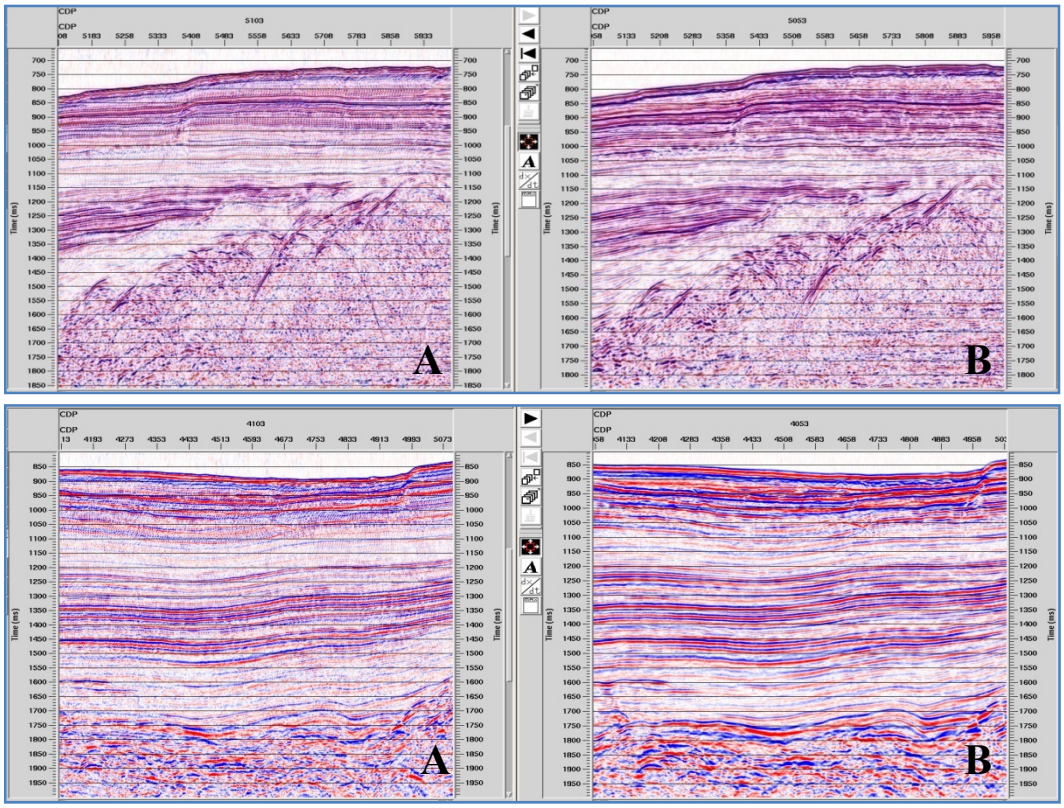


Fig. 4.22 - Different parts of TIR seismic lines showing the first stacked section (A, obtained using CVS velocities) and the final stacked section (obtained using spectral analysis velocities); improvements in horizon resolution and definition can be notice.

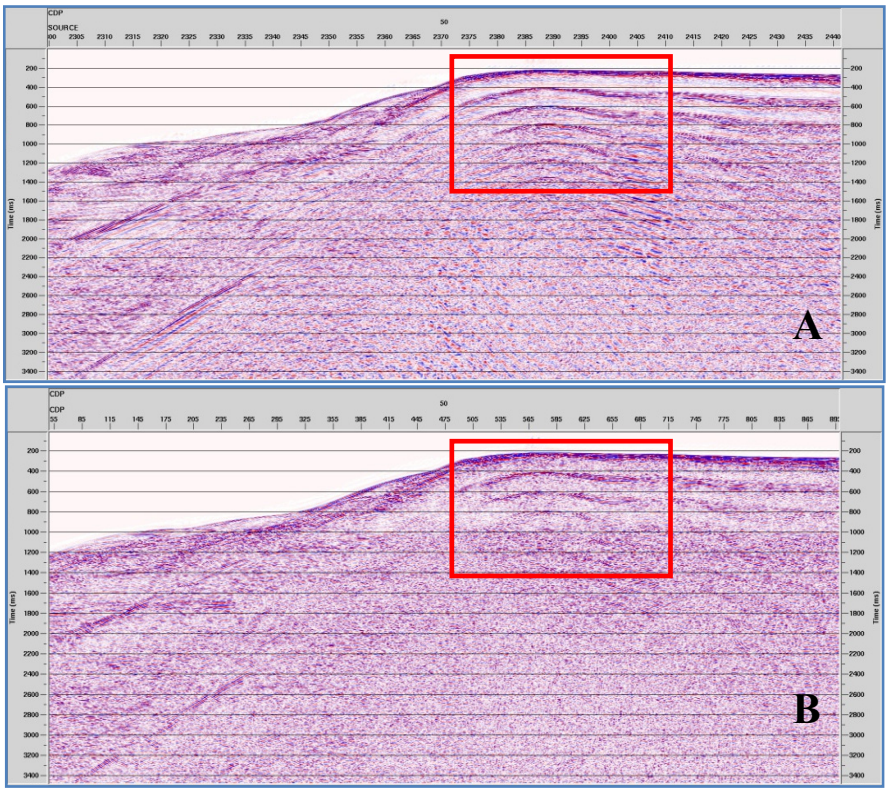


Fig. 4.23 - A and B same as Fig 4. 22. In this case the new velocity field was successful in removing multiple reflections.

### 4.2.9 Post-stack migration

Migration aims at better imaging by improving the correspondence between the stacked seismic line and the geological section in depth; this process moves dipping reflections to their original subsurface positions, collapsed diffractions and bowties and increase spatial resolution. Geometrically, migration has the effects of steepen and shorten reflectors and move them in the updip direction.

In this work, post-stack 2D (as seismic lines are 2D) time migration was applied; 2D migration assumes that the stacked seismic line does not contain energy reflected from outside the plane of recording, although in areas with complex structural setting this is not always true.

The number of existing migration algorithms is quite high; the algorithm chosen should be able to handle steep dips and lateral/vertical velocity variations with sufficient accuracy and at the same time to be cost effective. In this work different migration methods were tested extensively (Fig. 4.24): the phase shift and the Stolt migration, based on frequency-wavenumber implementation; the fast explicit FD time migration, based on the finite-difference solution; the Kirchhoff migration, based on the integral solution of the scalar wave equation.

| Migration Name | Category | Type | Velocity | V(x) | V(t/z) | Steep Dip | Run Time |
|---|---|---|---|---|---|---|---|
| Stolt 2D | F-K | Time | $V_{RMS}(x,t)$ | Poor | Poor | Fair | 0.2 |
| Phase Shift 2D | Phase Shift | Time | $V_{INT}(x,t)$ | None | Good | Good | 1.0 |
| Steep-Dip Explicit FD Time | F-D (70 deg)<br>(50 deg) | Time<br>Time | $V_{INT}(x,t)$<br>$V_{INT}(x,t)$ | Fair<br>Fair | Good<br>Good | Good<br>Fair | 21.0<br>10.0 |
| Fast Explicit FD Time | F-D | Time | $V_{INT}(x,t)$ | Fair | Good | Fair | 9.6 |
| Explicit FD Depth | F-D | Depth | $V_{INT}(x,z)$ | Good | Good | Good | 21.7 |
| Kirchhoff Depth | Kirchhoff/Im<br>Explicit<br>Mult. Arr. | Depth<br>Depth<br>Depth | $V_{INT}(x,z)$<br>$V_{INT}(x,z)$<br>$V_{INT}(x,z)$ | Fair<br>Good<br>Excel. | Good<br>Good<br>Excel. | Good<br>Good<br>Excel. | 7.3<br>12.0<br>64.0 |
| Kirchhoff Time | Kirchhoff | Time | $V_{RMS}(x,t)$ | Fair | Good | Good | 14.6 |
| Reverse-Time T-K | Reverse Time | Time | $V_{INT}(t)$ | None | Good | Good | 2.5 |

Fig. 4.24 - The different migration algorithms present in ProMAX software.

The best results were obtained by using the Kirchhoff technique; this method assumes that every point in the subsurface is a scatter point which spreads waves coming from a source point S. The wavefield collected at the earth's surface is a superposition of waves coming from every scatter point. In migration, we propagate the surface wavefield back to subsurface scatter points and collect wavefield at t = 0 to get the image of subsurface structure.

To compute the post-stack time migration, a velocity field must be supplied: this can be derived from, but is not identical, to the stacking velocity; so, the velocity field previously picked was smoothed (Fig. 4.25) and lowered of 10%. Two important parameters have to be

set in performing Kirchhoff migration: the aperture width (maximum horizontal distance that energy can move in the migration) and the maximum dip to migrate; if this latter parameter is too small, it can cause the attenuation of steeply dipping events and rapidly varying amplitude changes. On the other hand, large aperture means more computational time and degradation of the signal to noise ratio. It is important to notice that dip refers to apparent dip in diffractions and not to real dip of geological features; dip larger than the angle specified will not be migrated.

In the case of this work, for Kirchhoff migration aperture was tested from maximum to 3000 m and dip was chosen between values of 35°-50°, depending on the cases.

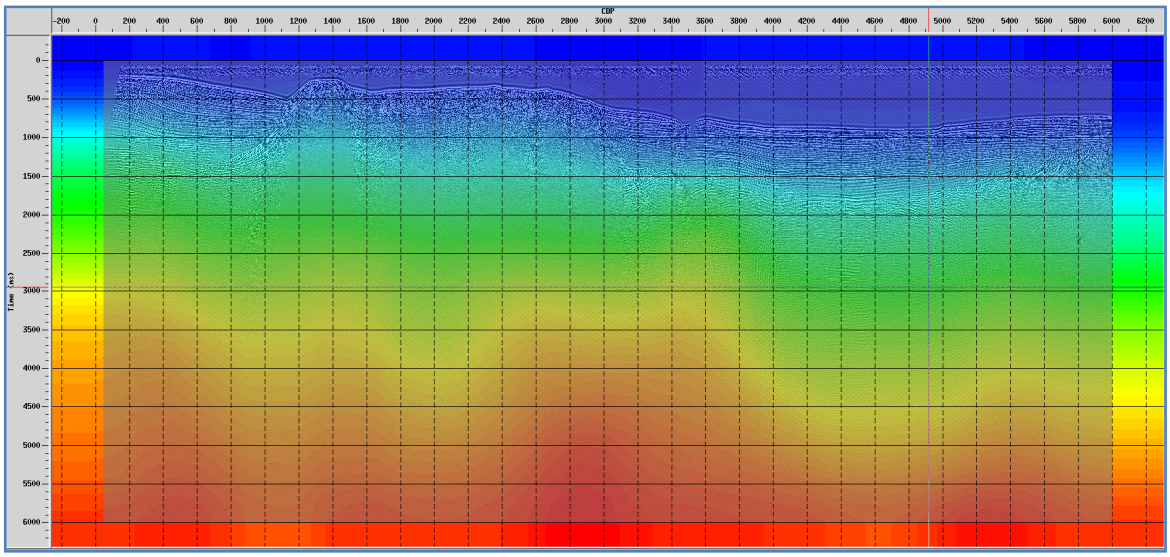


Fig. 4.25 - Smoothed velocity field (compare with Fig. 4.19) used in Kirchhoff migration.

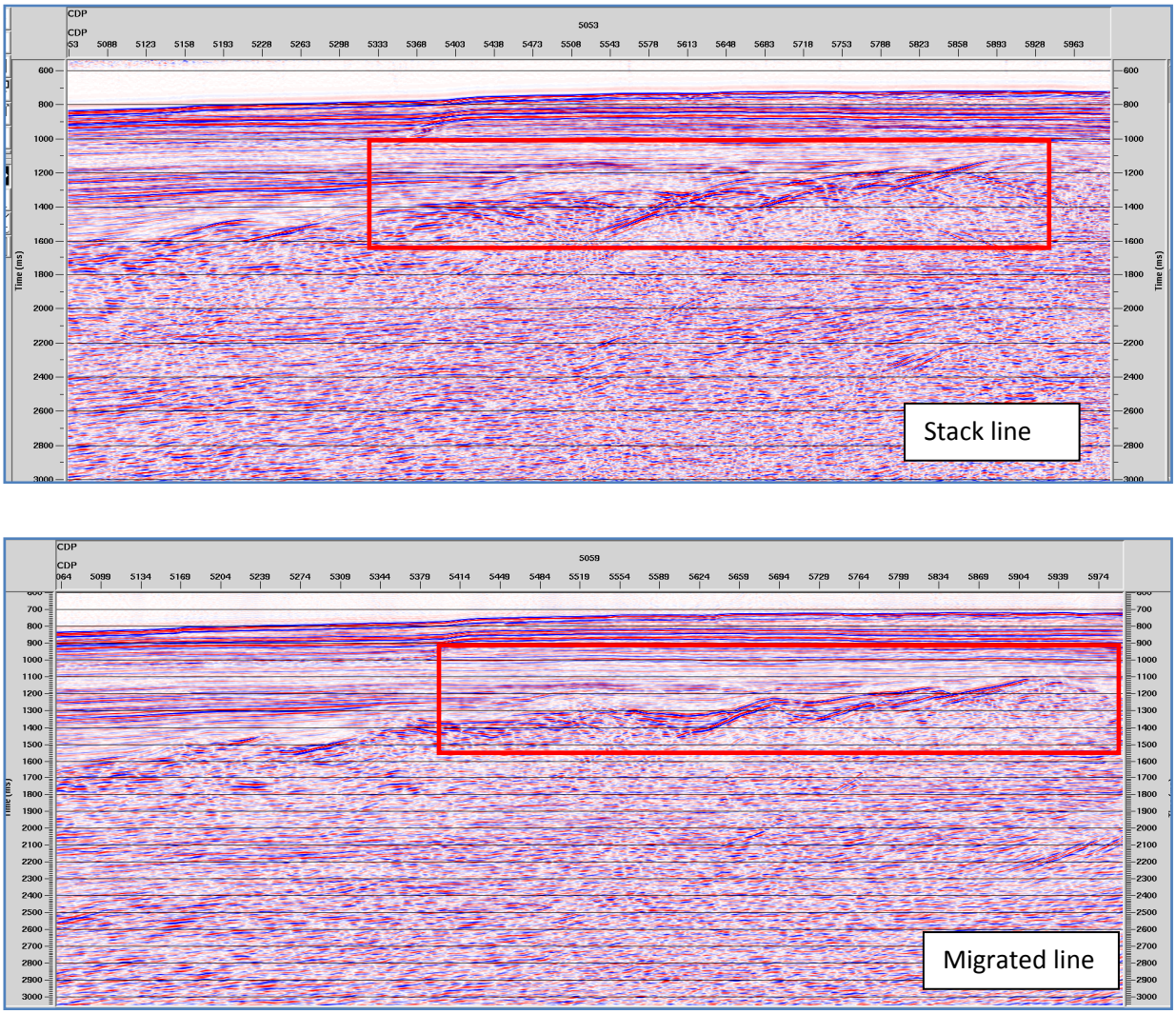


Fig. 4.26 - Effects of migration: diffractions are collapsed and the unconformity surface in the red rectangle is better visualized.

# CHAPTER 5

# Seismic Stratigraphic Analysis

Seismic stratigraphy is basically the interpretation of stratigraphic relationships based on the geometric configurations of reflector packages and patterns of vertical stacking and lateral continuity observed in seismic reflection data.

The definition of packages of reflections as seismic units is obtained through: a) the analysis of the contact relationships between the reflectors and the unconformity surfaces; based on different geometrical relationships these terminations are termed onlap, toplap, downlap or erosional truncation (Fig 5.1); b) the definition of the external shape of a seismic unit (sheet, lens, wedge, etc.); c) the definition of the internal characters of the unit, in terms of reflectors configuration (parallel, divergent, sigmoid, etc., Fig. 5.2) and continuity, amplitude, frequency.

As defined by Mitchum et al. (1977), a seismic facies is a group of seismic reflections whose parameters (configuration, amplitude, continuity, frequency and interval velocity) differ from those of adjacent groups; the main idea behind the facies analysis is to outline lithology and the characteristics of the depositional environment from seismic data.

In this section the seismic stratigraphic analysis of the study area is presented, as inferred from the analysis of the key horizons identified on the seismic sections, and their calibration with the few well data available in the area.

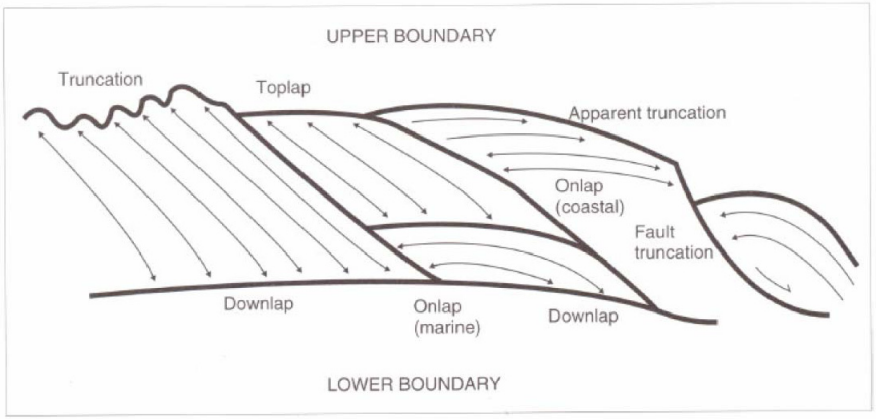


Fig. 5.1 - Different terminations of the reflectors on the unconformity surfaces (Emery & Myers, 1996).

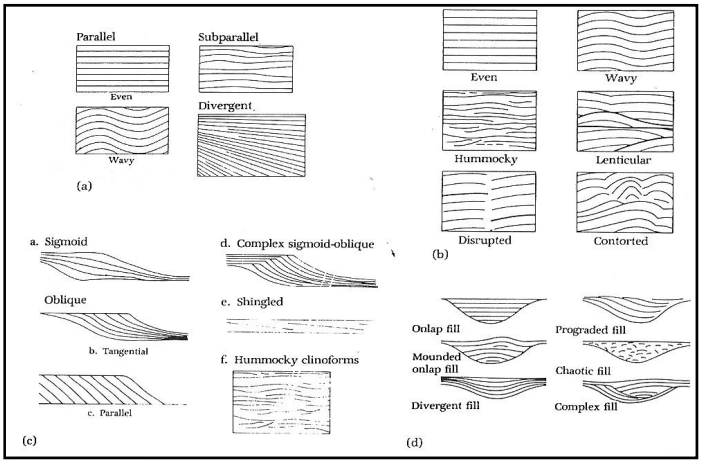


Fig. 5.2 - Possible internal configuration of the reflections (Mitchum et al., 1977).

## 5.1 Well data analysis

Well data are used in seismic exploration to calibrate key horizons in order to obtain a chronostratigraphic meaning for the seismostratigraphic units, and to constrain each seismic unit from a lithostratigraphic point of view.

In this study, well data are limited to some exploration wells located onshore along the coastal plains of the Latium and Campania regions (Fig. 5.3); they were drilled as part of research activities regarding hydrocarbon exploration on the coastal Italian sector, but the results were all negative, so the zone was abandoned from an industrial point of view. These wells are used in this work for indirect calibration of the seismic lines, in order to have a qualitative idea of the subsurface geology in the area. Two offshore wells (Michela 1 and Mara 1, Fig. 5.3) localized on the continental shelf, near the Italian coast, provide means for a direct calibration, although they are insufficient to cover the entire investigated dataset. Regarding the bathyal area, some ODP sites are present near the area of interest; their stratigraphic results (already described in Chapter 2.3) were taken into account in order to determine the stratigraphic setting in this area.

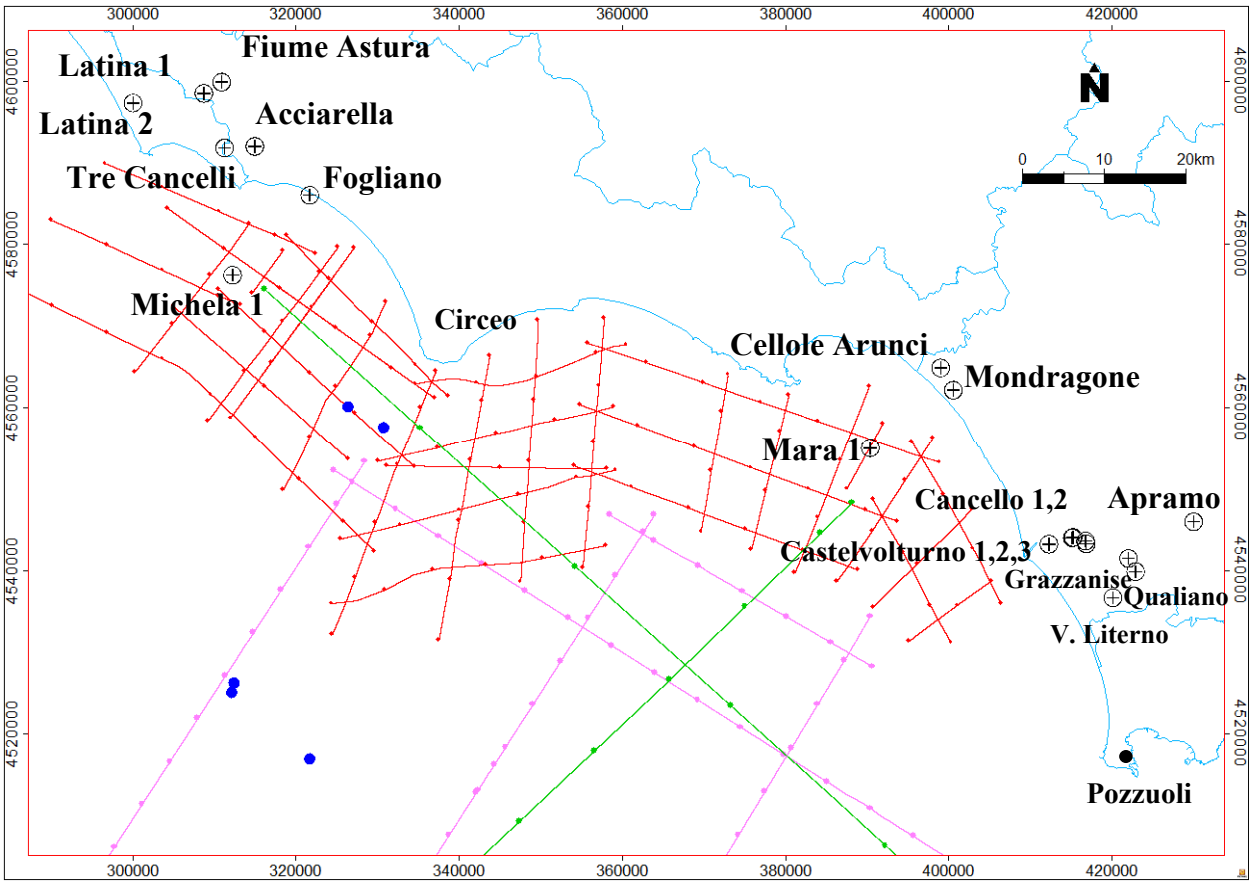


Fig. 5.3 - location of exploration wells used in this study; in red the E survey, in pink the TIR 2010 survey in green the CROP survey (Chapter 4). Blue dots correspond to some dredge and core samples.

The onshore wells are localized in three main sectors: the Pontina, Garigliano and Volturno plains (Fig. 5.3).

In the northernmost sector, the Pontina plain, is located the Fogliano well (Fig. 5.4), which reached a depth of 1000 m. The upper 407 m of sediments crossed by this well are composed by a Plio-Quaternary succession of sand and shales, followed by a 90 m thick succession of Messinian sandstones and of Aquitaniano-Langhian calcarenites. Down section, between 490 and 740 m of depth, marly limestones (Scaglia- type) of Eocene and Paleocene age are found and, finally, 250 m of limestones of the upper Cretaceous Scaglia Rossa Formation (Ippolito and Sgrosso, 1972).

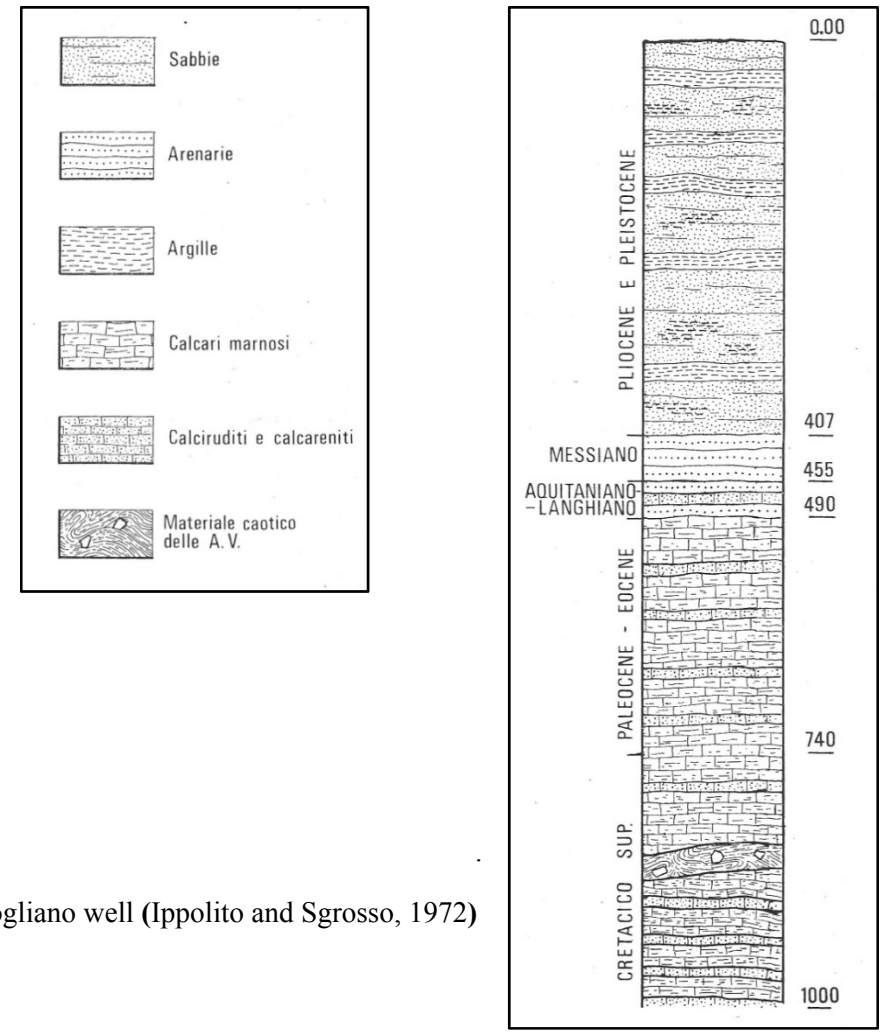


Fig. 5.4 - Fogliano well (Ippolito and Sgrosso, 1972)

Slightly to the North, Acciarella well (Fig. 5.5) was drilled for a total depth of 1041 m: it crossed 936 m of clays with intercalations of sands, Pliocene in age; the lower part crosses limestones with intercalations of marls and clays, of Miocene age.

Tre Cancelli 1 and Fiume Astura wells (Fig. 5.5) also drilled a Plio-Pleistocene succession for 1100 m and then crossed an Eocene or Cretaceous interval of marls and clays. Latina 1 and 2 shows a similar stratigraphy with a Plio-Pleistocene sequence overlying an allochthonous sequence Miocene in age, but they revealed the presence of a thinner succession of early Pliocene (73 m versus 287 m).

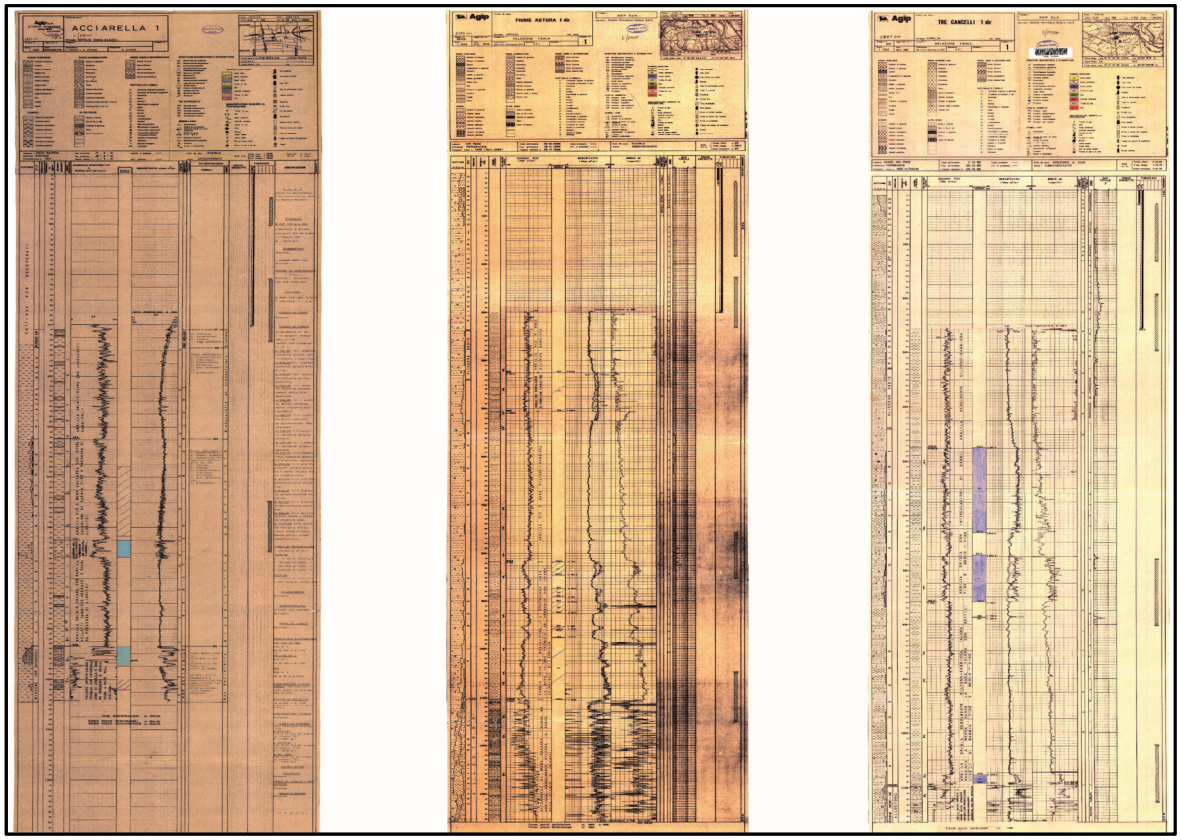


Fig. 5.5 - Acciarella1, Fiume Astura1 and Tre Cancelli 1 wells.

Michela 1 well (Fig. 5.6), which drilled a total depth of 2552 m, is located offshore between Anzio and Capo Circeo (Fig. 5.3). This is one of the two wells that allowed a direct calibration of the dataset. The first 1574 m encountered a succession of Pliocenic clays and shales, with sporadic levels of sands and gravel; it follows 400 m of a Miocene flysch deposit, overlying clays, marls and limestones of probably Cretaceous age, drilled to a depth of 2100 m; the bottom part of the well drilled anhydrites and dolomites of upper Triassic age, down to a total depth of 2552 m.

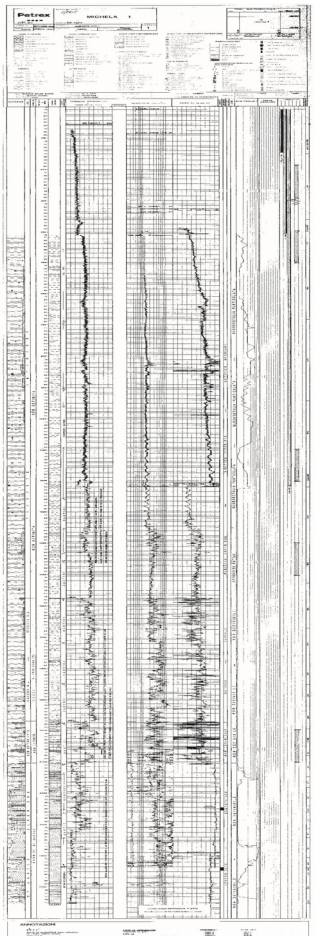


Fig. 5.6 – Michela 1 well.

Moving toward the south, in the Garigliano plain was drilled the Cellole Arunci 1 well (Fig. 5.7), for a total depth of 1500 m. According to Ippolito et al. (1973) the firsts 700 m of conglomerates, sands, clays and piroclastites are ascribed to the Quaternary, due to the presence of ostracoda as *Leptocyteretenera* and *Loxoconcaturbida*; between 700 and 875 m there is a barren interval of conglomerates; from 875 to 1220 m the succession of conglomerates, sandstones and clays is attributed to the early Pliocene, based on the presence of *Spaherodinellopsis*. The remaining part, formed by sandstones and clays, is dated as late Miocene. According to Ippolito et al. (1973), this is the only well in the central-southern sector which reached the Messinian sandstones and clays, after crossing the Plio-Quaternary succession of conglomerates, sands and clays. The authors indicate a depositional environment from infralittoral to deltaic plain. Regarding the barren conglomerates, the same authors affirm that they could belong or to the Quaternary cycle or to an intermediate cycle. They pointed out the presence, in the well proximities, of sandstones and clays locally with gypsum, strongly deformed, of late Miocene age; they are overlaid by transgressive discordant conglomerates with levels of sands and clays, referred to early Pliocene. The authors recognize two sedimentary cycles: Miocene to early Pliocene from 1500 to 875 m and Quaternary from 700 m to the surface.

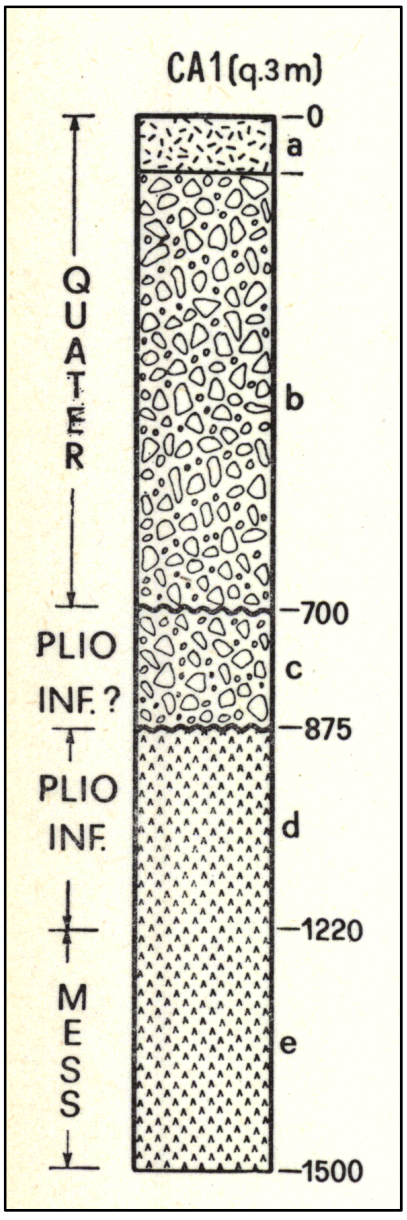


Fig. 5.7 – Cellole Arunci 1 well (Ippolito et al., 1973).

Near Cellole Arunci 1, is located the well Mondragone 1 (Fig. 5.8 A), 1966 m deep; it is localized on a structural high individuated through a seismic survey. The sediments drilled by this borehole are composed by a succession of clays and marls with frequent intercalations of polygenic conglomerates and in particular sandstones with gypsum in the bottom part. At the

depth of 675 m, the Quaternary sediments overlay deposits that could be ascribed both to Pliocene or Miocene age.

In this sector, but located offshore in the Gaeta Gulf, the Mara 1 well (Fig. 5.8 B) reached the depth of 2910 m, penetrating Pleistocene shales to a depth of 370 m, followed by a thick succession, about 850 m, of polygenic conglomerates, with intercalations of sands of undefined age. The rest of the well drilled clays and sandstone of Tortonian age, in flysch facies ("Flysch di Frosinone"), 350 m thick; then, there is a unit, probably overthrusted, of age comprised between Jurassic and Triassic, formed by limestones and dolostones, of about 1200 m thick. The last part of the well, from 2735 m to 2910, is formed by Paleocene-Eocene limestones and subordinately dolostones. This is the other well utilized for direct calibration of the seismic lines.

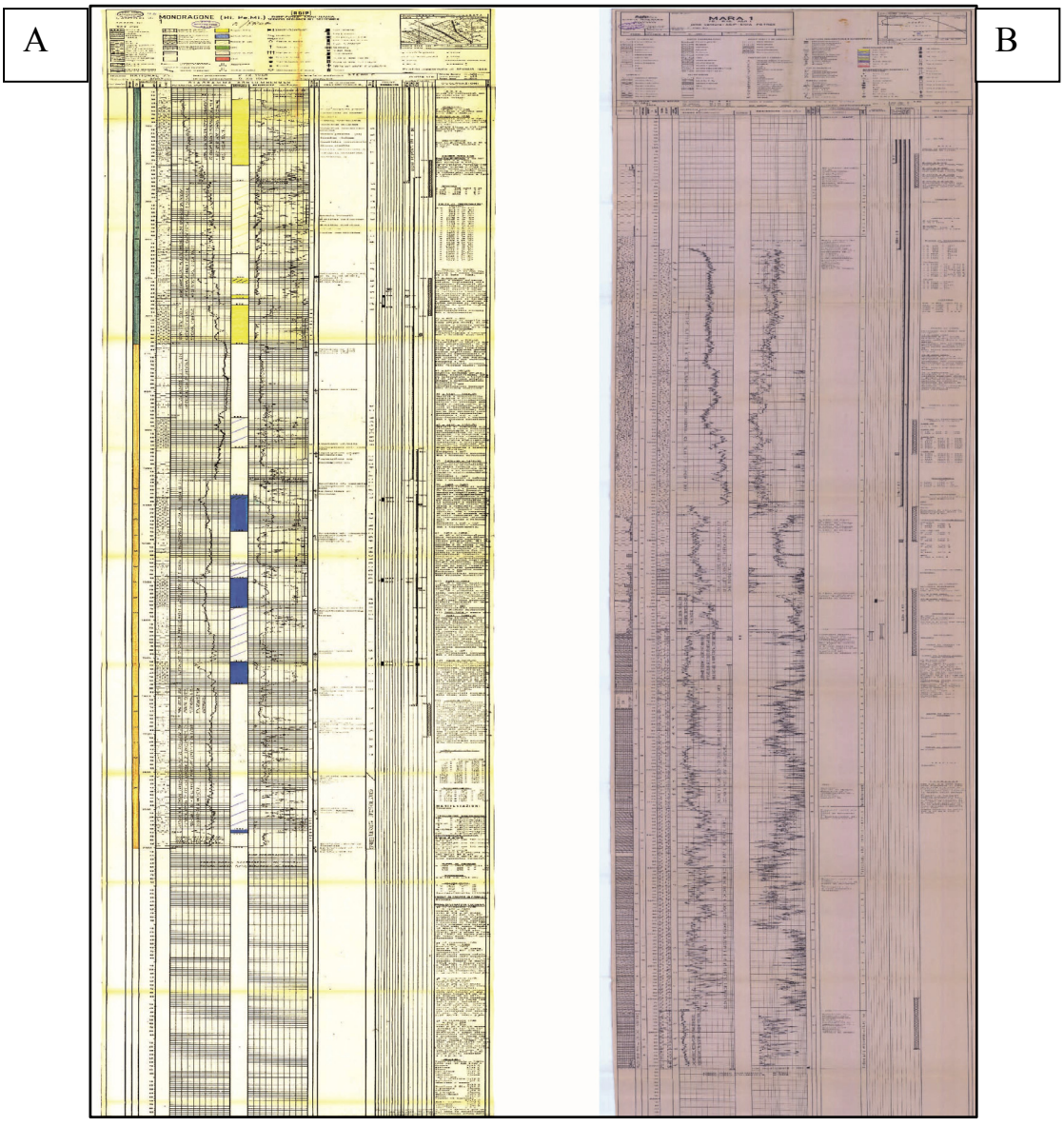


Fig. 5.8 - Mondragone 1 (A) and Mara 1(B) wells.

In the southern sector of the study area, the Volturno plain, separated from the Garigliano plain by the Massico Mountain, several wells were drilled. According to Ippolito et al. (1973), they only crossed Quaternary sediments, as inferred by the presence of *Hyalinea balthica*. Castelvolturno 1 and 3 wells (Fig. 5.9) reach 3000 m of depth, crossing a mainly siliciclastic succession made of conglomerates, sands and clays; depositional environment varies from pro-delta to delta plain and infralittoral.

The Castelvolturno 2, Grazzanise 1 and Qualiano 1 wells (Fig. 5.9) reach depths between 1200-1500 m; compared to the previously described wells, they are characterized by a succession of marine sediments and by several levels of pyroclastites and lavas. Ippolito et al. (1973) affirmed that the thick Quaternary succession highlighted in the Volturno plain, probably overlies Upper Miocene – Lower Pliocene sediments, transgressive on a carbonatic substratum. Thick volcanic complexes were drilled in the nearby wells Villa Literno 2 (Fig. 10) and Parete 2 wells (Villa Literno volcanic complex and Parete volcanic complex).

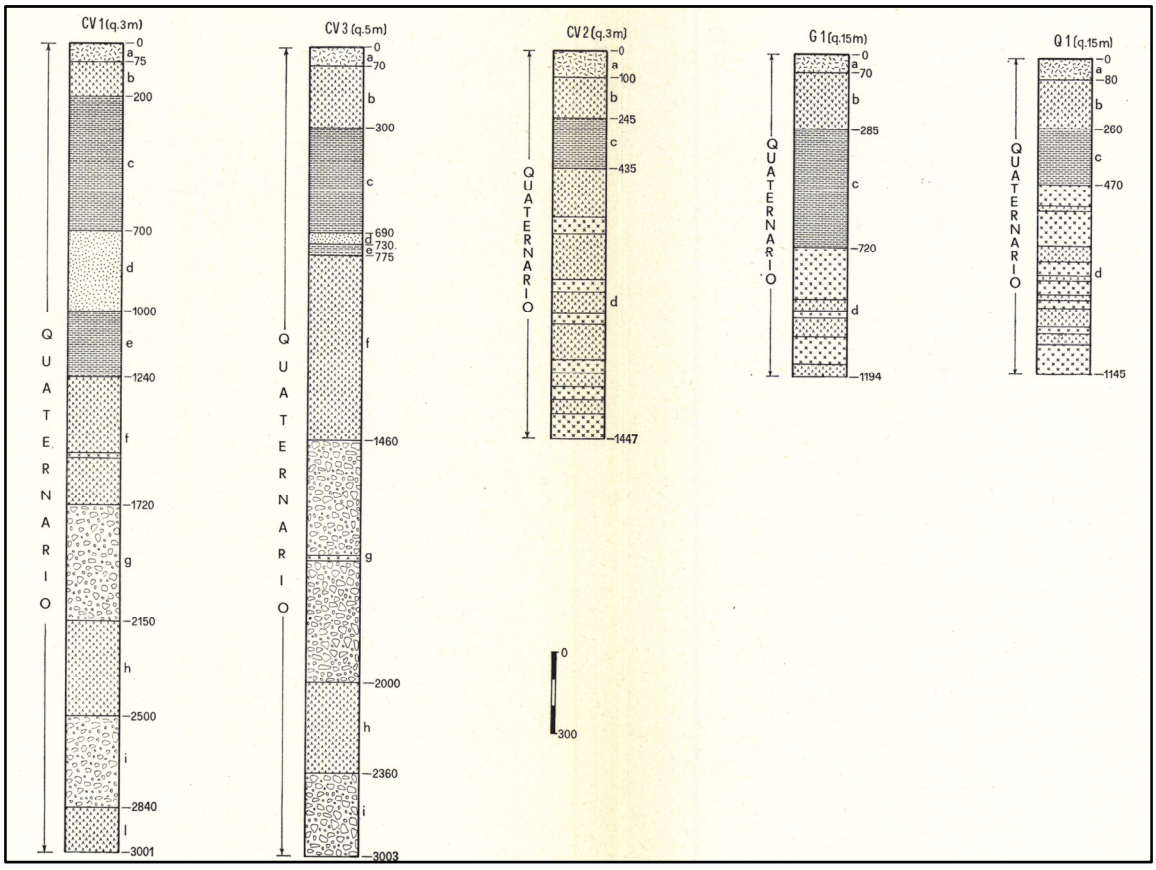


Fig. 5.9 - Castelvolturno 1, 2, 3 (CV), Grazzanise (G), Qualiano (Q) wells.

The logs of the Cancello 1 and 2 (Fig. 5.10) boreholes confirm the presence of a thick Pleistocenic sequence, crossed also by these wells for a depth of more than 3000 m; the only information about the substratum of the area is provided by the Apramo well (Fig. 5.10),

where under 1275 m of Pleistocene sequence, a Serravallian breccia overlaying Cretaceous limestones is encountered.

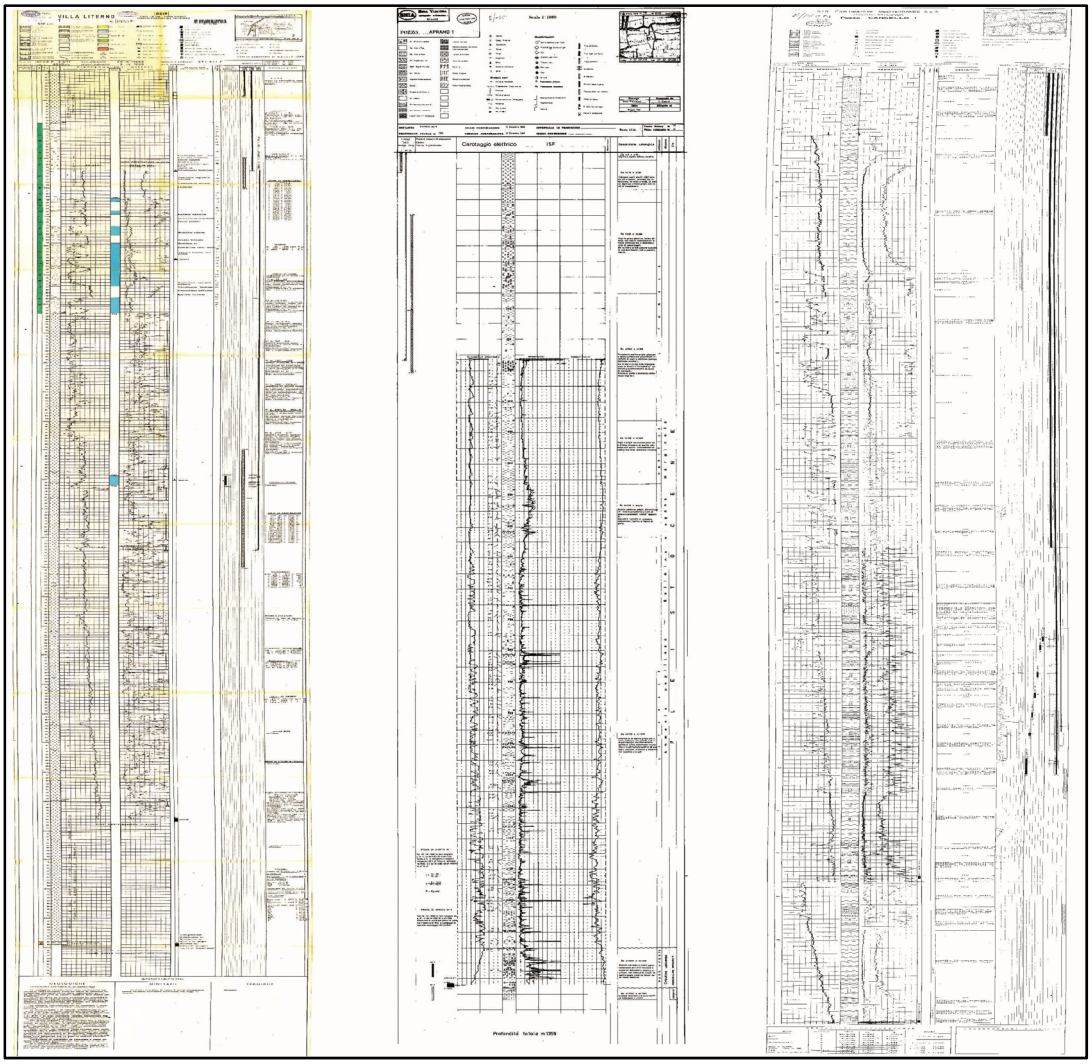

Fig. 5.10 – From left to right: Villa Literno, Apramo, Cancello 1wells.

## 5.2 Seismostratigraphic Units

The description of the identified seismic units is presented in this section. The unconformity surfaces were interpreted on those seismic lines where it was easier to define the geometry and terminations of the reflections, and the relationships between tectonic structures and sedimentation. The main unconformities were then correlated along all the dataset by the intersections between inlines and crosslines; however, due to the strong tectonic and the poor lateral continuity of the basins, in some areas the identification of the all sequences was not possible.

Some uncertainties in the interpretation can also arise where strong multiples are still present masking the real stratigraphic pattern, or where hard sea-bottom (calcareous or volcanic) reflected back a great part of the seismic energy causing poor penetration of the seismic signal. The lack of wells in the offshore area made the chronological calibration of the seismic units more complex, so correlation was done also taking into account all the previous studies done in the adjacent areas.

Based on all the available data, four main seismic units have been identified (named U1, U2, U3, U4), delimited by three main unconformity surfaces (named A, B and C) (Fig. 5. 12 and Fig. 5.13). The description of their characteristics is presented in the following sections; localization of lines shown in figures from Fig. 5.13 to Fig. 5.23, representing the seismic unit characters, is shown on Fig. 5.11.

Regarding the area beyond the continental slope, stratigraphic considerations where made taking into account the information provided by the ODP Sites (Chapter 2.3)

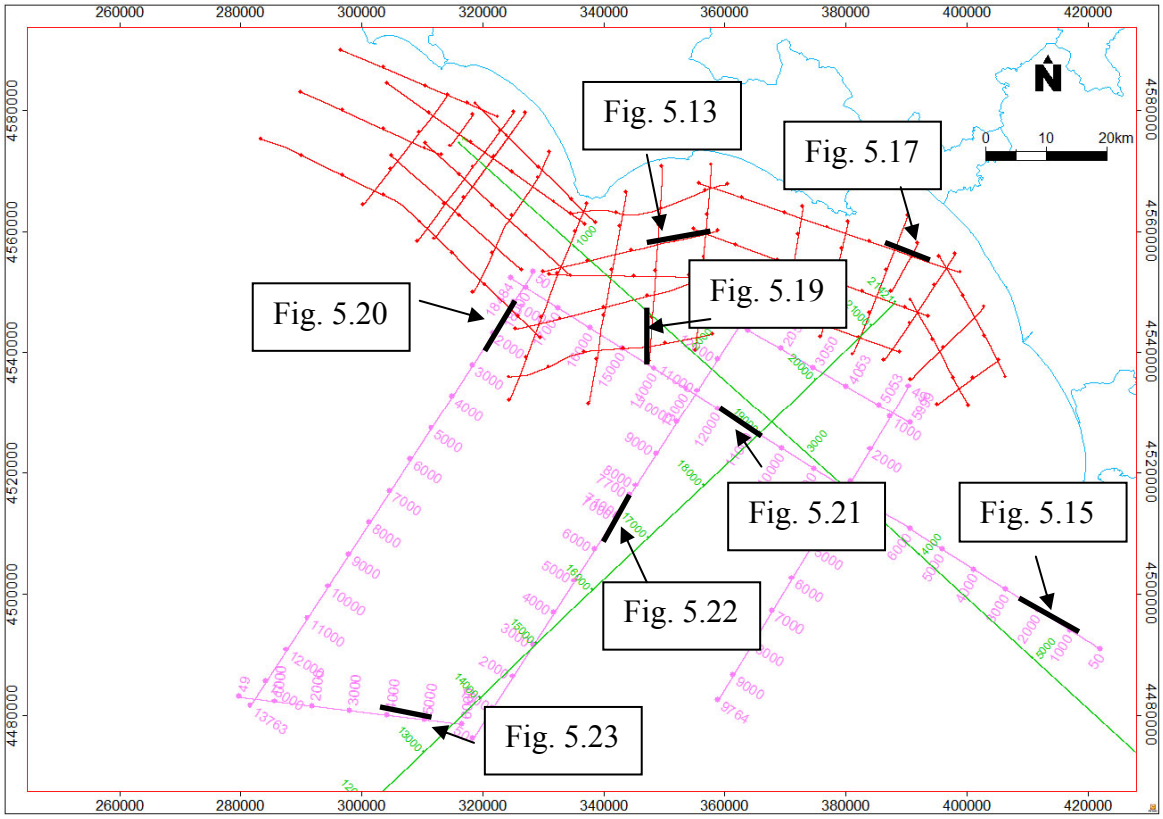


Fig. 5.11 – Localization of the following seismic profiles, with the main seismic units and unconformities identified.

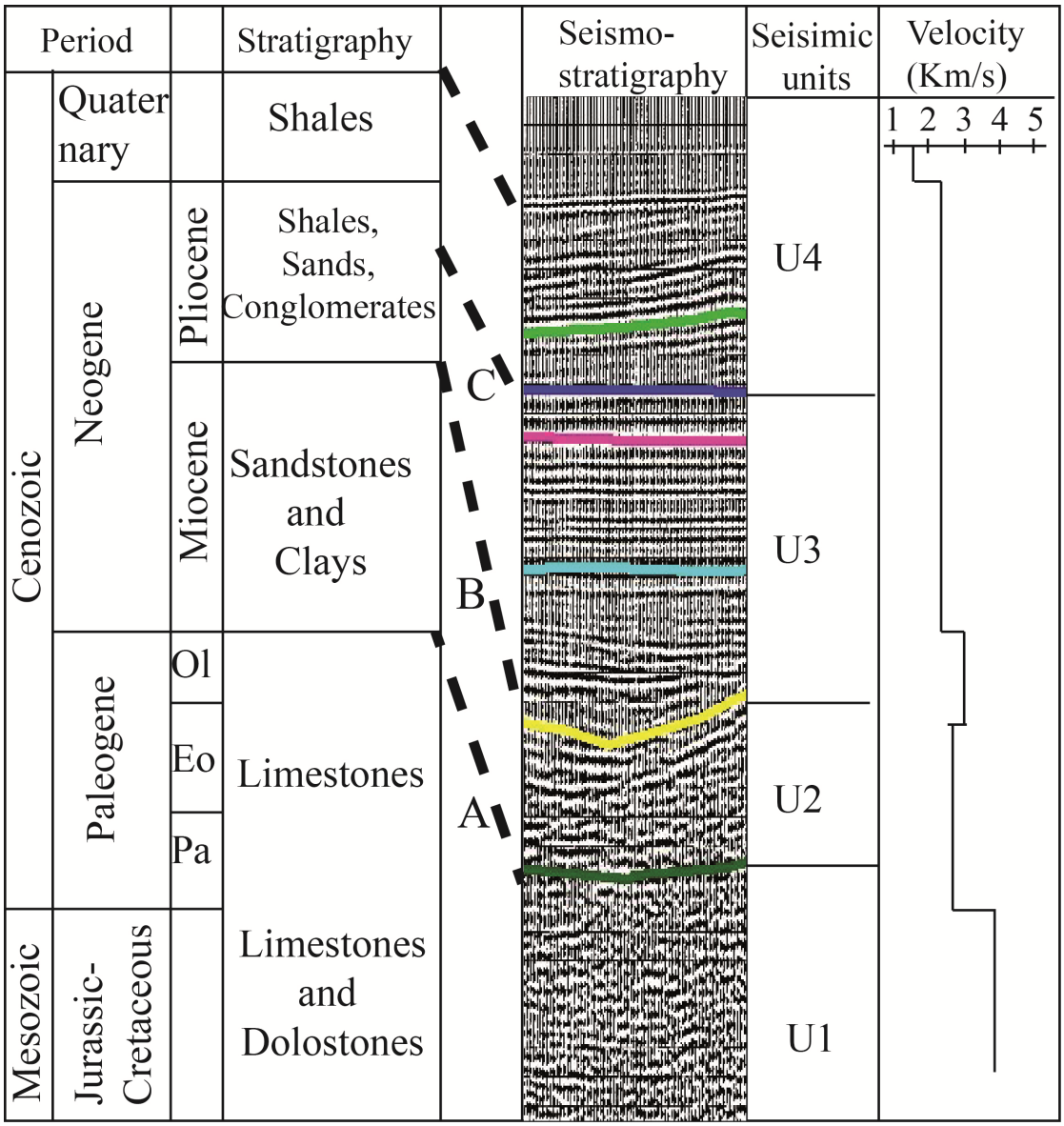


Fig. 5.12 - Seismostratigraphic scheme showing the main seismic units and main unconformities interpreted in this work. Correlation between seismic unit and stratigraphy is based on seismic facies analysis, well data and stratigraphic data available onshore close to the investigated margin.

Unit U4: Middle Pliocene p.p. - Pleistocene
Unit U3: Early Pliocene – Middle Pliocene p.p.
Unit U2: Miocene
Unit U1: Mesozoic – Cenozoic

C unconformity (blue line): Middle Pliocene p.p
B unconformity (yellow line): top Messinian
A unconformity (dark green): top Meso-Cenozic carbonates

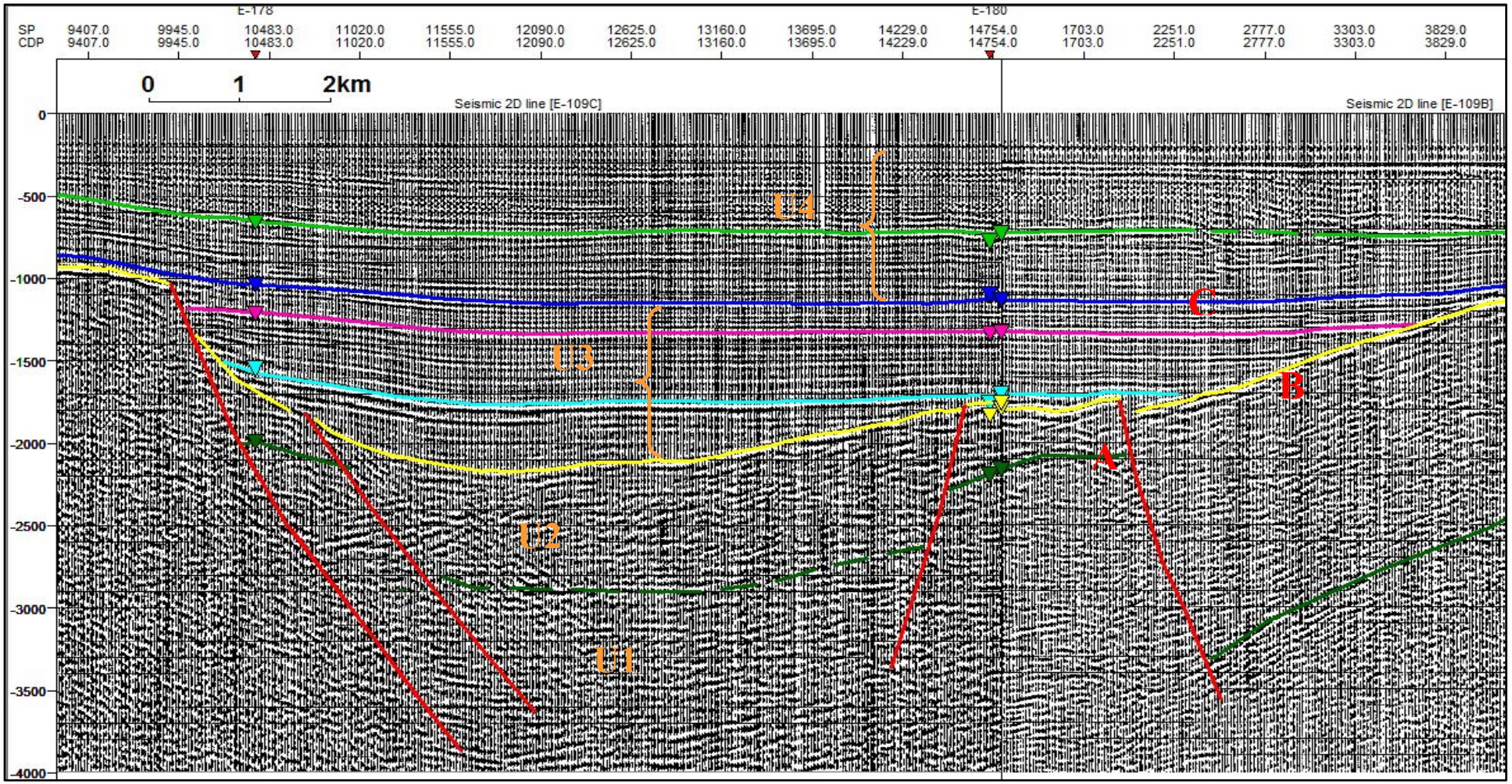


Fig. 5.13 – Seismostratigraphic units (orange) and main unconformities (red) defined: U1, Meso-Cenozoic; U2, Miocene; U3, Early Pliocene – middle Pliocene p.p.; U4, middle Pliocene p.p. –Pleistocene. A, top Meso-Cenozoic unconformity; B, top post-evaporitic Messinian unconformity; C, mid-Pliocene unconformity. For location see Fig. 5.11

### 5.2.1 Seismic units on the continental shelf

#### 5.2.1.1 Seismic Unit U1 (Mesozoic-Cenozoic)

This unit is the lowest seismic unit identified, characterized by a scarce penetration of the seismic signal. In most of the seismic lines it displays an undifferentiated seismic facies (Fig. 5. 14), whereas in few others, some strong reflections are visible. These latter are characterized by variable amplitude and frequency and are mostly discontinuous and chaotic, indicating lack of stratification. Probably the presence of compressive structures involving this unit are one of the reasons for the low quality of the data, as they cause internal reflection disturbances.

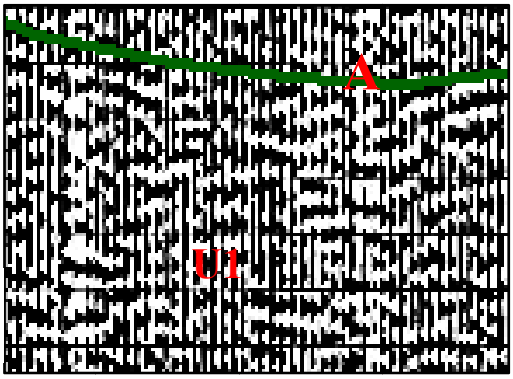


Fig. 5. 14 - Seismic facies of unit U1 and top unconformity (A).

The horizon A (Fig. 5. 14, Fig. 5. 15) at the top of Unit U1 generally reflects the major part of the seismic energy and appears discontinuous and with variable energy; this unit can be considered the acoustic substratum of the area.

U1 unit has been correlated for its characteristics to the Meso-Cenozoic carbonates widely cropping out in the near onshore areas, in the Lepini and Aurunci massifs, the Massico Mountain, Zannone Island and Circeo Mountain. Moreover, the unit U1 is drilled onshore by the Fogliano 1 well, which found marly carbonates sediments ("Scaglia type") at a depth of 500 m (so probably it drilled a structural high) and, more to the south, by the Apramo 1 well. Offshore, both Michela 1 and Mara 1 drilled this unit, at a depth of about 2100 m and 1500 m, respectively.

In literature, unit U1 correspond to the unit "C" of Zitellini et al. (1987), or to the "unit 4" of Bartole et al. (1990); the upper boundary corresponds to the "Z" unconformity of Zitellini et al. (1987), or "R1" horizon of Aiello et al. (2011) (see Chapter 3.2).

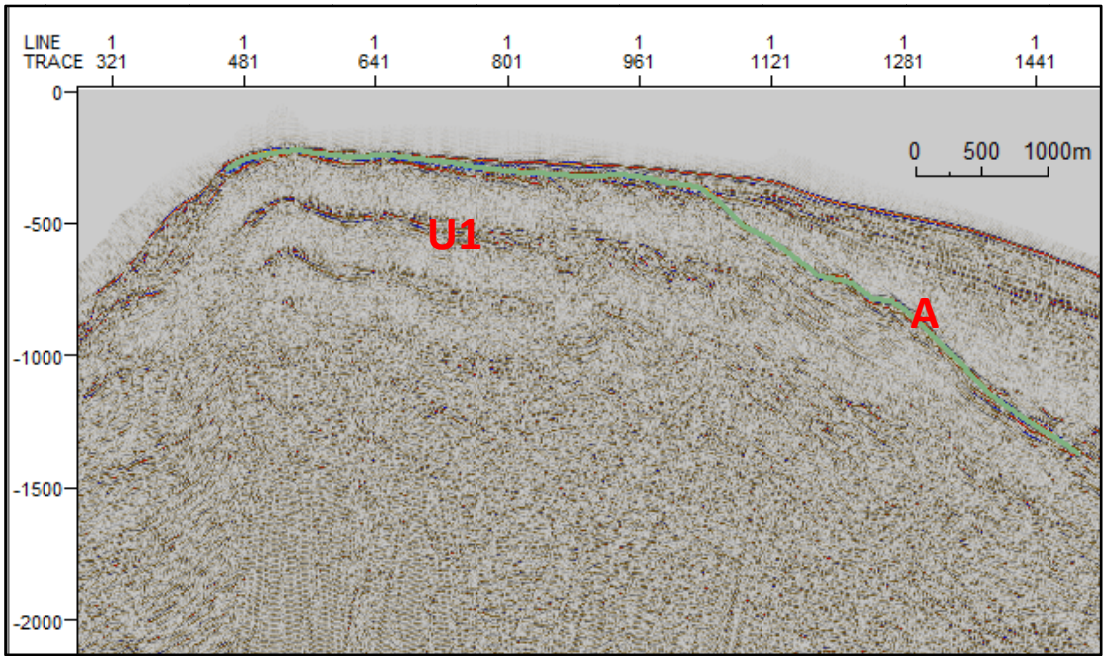


Fig. 5. 15 - Carbonatic structural high (Unit U1) and unconformity A. For location see Fig. 5.11.

### 5.2.1.2 Seismic Unit U2 (Miocene)

This unit is characterized by a chaotic seismic facies, with scattered discontinuous reflectors, medium amplitude and variable frequency, indicative of heterogeneous lithologies (Fig. 5. 16). As inferred by the geology outcropping in the Latium-Campania regions, this unit can be correlated with the Miocene flysch deposits («Units Sicilidi», «Units Liguridi», «Flysch of Frosinone», «Flysch of Cilento») (D'Argenio et al., 1973, Parotto and Praturlon, 1975). Some of the exploration wells drilled Miocene deposits like Mara 1 (1220 m of depth), Michela 1 (1574 m of depth), Fogliano 1 (410 m), Cellole Arunci 1 (1220 m), and probably Mondragone 1 (700 m); generally the Miocene succession is made of clays and sands, with locally interbedded conglomerates.

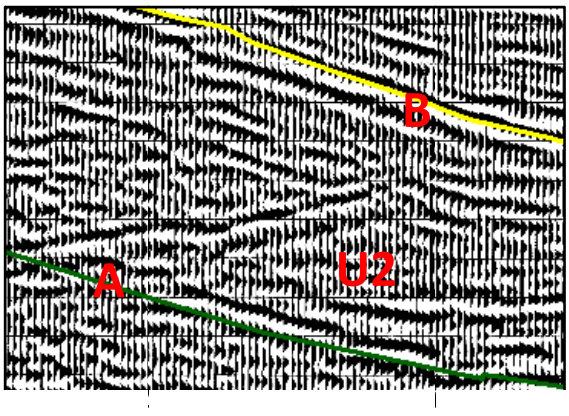


Fig. 5. 16 - Seismic facies of Unit U2

Unit U2 constitutes, together with the previous one (U1), the substratum of the area; it is not well displayed in all the seismic datasets, and it seem to be absent in the structural elevated areas where the substratum is composed only by the Meso-Cenozoic calcareous deposits. Maximum thickness observed is in the order of 1 sec. (twt).

The lower unconformity (A) of the unit has already been described; the upper unconformity (B) (Fig. 5.12 and Fig. 5.13) is a strong reflector, characterized by a high amplitude and strong impedance contrast; it is well visible in all the dataset, although

sometimes it is formed by several diffraction hyperbolas, more than a single and well defined seismic horizon. This unconformity has a regional importance, being linked to the top of the evaporites deposited during the late Messinian salinity crises or to an erosional unconformity formed during the late Messinian sea level drop (Malinverno, 1981); sometimes it has been observed erosional truncation geometry of the unit U2 on this unconformity (Fig. 5. 17).

Unconformity B corresponds to the "Y" horizon of Zitellini et al. (1987) and the unit U2 correspond to the "unit 3" of Bartole et al (1990).

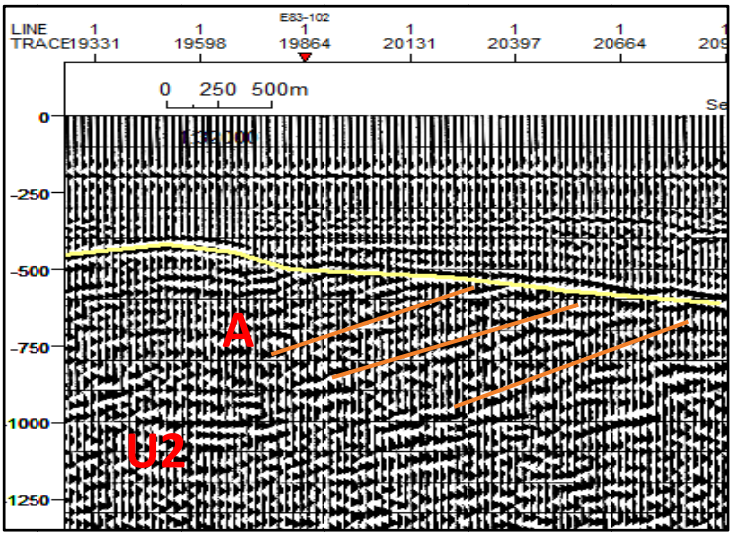


Fig. 5.17 - Erosive truncation of unit U2. For location see Fig. 5.11.

### 5.2.1.3 Seismic Unit U3 (Early Pliocene – middle Pliocene p.p.)

This unit lies upon the unconformity B that marks the top of the Messinian; basal reflections inside U3 are generally parallel to the B horizon, or they onlap it in presence of structural highs; locally B also displays an erosive character. The upper boundary of the unit is generally a well distinguishable surface, parallel to the upper reflectors of the unit (Fig. 5.13).

Internal reflections are generally continuous and well imaged, from low to medium amplitude, medium frequency, with a parallel to subparallel geometry and horizontal pattern; the overall unit shows wedge geometry, being thicker in the basin depocenters and progressively thinner in the proximity of the horsts that delimited the basins. The time

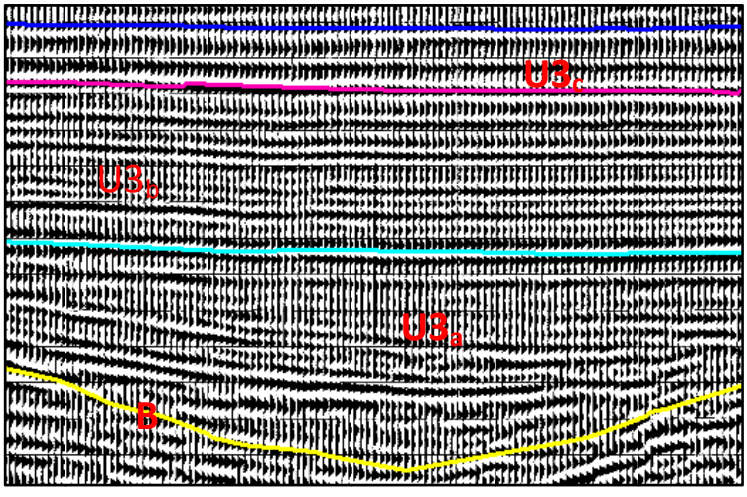


Fig. 5.18 - Seismic facies of unit U3 and subunits.

thickness of U2 varies due to the irregular morphology of the underlying unconformity, being maximum in the basin where it reaches about 1 second (twt) of thickness (Fig. 5.18).

In some sectors (i.e. the deepest areas) it is possible to divide the unit in a lower part ($U3_a$) formed by high amplitude reflectors progressively becoming a transparent facies, with low amplitude and high frequency, probably associated with a more fine grained clastic sediment. The overlain subunit ($U3_b$) is formed by continuous, well layered reflections, with medium amplitude and high frequency. The subunit at the top ($U3_{c)}$ is a thin sequence characterized by a higher amplitude of the reflections (Fig. 5.18).

According to the well analysis, unit U3 can be correlated with the Pliocene deposits drilled by almost all of the wells, which found a succession made in general of alternation of clays and sands, locally with intercalated conglomerates; these more coarse grained sediments are detected on the seismic lines by stronger and less organized reflections. Depositional environment is marine, infralittoral according to Ippolito et al. (1973).

In some portions of the seismic lines normal faults with limited (or null, for seismic resolution) offset are detected in this unit, and also folds are present; this highlight a still active tectonic and therefore the unit has a syntectonic signature.

Unit U3 has been correlated the unit "B1" of Zitellini et al. (1987) and it is formed by post evaporitic Messinian, early Pliocene and Middle Pliocene p.p. sediments.

#### 5.2.1.4 Seismic Unit U4 (middle Pliocene p.p. – Pleistocene)

This is the uppermost seismic unit, divided from the underlying unit U3 by a basal unconformity here named C (Fig. 5.12 and Fig. 5.13, blue line). This surface highlights an evident variation of the depositional geometries, marking the beginning of the progradation in the basin fill and apparently the end of the tectonics (no evident deformation is displayed in unit U4). Trincardi and Zitellini (1987) and Zitellini et al. (1987) already detected in other Tyrrhenian sectors a tectonically-enhanced unconformity (X) marking the transition from a synrift to a postryft stage; therefore the unconformity C is correlated with this regional unconformity X, of intra-middle Pliocene age.

The internal reflections configuration of unit U4 on the continental shelf sector consists in prograding clinoforms, probably of deltaic environment (Fig. 5.19); on seismic profiles parallel to the direction of progradation, it is possible to recognize topsets, foreset and bottomset beds of sigmoidal or oblique clinoforms. The deltaic system was probably supplied during Pleistocene times by the adjacent Latium-Campania plains, and the main direction of progradation was NW-SE basinwards. Offlap breaks seem to move seawards, which indicate a regressive trend of the marine and coastal facies. Several main unconformities are observed within the unit U4; the bottom part of the reflections display a slightly downlap termination on the basal unconformity surface, and then basinwards they became concordant with it.

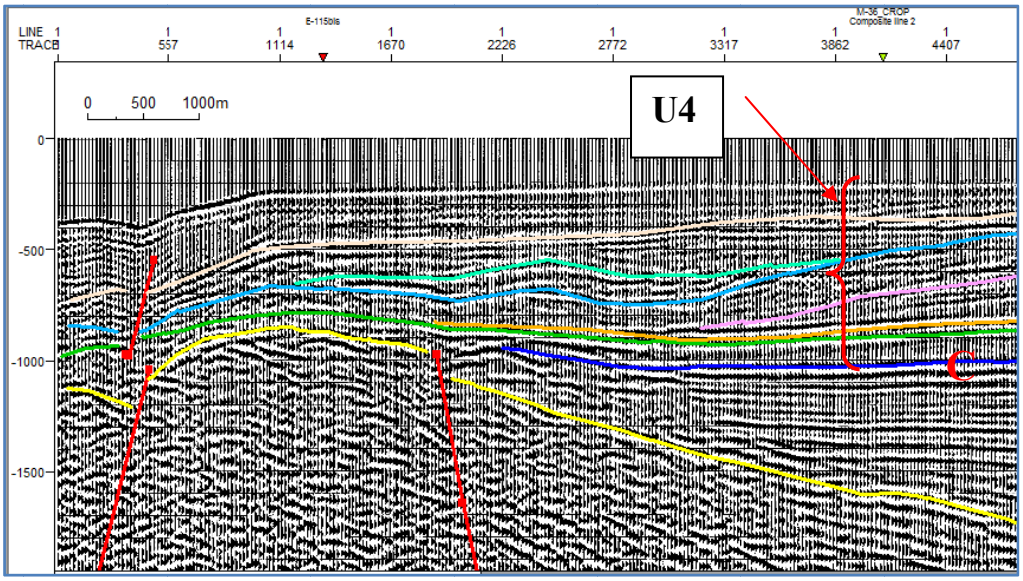


Fig. 5.19 - Prograding clinoforms in unit U4. For location see Fig. 5.11.

In addition to the continuous, low to medium amplitude reflectors above described, are also observed localized and chaotic reflections probably due to slumping, especially in the proximity of structural highs of the basements (Fig. 5.20) Another characteristic is the presence of cut and fillings of canyons or channels, sometimes in correspondence of moderns channels.

This unit is reached by all wells present in the area; it can be noticed that the Pleistocene sequence shows very different thickness along the area, minimum in the northern sector (around 1000 m) and maximum to the south (more than 3000 m), as already pointed out by the analysis of the well data.

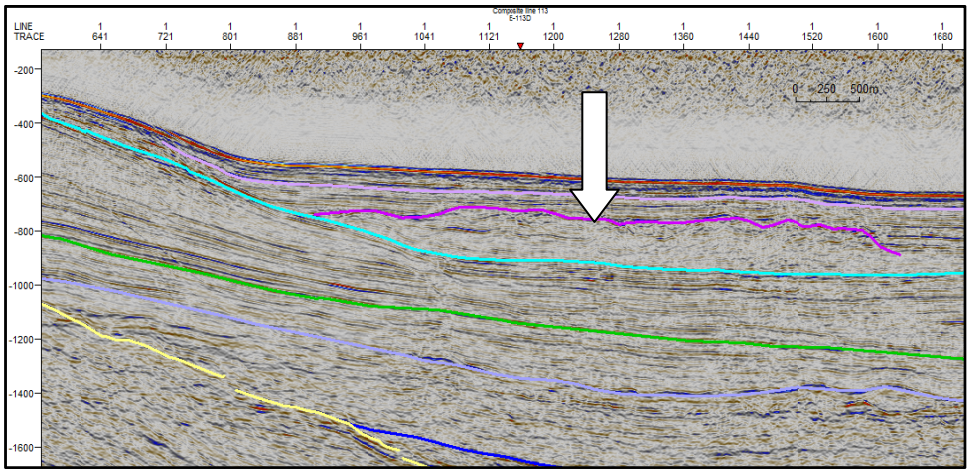


Fig. 5.20 - chaotic facies ascribed to instability phenomena. For location see Fig. 5.11.

The analysis of the seismic facies and the information provided by the wells identify the sequence as composed essentially by conglomerates, sands and clays of deltaic environment, evolving to a more marine environment in the upper part of the sequence. A middle Pliocene p.p.-Pleistocene age is assumed for this sequence.

#### 5.2.1.5 Volcanic unit (V)

In some seismic lines, an additional facies has been detected, included within the seismic unit U4; it is characterized by a low signal/ noise ratio due to the scattering of the seismic energy provoked by the presence of volcanic rocks. It occurred especially in the southeastern sectors on the line TIR-13, where some volcanic shape reflectors are detected, as it approximates the Ventotene volcanic region, and in the NW sector in correspondence with the Ponza high, whose substrate is probably of volcanic origin. The reflections appear chaotic, discontinuous and with high amplitude (Fig. 5.21).

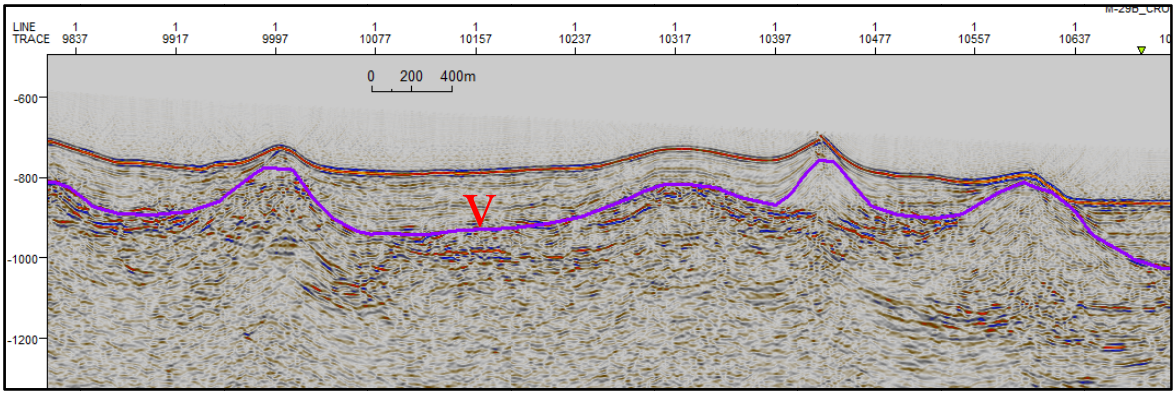


Fig. 5.21 - Volcanic complex near the island of Ventotene. For location see Fig. 5.11.

### 5.2.2 Seismic units on the continental slope and the Vavilov plain sector

Seismic units previously described were defined on the continental shelf sector; regarding the area of the continental slope and the Vavilov plain, which extends starting from the base of the escarpment, some considerations are here exposed.

On the steep continental slope, a thin succession of reflectors is observed, lying upon a basal unconformity characterized by strong acoustic impedance and which shows sometimes an erosive character; the internal reflections shows low amplitude and frequency, and sometimes a discontinuous pattern. Where the escarpment shows major inclination, the sequence is absent. In some sectors, chaotic facies are found, with discontinuous and

disrupted reflectors, due probably to instability phenomena, or bodies with mounded geometries and still visible internal reflections (Fig. 5.22).

The bathyal plain is investigated by only one seismic line of the dataset, the TIR-15 line, with a WNW-ESE trend (Fig. 5.23). Starting from the seabottom, a first seismic unit ($U_3$) is characterized by continuous, parallels and high amplitude reflectors; this unit overlays a thick, well-layered succession ($U_2$) (about 0,8 sec. twt), within which several sequences can be detected, separated by slight angular unconformities. They are characterized by continuous, parallel, subhorizontal reflections; sequence boundaries are subhorizontal, resulting in a tabular external geometry of the unit. An alternation of seismic facies is observed, from well layered reflectors with medium amplitude, to a more transparent seismic facies, due probably to fine grained sediments. According to Mascle and Rehault (1990), the deep Vavilov plain is filled locally with successions of ponded turbidites, ash layers, and hemipelagic sediments of lower Pliocene to Pleistocene age, locally thick as much as 800-1000 m; these sediments well fit with the facies observed in $U_2$. On the seismic line TIR15, a deeper unit ($U_1$) can be detected, underlying $U_2$, formed by more irregular and discontinuous reflectors, and pinching out against a strong diffractive basement (A) (Fig. 5.23).

In order to attempt a chronostratigraphic correlation for this sector, ODP site 651 can be taken into account, being this drilled on the flank of a broad basement swell located about 35 Km to the south respect to the line TIR-15. According to Mascle and Rehault (1990) three main seismic units are distinguished in this area: the upper unit is an almost transparent sequence of about 100 m of thickness, made of volcanogenic sediments (pumice or cemented volcanic breccias) interbedded with marly muds, Pleistocene in age. The seismic unit 2 is characterized by alternating high-low amplitudes reflectors, consisting of lower Pleistocene to upper Pliocene nannofossil ooze with subordinate volcanogenic turbidites, in slight unconformity on the underlying one; unit 3 includes two contrasting acoustic facies: the upper one is characterized by undulating reflectors, correlated with chalks to dolomites; the lower one shows high-amplitude and irregular reflectors and consist of a succession of lava flows and basaltic breccias; finally, topped by a strong reflector, the acoustic basement corresponds to serpentinized peridotites.

Therefore, tentatively, the diffractive basement shown on line Tir 15 could be correlated with the basement find at the bottom of ODP Site 651, and the immediately above seismic unit $U_1$ can be compared with the lava flows or basaltic breccias of seismic unit 2 of Mascle and Rehault (1990). The siliciclastic filling by consequence should have an upper Pliocene-Pleistocene age.

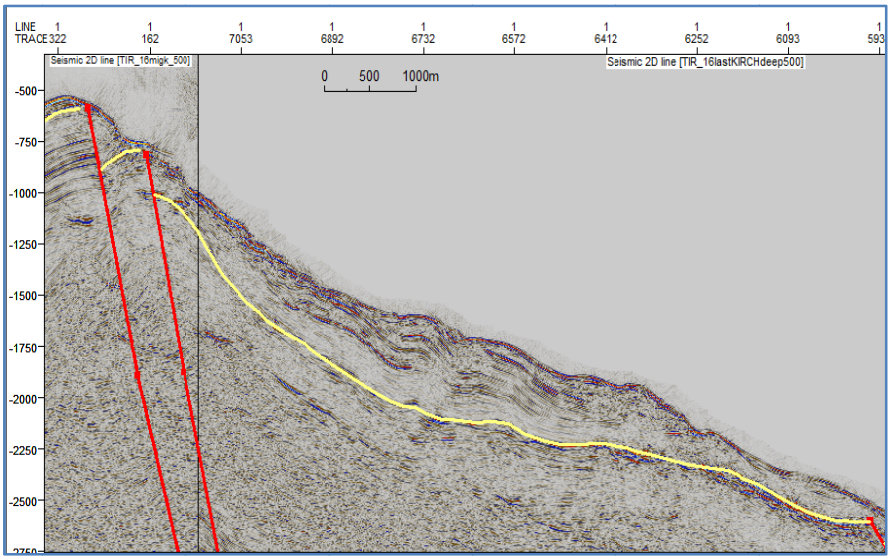


Fig. 5.22 - Detail of a chaotic deposit resting on the escarpment (conturite body?). For location see Fig. 5.11.

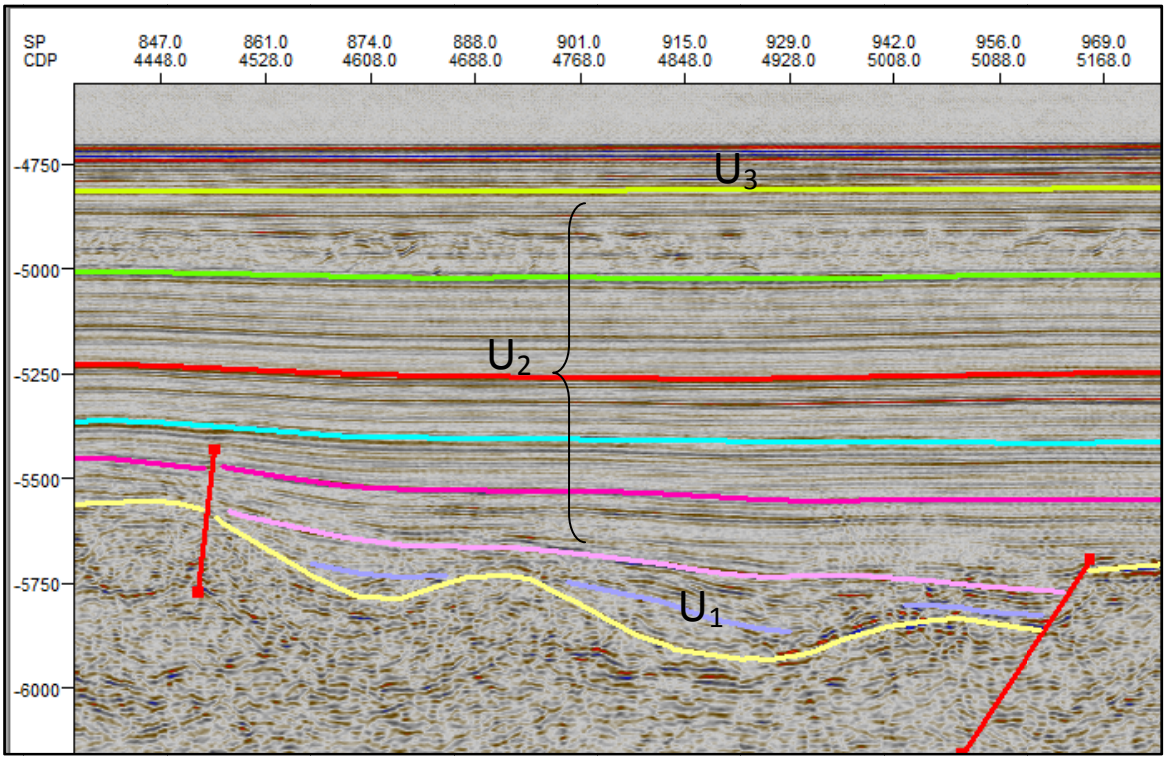


Fig. 5.23– Seismostratigraphic units in the Vavilov area (Tir 15 profile). For location see Fig. 5.11.

# CHAPTER 6

# Reconstruction of the Structural Setting

Seismic interpretation was carried out using Petrel 2012.1 software (Schlumberger) (Fig. 6.1), which allows to manage digital seismic data in seg-y format and to represent the dataset in a georeferenced environment; furthermore, three-dimensional visualization is an efficient tool in verify interpretation at the intersection of the lines, the horizons geometry or the structural trends within the entire 2D dataset.

The interpretation of the seismic profiles was aimed to unravel the tectonic and stratigraphic setting of the Latium-Campania rifted margin; the transition from the oceanic Vavilov basin to the surrounding continent crust occurs by means of a system of continental margins thinning toward the ocean, so the general setting shows a preponderance of extensional features. Peculiar is the steep escarpment -the main morphological feature- connecting a narrow continental shelf to the mostly flat bathyal plain.

In this chapter the main structural and stratigraphic features interpreted will be described in detail. Description is divided in three different paragraphs according to the principal morphological sectors: the continental shelf, the escarpment and the bathyal plain.

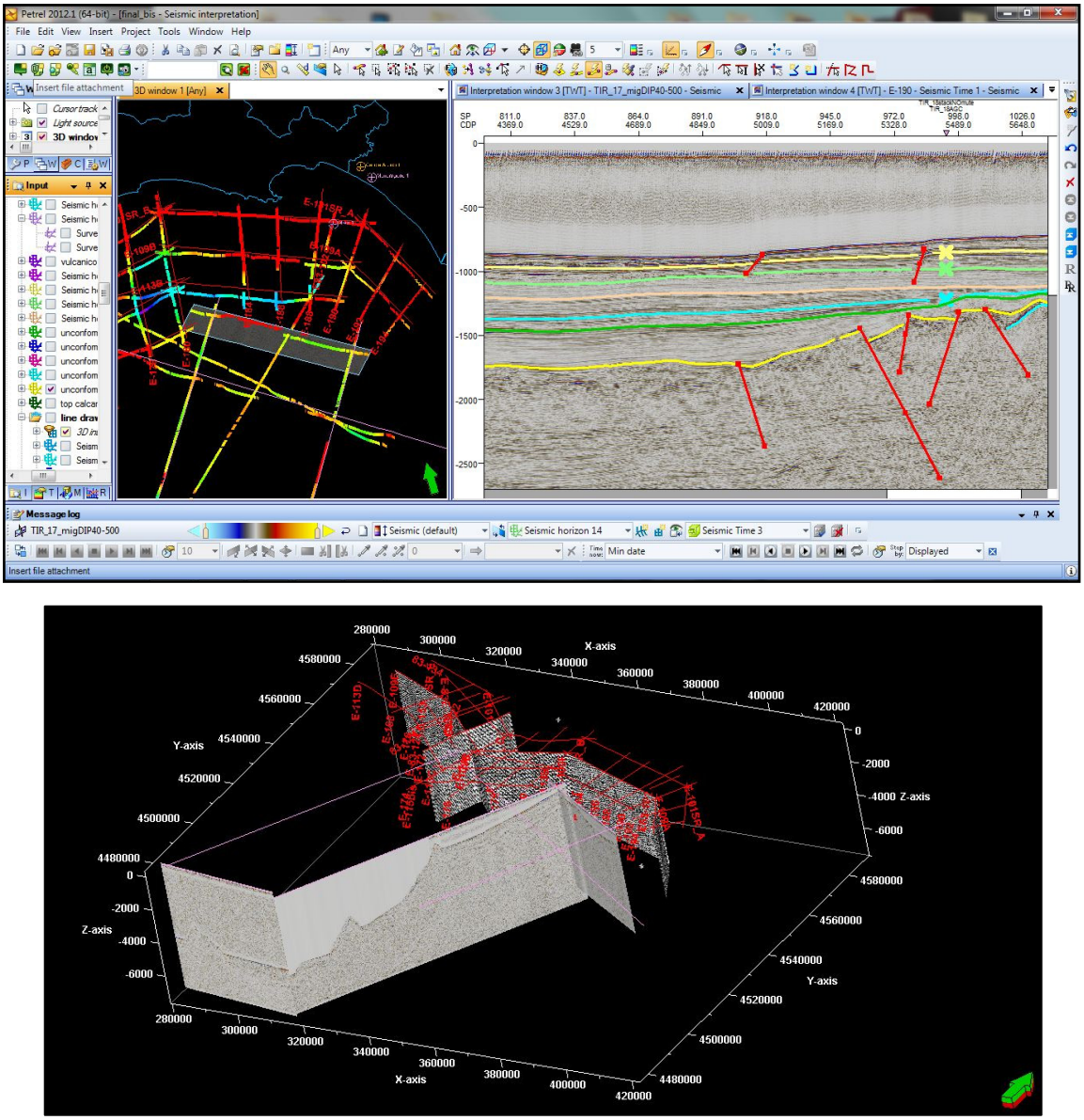


Fig. 6.1 - The Petrel environment

## 6.1 The continental shelf

The continental shelf is defined as the sector of the continental margin comprised between the shoreline and the shelf break. In the sector between Anzio and Volturno river, the shelf display a width of about 25 Km, with low inclination; however, offshore Circeo promontory, it surrounds the western Pontine archipelago (Ponza, Palmarola, Zannone), reaching an extension of 35 Km from the continent, determining a morphological continuity between the Italia peninsula and the islands. Shelf break is well defined and it is usually found at a depth between 150-200 m.

The tectonic setting of the shelf area has been studied by means of the E survey, which extensively investigates this area with a regular net of seismic profiles (spacing between the lines is in the order of 10 Km) acquired during the '80s for oil exploration purposes.

From a structural point of view, the interpretation highlighted a general horst and graben setting in this area. Several half-graben systems and fault bounded blocks are present, most of them showing small areal extension and continuity; as a consequence, correlation along the entire dataset is unable for these secondary faults. The identification of the main trends and the correlation of the master faults have been realized on the basis of the major offsets observed in the main unconformity present in the area (unconformity B, top Messinian); in this way the principal basins were identified, separated by the main structural high areas. In the following part, the principal morpho-structures pointed out by the interpretation and correlation will be described.

Starting from the northern sector, a main structural high is identified on the seaward extension of the Circeo Promontory, located in the mainland; on line E-101, this high can be observed between shotpoints (hereafter SP) 8676 (Line E-101D) and 7900 (Line E-101C), with a length of approximately 15 Km (Fig. 6.2 A). Moving seaward, on lines E-109 and E-113, the Circeo High is still evident but it displays different characters: structural elevation is lower and the morphological high becomes a wide area (about 20 km length) of smaller horsts dissected by high-angle extensional faults, with small displacements (SP 13700, Line E-109D to SP 7750, Line E- 109C; SP 27830 Line E-113D to SP 7166, Line E-113C) (Fig. 6.2 B and C).

The Plio-Quaternary cover above the main unconformity B (top Messinian, yellow line) is usually thin, especially in the northern sector (Line E-101, Fig. 6.2 A) where it is almost null at the top of the structure, probably due to sub-aerial erosion phenomena; moving seaward (Lines E-109, E-113, Fig. 6.2 B and C), maximum thickness is in the order of 1 sec. (twt). The seismic facies displayed by the structural high is characterized by a low signal/noise ratio and primary reflections are barely visible; these features fit with a carbonatic nature of the substratum, which is also confirm by the Meso-Cenozoic limestones cropping out in the mainland, in the area of the Circeo Promontory.

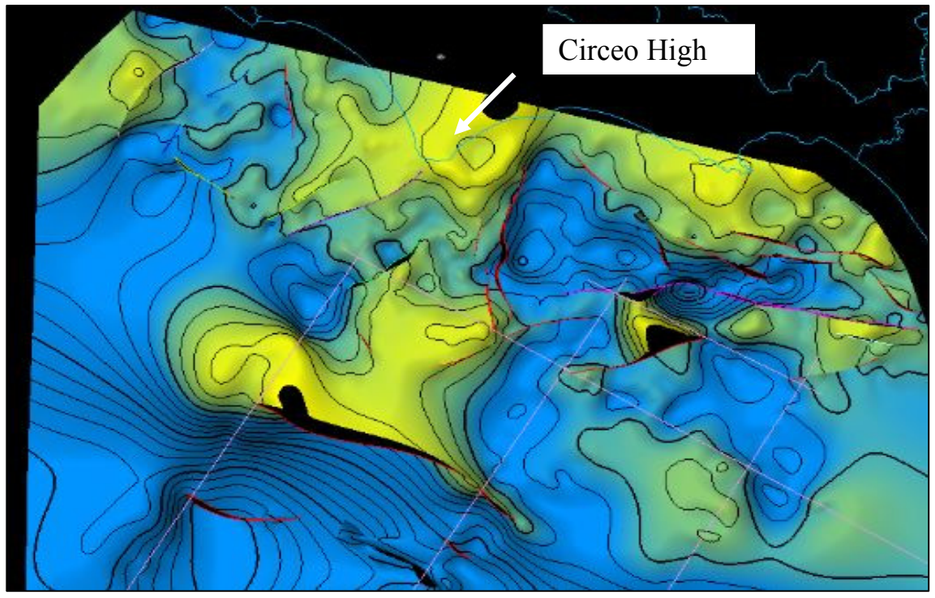


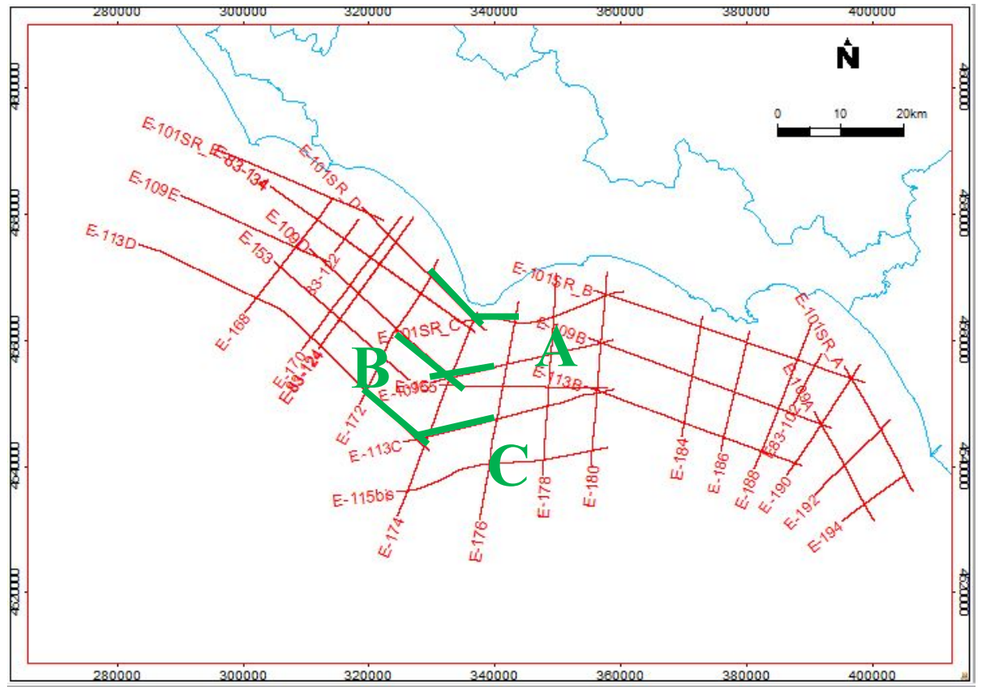


Fig. 6.2 - The Circeo High displayed on Line E-101 (A), Line E-109 (B), Line E-113 (C). Moving seaward, the structural high progressively decreases in elevation and sedimentary cover thickens. Also, from a single horst, the structural elevated area is formed by smaller horst disrupted by several faults toward the south.
Original seismic lines are available on the ViDEPI project website (www.videpi.com).

C unconformity (Middle Pliocene p.p)
B unconformity (top Messinian)
A unconformity (top Meso-Cenozic carbonates)

Generic unconformities correlated along all the dataset

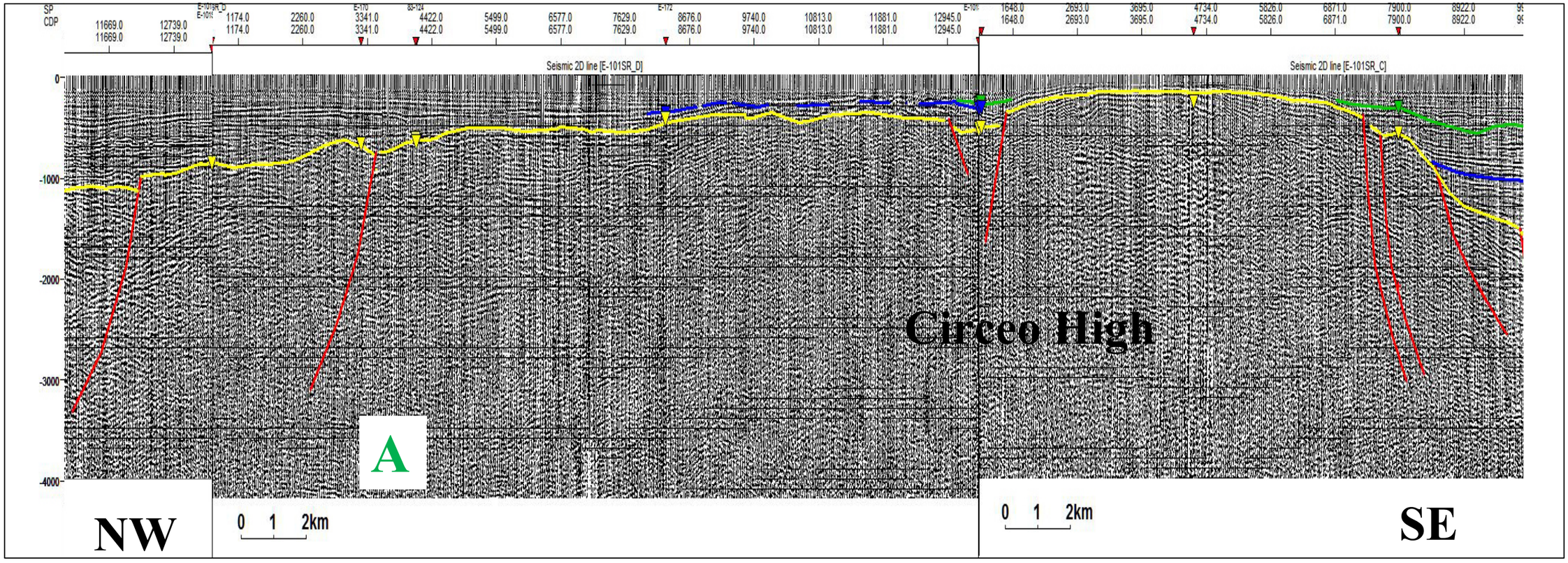

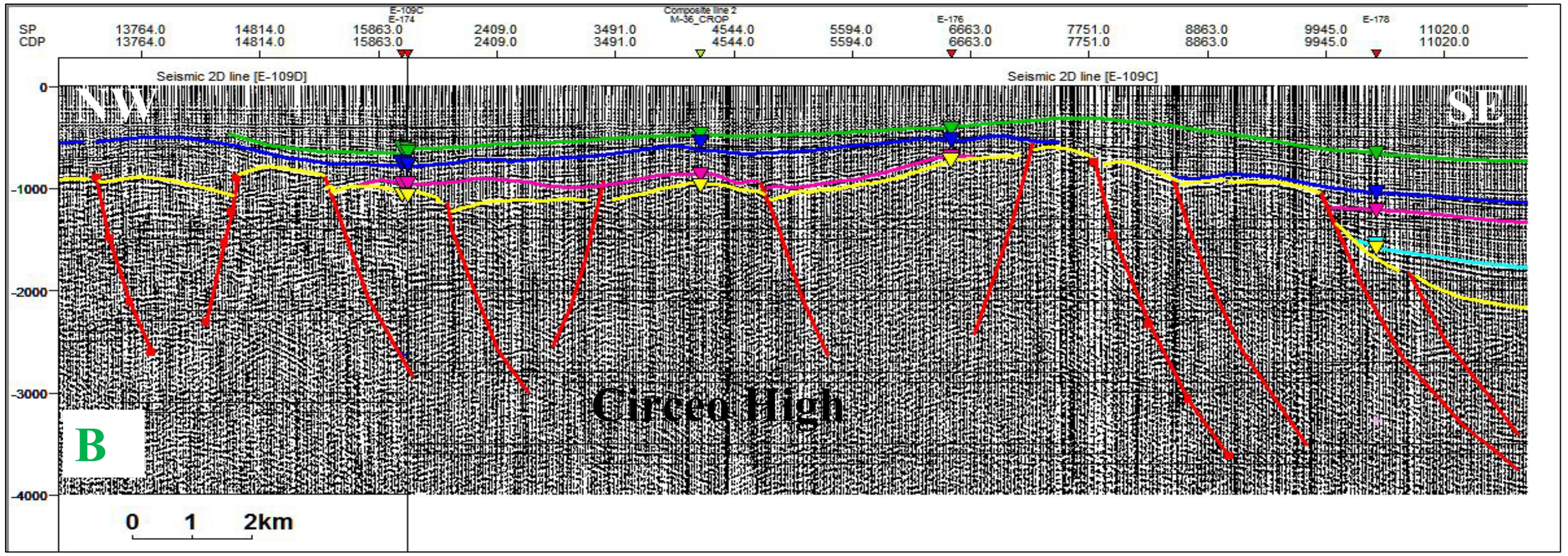
SP
CDP
13764.0
14814.0
15863.0
2409.0
3491.0
4544.0
5594.0
6663.0
7751.0
8863.0
9945.0
11020.0
E-109C
E-174
Composite line 2
M-36_CROP
E-176
E-178
Seismic 2D line [E-109D]
Seismic 2D line [E-109C]
NW
SE
0
-1000
-2000
-3000
-4000
Circeo High
B
0 1 2km

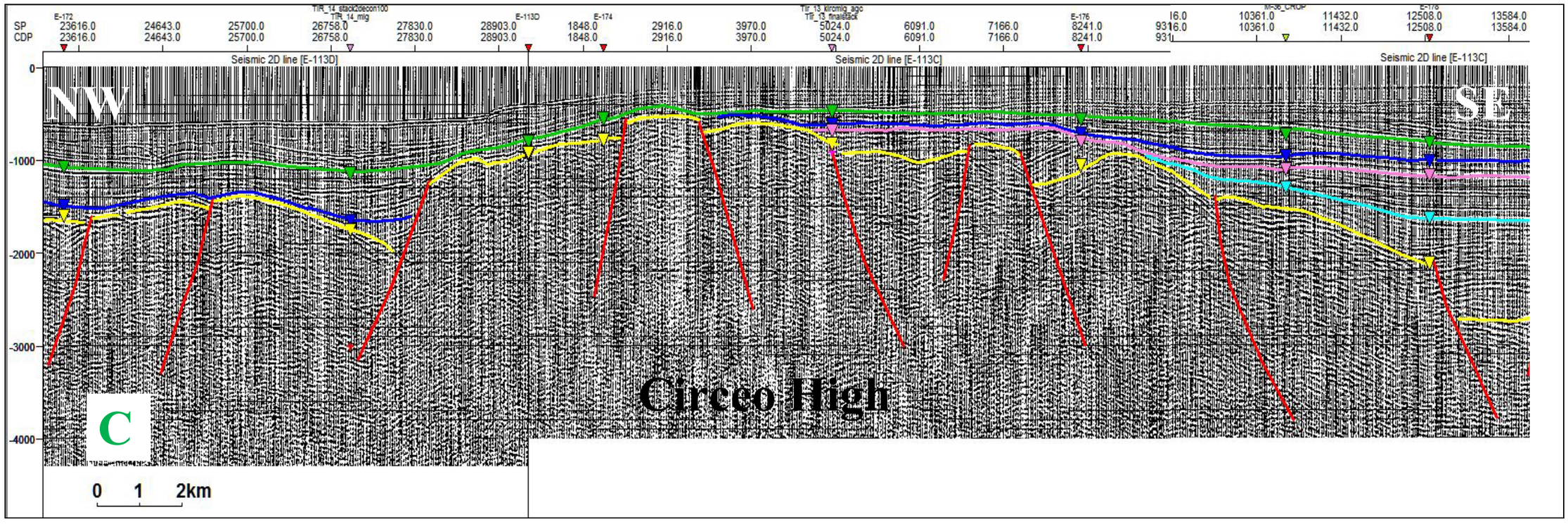
SP
CDP
23616.0
24643.0
25700.0
26758.0
27830.0
28903.0
1848.0
2916.0
3970.0
5024.0
6091.0
7166.0
8241.0
E-172
E-113D
E-174
E-176
E-178
Seismic 2D line [E-113D]
Seismic 2D line [E-113C]
NW
SE
0
-1000
-2000
-3000
-4000
Circeo High
C
0 1 2km

The Circeo High is bordered by sub-vertical normal faults; to the east, a NNE-SSW trending fault system is observed, which produces the transition to the adjacent basin, hereafter named the Terracina Basin. This basin is about 12 km long on Line E-101 (Fig. 6.3 A) and progressively widens seaward, until it merges with the basin (Gaeta Basin) to the west. The general setting is that of an half graben with a master fault system, NNE-SSW trending, bounding its western margin; here the throw is maximum, in the order of 1 sec. (twt), with the depocenter of the basin located near the master fault system. Several smaller synthetic and antithetic faults, closely spaced (few kilometers), are present, giving to the basin an articulated morphology (Fig. 6.3); they usually show small offsets and do not seem to involve the Plio-Quaternary sequence, unless sometimes in the basal part of the first infilling sequence.

The Terracina Basin infill show a maximum thickness of about 2.5-2.8 sec. twt, near its western margin; according to the seismic stratigraphic interpretation, the sediments are Plio-Quaternary in age and the main unconformities discussed in Chapter 5 (Section 5.2.1) are present. Observing Line E-178 (Fig. 6.4) which crosses the Terracina Basin in an almost N-S direction (perpendicular to the previous profiles discussed), it is possible to better outline the relationships between tectonics and stratigraphy: the basal group of seismic sequences, until the C unconformity (blue line, mid-Pliocene unconformity), shows approximately parallel reflectors, with onlap termination on the basal unconformity B (yellow line); their wedge shape, and the thickness which increases toward the master fault, let to infer a synsedimentary nature for these reflectors. C unconformity marks a change in tectonic behavior, considering that the above reflectors show an essentially progradational setting, with direction of progradation toward the south. Regarding the substratum below the B unconformity, in this sector is mostly non reflective; even tough, on Line E-178 between SP 557-1670 is possible to see reflectors of the sequence U1 (Miocenic flysch-type sediments) truncated by the main unconformity B (erosional truncation).

The western flank of the Circeo High is formed by a NE-SW trending normal fault system which downthrown the acoustic basement, dividing the horst from another basin area (Fig. 6.5); the latter display a graben setting and extends until offshore Anzio city, where another horst is present, bounded by another NE-SW trending fault, dipping toward the SE. Unconformity B is well visible all over the basin, and it is cut by several minor faults, sometimes showing lower angles or listric geometries, with opposite dipping; as a consequence, the basin substratum is very articulated. Maximum offsets are localized at the horst-bounding faults and are in the order of 0.7-0.8 sec twt. The Plio-Quaternary infill reaches the maximum thickness of 1.8 sec twt on Line E-113: seismic unconformities are not distinguishable in this sector and, as it occurs on the Terracina Basin, they seem to be mostly undeformed. The crossline E-172 (Fig. 6.5 B) shows that the basin substratum lowers also toward the south and the Plio-Quaternary cover shows a progradational setting in its upper part.

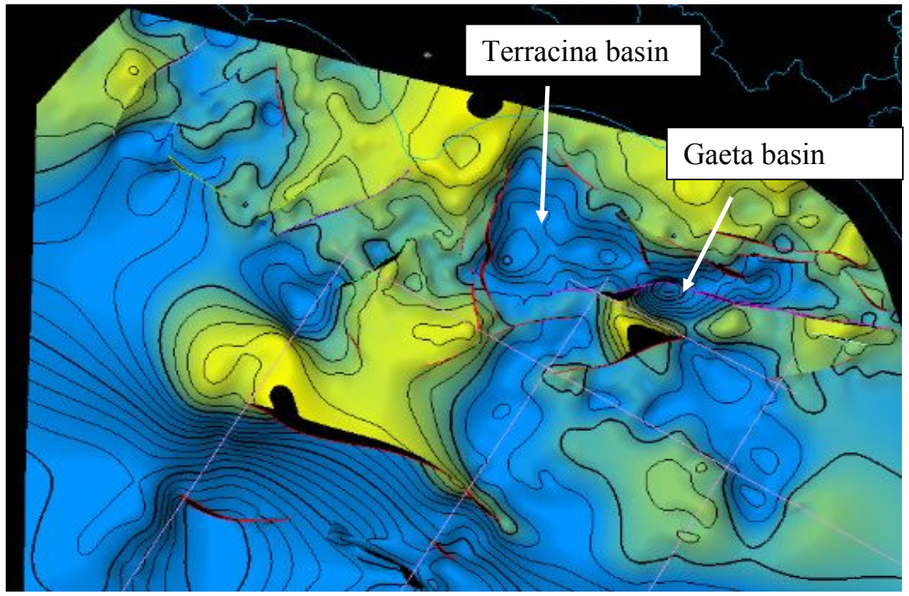


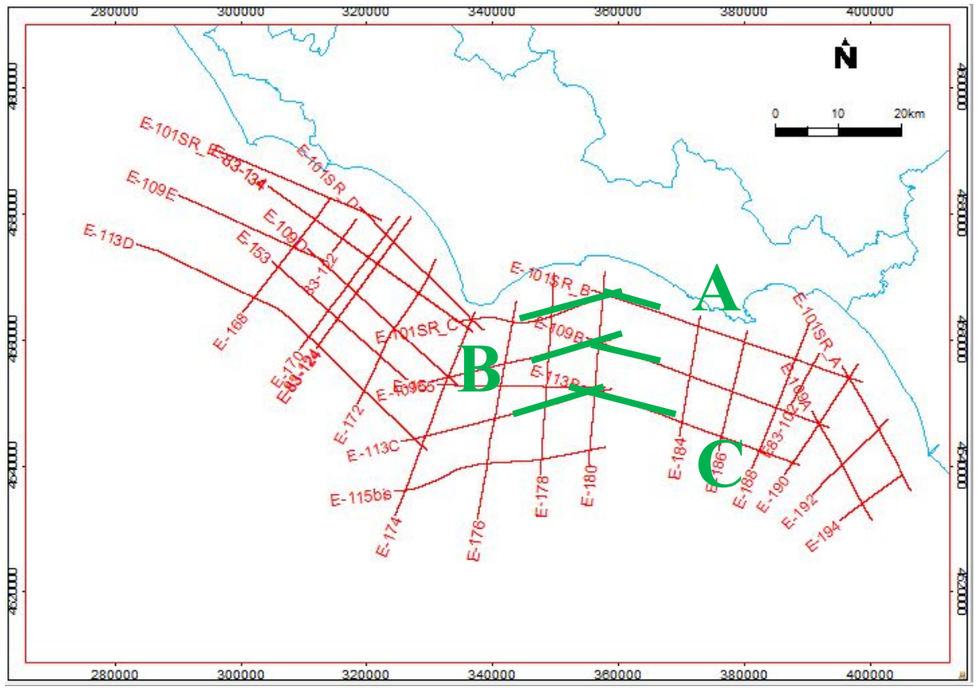


C unconformity (Middle Pliocene p.p)
B unconformity (top Messinian)
A unconformity (top Meso-Cenozic carbonates)
Generic unconformities correlated along all the dataset

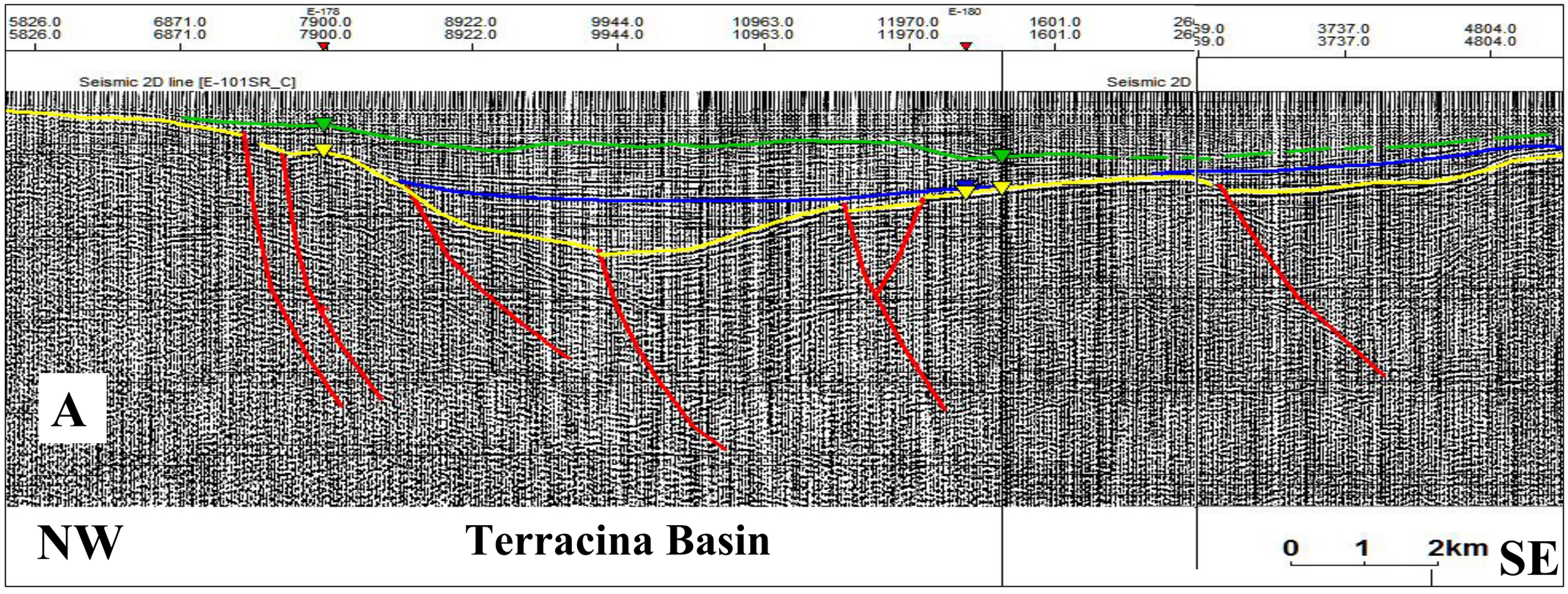


Fig. 6.3 - The Terracina Basin displayed on Lines E-101 (A) and E–109 (B). Moving seaward the basin merges with the Gaeta basin, like display on Line E-113 (C). Original seismic lines are available on the ViDEPI project website (www.videpi.com).

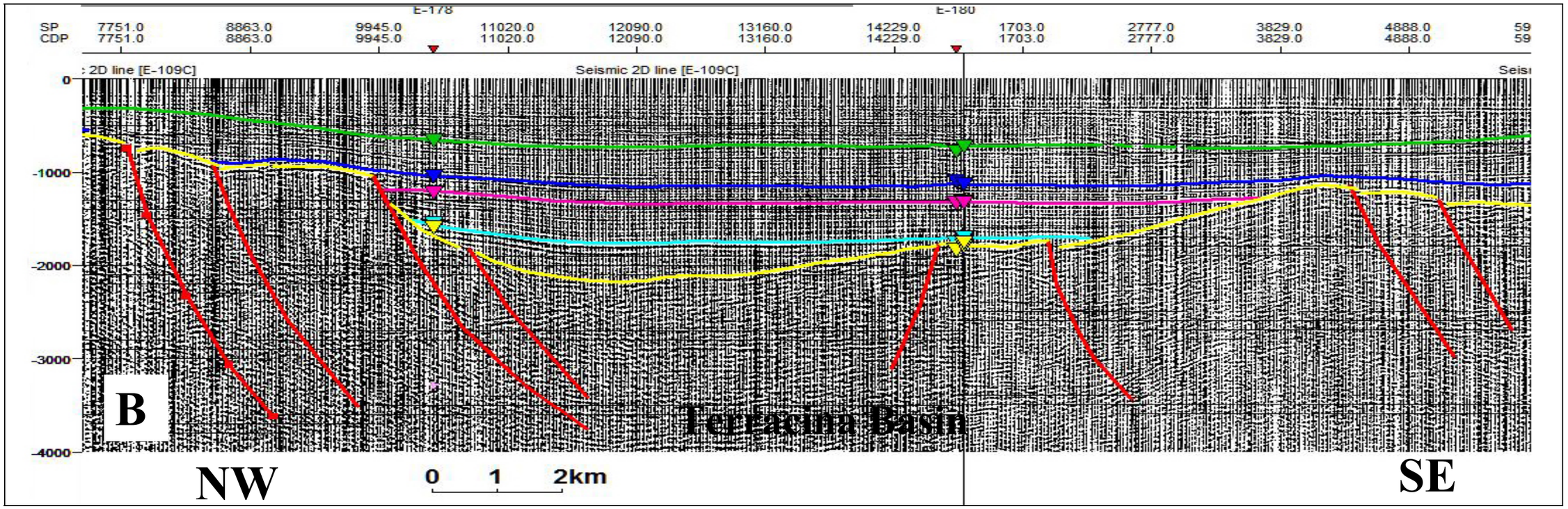
SP
CDP
E-178
E-180
: 2D line [E-109C]
Seismic 2D line [E-109C]
0
-1000
-2000
-3000
-4000
B
Terracina Basin
NW
0 1 2km
SE

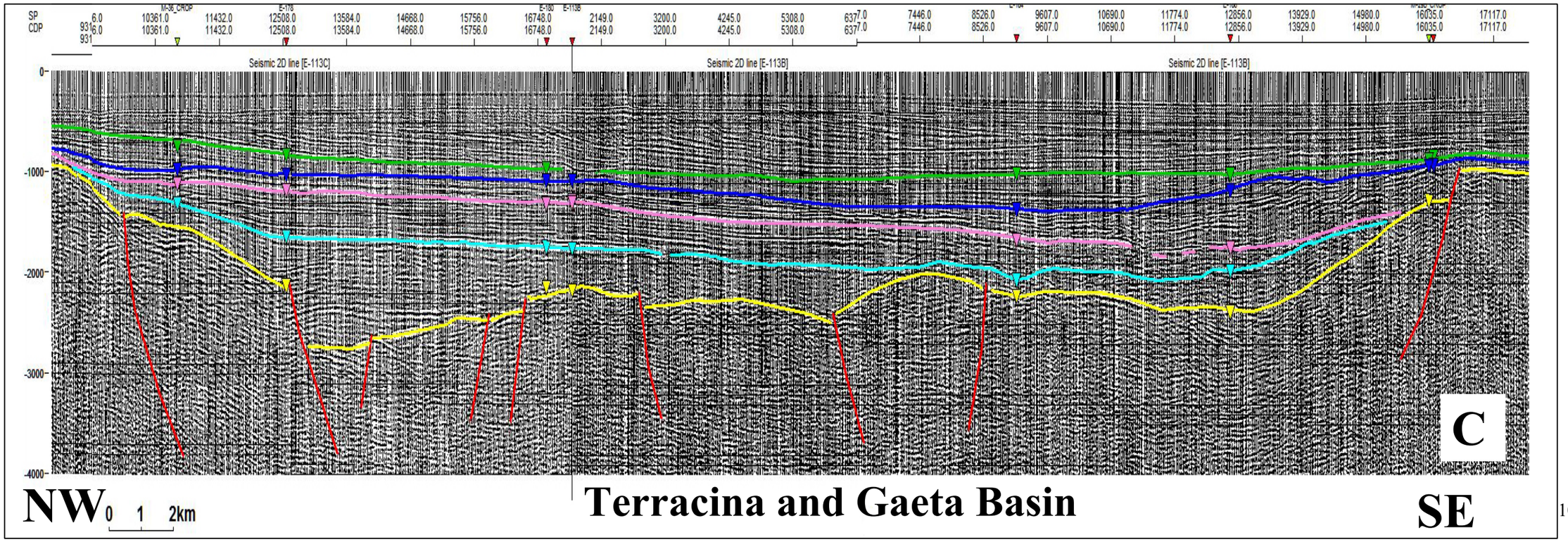
SP
CDP
M-36_CROP
E-178
E-180
E-113B
Seismic 2D line [E-113C]
Seismic 2D line [E-113B]
Seismic 2D line [E-113B]
0
-1000
-2000
-3000
-4000
C
NW
0 1 2km
Terracina and Gaeta Basin
SE

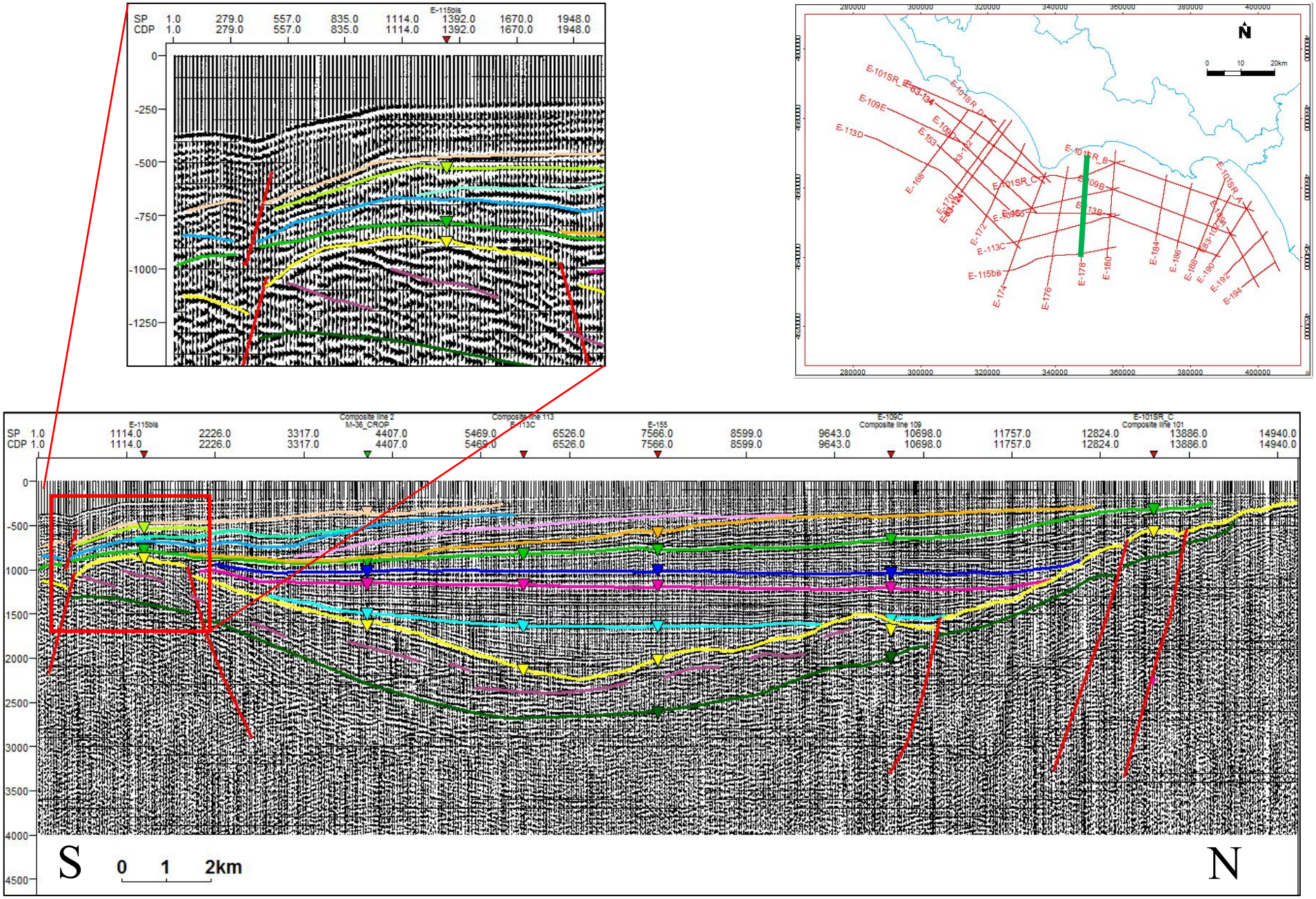


Fig. 6.4 – Line E-178, N-S trending, crossing the Terracina basin. Upper part, a detail (red box) showing reflectors of the sequence U1 truncated by the main unconformity B (yellow line). Original seismic line available on the ViDEPI project (website www.videpi.com). Colors same as Fig. 6.3.

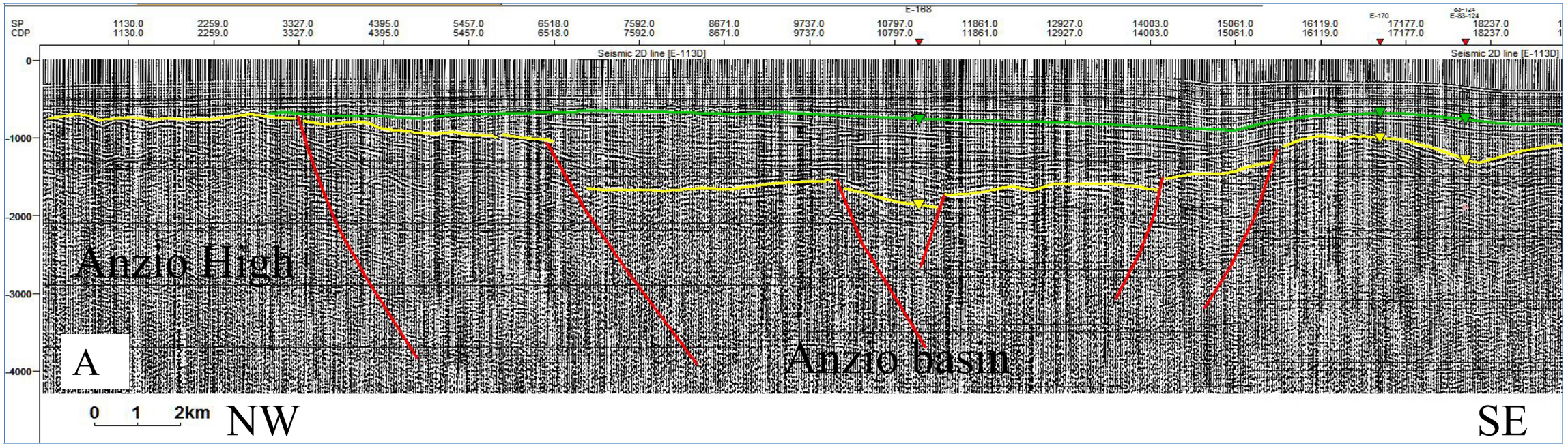


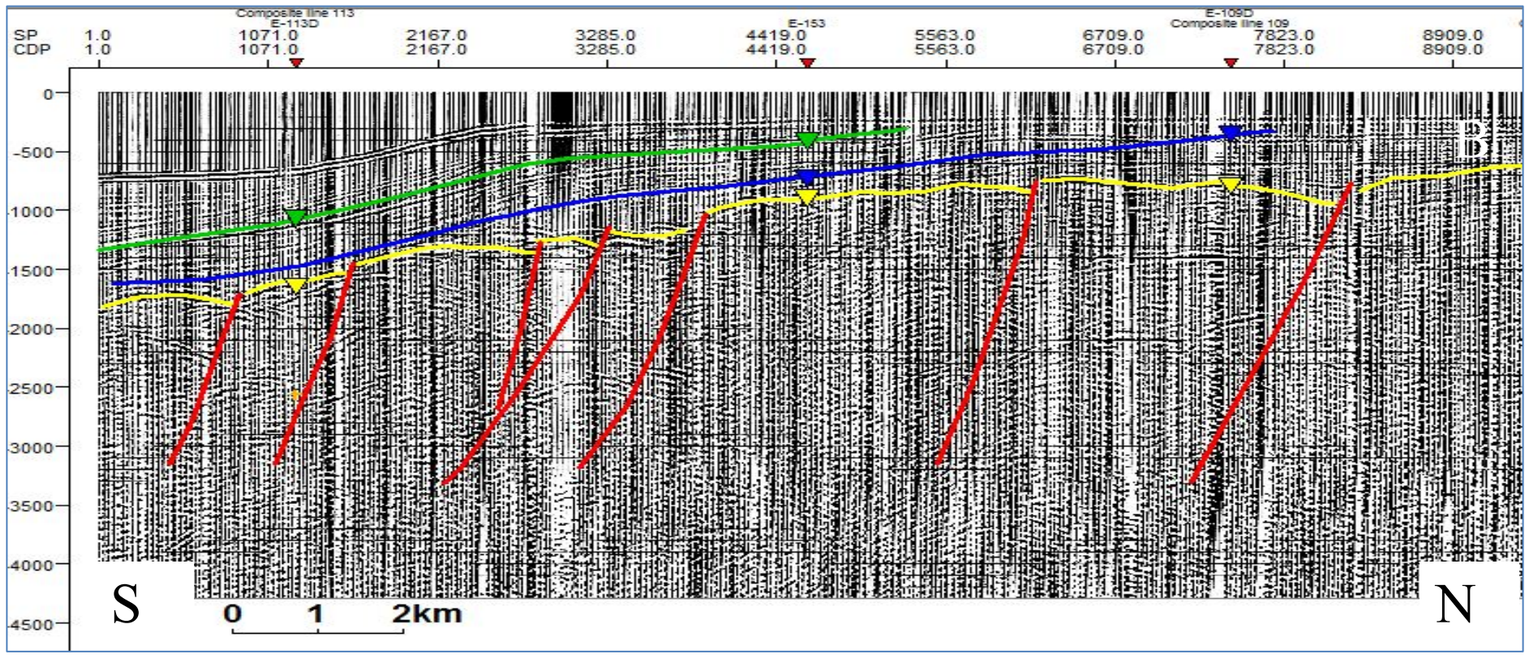


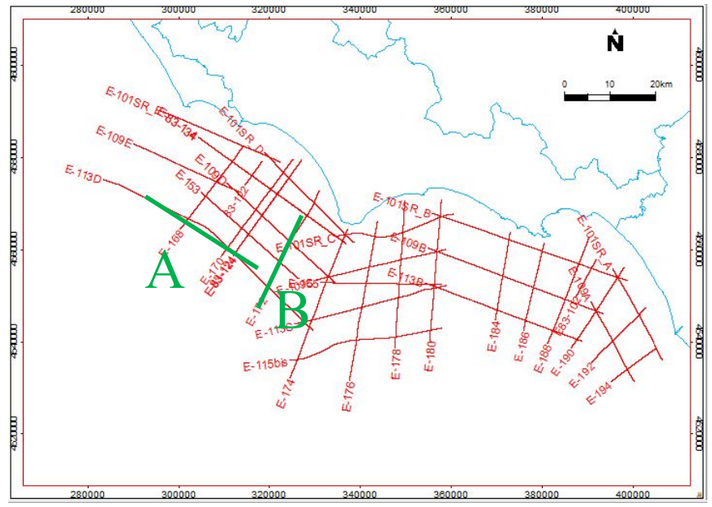


C unconformity (Middle Pliocene p.p)
B unconformity (top Messinian)
A unconformity (top Meso-Cenozic carbonates)

Generic unconformities correlated along all the dataset

Fig. 6.5 – Anzio basin and Anzio High on Line E-113D (A). In B the N-S trending Line E-172, showing the substratum lowered toward the south and progradational clinoforms in the upper part.
Original seismic lines are available on the ViDEPI project website (www.videpi.com).

The Terracina basin is divided from another basin, the Gaeta basin, by the presence of another structural high located on the offshore extension of the Gaeta Promontory; it is visible on line E-101 between SP 6946-14518 (Fig. 6.6 A), where it displays its maximum structural elevation, with an almost horizontal top probably testifying sub-aerial exposure. Moving seaward the simple horst visualized on Line E-101 becomes a wide area of structural highs, showing lower structural elevation (Fig. 6.6 B, SP 8140-15630); finally, on Line E-113, the two basins - Terracina and Gaeta – merge to form a single basin, W-E trending (Fig. 6.3 C). The horst, located offshore, for its seismic facies characteristics (substratum no reflective or poorly reflective, chaotic reflectors) can be considered of carbonatic nature and it matches the carbonatic outcrops present in the mainland, in the Aurunci Massifs.

The western flank of this structural high is formed by a high angle, NW-SE trending master fault, which delimits toward the east the Terracina basin; thereby, the basin assumes a triangular shape, bordered toward the south by W-E trending normal faults. This latter trend is the extensional feature responsible for the formation of the Gaeta basin: this basin is delimited to the north and to the south by W-E antithetic normal faults which downthrown the acoustic basement; maximum offsets are in the order of 0.5-0.8 sec (twt). This W-E trend is characterized by a lower dip angle and an approximately listric geometry. The basin fill reaches a maximum thickness of the order of the 2 sec (twt) and it shows the same seismic units already recognized in the Terracina basin and correlated along the entire dataset; even though, in this sector the sedimentary cover seems to be more involved in the deformation, with faults cutting also the C unconformity (blue line, Fig. 6.7 A and B).

Gaeta basin is limited in its eastern margin by a horst structure (Fig. 6.8), representing the seaward extension of the Mt. Massico, which divides the Garigliano and the Volturno plains onshore. From the directions observed in the mainland, the Massico horst is bordered by two antithetic NE-SW trending faults. Offshore, on the profile E-101, the Massico horst is located between crosslines E-190 and E-192; on the line E-109, located about 8 Km seaward, it is located between lines E-192 and E-194: this means that the horst is shifted of about 8 km. As already pointed out by Bruno et al. (2000) and how is possible to notice in (Fig. 6.8 B), the horst display a roughly flat morphology at the top and prograding beds along the sub vertical fault boundaries, which show a downlap termination on unconformity B (yellow line). The above reflectors onlap the structure, until the structural high is completely blanket and the reflectors bypass the structure in the uppermost part of the Plio-Quaternary sequence. The prograding beds seem to be characterized by slumping structures.

Eastern of the Massico structural high the Volturno basin is present, which lays outside the area investigated by this research; according to Aiello et al. (2011), Volturno basin is an half graben characterized by downthrown blocks along normal faults; Plio-Quaternary cover is formed by deltaic sediments coming from the Volturno river. As also pointed out by the well analysis in Chapter 5, here the Plio-Quaternary sediments reach their maximum thickness, both onshore (3000 m of Quaternary in Castelvolturno well) than offshore (maximum thickness above the substratum is around 2.5 - 3 sec twt according to Aiello et al., 2011).

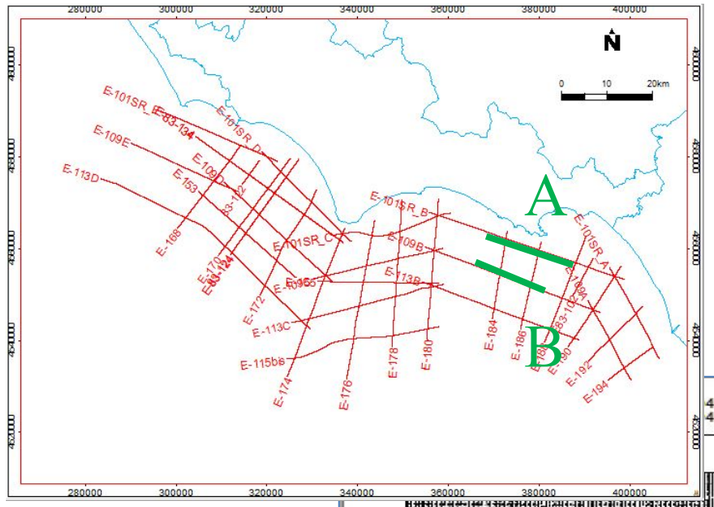


Fig. 6.6 - Gaeta High shown on Lines E-101 (A) and E-109 (B); this structural high divides the two basins of Gaeta to the east and Terracina to the west. On line E109 (B) the high shows minor structural elevationand is formed by a wider area of faulted blocks. Original seismic lines are available on the ViDEPI project website (www.videpi.com).

C unconformity (Middle Pliocene p.p)
B unconformity (top Messinian)
A unconformity (top Meso-Cenozic carbonates)

Generic unconformities correlated along all the dataset

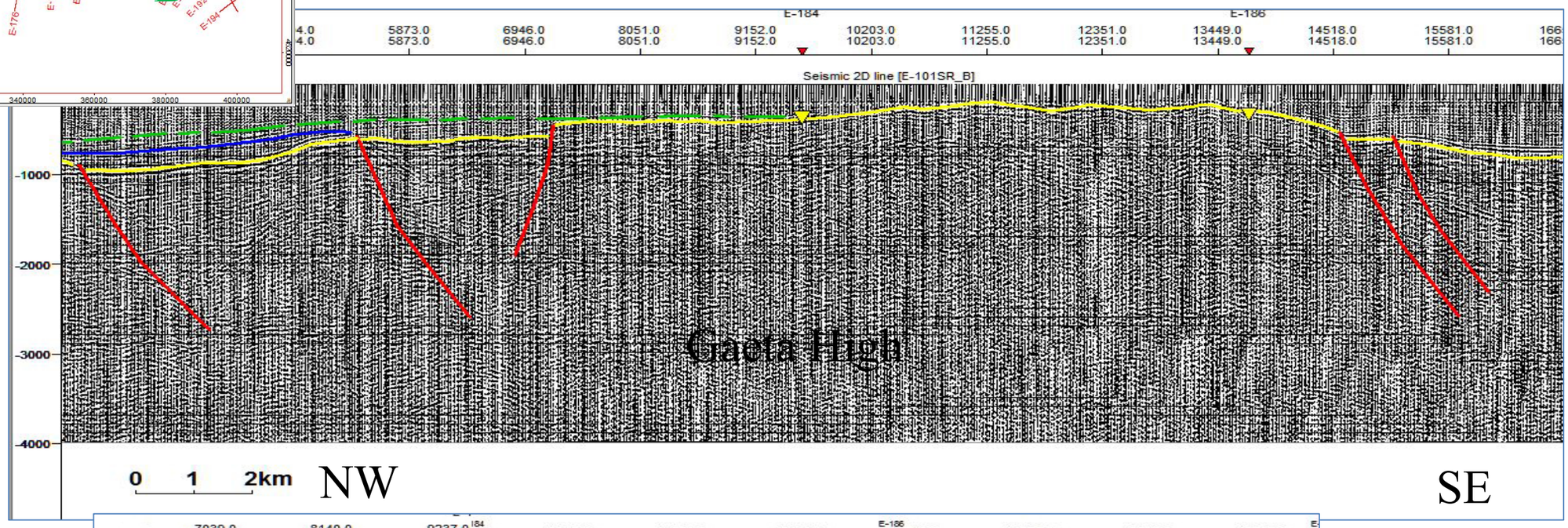


A

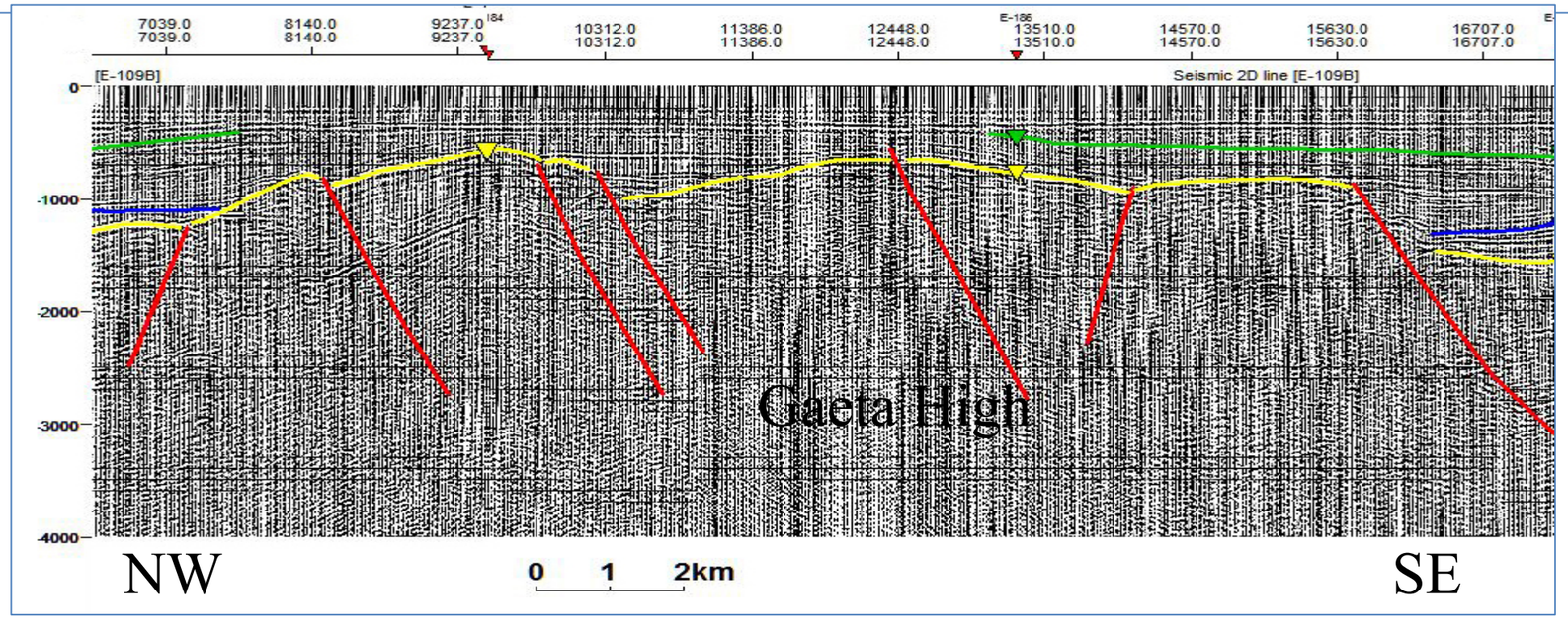


B

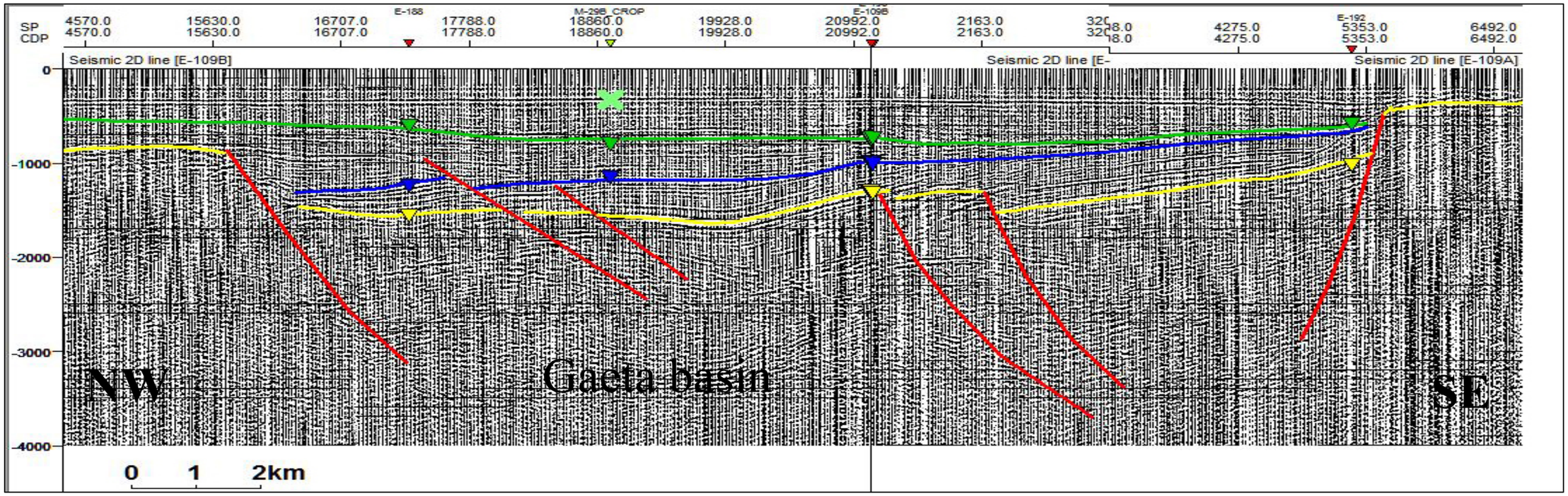


A

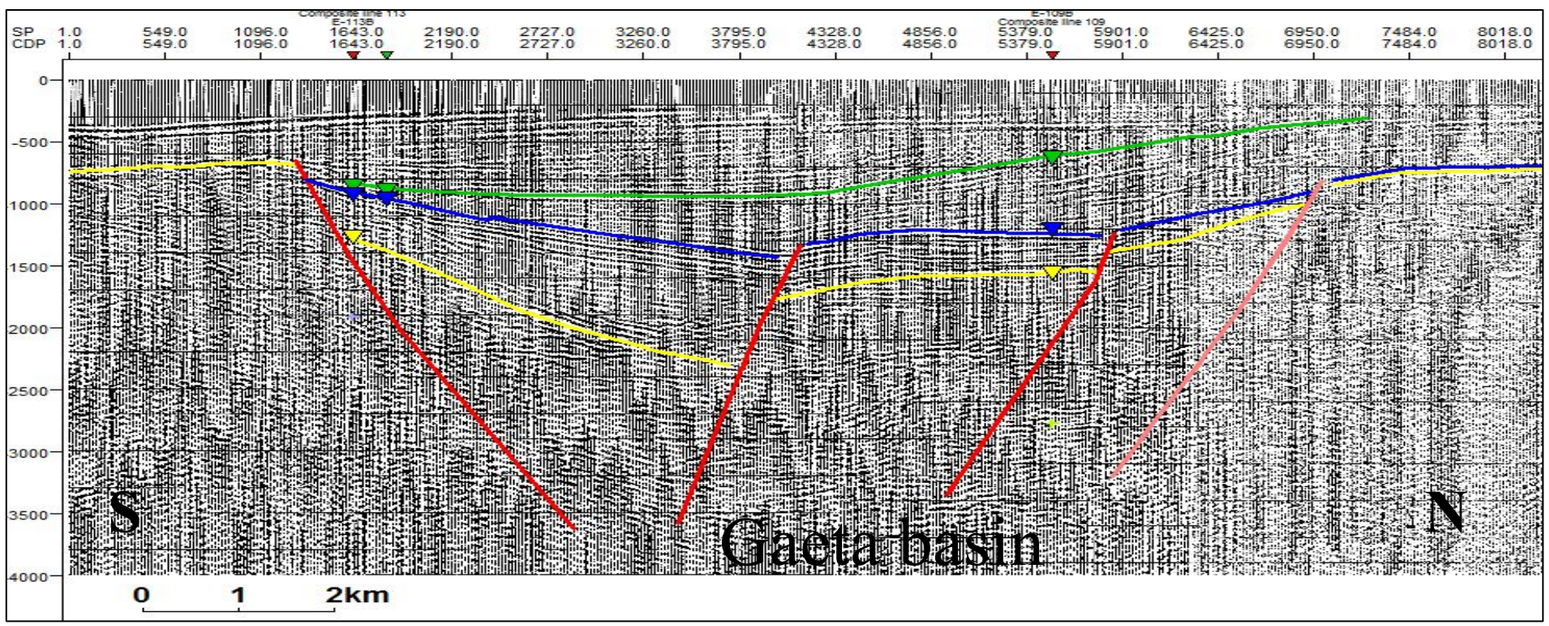


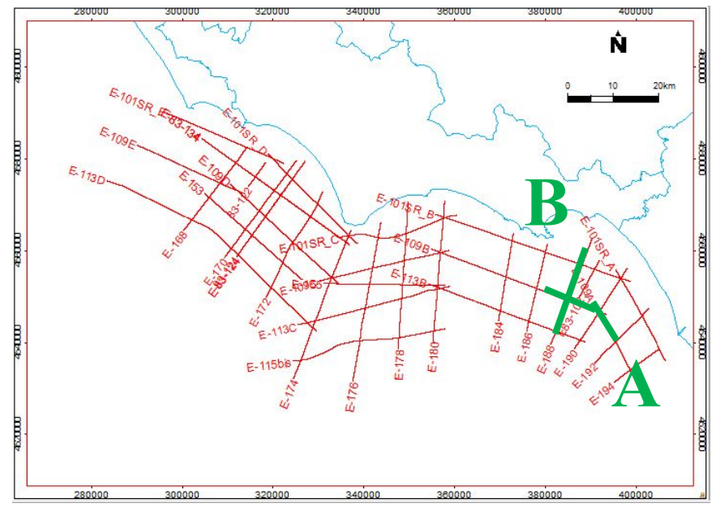


Fig. 6.7 - Gaeta basin displayed on two perpendicular profiles: E- 109 (A) and E-188 (B). C unconformity in this sector is offset by the extensional faults. Original seismic lines are available on the ViDEPI project website (www.videpi.com). Horizon colors same as Fig. 6.6.

B

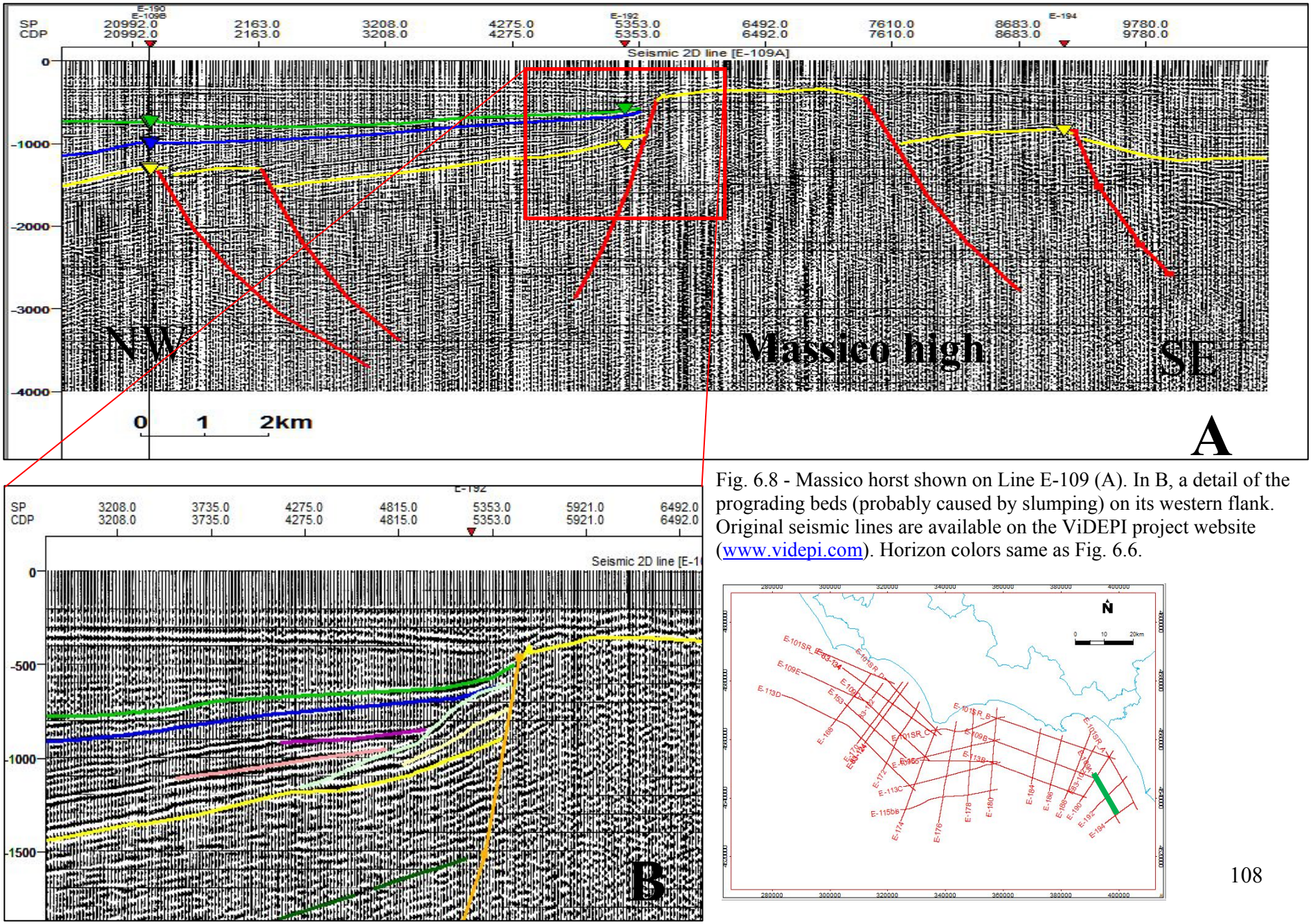


Fig. 6.8 - Massico horst shown on Line E-109 (A). In B, a detail of the prograding beds (probably caused by slumping) on its western flank. Original seismic lines are available on the ViDEPI project website (www.videpi.com). Horizon colors same as Fig. 6.6.

## 6.2 The continental slope sector

### 6.2.1 The intraslope basins

The investigated area is characterized by a complex slope sector that border the Vavilov abyssal plain, situated toward the east and 3500 m deep; the slope is about 15 Km large around the Western Pontine Archipelago and it progressively widens toward the south.

The upper-slope sector is characterized by the presence of two intraslope basins, named the Palmarola Basin and the Ventotene Basin (Zitellini et al., 1984), located respectively to the NW and to the SE of the Capo Circeo-Ponza alignment.

The southeastern portion of the Palmarola Basin is investigated by the initial part of Line TIR-14, from SP 101 to 580 (Fig. 6.9); this seismic profile extends for a length of about 85 Km in a NE-SW direction; it starts on the edge of the continental shelf, offshore Circeo promontory, and crosses the Palmarola basin east of Palmarola island, continuing then until the Farfalla seamount.

At the NE extremity of the line a set of prograding units are displayed, equivalents to the prograding units observed on the parallel profiles E-172 (Fig. 6.5 B); these sequences extends from the continental platform into the basin, filling it. The maximum thickness of the sedimentary infilling is in the order of 1,5 sec twt and three main unconformities are recognize by means of correlation from seismic profiles of the E survey: the lower unconformity correspond to the top of the Messinian (B unconformity, yellow) and shows a variable depth between 1 and 2,2 sec (twt), deepening seaward. Several extensional faults, NW-SE trending and dipping seaward, are responsible for the lowering of the substratum and the formation of the basin; they do not affect the sedimentary fill of the basin, except probably the bottom part of the lowest sequence. The seaward margin of the basin is formed by an antithetic fault (NW trending, dipping toward the mainland) which shows a throw of more than 1 sec twt and that bound the Palmarola structural high. This is the master fault that probably controlled the formation of the basin; the extension provoked by this feature started during late Messinian-early Pliocene but probably acted until Quaternary times. Above the Messinian unconformity the lower Pliocene unit (U2) lays, characterize by sub-parallel reflectors, with low amplitude and frequency, onlapping the unconformity B. Above the latter surface, the mid Pliocene-Pleistocene sequence is displayed: the lower part shows low to medium amplitude and frequency reflectors, with a discontinuous pattern in the lower part, sub-parallel in the upper part; starting from the unconformity signed by the green line, the progradational pattern become evident. Another important unconformity surface seems to be the one localized around 0.8 sec. (twt); the upper reflections seems to onlap this surface whereas the presence of localized chaotic reflections “resting “ on this unconformity, presumably represents a slumping deposit.

The Palmarola Basin in this sector is delimited seaward by the Palmarola-Ponza High (Fig. 6.10); this feature is shown on seismic line TIR-14 between the SP 580-900. Seafloor is localized around 0.1 sec (twt) and in this sector no real reflections are displayed on the seismic line below.

Fig. 6.9 - Palmarola basin shown on TIR 14 Line, bordered to the southwest by a master fault trending NW-SE, dipping toward the mainland; the arrow indicates a deposit probably due to instability phenomena.

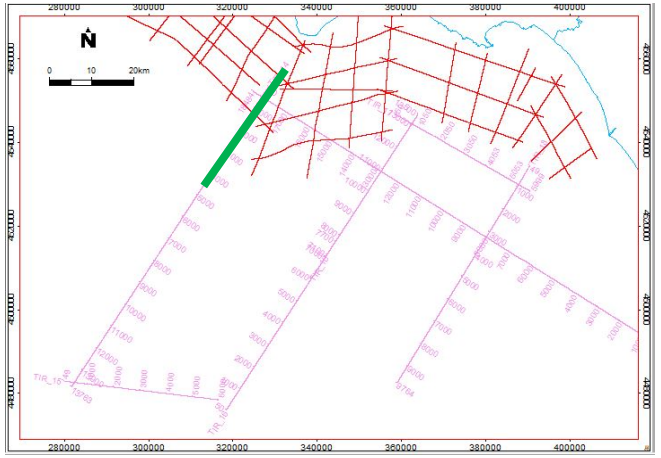


TIR-14

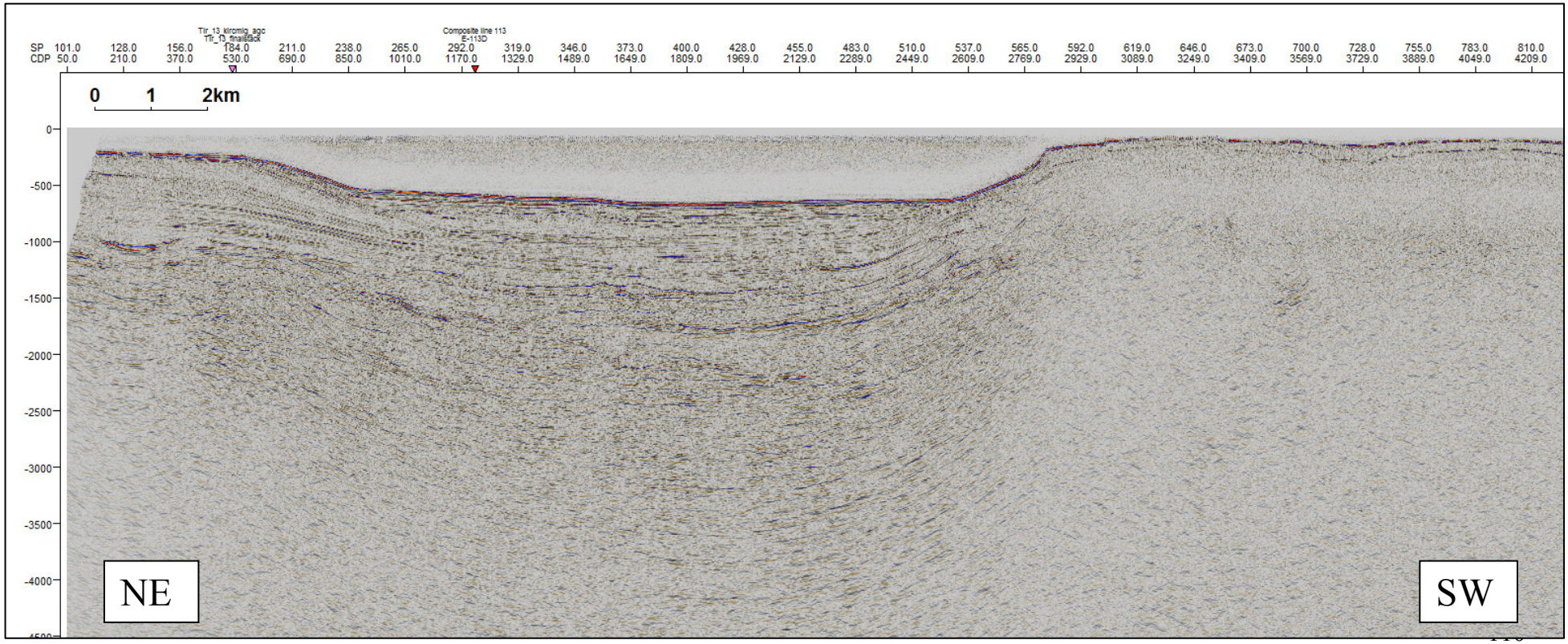

C unconformity (Middle Pliocene p.p)

B unconformity (top Messinian)

A unconformity (top Meso-Cenozic carbonates)

Generic unconformities

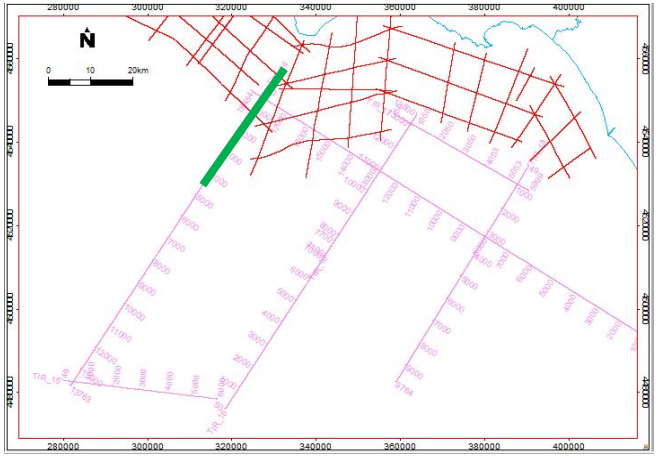

TIR-14

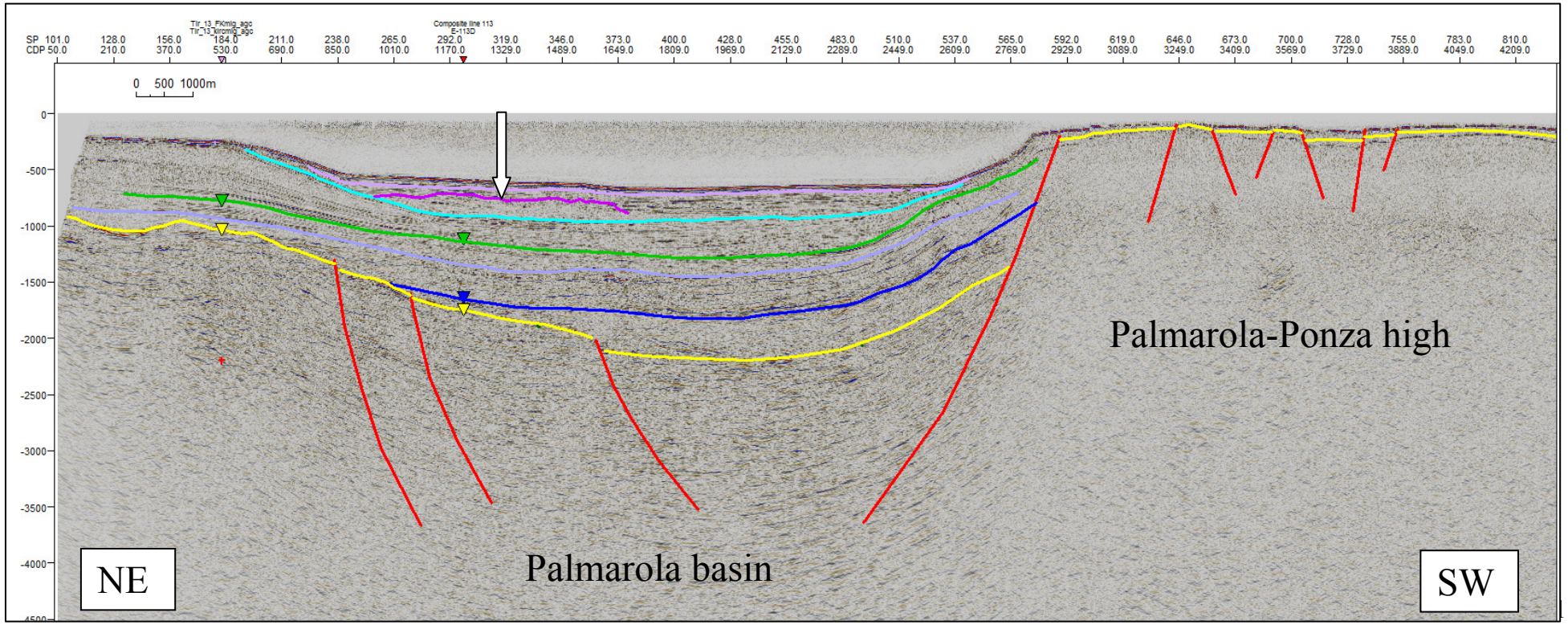

The seabottom reflector, also because strong multiple reflections are present, was not completely eliminated by the processing. The strong reflectivity of this horizon let to infer the presence of a hard substratum that could be linked to the volcanic nature of Ponza and Palmarola products, or to the Meso-Cenozoic carbonatic basement, here in an elevated structural position.

Actually, Paleozoic metamorphic and Meso-Cenozoic sedimentary units crop out in the near island of Zannone, the only island of the archipelago showing a sedimentary sequence in outcrop. Both the flanks of the horst are delimited by extensional, high-angle normal faults, the one previously mentioned dipping toward the Palmarola basin, and the antithetic fault system dipping southwestward; this system is indeed the responsible of the formation of the steep escarpment facing the Vavilov basin. Several minor discontinuities are visible on the structural high, with little offset, cutting the present seafloor. This same structural high also borders the eastern margin of the Palmarola basin and separates it from the adjacent Ventotene basin; according to De Rita et al. (1986) a NE-SW en-echelon trending faults affects in this sector the margins of Palmarola - Ponza high in Fig. 6.10 (bottom), producing the lowering southeastwards to the Ventotene Basin and less abruptly, to the NW, toward the Palmarola Basin.

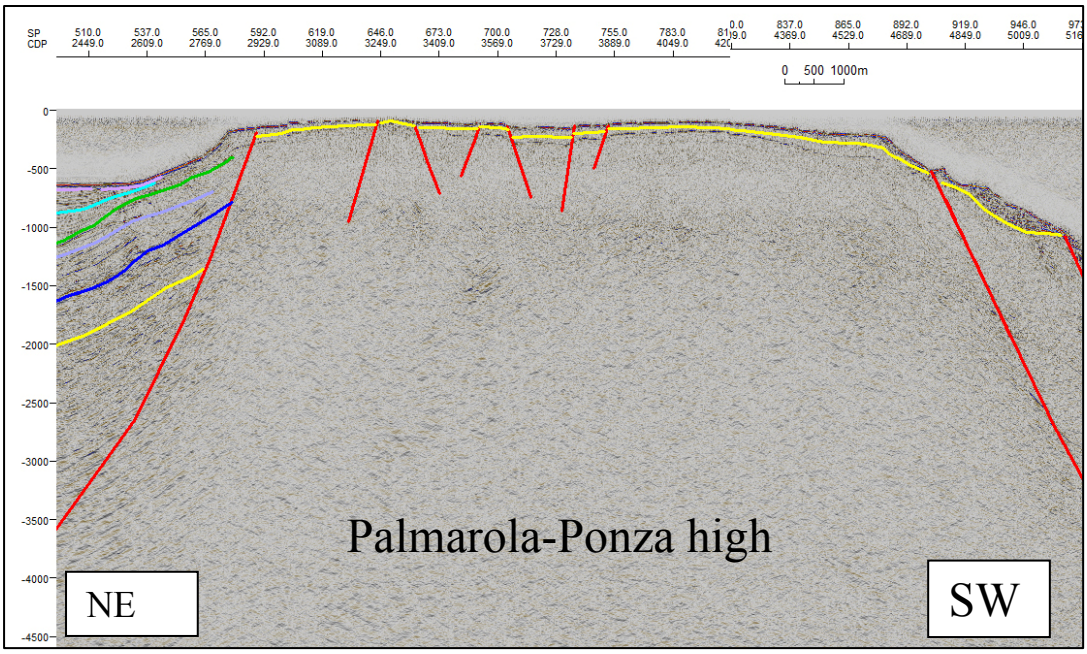


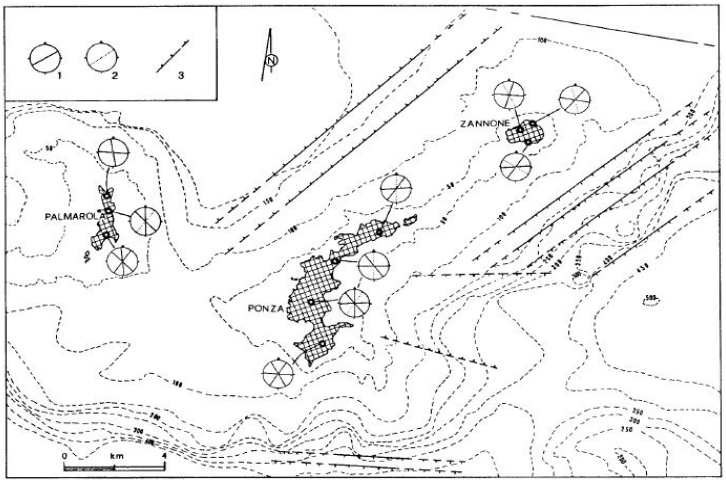


Fig. 6.10 Above, the Palmarola-Ponza high; bottom, fault systems bordering the structural high (De Rita et al 1986)

Ventotene basin extends east of the Capo Circe-Ponza alignment, reaching approximately the Ischia island; the islands of Ventotene and Santo Stefano represent the sub-aerial portion of a large submerged strato-volcano emplaced at the centre of the basin. Several lines investigate this portion of the Latium-Campania upper slope.

TIR-17 seismic profile (Fig. 6.11 A) runs in a NW-SE direction for a length of about 37 Km and it is localized on the northern border of the Ventotene basin, just south of the -200 m isobaths. In its initial part, at the NW side, the line displays a 1 sec. (twt) thick sedimentary infill, lying above an acoustic substratum affected by extensional tectonic. Reflections are discontinuous in the lowermost part, where they seem to be affected by the extensional or transtentional faults system involving the basement. The upper seismic reflectors are continuous and parallel, they display a prograding pattern in the uppermost part and are not involved in the deformation.

Moving to the SE along the line, a cone-shaped structure deforms the acoustic substratum; according to the geometry displayed by de termination of the sedimentary reflectors on the western flank of this object, no fault is detected: reflectors are interpreted to be folded but not cut. So the origin of the cone-like structure is inferred to be more likely link to some volcanic origin rather than structural. Available magnetic data show a positive magnetic anomaly in correspondence of this structure, supporting the volcanic origin, but not excluding some other hypothesis. It must to be notice that also the sea bottom is deformed in correspondence of the western flank of the structure. Its eastern flank instead is more clearly affected by normal faulting, which involves the entire basement further display, here localized at shallow depths, less than 0.5 sec. (twt). This morpho-structural high zone (SP 340-580) is characterized by a strongly dissected basement overlain by thin layers of sedimentary cover; they seem to form small basins often bounded by tilted blocks and display strong wedging and strata growth. Seismic signal scarcely penetrates the basement, so the acoustically transparent seismic facies is interpreted as the carbonatic unit of Meso-Cenozoic age. At shot point 584 the seismic line intersects a main tectonic alignment which causes the down-throwing of the structural high zone: the offset is about 1.2 sec. (twt) and this master fault bounds the Ventotene basin which developed toward the rest of the line. The basin in this sector shows a gentle syncline geometry, with the basement rising again toward the SE and dissected by extensional faults, especially at the margins of the basin, where tilted faulted blocks are displayed. The infilling succession is composed in general by parallel to sub-parallel seismic reflectors, from high to low amplitude, mostly continuous; the lowermost seismic unit seems to be syn-tectonic, with a wedge geometry thinning to the SE on the basement highs. A relic prograding wedge is interpreted at the hangingwall of the master fault bordering the western flank of the Ventotene basin. Also along this line, in the south-eastern sector, some incipient faulting seems to affect the upper part of the quaternary sequence, as faults (which show no offset) develop and reach the sea-bottom.

The Plio-Quaternary filling of the Ventotene basin lies above a seismic unit displaying a chaotic acoustic facies, with weak discontinuous and disrupted reflectors; they could be tentatively refer to a flysch deposit, also suggested by correlation with the onshore geology (Flysch del Cilento). The deepest seismic unit, showing an acoustically transparent facies, is

instead interpreted as the Meso-Cenozoic carbonates, which constitutes the bulk of the stratigraphic architecture of the margin.

Also TIR-13 (Fig. 6.11 B) crosses the Ventotene basin in a NW-SE direction, but it investigates the central part of the basin, just north of the islands. At SP 4740 the NE-SW trending master fault that determines the transition from the Ponza-Palmarola high to the Ventotene basin is displayed: it is formed by a system of en-echelon listric faults, dipping toward the SE, with some small antithetic faults present. The sedimentary infill is composed by different sequences bordered by main surface unconformities, laterally thinning and onlapping the basal acoustic basement unconformity. The internal organization of the seismic sequences is characterize by parallel to subparallels reflectors, mostly continuous and the main unconformities correspond to the top of the Messinian (B unconformity), mid-Pliocene (C unconformity) and the general unconformities comprised in the mid-Pliocene-Pleistocene sequences are recognized. Maximum thickness is in the order of 1 sec. (twt), which means about 1100 m of thickness using velocities around 2200-2300 m/s. The basin has a general syncline setting, but it is divided in two depocenters by the structures visible between shot points 4400-4250: a graben is displayed, bordered by two conjugate faults; at the center of the graben cone shaped structures are then visible, deforming also the sea bottom, whose origin seems to be volcanic rather than tectonic; in the literature no volcanic bodies are pointed out in this sector. The basin continues further of this structure, with the basement localized around 1,5 sec (twt) of depth; at SP 4100 until 3790 small cone shaped structures affecting also the seafloor are shown and in this case, considering the proximity with the Ventotene island, they are considered part of the Ventotene volcanic complex. A thin sedimentary cover drapes the volcanic structures, being thinner the ones proximal to the Ventotene island, more to the SE. Moving southeastward, TIR-13 line enters in the eastern portion of the Ventotene basin, which displays characteristics similar to the previous described sector, until it reaches the Ischia island area, which is not part of this research.

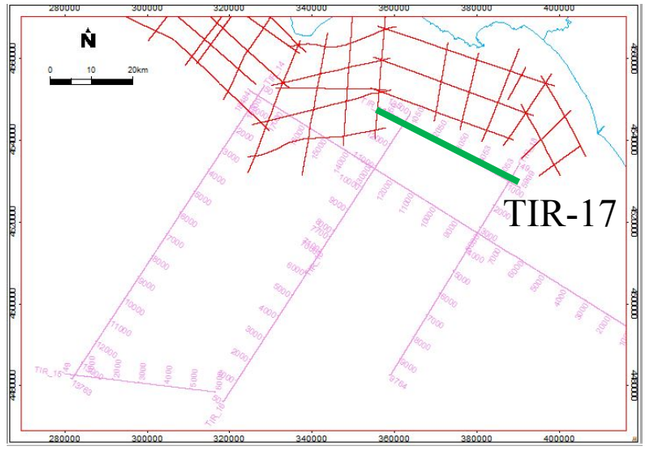


Fig. 6.11 A – Structural setting of Ventotene basin shown on seismic profiles TIR-17. White arrows indicate the probably volcanic features find in the area, not indicated by the structural map of Italy (1991).

C unconformity (Middle Pliocene p.p)

B unconformity (top Messinian)

A unconformity (top Meso-Cenozic carbonates)

Generic unconformities

A

TIR-17

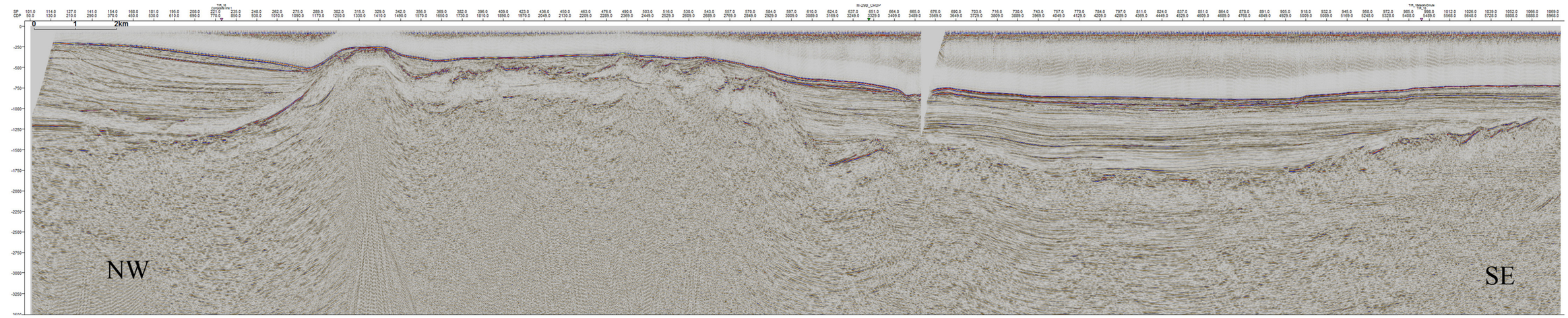


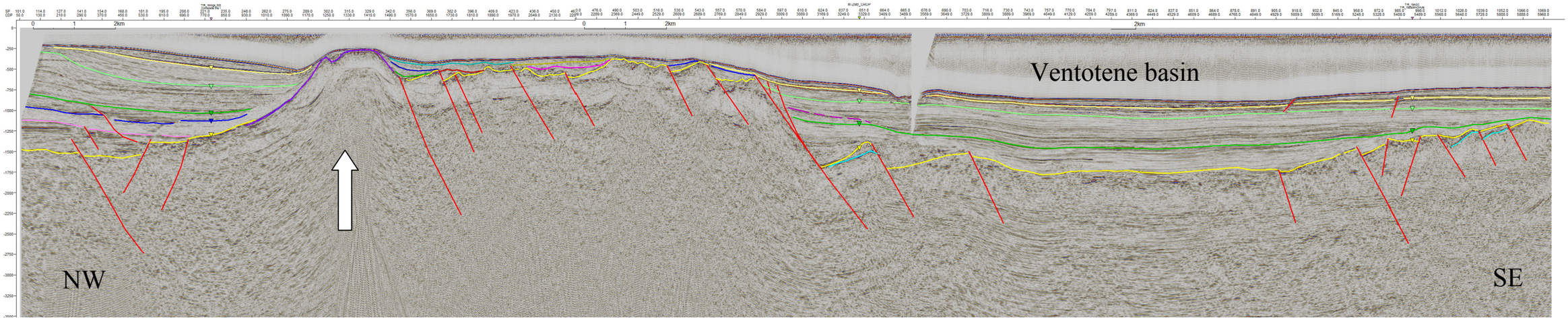

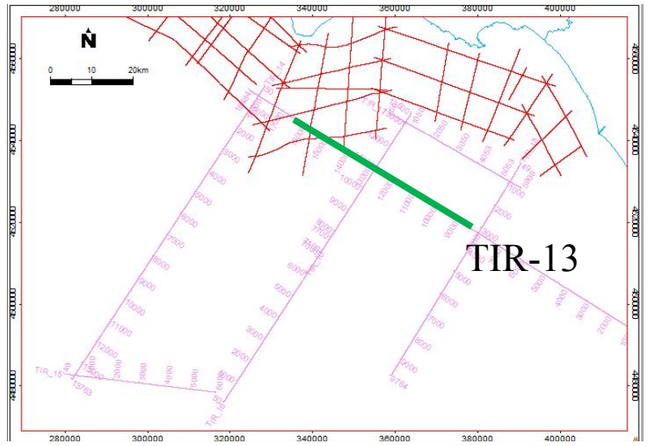


Fig. 6.11 B – Structural setting of Ventotene basin shown on seismic profiles TIR-13. White arrows indicate the probably volcanic features find in the area, not indicated by the structural map of Italy (1991).

C unconformity (Middle Pliocene p.p)
B unconformity (top Messinian)
A unconformity (top Meso-Cenozic carbonates)

Generic unconformities

B

TIR-13

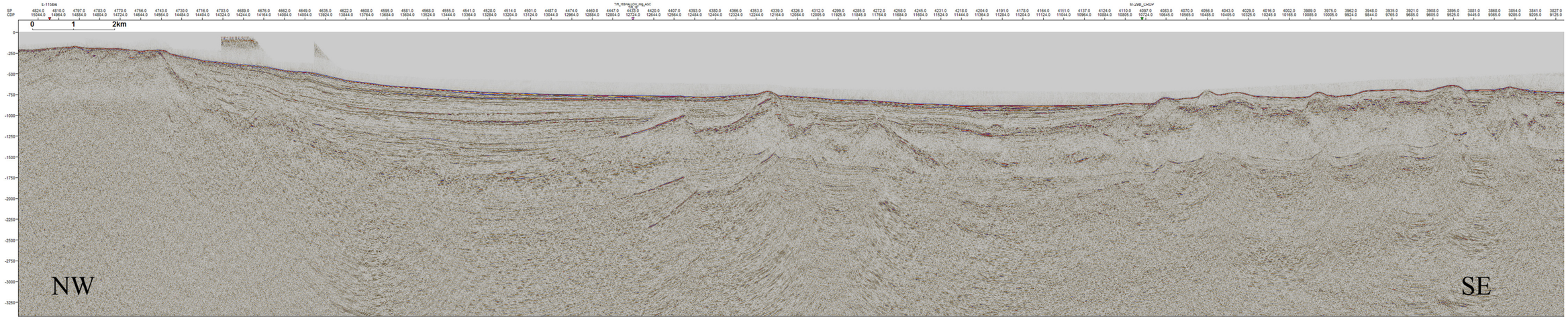


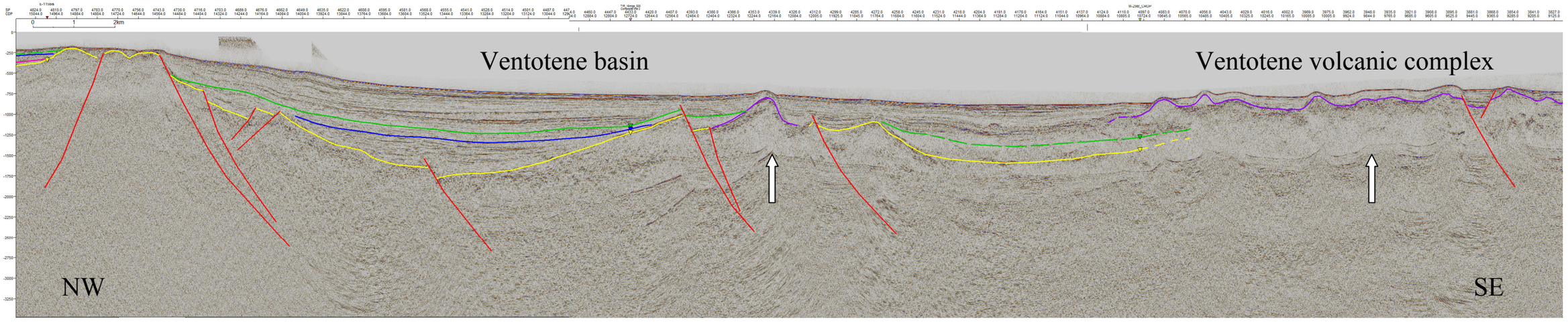

Three different lines cross the Ventotene basin in a NE-SW direction. Line TIR-16 (Fig 6.12 A) starts on the edge of the continental shelf in the sector of the Gaeta Gulf and it investigates the northwestern portion of Ventotene basin, between the western Pontine islands (Ponza, Zannone, Palmarola) and the eastern group (Ventotene and Santo Stefano). The basin in this sector shows its maximum thickness in the initial part of the line, around 1,1-1,2 sec. (twt); the basal unconformity B is still affected by extensional faults, but in small extent and the faults do not affect the sedimentary cover. It can be noticed that the substratum is characterized by an undulate morphology: a swell is observed between SP 1977 and 1790, onlapped by the lowermost part of the Plio-Pleistocene sequence; between SP 1650 and 1570 instead, the sedimentary cover is deformed by symmetric folds. Moving toward the SW, the Plio-Quaternary sequence progressively thins and onlap a structural high delimited by a high angle normal fault, NW-SE trending and dipping to the NE, which delimited the Ventotene basin seaward. The folds present in the sedimentary cover could be linked to a transtensive fault system, although this is not well clarified by the seismic data.

The line CROP 29B, NE-SW trending, intersects the central part of the basin and the structural and stratigraphic setting shown is similar to the one on the profile TIR-16. Even though, on the CROP profile extensional faults cutting the basal unconformity are more evident and between SP 18670 and 18200 the volcanic complex of Ventotene is imaged. On the initial part of the line (NE) prograding units from the continental platform area are shown, which form the infill of the basin in this sector.

Finally, the TIR-18 (Fig. 6.12 B) profile crosses the Ventotene basin in its eastern sector, between Ventotene and Ischia islands. The basin substratum is dissected by several extensional faults, probably linked to the NE-SW system affecting this sector toward the Ischia island. The basin infill, formed by parallel and continuous reflectors, is thicker in the first part of the line, with a maximum of 0.7 sec. (twt). Then it progressively thins southwestward, and probably intersects the Ventotene volcanic complex (SP 625-730). The basin is limited seaward by the NW-SE trend related to the escarpment sector.

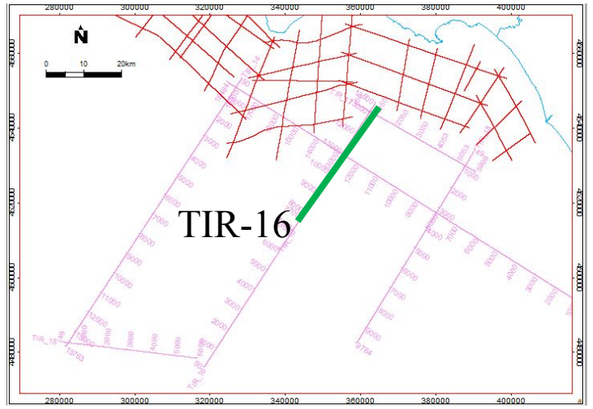


Fig. 6.12 A- TIR-16 profile crossing the Ventotene basin in a NE-SW direction.

C unconformity (Middle Pliocene p.p)
B unconformity (top Messinian)
A unconformity (top Meso-Cenozic carbonates)

Generic unconformities

TIR - 16

A

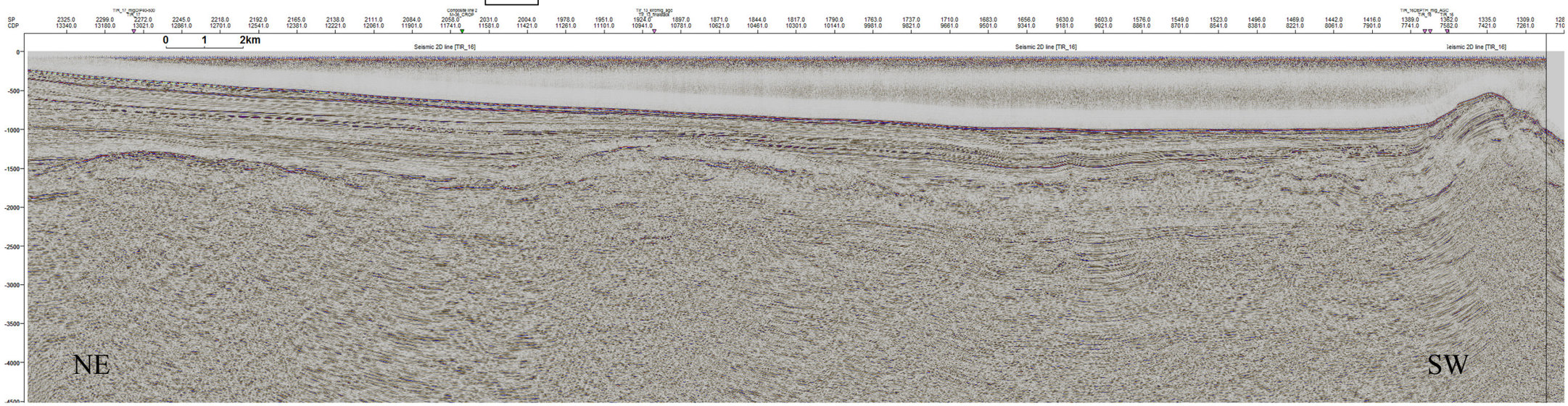


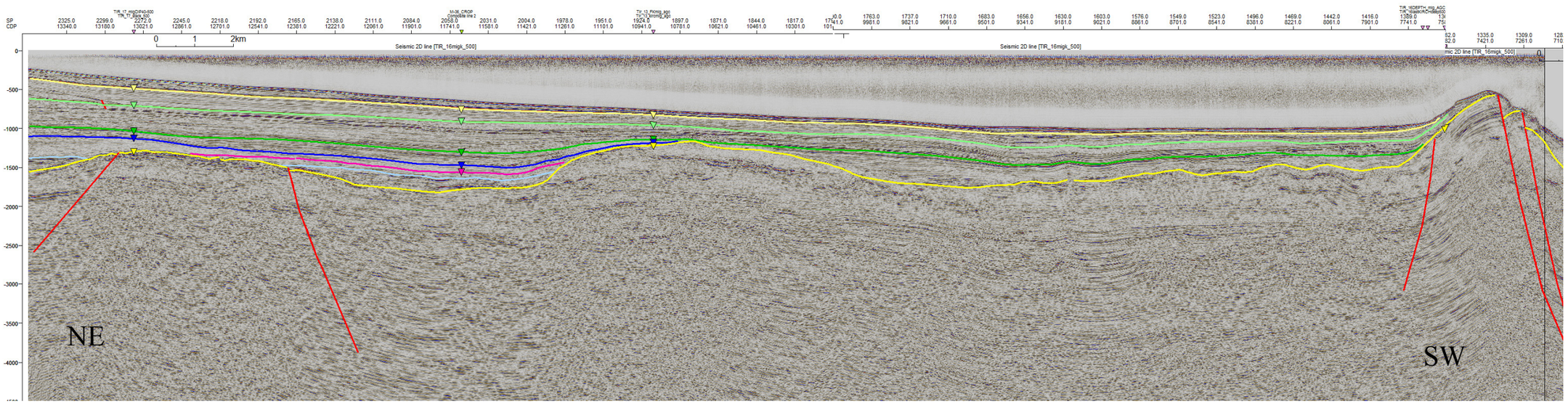

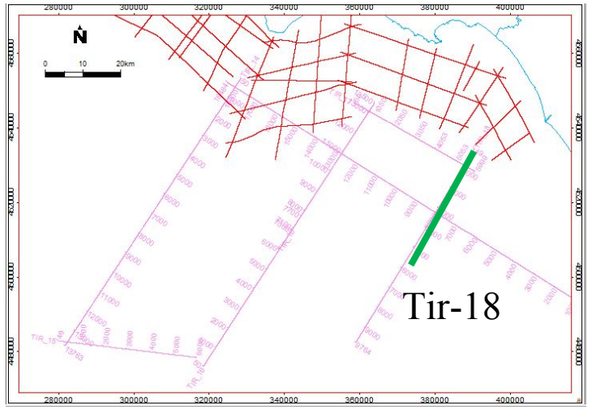


Fig. 6.12 B - TIR-18 profile crossing the Ventotene basin in a NE-SW direction.

C unconformity (Middle Pliocene p.p)
B unconformity (top Messinian)
A unconformity (top Meso-Cenozic carbonates)

Generic unconformities

B

TIR - 18

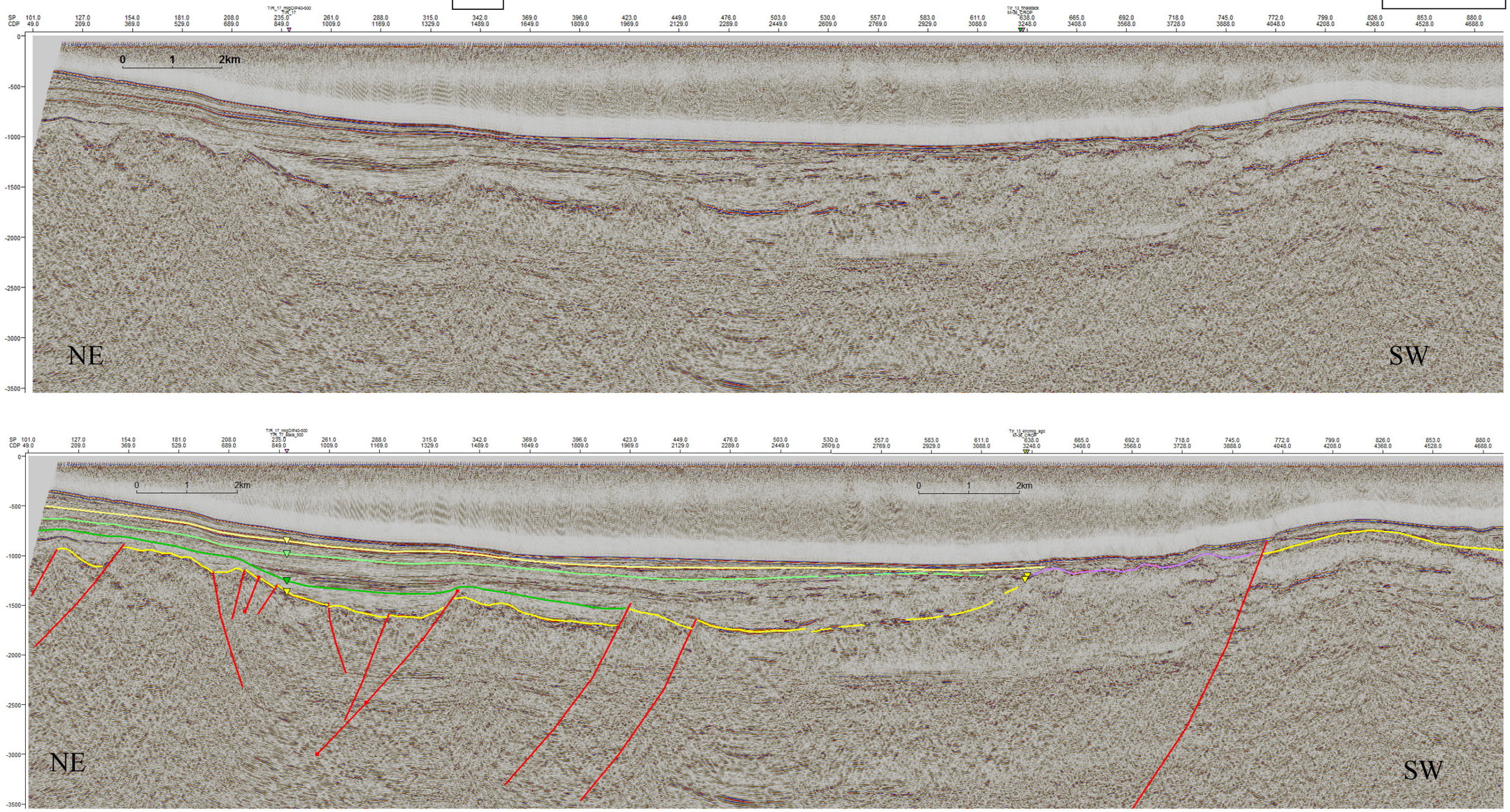

### 6.2.2 Pontine islands escarpement

The seismic profiles TIR-14, TIR-16 and TIR-18, NE-SW trending, provide an overall view of the complex escarpment that characterize the Pontine Archipelago.

On the TIR-14 line (Fig. 6.13) the slope offshore Palmarola is represented, visible from SP 880, just beyond the structural high area. Here the slope shows its minimum width, around 15 km, and maximum gradient, locally up to 30°. It appears clear that the slope is structurally controlled by a NW-SE trending normal fault system, responsible for the lowering of the margin down to the deep bathyal plane localized at 3500 m of depth. On the upper slope sector, faults are organized in an-echelon pattern and three main fault scarps are identified, producing as many morphological steps within the slope. Fault plains are closely spaced, with a listric geometry, probably merging on a low angle detachment fault. Other faults are probably present along the line until the base of the escarpment is reached. It is possible to notice that, particularly in its initial and more steep part, along the slope the seafloor displays an uneven morphology and the sedimentary cover is very thin or absent. Actually, in this sector, the interplay between main tectonics lineaments and instability processes can produce basement highs where the substratum is exposed.

The general morphological setting of the slope offshore Ponza and Palmarola islands is formed by three main ridges oriented NE-SW separated by broad channels and the TIR-14 line is located on the flank of one of this channels. According to Chiocci et al. (2003), the western Pontine slope seafloor is affected for 98% of its area by erosive and instability processes which cause the slope retreat and produce a complex pattern of features; according to the same authors, the steepest areas are characterized by linear channels, gullies and canyons which produce sliding and punctual mass transport processes. This seems to be well displayed by the seismic line TIR-14 where no sediments are displayed on the steep portions, probably associate with fault scarps and/or with the erosive and instability processes; on the contrary, the thin and localized sedimentary cover could be associated to mass wasting phenomena: they show chaotic and discontinuous, internal reflections, variable amplitude and frequency. In the lower part of the continental slope, processes of transport and sedimentation are more common; actually, moving further along the TIR-14 line, it can be seen that a thicker sedimentary cover is present at the footwall of the escarpment.

TIR-16 seismic profile (Fig. 6.14) investigates the escarpment in the sector between the western and the eastern Pontine archipelago. In this part the slope extends on a wider area and it displays a more articulated structure. The lowering toward the Vavilov plain is always controlled by extensional faults NW-SE trending, but in this case fault planes seems to be more spaced; the listric faults bound tilted blocks forming basements high and intraslope basins, which act as the main loci for sedimentary deposition. In the upper part of the escarpment, between SP 1250 and 1100, a mass flow deposit can be recognized: it is characterized by a mounded geometry, a transparent seismic facies at the bottom and visible strong and continuous reflectors in the upper part, probably due to coarser sediments; it could be correlated with a slumping resulting from mass wasting degradation of the adjacent structural high. At SP 950 a basin is displayed above a basement depression bordered by a fault plane: the infilling shows a syncline geometry; it is possibly to attribute this geometry to

a gravity flow event, originated from the margin to the NE; alternatively a tectonic origin can be presume, with a strike slip component.

Further along the line, between shot point 680-430, a faulted block, 6-7 Km long is displayed; it can be interpreted as a rotated block of the substratum, even if a volcanic nature can also be possible; it shows asymmetric flanks, being the north-eastern one (left) steeper than the south-western one (right); in fact, a thin sedimentary succession covers the flank: it is characterized by closely spaced reflections, with low to poor amplitude, slightly continuous and low acoustic impedance contrast, resulting somewhere in a transparent facies; such characteristics let to suppose a pelitic or hemipelagic nature of the sediment covering the basement high. The faults that dissect the western margin of the block is part of a bigger escarpment slightly NNE-SSW trending, which represents a tectonic feature through which the lower continental slope is divided in more steps.

Finally, the line TIR-18 (Fig. 6.15) intersects the escarpment south of Ventotene island. Here the escarpment morphology is even less steep and it extends over a wider area of the continental margin, so the down-stepping toward the Vavilov basin results in a more gentle morphology. Fault system lowering the margin belongs to the NW-SE system that characterized the entire area of research and higher fault spacing is observed. A thin succession (no more than 0,2 sec twt) overlie the substratum and generally no fault scarps are exposed, testifying a slope sector where instability and erosive processes are replaced by depositional processes. At the end of the seismic line, a basin with an almost 1 sec. (twt) infill is display, formed by mostly continuous sub-parallel reflections, onlapping toward the SW a rising basement. TIR-18 line is shorter respect to the previous described and it does not reach the Vavilov basin, so it does not investigate the entire stepping margin.

Fig. 6.13 - Slope sector on TIR-14. Listric faults progressively lower the margin until the bathyal area. Erosive/instability phenomena prevails in this sector.

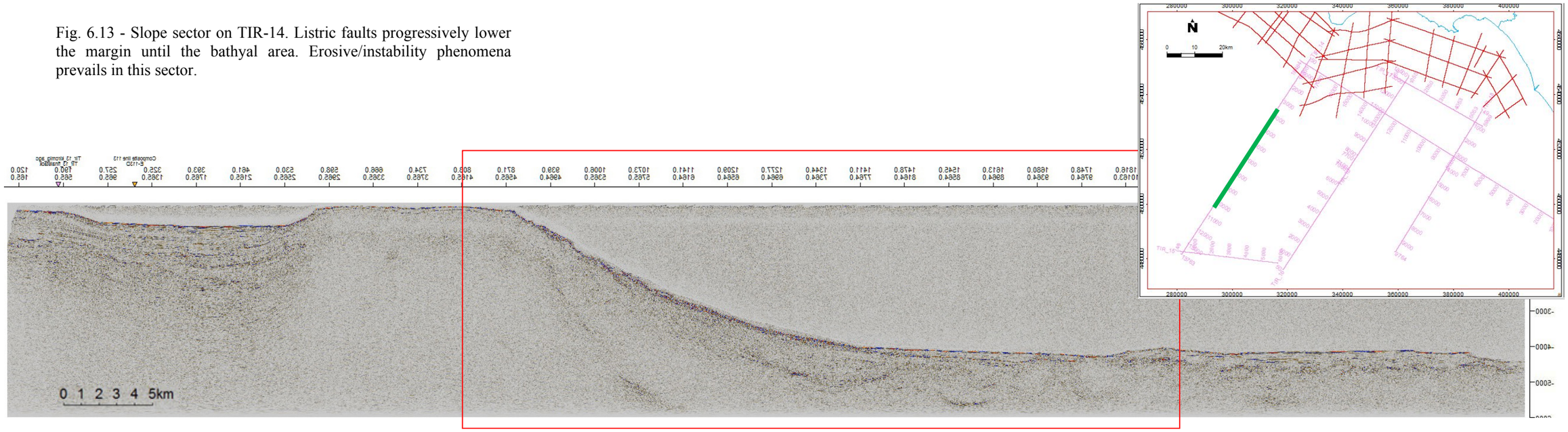


TIR - 14

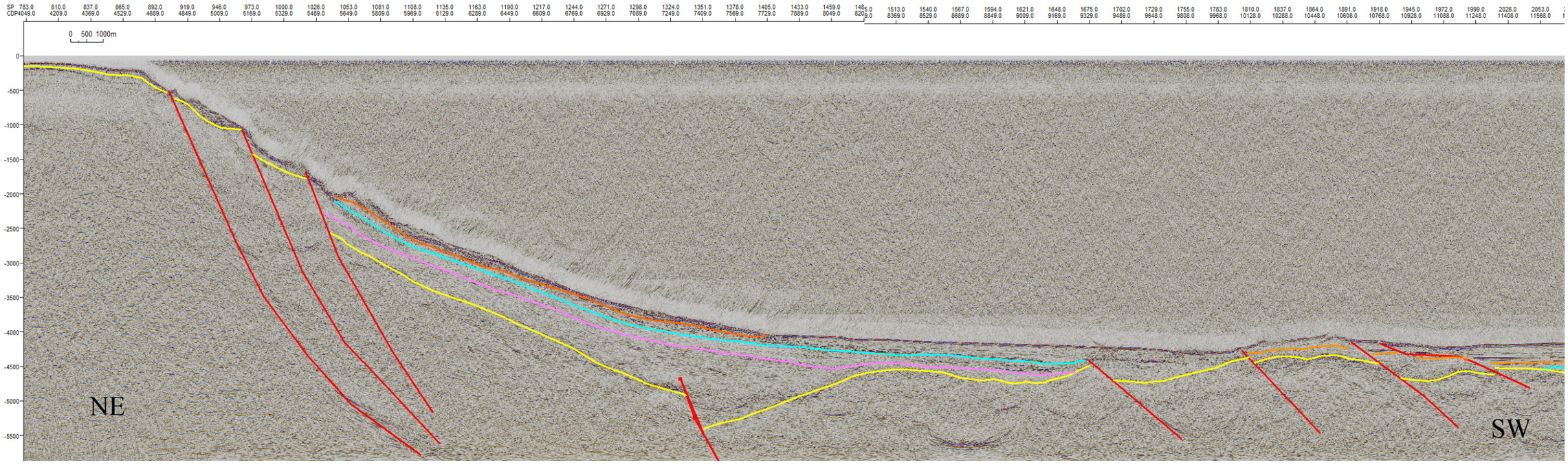

Fig. 6.14 - Slope sector on line TIR-16. The slope extends on a wider area and is more articulated. The folded reflectors could be refer to a big slump deposits originated from the margin, or in alternative a strike slip component for the faults could be supposed.

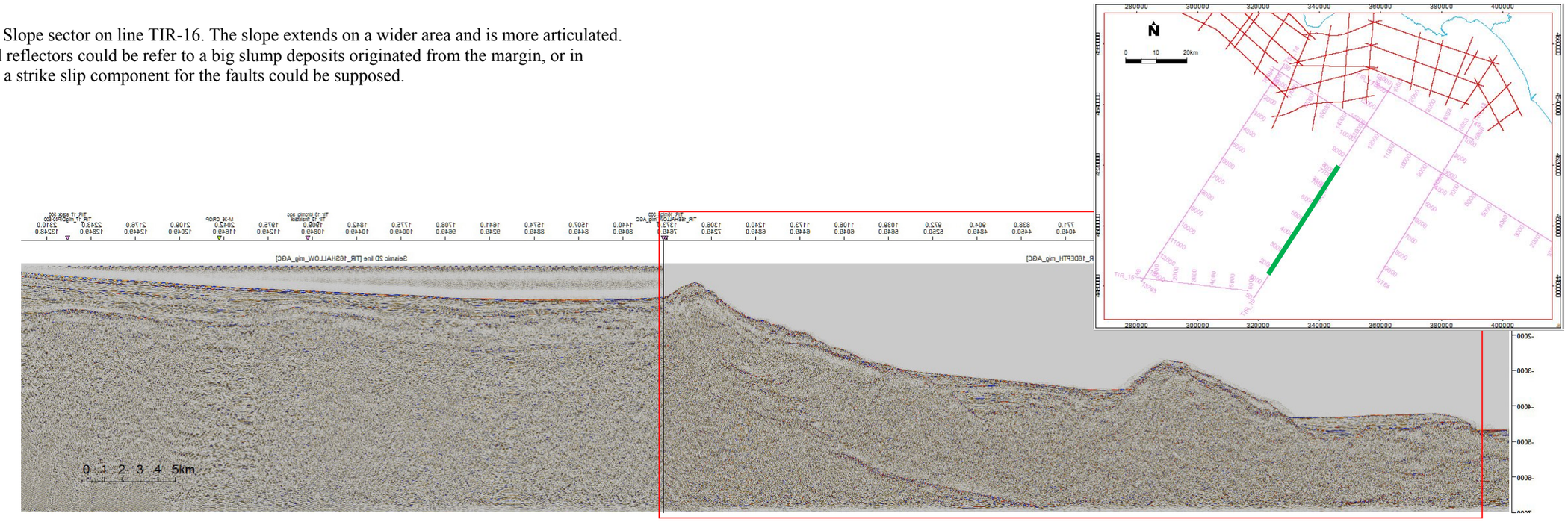

Fig. 6.15 - Slope sector on TIR-18. In this sector a thin deposition along the escarpment is pointed out; several and more spaced faults lowered the margin and at the base of the escarpment a basin is displayed.

TIR - 18

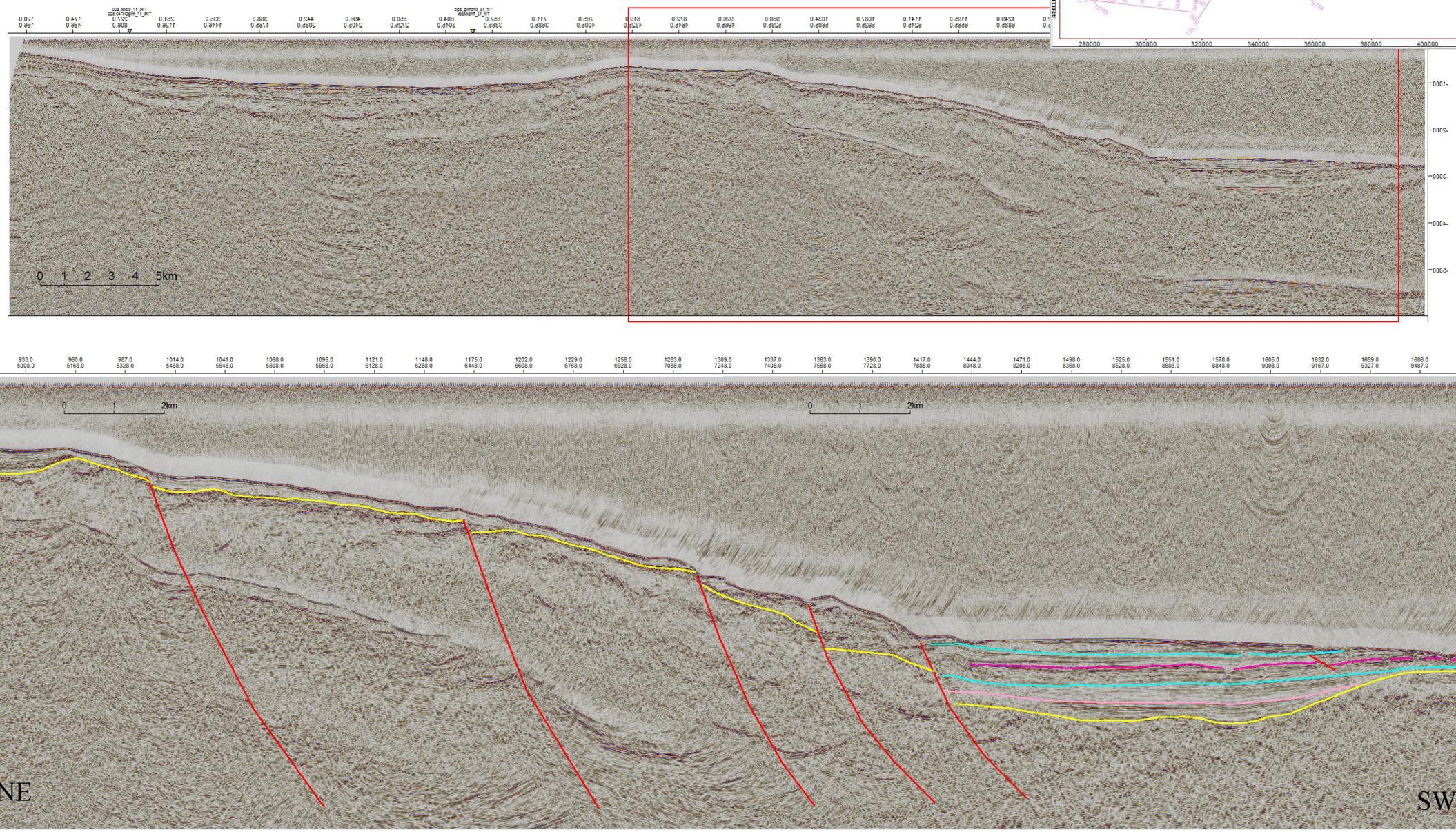

### 6.2.3 The Vavilov basin

The only seismic section of the new TIR dataset which effectively crosses the bathyal plain of the Vavilov basin is the TIR-15 profile, in a WNW-ESE direction; the CROP profile 29B also crosses the Vavilov basin and actually reaches the Sardinian margin; only the part related to the abyssal plain facing the Pontine margin will be taken into account.

Line TIR-15 (Fig. 6.17) is localized in the northern vertex of the triangular shaped Vavilov basin, also called Gortani basin in this sector. Starting from the western part, the seismic section shows the Farfalla seamount, which constitutes the western border of the Vavilov basin; this is one of the numerous volcanic seamounts present in the central Tyrrhenian basin. It has an asymmetric shape, with the western flank steeper respect to the eastern one; according to Piangiamore et al. (2004), in correspondence of this seamount, a negative magnetic anomaly is displayed, which is an apparent contradiction, as the sector should show a positive magnetic anomaly. Some hypothesis to explain this phenomenon are related to the demagnetization of the rocks as they reach the Curie temperature, due to the high heat flow of the area (Zito et al., 2003); another explanation could be the intense deformation that caused fracturing and cataclasite formation, which facilitate the rocks alteration and the oxidation of magnetite; also hydrothermal alteration could be a possible explanation. The margins of the seamount appear faulted by extensional faults, NNE-SSW trending, dipping toward the west (on the western margin) and the east (on the eastern margin). The tilted faulted blocks constitutes the preferred location for a thin sediment deposition, in the order of 0,1 sec. (twt).; the wedge shape of the deposit let to infer a syn-sedimentary activity of the fault.

Immediately to the east of the Farfalla Smt., a cone-like structure is visible, that might represent a volcanic feature. Its eastern flank is interested by a listric normal fault, with growth strata displayed at the hangingwall.

Further along the line, the Vavilov basin is shown. It is formed by a sedimentary infill of maximum thickens of 1,2 sec. (twt), thinner toward the east, near the basin margin; it shows mostly continuous and parallel reflections, with variable amplitude; between 4.9 and 5 sec. a transparent and more chaotic facies is present. These seismic characteristics are compatible with distal turbidites with a basin-wide areal extent (Gamberi & Marani, 2004). Several faults seem to dissect the substratum and the bottom part of the sedimentary cover and overlay it. They are high angle faults with minimum offset and could represent preferential paths for fluid escaping. The older stratigraphic units covered by the sedimentary units seem to be composed by an upper set of week reflectors, locally very bright (between shot points 996 and 1050) and a lower one characterized by discontinuous reflectors displaying no clear dipping attitude. Taking into account the drilling data of the ODP site 651 located about 35 Km south of TIR-15 line, the upper unit could correspond to an interval made of lava flows and the lower one to the basement of serpentinized peridotites (as already discussed in the stratigraphy Chapter 5).The seismic section ends to the east where the eastern escarpment bordering the Vavilov basin is intersected: this seems to be part of a major extensional fault system with an almost N-S direction, running from the Flavio Gioia Seamount localized to the south, until the base of the NW-SE escarpment bordering the

margin offshore Ponza island.

Evidence supporting the hypothesis of the presence of oceanic crust in the Gortani basin could be provided by the CROP 29B profile that intersects the TIR-15 line at SP 13491. On this profile, the almost N-S trending margin that determines the lowering to the basins is intercepted at SP 13680; the sedimentary infill of the basin is then display with the same seismic facies characteristics previously describes. Between SP 9700 and 10600 is imaged the Gortani ridge, a linear morphological high of maximum elevation in the order of 300-400 m. On this feature, ODP site 655 was drilled (Fig. 6.16): there were recovered 120 m of tholeiitic basalts (pillow lavas), overlain by 80 m of upper Plio-Pleistocene marly nannofossil ooze; the basalts were dated between 3.4-3.6 Ma old and are considered by Kastens & Mascle (1990) the earliest evidence for emplacement of oceanic crust in the basin.

Mascle & Rehault (1990) analyzed a seismic dataset named ST, collected during the Site Survey cruise SITHERE, preparatory for ODP Leg 107, carried out in 1985 by the French Institutions IFREMER-IFP-CNRS on the R/V Noroit. Particularly interesting for this work are the lines ST-4 and ST-3, whose location respect to the TIR dataset is provided by the Fig 6.18: ST 4, WNW-ESE trending, is essentially parallel but shifted about 15 Km to the south respect to seismic line TIR-15; line ST-3, N-S trending, crosses both the previous lines mentioned and ODP Site 651, where evidence of basalts and serpentinized peridotites where found (Chapter 2.3, Fig. 2.15), is located on this line. The seismic signature of the acoustic basement is characterized most of the time by a rugged and diffractive topography interpreted by the authors to be typical of the top of oceanic layer 2. In the proximity of basement highs or swells, they observe a rather regular basement, characterized by high interval velocities (between 4.0 and 6.0 km/s); this should correspond to thick piles of poorly altered lavas flows and/or to serpentinized peridotites. Along the swell flanks and in general on topographic depressions, they interpreted an irregular basement (with interval velocities between 2.5 and 3.5 km/s) characterized by weak seismic signal interpreted as indicative of interbedded lava flows.

Thus, taken into account these previous studies and the new data provided by TIR-15, it is possible to affirm that oceanic crust could occur also in the zone investigate by TIR-15, or at least in its very proximities; the boundary between continental and oceanic crust could occur along the last fault system, NNW-SSE trending, imaged on the CROP 29B and TIR-16 lines and in part also visible on TIR-15.

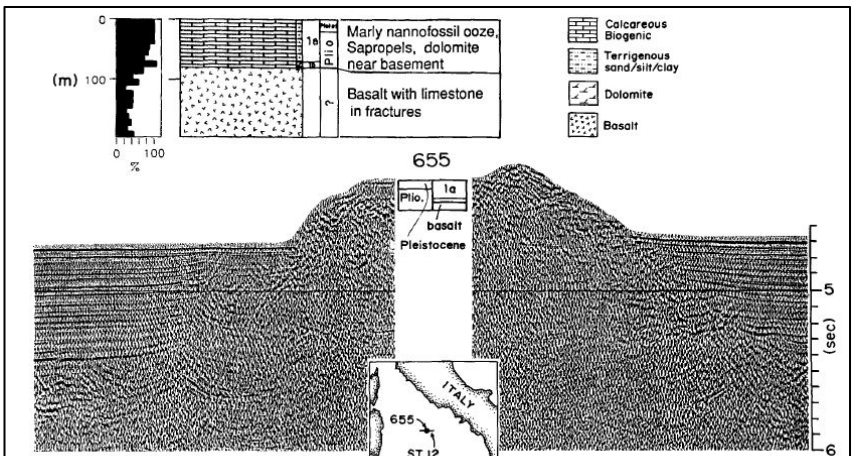

Fig. 6.16 - ODP site 655 drilled on Gortani Ridge (localization on Fig. 6.18)

Fig.6. 17 – Upper CROP M-29B profile from the intersection with TIR-15 to the Gortani ridge (localization also in Fig. 6. 18). Bottom, the TIR- 15 profile, showing the Farfalla Smt. to the WNW and the Vavilov basin toward the ESE.
A original data, B interpreted data.

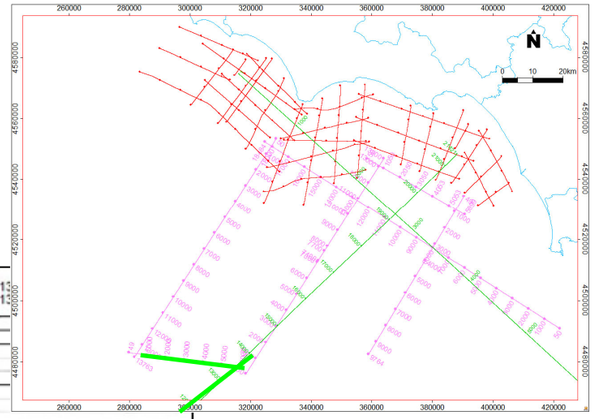

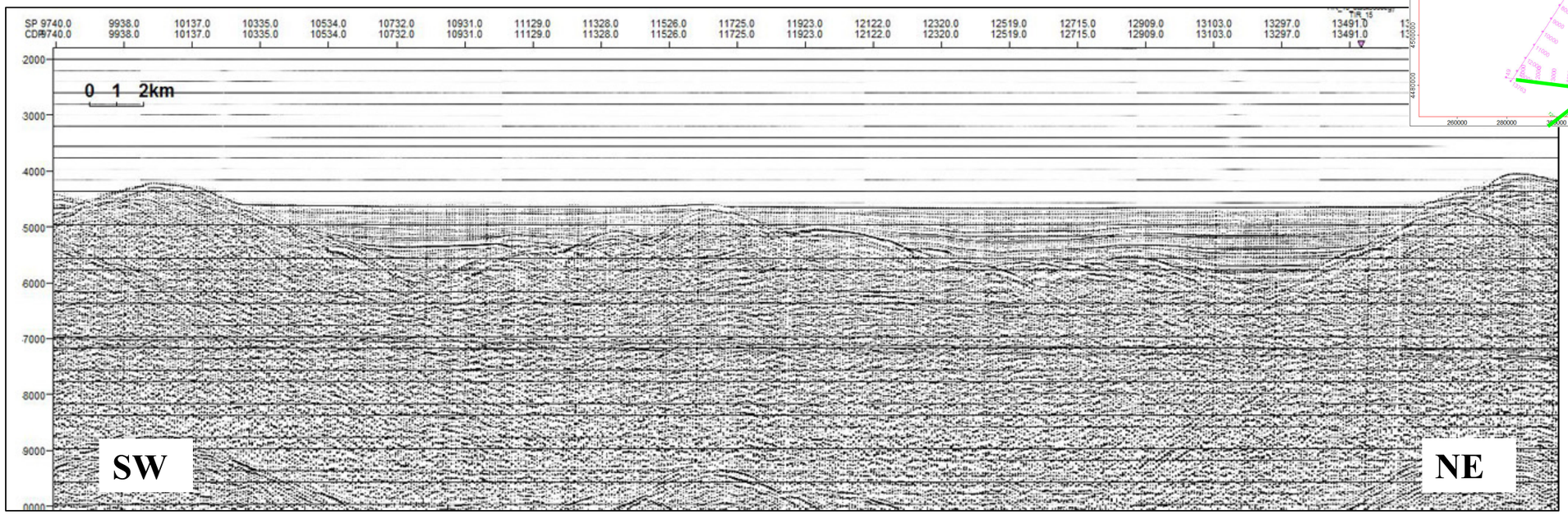


A

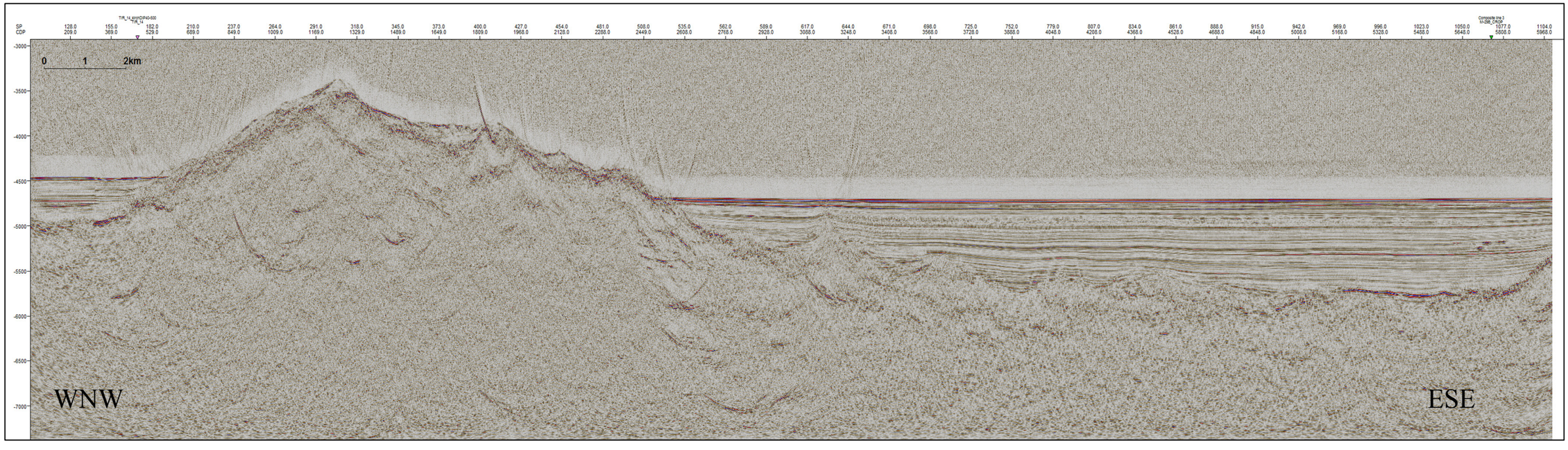

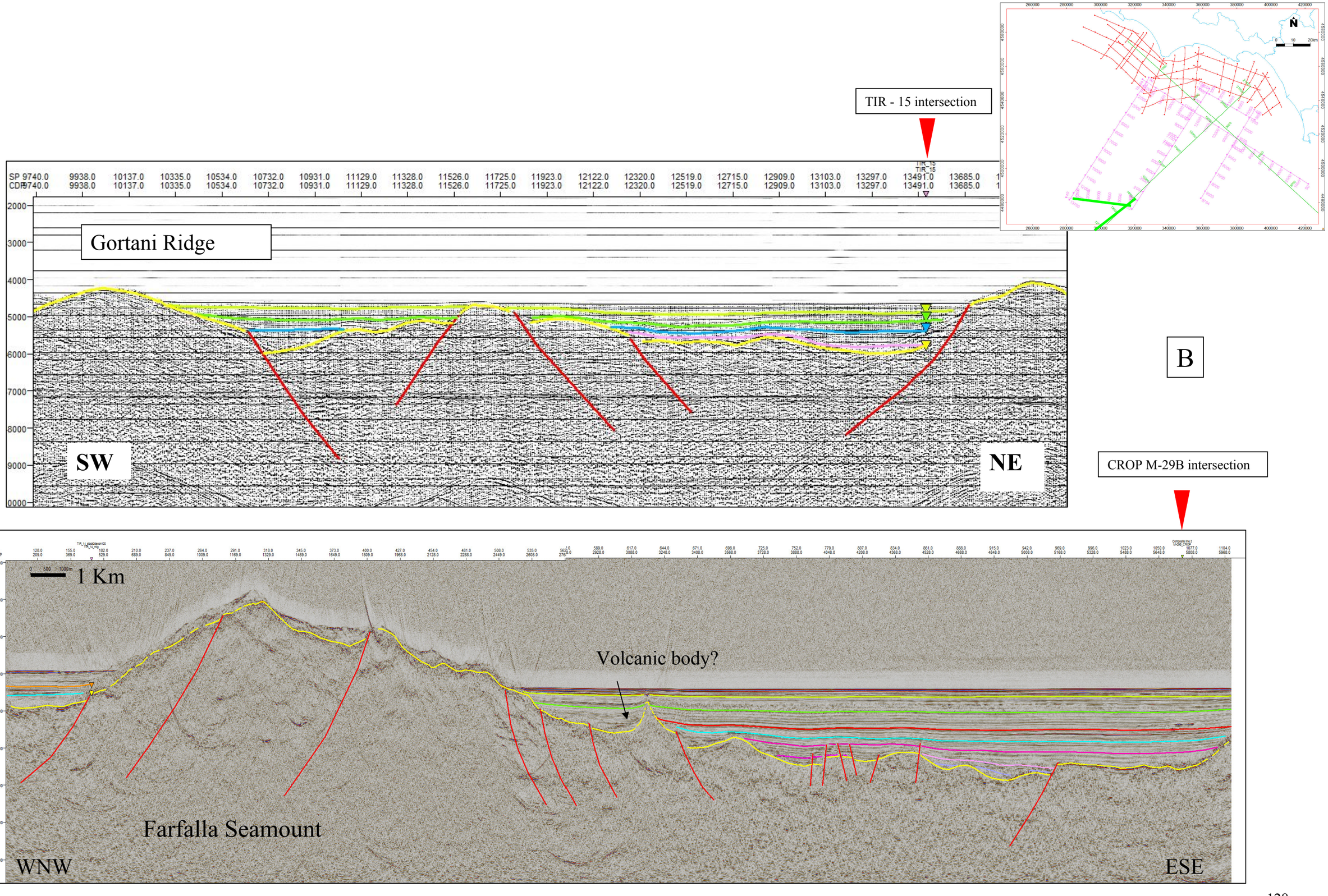
TIR - 15 intersection
Gortani Ridge
SW
NE
B
CROP M-29B intersection
1 Km
Volcanic body?
Farfalla Seamount
WNW
ESE

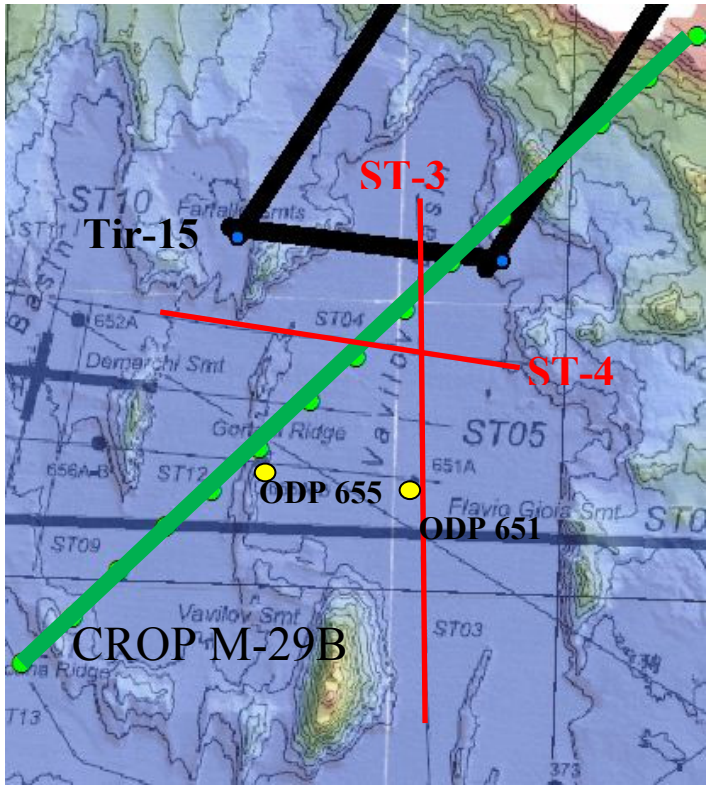


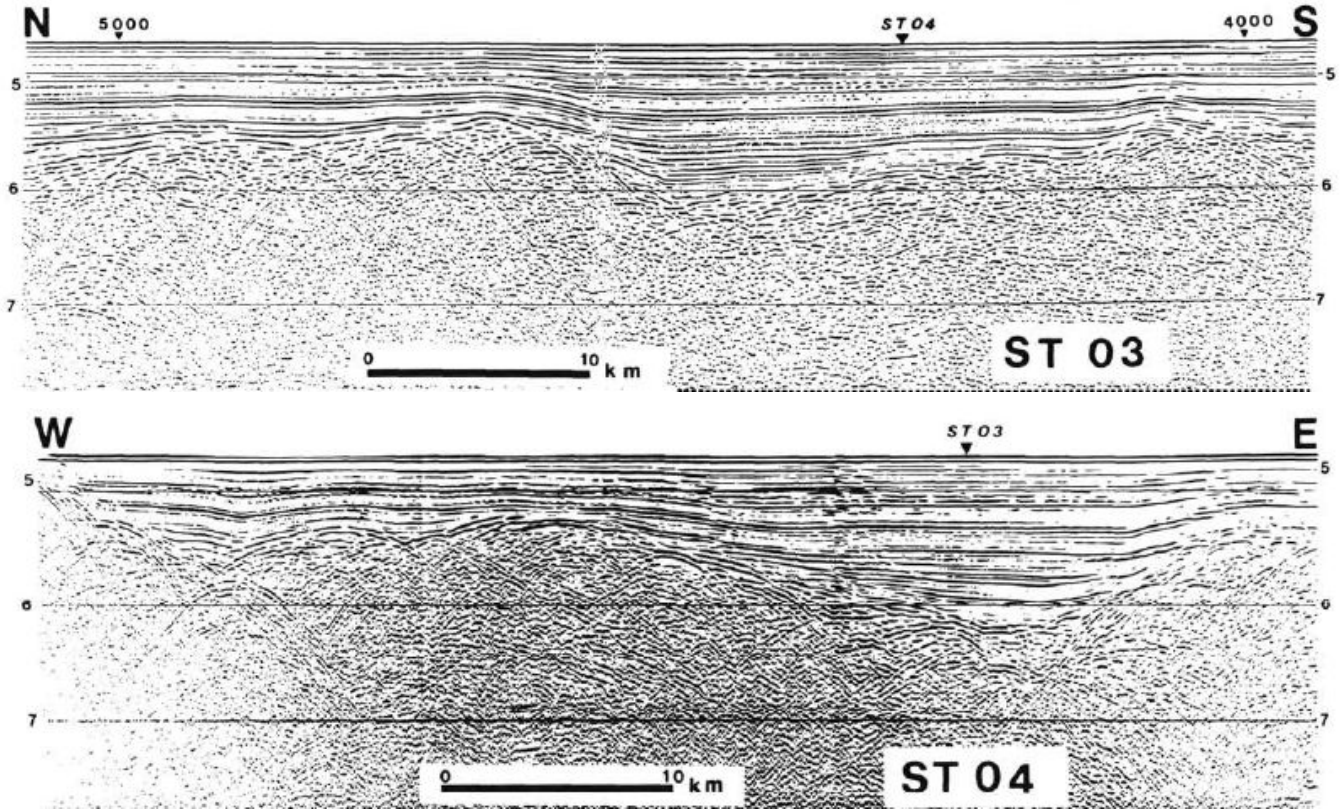


Fig. 6.18 – ST03 and ST04 profiles (Mascle & Rehault, 1990). The rugged and diffractive topography is referred by the authors to lavas flows and/or to serpentinized peridotites (vv in the interpreted line ST-04, bottom). Yellow dots are ODPsites.

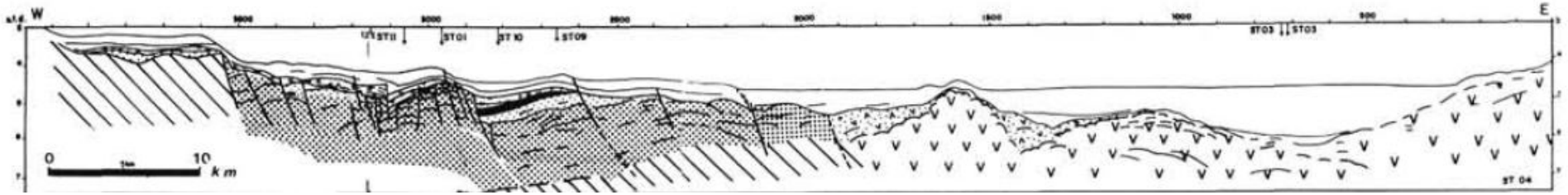


**ST-4**

# CHAPTER 7

# Tectonic Evolution

In this work the Tyrrhenian margin sector between Anzio and the Volturno river has been analyzed, from the continental shelf sector to the Vavilov bathyal plain. The interpretation of the new multichannel TIR seismic profiles, integrated with the "Reconnaissance Seismic" and the CROP profiles, plus the stratigraphic information provided by onshore and offshore wells, contributed to identify the processes that shaped this portion of Tyrrhenian margin.

The structural and stratigraphic features highlighted by the analysis allow to unravel the main tectonic phases in the study area, and to integrate them in the general evolutionary context of the Tyrrhenian basin.

### 7.1 Miocene orogenic phase

The older tectonic phase highlighted in the area is the one responsible for the overthrusting of the Meso-Cenozoic units, which involved the units labelled U1 and U2 (Chapter 5, Fig. 5.12 and 5.13). The effects of this orogenic deformation are masked on the slope sector by the following deformational phases, whereas they should be more evident on the shelf area. Unfortunately, the available data (the old E survey) do not display the necessary penetration and resolution to resolve the internal configuration of the units; moreover, in some sectors these units constitute a "non reflective" substratum. In Fig. 7.1 an example of a thrust structure involving the substratum can be observed; Bartole et al. (1984) identifies two main orogenic features in the area, as already discuss in Chapter 3.2 (Fig. 3.5 A): the "Palmarola-Terracina overthrust", NE trending, of Messinian age, and the "Zannone-Volturno overthrust", E-W trending, of middle Miocene-Pliocene age. Zitellini et al. (1984) indicated different orogenic phases responsible for the formation of the Apenninic chain in the surrounding mainland regions, ranging from lower Tortonian until Messinian.

During the research work, a short campaign was carried out on Ponza and Zannone islands, with the aim to collect structural data and measure parameters of faults and fractures to compare with the main trends observed on the seismic lines. On Zannone island it was possible to observe the substratum cropping out on the northern and eastern portion of the island. As already pointed out (Chapter 3.2.5, Fig. 3.13) this is the only outcrop of pre-volcanic units that occurs in the archipelago; in Fig. 7.2 the contact between the Paleozoic low grade metamorphic sediments (phillites) and the Triassic limestones is shown. Above these sediments, the Cretaceous-Miocenic succession lays, formed by pelagic limestones ("Scaglia Rossa") and flysch deposits. Several evidence of different deformational phases have been inferred and the principal direction observed are generally in agreement with previous studies carried on by De Rita et al. (1986), Pantosti & Velona (1986) or the recent work by Schnyder et al. (2012). The older tectonic phase is pre-Triassic in age, and could be connected either with the Hercynian cycle or the Alpine one; the phase responsible for the overthrusting of the Meso-Cenozoic succession is dated late Miocene and display a NW-SE strike and tectonic transport towards the NE.

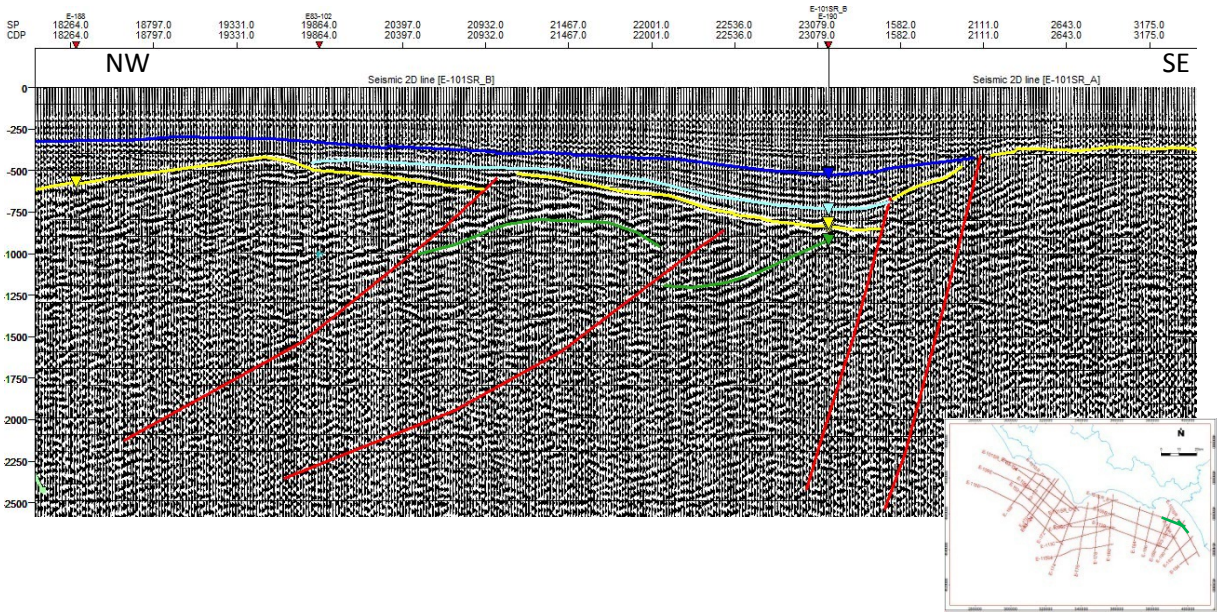


Fig. 7.1 – Example of thrust activity involving units U1 and U2 (Line E-101B).


Fig. 7.2 – Low grade metamorphic units (phillites, Paleozoic) in contact through an erosive surface with Triassic limestones.

### 7.2 Early Pliocene-middle Pliocene p.p.

At the Messinian-Early Pliocene transition, the investigated area is interested by an extensional tectonic phase, which plays a major role in the control of the present day physiography of the Latium-Campania margin. Indeed, the extensional phase is responsible

for the general horst and graben setting highlighted on the continental shelf by the interpretation, and of the steep escarpment connecting the continental platform to the Vavilov basin, as well as of the intraslope basins (Palmarola and Ventotene).

The unconformity surface (B in the text, Chapter 5, Fig. 5.12 and 5.13) marking this major change in tectonic pattern has a regional importance and has been interpreted along over the entire Tyrrhenian basin (Selli & Fabbri, 1971; Zitellini et al., 1986): it marks the top of the evaporitic deposits or, as in the studied area, it is associated to the erosional surface corresponding to the Messinian sea-level drop (i.e., the Messinian crisis). The sedimentary infilling lying above this surface is Plio-Pleistocene in age, although the presence of a post-evaporitic Messinian unit cannot be rule out; in fact, because of the trasgressive nature of the post-evaporitic Messinian, this latter unit would be formed by clastic sediments, indistinguishable from the lower Pliocene unit.

The extensional tectonic phase acted through structural lineaments with various orientations, which lead to the formation of different sectors along the margin characterized by differential tectonic movements. Main tectonic directions recognized are NW-SE, NE-SW, NNE-SSW and E-W, visible in Fig. 7.3; this map reproduces the depth (in ms) of the B unconformity (top Messinian) correlated along the entire dataset, and the main structural trends. In the north-western portion of the studied area (from Anzio to the Circeo Promontory) the principal structural directions interpreted are NE-SW striking; in the south-eastern portion instead (from Circeo Promontory to Volturno river) roughly E-W trend prevails, and in minor extent NNE-SSW and NW-SE trends are also present. The intraslope basins of Palmarola and Ventotene are instead controlled by structures NW-SE striking, the same trend characterizing the continental slope.

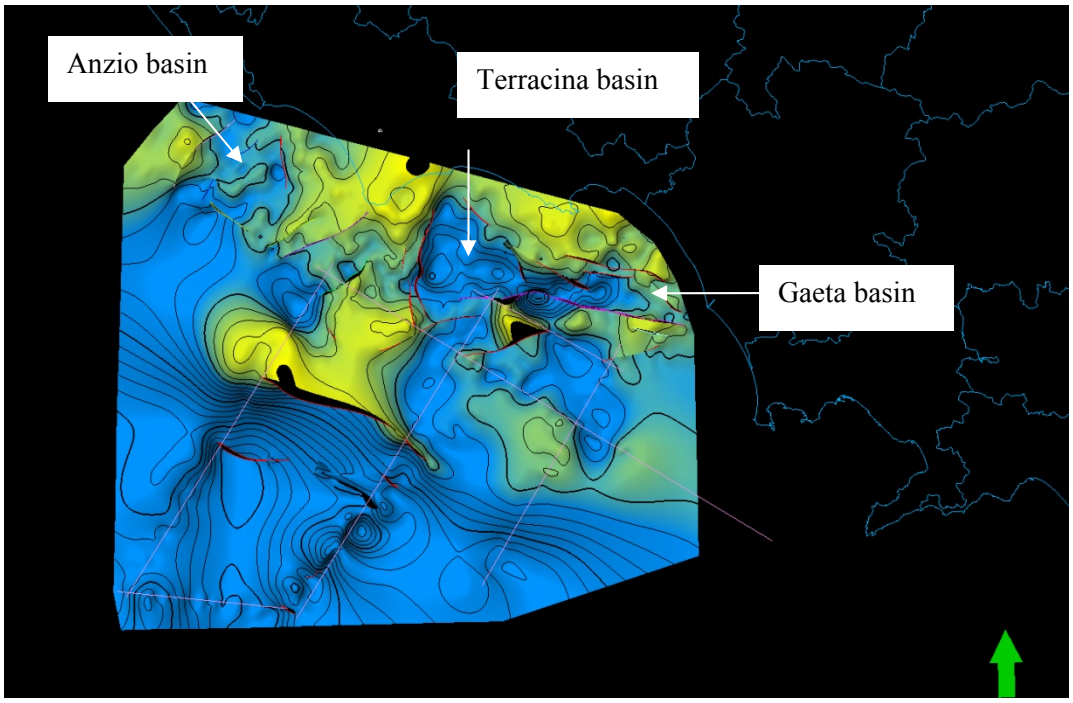


Fig. 7.3 - B unconformity (Top Messinian) correlated over the entire dataset and main tectonic trends interpreted (map in ms).

Summarizing, on the continental shelf sector from Anzio (NW) to the Volturno River (SE), the principal structures interpreted are:

- the Anzio basin, an extensional basin bordered by normal faults trending NE-SW, extending approximately from Anzio to the Circeo Promontory, characterized by an articulated substratum where smaller horsts, NW-SE trending, are present (Fig. 6.5).
- The Circeo High, a structural high roughly NE-SW trending, matching the carbonatic outcrops of the Circeo Promontory (Fig. 6.2, Chapter 6).
- The Terracina basin, an half graben NNE-SSW trending, which enlarges and merges the Gaeta basin toward the south (Fig. 6.3, Chapter 6).
- The Gaeta high, a wide area of structural highs dividing the Terracina and Gaeta basins in the northern sector, located approximately in correspondence of the carbonatic outcrops of the Aurunci massif (Fig. 6.6, Chapter 6).
- The Gaeta Basin, an extensional basin roughly E-W trending, joining laterally the Terracina basin (Fig. 6.7, Chapter 6).
- The Massico High, a NE-SW elongated horst structure, representing the prosecution of the Massico Mountain onshore (Fig. 6.8, Chapter 6).

All these features are generally recognized also by Aiello et al. (2000), Bruno et al. (2000), and the directions interpreted agree well enough with the Structural model of Italy (1991).

On the continental slope, the lower early Pliocene extensional phase is responsible for the formation of the two major basins of Palmarola and Ventotene and the individuation of the escarpment. Dredge T71-7 reported by Zitellini et al. (1984) and localized on the slope SE of Ventotene island, sampled an early Pliocene hemipelagic marls belonging to the *G. margaritae* and *Sphaerodinellopsis* zone. This dredge is localized on one of the faulted tilted blocks that form the escarpment, so a Pliocene age can be inferred for this structure.

Extensional tectonic took place both at the borders than within the basins, so the lower Pliocene surface (unconformity B) is very articulated. Major offsets occur along the faults bounding the basin margins (master faults) and are in the order of 0.5-1 sec. (twt), whereas the minor faults (synthetic and antithetic) show smaller displacements, general in the order of 0,1-0,2 sec (twt). The same relationship can be observed for the fault length; in fact, whereas the minor faults which dissect the basin are generally difficult to map through different seismic profiles, due to their limited extension, master faults bordering the basins have a length generally of the order of tens of kilometers. Faults have generally high angle dipping planes and the ones related to the basin margins show a listric geometry.

Fault activity seems to be stronger in the lower part of unit U3, testified by wedging, growth geometries and onlap of the lower sequences on the top of the acoustic basement. The minor faults within the basins dissect the basal part of the early Pliocene sequence, but moving upsection they are progressively abandoned and strain is localized on the master faults bordering the basin margins. This is in agreement with the observations made by Walsh et al. (2003), who analysed the progressive strain localization during fault systems growth in

the Northern North Sea (Fig. 7.4). The basic fault pattern is established early in the basin formation and faulting becomes increasingly localized onto the largest faults; this localization is accompanied by the death of smaller faults, determining a diminishing contribution to fault-related strain. Simultaneously, fewer and better connected faults extending across the area developed, which represent the most efficient means of accommodating fault-related deformation. According to the authors, this is a fundamental characteristic of the spatio-temporal evolution of fault systems.

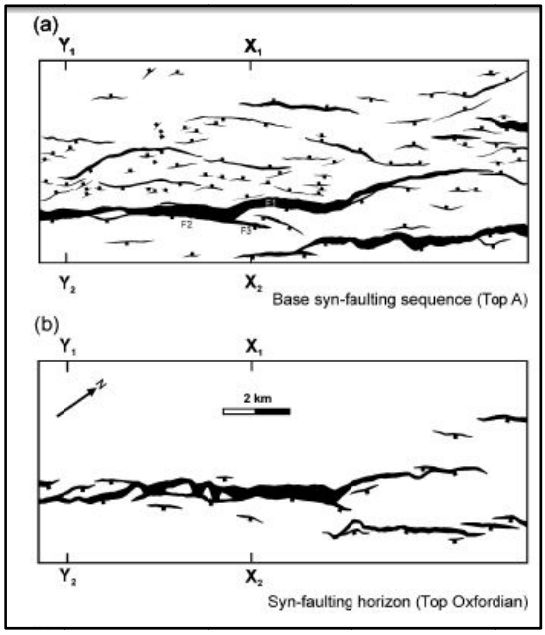


Fig. 7.4 – Faults map for the base of the synrift sequence (a) and for an horizon within the syn-faulting sequence, showing localization of the strain (Walsh et al 2003).

The extensional tectonic strongly involved also the older units; at Zannone is possible to observe extensional planes NE-SW oriented cutting the high angle stratified (probably folded) Triassic limestones (Fig. 7.5).

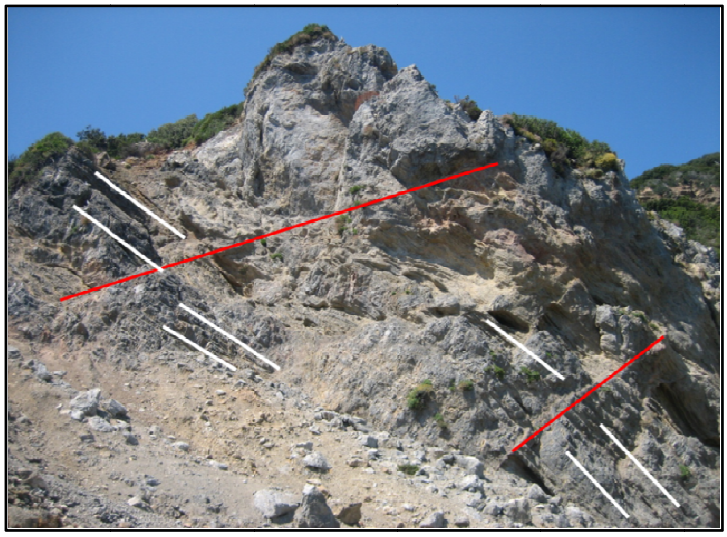

Fig.7.5 - NE-SW trending normal faults cutting Triassic limestones showing high angle stratification.

### 7.3 Middle Pliocene p.p. – Pleistocene

Extension activity continued during middle-late Pliocene up to Quaternary in the continental slope sector; on the shelf instead, two different situations are observed: in the northwestern sector (Fig. 7.6 A) (respect to the Capo Circeo-Ponza alignment) a tectonically-enhanced unconformity (C) seems to fossilize the extensional faults activity. Above unconformity C a main variation in depositional geometries is observed and a prograding sequence is displayed in the upper part; this means that during this time interval a deltaic system developed on the present day continental platform, which caused the deposition of these units prograding towards the sea. No evidence of extensional tectonic is observed. In the south-eastern sector, especially in the zone of the Gaeta Gulf, a different situation is displayed (Fig. 7.6 B): wedge shaped units are present in the basins, testifying a syn-depositional fault activity also after the C unconformity. So, in the southeastern sector, after a first activity stage during lower Pliocene, responsible for the deposition of the U3 unit (section 7.2), a second stage occurs, upper Pliocene-Pleistocene in age and provoked the deposition of a thinner syn-depositional sequence. The final upper part of unit U4 shows a progradational character also in the Gaeta sector.

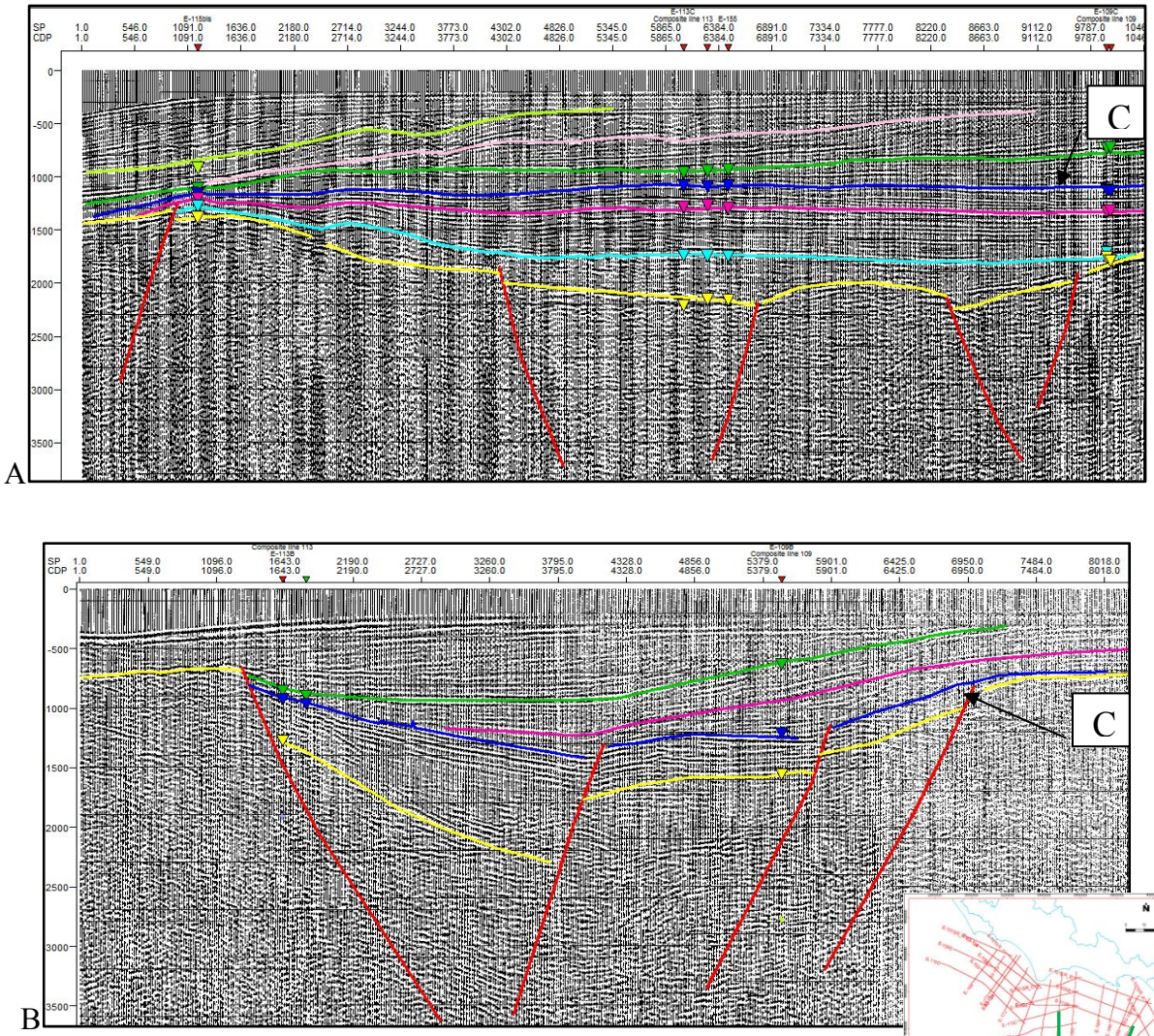


Fig. 7.6 – Line E-178 (A) and E-188 (B) showing how C unconformity (blue line) is affected by dislocation in the southeastern sector.

The upper Pliocene-Pleistocene fault activity seems to act principally through the E-W lineaments and created a depocenter in the Gaeta basin (Fig. 7.7). The E-W directed fault system, as previously pointed out (Chapter 6.1), shows a strike-slip component of movement; the translation of Mt. Massico is consistent with a left-lateral motion. In this zone the so called 41$^{st}$ Parallel line occurs, associated with an E-W trending magnetic anomaly (Chapter 2.1); the observations in this work support the hypothesis of a left-lateral strike slip kinematic for this lineament, in agreement with Bruno et al. (2000).

According to Milia et al. (2013), the youngest structures, post 0.4 My, are located south of Volturno River, outside of the studied area; they controlled the deposition of a large thickness (2.3 sec) of sediments, while in the northern sectors Quaternary progradational units were deposited.

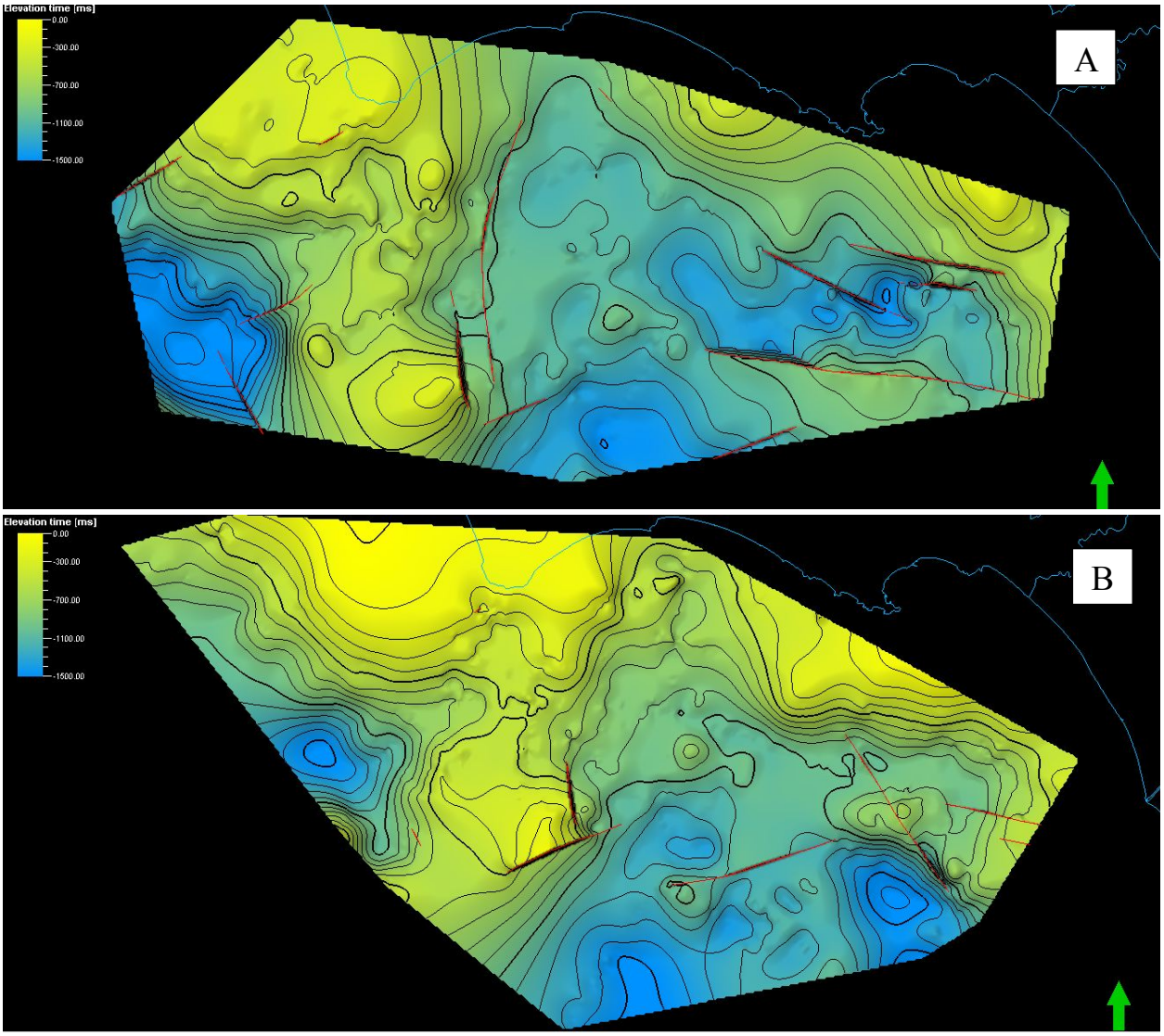


Fig. 7.7 – A) The "C" unconformity correlated over the entire dataset and main tectonic trends interpreted. B) General unconformity within the unit U4 (green line on the interpreted lines) and main tectonic trends. Surfaces are in ms (twt). Fault activity is progressively localized in the eastern sectors (B).

From a general point of view, the poly-phased evolution of the area shows how extension moves essentially towards the SE, where the activity is younger. This fact is reflected also by the stratigraphic record, both offshore than in the onshore sectors: from the offshore area analysed is possible to see that in the Anzio basin, in the northern sector, the Plio-Pleistocene sequence shows a total thickness around 1000 m (assuming an average velocity of about 2100-2200 m/s for the entire Plio-Quaternary succession); moving to the south, Gaeta basin shows a sedimentary infill of around 2000 m and Terracina basin of 2500-2600 m. In the Volturno basin Marani and Prato (1988) reported a Plio-Pleistocene thickness of about 4200 m. These observations partly fit with what is observed onshore by means of the well data, where a general sinking of the substratum is observed toward the south: the wells localized on the Volturno plain drilled a Pleistocene sequence of more than 3000 m thickness (Chapter 5.1, Fig. 5.9), without reaching the base of the Quaternary sequence.

Also volcanic features show younger ages moving toward the south; this is well displayed by TIR-13 line (Fig. 7.8), along which different volcanic features are observed: a first volcanic structure occurs between SP 4380-4310, a second at SP 4100-3800 more to the SE, and other volcanic edifices are present in the area of Ischia island (south of the investigated area). The progressive youngest age of this volcanic edifices is infer by the thickness of the sedimentary deposits which show onlap terminations above the volcanic flanks and blanket the top of the volcano: moving toward the SE, this thickness is progressively thinner, until is almost absent on the Ischia volcanic complex, testifying the younger age of this volcanism. The volcanic feature localized between SP 4380-4310 (1 in Fig. 7.8) is not reported on the Structural model of Italy, but for its proximity to Ventotene island, has been assigned to this volcanic district. Probably, another volcanic structure is shown on line TIR-17, more to the NW, localized for the first time thanks to this survey.

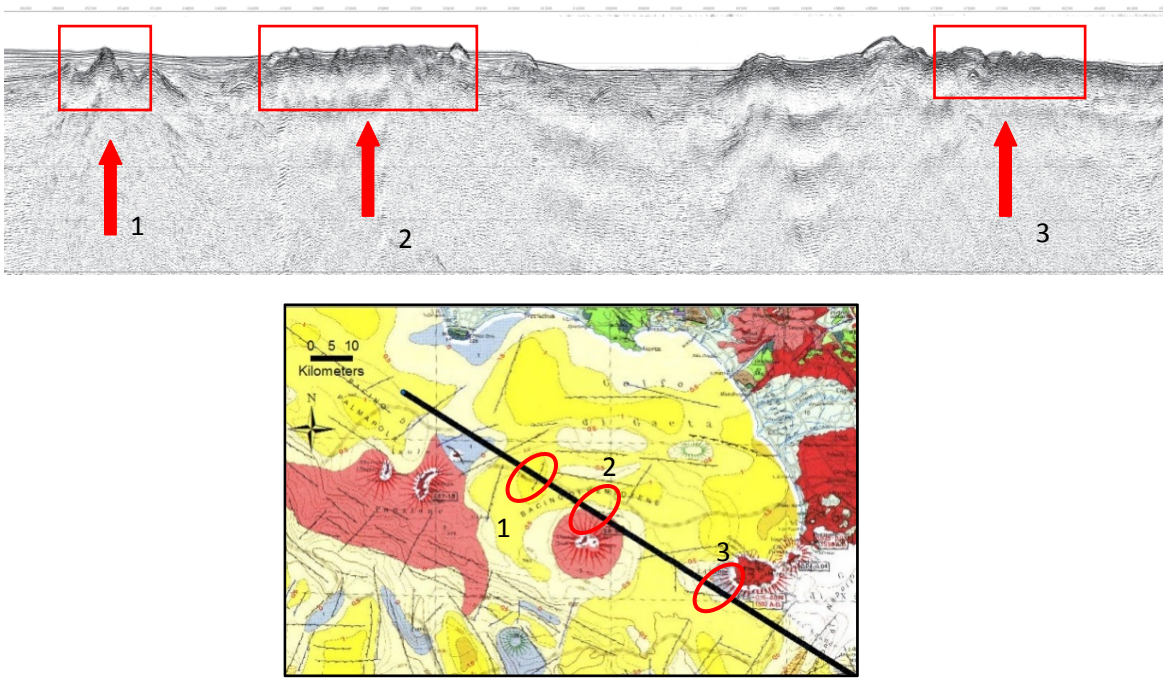


Fig. 7.8 – Volcanic structures pointed out on Line TIR-13 and corresponding localization.

In the continental slope area, the extension started during the early Pliocene (section 7.1) continues throughout the rest of the Pliocene time and during Quaternary, determining the formation of the subsiding basins of Palmarola and Ventotene and of the steep escarpment. Deformation is concentrated along the basin margins, whereas minor activity is observed in the inner portion. Occasionally, strike-slip movements or gentle folding are associated to the extension in the basal part of the basin infilling, and rare minor faults with sub-seismic offset cut the seafloor in some areas (Fig. 7.9).

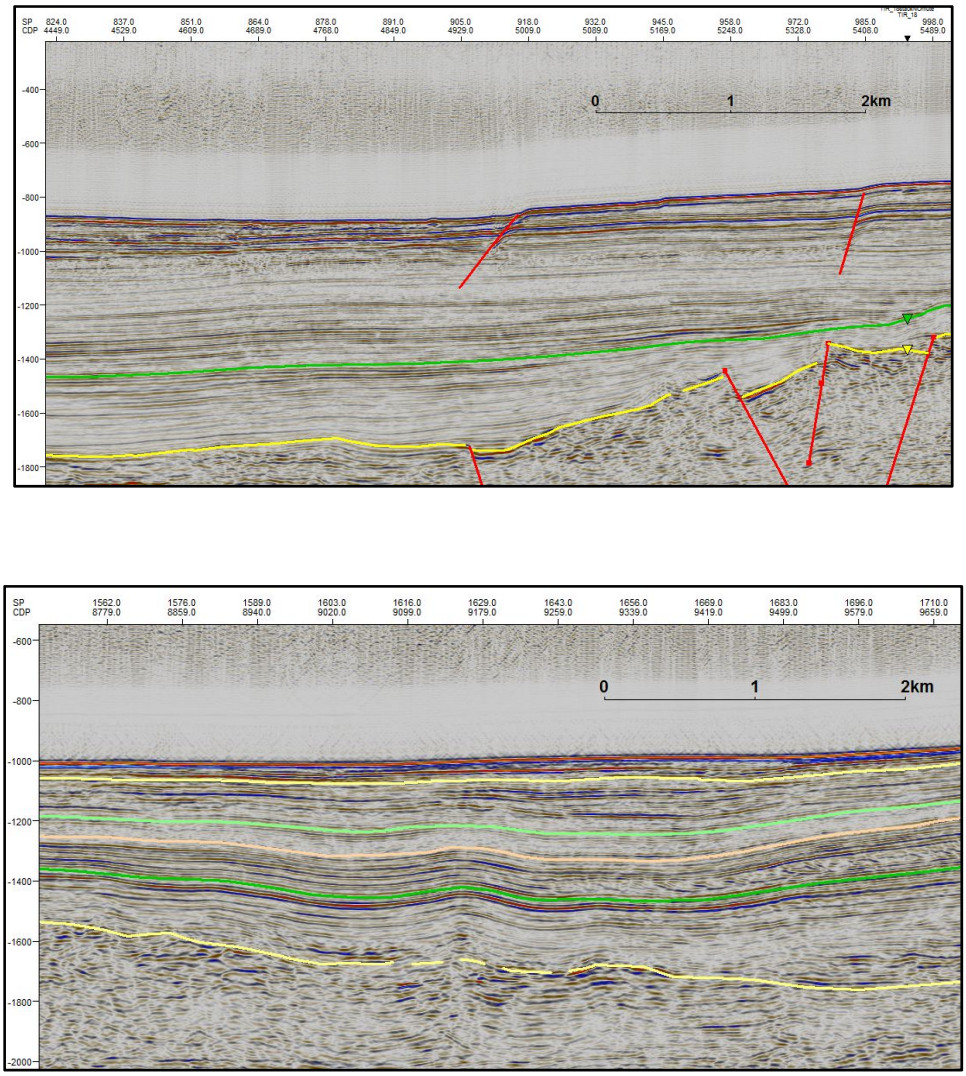


Fig.7.9 – Examples of small faults offsetting the seafloor or the upper part of the sedimentary sequence (upper) and small buckled folds (bottom).

According to Bruno et al. (1995) background seismicity is absent in the Campania-Latium continental margin, with the exception of earthquakes related to volcanic centers; this is in agreement with the Quaternary sediments not affected by fault.

Regarding the escarpment, the NW-SE trending fault system acts until Quaternary and especially in the northern sector it provokes morphological control on the present day

seafloor. Comparing the three NE-SW trending lines (TIR 14, 16, 18 profiles) the along strike variability of this important structural feature is highlighted: the fault system that progressively downthrown the escarpment toward the Vavilov basin is characterized by a different spacing of the fault plains, bigger toward the south. This could determine major slope gradients and structural elevation in northern sector, as can be noticed on TIR-14 profile (Fig. 6.13, Chapter 6): here the slope developed from 0,2 sec. (twt) of depth to 4 sec.(twt) in a relative little distance, about 15 Km; so in this sector the escarpment is narrow, and erosive and instability phenomena prevails onto deposition, and cause the progressive cannibalization of the slope (Chiocci et al, 2003) and an uneven morphology along the slope, where the rocky substrate is sometimes exposed. Instead, observing the continental slope as imaged by TIR-18 18 profile (Fig. 6.15, Chapter 6), it can be noticed that the gradient is lower, as the slope edge is around 0,75 sec. (twt) and the bottom at 2,5 sec. (twt), over a distance of about 25 Km; in addition, less erosive and instability processes are observed, whereas a thin sedimentary succession covers the slope. This let infer a minor activity of the faults in the southern sectors of the escarpment. The previous observations are in good agreement with the study by Conti et al. (2013), where the authors analyzed rock samples dredged along the upper and lower slope area; they infer that the Pontine continental slope experienced during Plio-Pleistocene periods of volcanic products and/or sediment deposition alternate with periods of non deposition. In fact, tectonically induced topography (confirmed by the seismic data here provided), together with erosive/instability processes (Chiocci et al. 2003), volcanic processes and distance from the mainland led to the formation of a sediment starved and complex slope morphology, which differ from the other margins of the Mediterranean region, where stacking of the shelf/slope sediments is observed (Chiocci et al., 1997; Ridente & Trincardi, 2002).

Tectonic activity in the bathyal sector seems to be still active, as testified by the fault planes interpreted, which clearly offset the seafloor (Fig. 7.10). These fault systems bordering the Vavilov margins are sometimes responsible for the formation of small basins localized on the hangingwall of the fault; the sedimentary cover lying above the substratum has an upper Pliocene-Pleistocene age, according to the results of the ODP 651, and sometimes show a syn-kinematic wedging. In the bathyal area crossed by TIR-15 profile, the occurrence of oceanic crust is supposed, on the basis of several evidences as the proximity of the ODP site 651, the correlation with seismic lines ST-4, ST-3 and the CROP M-29B profile (Chapter 6); in addition, the higher velocities used for the processing of TIR-15 line also can be related to the presence of oceanic layers, which are characterized by higher values.

Seismicity in this portion of the Tyrrhenian Sea, and also along the margin, is characterized by low activity both in occurrence and energy (Favali et al., 2004) (Fig. 2.8 A, Chapter 2 and Fig. 7.11). The long and well developed and continental slope could potentially generate earthquakes with high magnitude, but probably the occurrence of high heat flow reduces the elastic thickness and the differential stress in the area (TIR10 report, 2010).

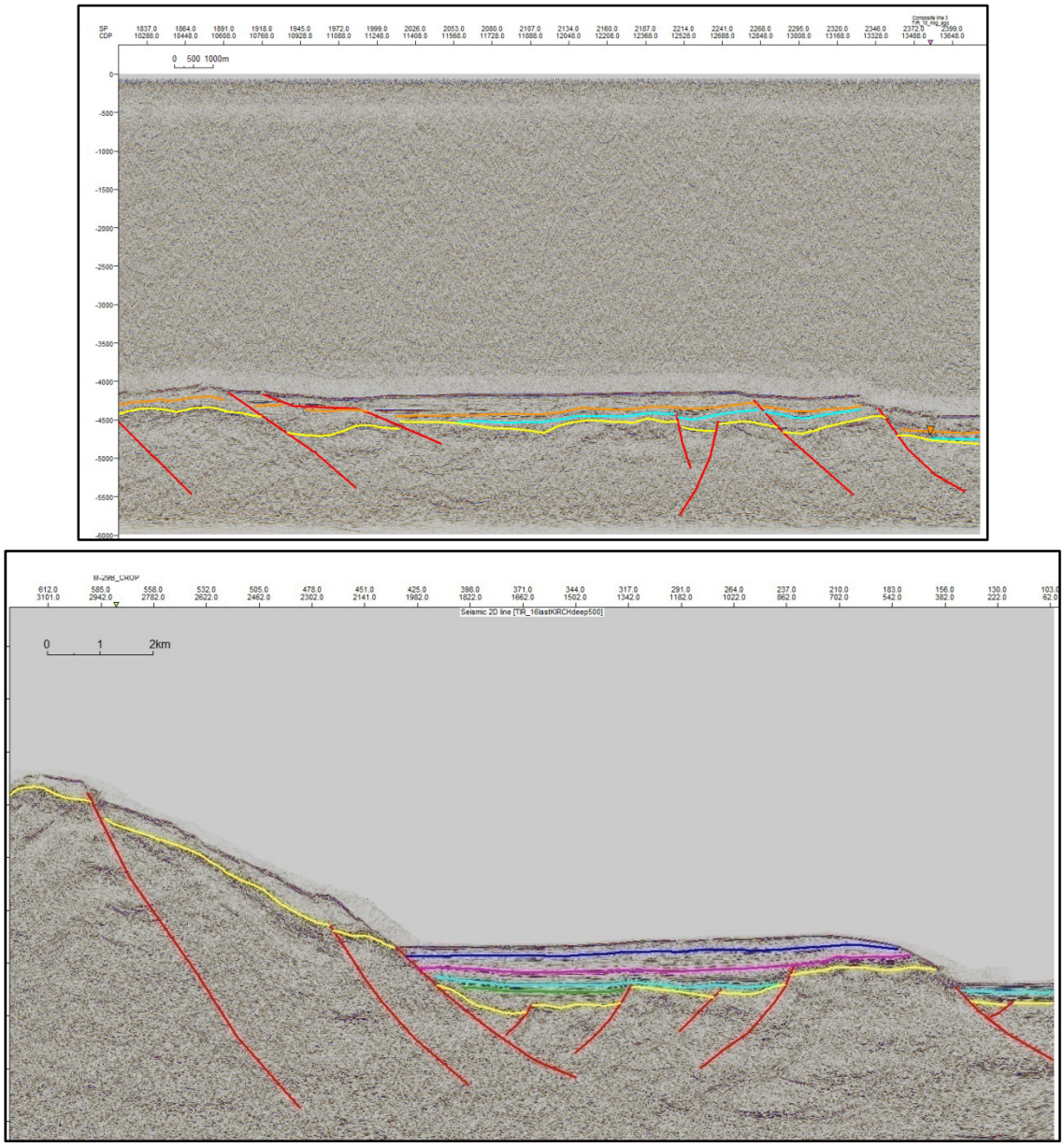


Fig.7.10 – Examples showing faults offsetting the seafloor in the bathyal area (TIR-14 upper, TIR-16 bottom).

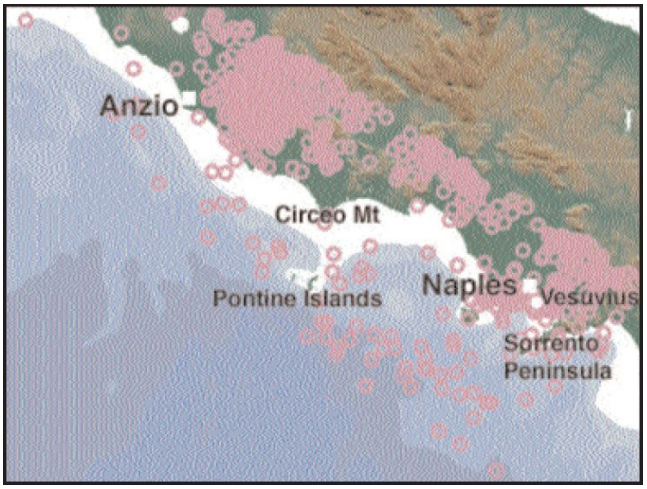


Fig. 7.11 - Map of the instrumental seismicity located along the Italian coasts of the northern and central Tyrrhenian Sea (1983-2003; INGV, 2004) (Favali et al., 2004).

# CHAPTER 8

# Conclusions

The investigation presented in this work focused on the central-eastern passive margin of the Tyrrhenian Sea, in particular on the Pontine archipelago sector, between the city of Anzio and the Volturno River delta. The studied area includes the continental shelf, the Vavilov plain and the steep escarpment connecting these sectors.

The Tyrrhenian Sea is the youngest back-arc basin of the western Mediterranean region and its extension is linked to the roll back of the Apennines subduction (Malinverno and Ryan, 1986; Doglioni, 1991); it developed from intra-Tortonian until the present day (Lustrino et al., 2011 and reference therein), so it is a relative young rift, which provides ideal conditions to study the early stage processes leading to the development of rifted passive margins and to the emplacement of oceanic crust.

Aim of the research is to propose a reconstruction of the central-eastern Tyrrhenian margin in terms of tectonic (geometry, kinematics and timing of the deformation) and seismostratigraphic setting, in order to contribute to the knowledge of the processes involved in the evolution of the rifted margins of peninsular Italy, a less constrained sector of the Tyrrhenian margin.

The investigation was carried out essentially by means of multichannel seismic reflection profiles, for a total length of 1300 km of interpreted lines (Fig. 4.1, Chapter 4). New seismic data were provided by an oceanographic cruise named TIR 2010, carried out in the Tyrrhenian Sea in October 2010 on the R/V Urania research vessel and funded by CNR of Italy. The advantage of this new set of data is given by the fact that they cover the rifted margin from the continental platform to the bathyal area, providing an overall view, especially regarding the escarpment, the more relevant morphological feature of the area. Nevertheless, also the network of lines acquired in 1986 by Western Geophysical Co. for the Agip oil company (Zone E), which investigates exclusively the continental platform sector, have been analyzed; they provided, together with the analysis of the exploration wells, a better constrain to the definition of the seismostratigraphy of the area.

A fundamental step to carry on the research was the processing of the TIR profiles, aimed to realize post-stack migrated sections. The main achievement was the suppression of the multiples reflections, caused by the hard sea-bed and by shallow depths; the processing of the seismic data removed most of the multiple energy by means of predictive multi-channel deconvolution and stacking, and depicted the geological structures in the subsurface down to approximately 3-3.5sec. (twt).

First step in interpreting the data has been the definition of the seismostratigraphic setting. Regarding this topic, the scarcity of well data for direct calibration must be highlighted: there are only two offshore wells (Mara 1 and Michela 1, Fig. 5.3, Chapter 5) that could be used for direct calibration of seismic profiles, whereas the onshore wells provided a useful but qualitative calibration. For this reason previous studies about the area, and in general regarding the entire Tyrrhenian basin, have also been taken into account. Furthermore, the complex tectonic setting of the area makes sometimes difficult to follow for great distances the same unconformity. Four main seismostratigraphic units have been defined, bounded by main unconformities (Fig. 5.12 and 5.13, Chapter 5), ascribed to the top of the Meso-Cenozoic carbonate sequence (unconformity A), the top of the evaporitic Messinian (unconformity B) and to mid-Pliocene (unconformity C). This analysis in general agrees with

the main unconformities defined by Zitellini et al. (1986) on the Sardinia passive margin, thus confirming the linking between the Sardo-Corso and the Latium-Campania sectors (conjugate rifted margins) and the regional meaning of the main unconformities. According to the authors, the unconformity Y (B in this work) is linked to the regional salinity crisis of upper Messinian age and the unconformity X (C in this work) is linked to the end of the extensional tectonic. The sedimentary infilling above the unconformity B is in this work referred to Plio-Pleistocene, whereas other authors (i.e. Aiello et al., 2000; Milia et al., 2013) assigned only a Pleistocene age to it, and by consequence also the unconformity C is considered of Quaternary age.

The performed structural analysis pointed out the main directions of tectonic lineaments: NE-SW, NNE-SSW, NW-SE and E-W.A general horst and graben setting is characteristic of the continental shelf area; faulted tilted blocks generate mainly half-grabens, with a strongly deformed substrate in the early stage of basin formation. Strain localization (Walsh et al., 2003) on major normal faults is a common mechanism of the spatio-temporal evolution of fault systems, which lead progressively to deactivation of the inner smaller faults.

The area of the continental slope is dominated by the occurrence of a steep escarpment which connects the continental platform to the bathyal Vavilov plain. The new Tir seismic lines provide new evidence of listric faults, trending NW-SE, that progressively downthrown the Latium-Campania margin; along strike, some differences have been pointed out: the escarpment shows a major morphological elevation in the northern sector, where in addition non deposition prevails and erosive/instability phenomena are widespread, in agreement with the works of Chiocci et al. (2003) and Conti et al. (2013). Moving toward the south, the escarpment progressively loose part of its morphological elevation and a thin sedimentation is observed. This change along strike has been ascribed to the higher fault spacing pointed out from north to south. Extensional tectonics is still active along the escarpment and it is also responsible for the formation of the two intraslope basins (Palmarola and Ventotene basins) which constitute the major areas of sedimentation in this sector. Although kinematic is essentially extensional, observed structures are compatible with a strike-slip component.

Regarding the bathyal plain, the new data provided evidence of faults offsetting the seafloor, thus implying recent tectonic activity; both sectors are although characterized by low frequency seismicity and low intensity (Favali et al., 2004), which could be explained by the occurrence of high heat flow that reduces the elastic thickness and the differential stress in the area. The northern apex of the Vavilov plain investigated by the TIR lines is floored with oceanic crust, or at least is a zone of continent-ocean transition, as inferred by the seismostratigraphic analysis of the TIR-15 profile, by correlation with previous seismic surveys and results of ODP sites 651 and 655; probably the continent ocean transition occurs in the proximity of the border of the Flavio Gioia Smt. and continues to the north along the almost N-S trending border of the basin.

The seismostratigraphic and structural interpretation allowed to outline the main evolutionary phases that interested the area: the first phase visible on the seismic profiles is the compressive Miocene phase, responsible for the folding and thrusting of the Meso-Cenozoic units; at the transition between Messinian and early Pliocene, an extensional phase took place, responsible for the actual setting of the margin. The extension acted through

different directions: NE-SW, prevalent on the northwestern sector of the continental shelf; NW-SE, typical of the slope and intraslope basins; NNE-SSW and E-W, characteristic of the southeastern area. The latter sector also experienced two main phases of extension, one in the early Pliocene and a second one probably during upper-Pliocene-Pleistocene; on the other hand, to the northwest, the extensional activity lasted until early Pliocene and the mid-Pliocene unconformity mark its ending. After the extensional phase, in both areas a main change occurs with the deposition of Quaternary progradational units, probably linked to fluvial-deltaic environments; extension is still active in the slope and bathyal sectors.

The results herein presented well fit in the general geodynamic context of the Tyrrhenian basin formation and provide further evidence about the evolution of the basin, which can contribute to the understanding of extensional processes involving rift basins and passive margin development.

In the Tyrrhenian Sea extensional tectonics was first active to the west, along the Sardinian margin, during Tortonian-Messinian p.p.; then it propagates to E-SE, reaching during Messinian- Early Pliocene the eastern Tyrrhenian margin. Rift propagation is confirmed by the drilled sites of ODP Leg 107 (Kastens et al., 1988), which pointed out older synrift deposits on the upper Sardinia margin (Tortonian to Messinian p.p., Site 654) and younger synrift deposits on the lower Sardinia Margin (Messinian to Pliocene, Site 652). The age ascribed by this research work to the synrift sediments of Latium-Campania margins is Early–Middle Pliocene, therefore it confirms the trend of the E-SE propagation of extension. Volcanic edifices have been highlighted by the new seismic data, in particular along TIR-13 profile, which runs in a direction parallel to the Italian mainland (Fig. 7.8, Chapter 7): the first volcanic feature occurs in the northwestern sector, in an area where no volcanic edifices are point out according to the structural map of Italy; then, moving towards the southeast, the Ventotene volcanic complex and then the Ischia volcanic complex are shown. The progressive youngest age of these volcanoes moving towards the south is inferred by the stratigraphic relationships with the sedimentary deposits (Fig. 7.8, Chapter 7); the generation of magma could be due to crustal thinning and consequent mantle decompression or might be link to the migration of a volcanic arc.

Compared with others rifted margins (i.e. the Iberian-Newfoundland Margin), the Tyrrhenian Sea shows several similarities, as for example asymmetric rifted margins (Doglioni et al., 2004) or the occurrence of serpentinized peridotites in the basin (Kastens et al., 1988). However, extensional rates are higher in the Tyrrhenian Sea, almost one order of magnitude respect to the case of the Atlantic Ocean (Sartori et al., 2004), and stretching affected Alpine–Apenninic fold and thrust belt units whose last shortening events (Miocene) just predated the onset of extension; this might have create zones of weakening from a rheological point of view, which conditioned extensional rates (Sartori et al., 2004).

The investigated area shows a poliphasic activity, characterized by a different temporal activity of the faults related to the opening of the basin and by different orientations. This might be linked to the peculiar location of the studied sector: probably continent-ocean transition occurs at the base of the steep continental escarpment or at least in the proximities, in the Vavilov abyssal plain. Besides, and more important, the area might be influenced by the interplay between the Northern Apenninc Arc and the Southern Apenninc Arc. According to

Turco et al. (2006) this two distinct kinematic elements, moved independently: during first stage (3.5-0.78Ma), the Northern Arc moved toward the NE and the Southern Arc toward the SE; in the second stage (0.78 Ma- present), the Northern Apenninic Arc stopped its migration (Di Bucci & Mazzoli, 2002), while the Southern Apenninic Arc continued moving toward the SE. This different behavior might have generated the different faults orientations observed and the different timing of the extensional phases. Conventionally the limit between the Northern Tyrrhenian domain and the Southern Tyrrhenian domain is considered the 41$^{st}$Parallel Line, which cross the investigated area; this magnetic E-W trending anomaly has been ascribed to different tectonic settings: in this work a left lateral strike-slip movement is supposed along this feature by the structural evidences; this line merge along the Latium-Campania margin with the Ortona – Roccamonfina line, which is considered a dextral strike slip fault system (Patacca et al., 1990) that separates the two Apenninc arcs mentioned.

# References

- Aiello, G., Marsella E. and Sacchi M. (2000) - Quaternary structural evolution of Terracina and Gaeta basins (eastern Tyrrhenian margin, Italy), Rend. Lincei Sci. Fis., 9, 11-41.

- Aiello, G., Marsella, E., Cicchella, A.G. and Di Fiore, V. (2011) - New insights on morpho-structures and seismic stratigraphy along the Campanian continental margin (Southern Italy) based on deep multichannel seismic profiles. Rendiconti di Scienze Fisiche e Naturali Accademia dei Lincei, 22, 349-373.

- Aiello G., Cicchella A. G., Di Fiore V, Marsella E (2011) - New seismo-stratigraphic data of the Volturno Basin (northern Campania, Tyrrhenian margin, southern Italy): implications for tectono-stratigraphy of the Campania and Latium sedimentary basins. Annals of Geophysics, 54, 3, 2011

- Aiello G., Cicchella A.G., Di Fiore V., Marsella E. (2010) - Morfo-strutture regionali sul margine continentale della campania in base a nuovi dati di sismica multicanale profonda. GNGTS- Atti del 29° Convegno Nazionale.

- Badley M.E. (1985) - Practical Seismic Interpretation. International Human Resources Development Corporation.

- Barberi, F., Borsi, S., Ferrara, G., Innocenti, F., (1967) - Contributo alla conoscenza vulcanologica e magmatologica delle Isole dell'Archipelago Pontino. Memorie della Società Geologica Italiana 6, 581–606.

- Bartole, R. (1984) - Tectonic Structure of the Latian–Campanian Shelf (Tyrrhenian Sea). Boll. Ocean. Teor. ed Appl. 3, 197–230.

- Bartole, R., Savelli, C., Tramontana M. and Wezel F.C. (1983) - Structural and sedimentary features in the Tyrrhenian margin off Campania, southern Italy, Mar. Geol., 55, 163-180.

- Bellucci, F., Grimaldi, M., Lirer, L., Rapolla, A., (1997) - Structure and geological evolution of the island of Ponza, Italy: inferences from geological and gravimetric data. J. Volcanol. Geother. Res. 79, 87–96.

- Bellucci, F., Lirer, L., Munno, R. (1999) - Geology of Ponza, Ventotene and Santo Stefano Islands (with a 1:15,000 scale geological map). Acta Vulcanologica 11, 197–222.

- Boccaletti M., Calamita F., Deiana G., Gelati R., Massari, F., Moratti G., Ricci Lucchi F. (1990) - Migrating foredeep-thrust belt system in the northern Apennines and southern Alps. Palaeogr. Palaeoclimatol. Palaeoecol. 77, 3-14.

- Boillot, G., Grimaud, S., Mauffret, A., Mougenot, D., Kornprobst, J., Mergoil-Daniel, J., Torrent, G., (1980) – Ocean Continent boundary off the Iberian margin: a

serpentinite diapir west of the Galicia Bank. Earth and Planetary Science Letters 48, 23-34.

- Brandano, M., Civitelli, G., (2007) - Non-seagrass meadow sedimentary facies of the Pontinian Islands, Tyrrhenian Sea: a modern example of mixed carbonate–siliciclastic sedimentation. Sedimentary Geology 201, 286–301.

- Bruno, G., Moretti, A., Guerra, I. (1995) - Meccanismi focali di terremoti intermedi e profondi del Tirreno meridionale. Proceedings 14th meeting G.N.G.T.S. 1, 103–114.

- Bruno, P.P., Di Fiore, V. and Ventura, G. (2000) - Seismic study of the '41st Parallel' Fault System offshore the Campanian–Latial continental margin, Italy. Tectonophysics, 324, 37–55.

- Cadoux, A., Pinti, D.L., Aznar, C., Chiesa, S., Gillot, P., (2005) - New chronological and geochemical constraints on the genesis and geological evolution of Ponza and Palmarola volcanic islands (Tyrrhenian Sea, Italy). Lithos 81, 121–151.

- Calcagnile G., Fabbri A., Farsi F., Gallignani P., Gasparini C., Iannaccone G., Mantovani E., Panza G.F., Sartori R., Scandone P. & Scarpa R. (1981) - Structure and evolution of the tyrrhenian Basin. Rapp.Comm.int. Mer Medit., 27 88), 197-208.

- Carmassi, M., De Rita, D., Di Filippo, M., Funiciello, R., Sheridan, M.F., (1983) - Geology and volcanic evolution of the Island of Ponza (Italy). Geol. Rom. 22, 211 – 232.

- Carminati E. & Doglioni C. (2005) - Mediterranean tectonics. In Encyclopedia of Geology, Elsevier, 135-146

- Carminati E., Wortel M.J.R., Spakman W., R. Sabadini (2008) - The role of slab detachment processes in the opening of the western–central Mediterranean basins: some geological and geophysical evidence. Earth and Planetary Science Letters 160, 651–665.

- Carminati, E., Lustrino M. and Doglioni, C. (2012) Geodynamic evolution of the central and western Mediterranean: Tectonics vs. igneous petrology constraints. Tectonophysics, 579, 173-192.

- Carminati, E., Wortel, M.J.R., Spakman, W. and Sabadini, R. (1998) - The role of slab detachment processes in the opening of the western-central Mediterranean basins: some geological and geophysical evidence. Earth and Planetary Science Letters, 160, 651–665.

- Carrara, C., Conato, V., Dai Pra, G., (1986) - Segnalazione di sedimenti plioceni nell'Isola di Palmarola (Isole Pontine, Italia centrale). Mem. Soc. Geol. Ital. 35, 127–131.

- Cataldi R., Mongelli F., Squarci P., Taffi L., Zito G. & Calore C. (1995) – Geothermal ranking of the Italian territory. Geothermics, 24: 115-129.

- Chiocci F.L., Orlando L. (1994) - Terrazzi deposizionali sommersi alle Isole Pontine (Lazio Meridionale). Mem. Descr. Carta Geol. d'It. LVIII, pp. 37-48.

- Chiocci, F.L., Ercilla, G., Torres, J., (1997) - Stratal architecture of western Mediterranean margins as the result of the stacking of Quaternary lowstand deposits below glacio-eustatic fluctuation base level. Sedimentary Geology 112, 195–217.

- Chiocci, F.L., Martorelli, E., Bosman, A., (2003) - Cannibalization of a continental margin by regional scale mass wasting: an example from the central Tyrrhenian Sea. In: Locat, J., Mienert, J. (Eds.), Submarine Mass Movements and Their Consequences. Kluwer Academic Publishers, Dordrecht, pp. 409–416.

- Chiocci, F.L., Martorelli, E., Sposato, A., and T.I.VOL.I research group (1998) - Prime immagini TOBI dei fondali del Tirreno centro-meridionale. (settore orientale). Geologica Romana Vol. 34, 207-222.

- Chiocci, F.L., Orlando, L., (1996) - Lowstand terraces on Tyrrhenian Sea steep continental scope. Marine Geology 134, 127–143.

- Colantoni P., Lucchini F., Rossi P.L., Sartori R. & Savelli C. (1981) - The Palinuro Volcano and magmatism of the south-eastern Tyrrhenian Sea (Mediterranean). Marine Geology 39: M1-M12.

- Colantoni, P., Fabbri, A., Galignani, P., Sartori, R., Rehault, J.P., (1981) - Carta litologica e stratigrafica dei mari italiani. Litografia Artistica Cartografica, Firenze.

- Conte A.M. and Savelli C. (1994) - Vulcanismo orogenico dell'Isola di Poza: rioliti calcalcaline ed evoluzione trachiti-comenditi di serie shoshonitica. Mem. Descr. Carta Geol It. XLIX: 333-346

- Conte, A.M. and Dolfi, D., (2002) - Petrological and geochemical characteristics of Plio-Pleistocene volcanics from Ponza Island (Tyrrhenian Sea, Italy). Mineralogy and Petrology 74, 75–94.

- Conti M. A., Girasoli D.E , Frezza V., Conte A.M., Martorelli E., Matteucci R., Chiocci F.L (2013) - Repeated events of hardground formation and colonisation by endo-epilithozoans on the sediment-starved Pontine continental slope (Tyrrhenian Sea, Italy). Marine Geology 336 (184-187).

- Curzi P.V., Castellarin A., Vai G.B. & Zitellini N. (2003) – Raimondo Selli e Renzo Sartori una staffetta generazionale della geologia marina italiana. In: Convegno in memoria di Raimondo Selli e Renzo Sartori. La geologia del Mar Tirreno e degli Appennini. Bologna, 1-12 December 2003.

- D'argenio B., Pescatore T.S. & Scandone P. (1973) - Schema geologico dell'Appennino meridionale (Campania e Lucania) - Atti Accad. Naz. Lincei Quad. 183; 49-72

- De Rita D., Giordano G., Cecili A. (2001) - A model of submarine rhyolite dome growth: Ponza Island (central Italy). Journal of volcanology and geothermal research 107 (221-239).

- De Rita, D., Funiciello, R., Pantosti, D., Salvini, F., Sposato, A. and Velona, M. (1986) -Geological and structural characteristics of the Pontine islands (Italy) and implications with the evolution of the Tyrrhenian margin. Memorie della Società Geologica Italiana, 36, 55-65.

- De Vivo, B., Torok, K., Ayuso, R. A., Lima, A. and Lirer L. (1995) - Fluid inclusion evidence for magmatic silicate/saline/CO2 immiscibility and geochemistry of alkaline xenoliths from Ventotene Island, Italy. Geochimica et Cosmochimica Acla. Vol. 59, No. 14. pp. 2941-2953.

- Della Vedova, B., Bellani, S., Pellis, G., Squarci, P., (2001) - Deep temperatures and surface heat flow distribution. In: Vai, G.B., Martini, I.P. (Eds.), Anatomy of an Orogen: The Apennines and Adjacent Mediterranean Basins. Kluwer Academic Publishing, Great Britain, pp. 65– 76.

- Della Vedova, B., Pellis, G., Foucher, J.P. and Rehault, J.P. (1984) - Geothermal structure of the Tyrrhenian Sea. Marine Geology, 55, 271– 289.

- Di Bucci, D. & Mazzoli S. (2002) - Active tectonics of the northern Apennines and Adria geodynamics: new data and a discussion. J. Geodynamics 34, 687-707.

- Doglioni, C. (1991) - A proposal for the Kinematic modelling of the Tyrrhenian-Apennines system. Terranova, 3, 423- 432.

- Doglioni, C., Innocenti, F., Morellato, C., Procaccianti, D. and Scrocca, D. (2004) - On the Tyrrhenian Sea opening. Memorie Descrittive della Carta Geologica d'Italia, 64, 147–164.

- Emery, D. & Myers, K. J. (eds) (1996) - Sequence Stratigraphy. 297 pp. Oxford: Blackwell Science.

- Fabbri A., Gallignani P. & Zitellinini N. (1981) – Geological evolution of the peri-Tyrrhenian sedimentary basins. In WEZEL F.C. (Ed.): "Sedimentary basins of Mediterranean margin". Tecnoprint Bologna, 101-126.

- Fabbri A., Ghisetti F. & Vezzani L. (1980) – The Peloritani- Calabria range and the Gioia Basin in the Calabrian arc (southern Italy): relationships between land and marine data. Geol. Rom., 19: 131 150.

- Fabbri, A., Curzi, P., (1979) - Distribution of the Messinian deposits in the Tyrrhenian Sea, Giornale di Geologica, Vol. 43, Pl. 29

- Faccenna, C., Becker, T. W., Lucente, F. P., Jolivet, L. and Rossetti, F., (2001) - History of subduction and back-arc extension in the Central Mediterranean. Geophysical Journal International, 145: 809-820.

- Faccenna, C., Funiciello, F., Civetta, L., D'Antonio, Moroni, M., Piromallo, C. (2007) - Slab disruption, mantle circulation, and the opening of the Tyrrhenian basins. Geological Society of America Special Paper 418, 153–169.

- Faccenna, C., Mattei, M., Funiciello, R., Jolivet, L. (1997) - Styles of back-ark extension in the Central Mediterranean. Terra Nova 9, 126–130.

- Faccenna, C., Piromallo, C., Crespo-Blanc, A., Jolivet, L., Rossetti, F. (2004) - Lateral slab deformation and the origin of the western Mediterranean arcs. Tectonics 23, TC1012.

- Faggioni O., Pinna E., Savelli C., Schreider A.A. (1995) - Geomagnetism and age study of Tyrrhenian seamounts, Geophys. J. Int., 123: 915-930.

- Favali P., Beranzoli L., Maramai A. (2004) - Review of the Tyrrhenian Sea seismicity: how much is still to be known? Mem. Descr. Carta Geol. d'It. XLIV (2004), pp.57-70.

- Fedele, L., Bodnar, R.J., DeVivo, B. & Tracy R. (2003) - Melt inclusion geochemistry and computer modeling of trachyte petrogenesis at Ponza, Italy. Chemical Geology 194 (2003) 81– 104

- Florio, G., Fedi M. and Cella F. (2011) - Insights on the spreading of the Tyrrhenian Sea from the magnetic anomaly pattern. Terra Nova, 00, 1–7.

- Franke, D. (2013) - Rifting, lithosphere breakup and volcanism: Comparison of magma-poor and volcanic rifted margins. Marine and Petroleum Geology 43, 63-87.

- Gamberi F., Marani M. P. (2004) - Deep-sea depositional systems of the Tyrrhenian basin - Mem. Descr. Carta Geol. d'It. XLIV (2004), pp.127-146

- Gamberi, F., Marani, M., (2006) - Hinterland geology and continental margin growth: the case of the Gioia Basin (southeastern Tyrrhenian Sea). In: Moratti, G., Chalouan, A. (Eds.), Tectonics of the Western Mediterranean and North Africa: Geological Society London Special Publication, 262, pp. 349–363.

- Gennesseaux M., Rehaul, J., Thomas, B., Colantoni, P., Fabbri, A., Lepvrier, C., Mascle, G., Mauffret A., Polino, R., Robin, C., and Vanney, J.R. (1986) - Resultats des plongees en submersible Cyana sur le blocs contintaux bascules et le volcan Vavilov (mer Tyrrhenienne central). C. R. Acad. Sci. Ser. 2, 12: 785-792.

- Gueguen, E., Doglioni, C. and Fernandez, M. (1998) - On the post 25 Ma geodynamic evolution of the western Mediterranean. Tectonophysics, 298, 259-269.
- Gueguen, E., Doglioni, C., Fernandez, M., (1997) - Lithospheric boudinage in the Western Mediterranean back-arc basin. Terra Nova 9, 184–187.
- Hsu et al., 1973 Hsü, K.J., Montadert, L., Bernoulli, D., Cita, M. B., Erickson, A., Garrison, R.E., Kidd, R.B., Melieres, F., Müller, C. and Wright, R., (1977) - History of the Mediterranean salinity crisis, Nature 267, 399-403.
- Ippolito F. & Sgrosso I. (1972) - Sulle ricerche di idrocarburi nell'area litorale del Lazio e sulla loro interpretazione - Riv. Min. Siciliana 133-135; 1-16
- Ippolito F., Ortolani F., Russo M., (1973) - Struttura marginale tirrenica dell'Appennino campano: reinterpretazione di dati di antiche ricerche di idrocarburi. Mem. Soc. Geol. Ital., 12, 123-132.
- Kastens, K. and Mascle, J. (1990) - The geological evolution of the Tyrrhenian Sea: an introduction to the scientific results of ODP Leg 107. In: Kastens, K. and Mascle, J. et al. (Eds.), Proceedings of the Ocean Drilling Program, Scientific Results, 107, 3–26.
- Kastens, K.A., Mascle, J. and Others (1988) - O.D.P. Leg 107 in the Tyrrhenian Sea: insights into passive margin and back-arc basin evolution. Geological Society of American Bulletin, 100, 1140– 1156.
- Lustrino M., Duggen S.,. Rosenberg C. L. (2011) - The Central-Western Mediterranean: Anomalous igneous activity in an anomalous collisional tectonic setting. Earth-Science Reviews 104, 1–40
- Malinverno A. & Ryan W. B. F. (1986) - Extension in the Tyrrhenian Sea and shortening in the Apennines as result of arc migration driven by sinking of the lithosphere. Tectonics, 5, 227-245.
- Mantovani, E., Albarello, D., Tamburelli, C., Babbucci, D., (1996) - Evolution of the Tyrrhenian basin and surrounding regions as a result of the Africa–Euroasia convergence. J. Geodynamics 21 (1), 35–72.
- Marani M. P., Gamberi F. (2004) - Structural framework of the Tyrrhenian Sea unveiled by seafloor morphology. Mem. Descr. Carta Geol. d'It. XLIV (2004), pp.97-108
- Marani, M. & Zitellini, N. (1986) - Rift structures and wrench tectonics along the continental slope between Civitavecchia and C. Circeo. Memorie Società Geologica Italiana, 35: 453-457.
- Mariani, M., Prato, R., (1988) - I bacini neogenici del margine tirrenico: approccio sismico stratigrafico. Mem. Soc. Geol. It. 41, 519–531.

- Mascle, J. and Rehault, J.P. (1990) - A revised seismic stratigraphy of the Tyrrhenian Sea: implications for the basin evolution. In: Kastens, K.A., Mascle, J. et al. (Eds.), Proceedings of the Ocean Drilling Programme, Scientific Results, 107, 617– 636.

- Mascle, J., Chaumillon, E., (1997) - Pre-collisional geodynamics of the Mediterranean Ridge and Tyrrhenian Sea. Annali di Geofisica 40, 569–586.

- Mauffret, A., and Contruccci, I. (1999) - Crustal structure of the North Tyrrhenian Sea: first results of the multichannel seismic LISA cruise. In: Durand, B., Jolivet, L., Horvath, F. and Seranne, M. (Eds) The Mediterranean Basins: Tertiary Extension within the Alpine Orogen. Geological Society London, Special Publications, 156, 169-193.

- McKenzie, D., (1978) - Some remarks on the development of sedimentary basins, Earth and Planetary Science Letters, 40, 25-32.

- Metrich, N., Santacroce, R., Savelli, C., (1988) - Ventotene, a potassic quaternary volcano in central Tyrrhenian Sea. Rend. Soc. Ital. Mineral. Petrol. 43, 1195–1213.

- Milia A., Torrente M.M., Massa B., Iannace P. (2013) - Progressive changes in rifting directions in the Campania margin (Italy): New constrains for the Tyrrhenian Sea opening. Global and Planetary Change 109, 3–17.

- Mitchum, R. M., Jr. (1977) - Seismic stratigraphy and global changes of sea level, part 11: glossary of terms used in seismic stratigraphy. In: Payton, C. E. (ed.), Seismic Stratigraphy – Applications to Hydrocarbon Exploration. American Association of Petroleum Geologists Memoir 26, 205–212.

- Mongelli F., Loddo M. & Calcagnile G. (1975) - Some observations on the Apennines gravity field - Earth Planet Sci. Lett. 24; 385-393.

- Mongelli, F., Zito, G., Della Vedova, B., Pellis, G., Squarci P. & Taffi, L. (1991) – Geothermal Regime of Italy and surrounding Seas. In: "Exploration of the deep continental crust", Springer-Verlag: 381-394, Berlin.

- Moussat E., Rehault J.P. & Fabbri A. (1986) - Rifting et evolution tectono-sédimentaire du Bassin tyrrhenien au cours du Néogène et du Quaternaire. Giorn. Geol., 48 (1/2): 41-62.

- Musacchio M., Carrarra G., Gamberi F., Marani M. (1999) - Tectonic setting of the eastern Tyrrhenian margin. Geoitalia, 2° Forum FIST, Riassunti, 1: 184-185.

- Nicolich R. & Dal Piaz G.V. (1992) - Moho isobaths. Structural Model of Italy. Scale 1:500,000. Quaderni de "La Ricerca Scientifica", 114 (3), CNR.

- Nicolich R. (2001) - Deep seismic transects. In: Vai G.B. & Martini I.P. (Eds.): "Anatomy of an orogen: the Apennines and adjacent Mediterranean basins". Kluwer Academic Publishers: 47- 52, Dordrecht, The Netherlands.

- Nicolosi, I., Speranza, F. and Chiappini, M., (2006) - Ultrafast oceanic spreading of the Marsili Basin, southern Tyrrhenian Sea: evidence from magnetic anomaly analysis. Geology, 34, 717–720.

- Oldow J. S., D'Argenio B., Ferranti L., Marsella E., Pappone G., Sacchi M., (1993) - Large scale longitudinal extension in the Southern Apennines contractional belt. Geology, 21: 1123-1126.

- Pantosti D. & Velona M (1986) - Tettonica recente nell'isola di Zannone e nella piattaforma circostante (arcipelago Pontino, Italia centrale). Mem. Soc. Geol. It. 35, 623-629.

- Panza G.F., Scandone P., Calcagnile G., Mueller S. & Suhadolc P. (1992) – The lithosphere-asthenosphere system in Italy and surrounding regions. Quaderni de "La Ricerca Scientifica", 114 (3), CNR.

- Parotto M. (1980) –Appenin central. In "Introduction à la géologie génerale d'Italie". Soc. Min. Petr. Ital., 33-37.

- Parotto, M. and A. Praturlon (1975) - Geological summary of Central Apennines, Quaderni de "La Ricerca Scientifica", CNR, Roma, 90, 257-311.

- Patacca E., Scandone P and Meletti C. (1997) - Variazione di regime tettonico nell'Appenino meridionale durante il Quaternario. Proceedings of AIQUA meeting. Parma 25-27 February, 21-22

- Patacca, E., Sartori, R., Scandone, P., (1990) - Tyrrhenian basin and Apenninic arcs: kinematic relations since late Tortonian times. Memorie Società Geologica Italiana 45, 425–451.

- Pepe F., Bertotti G., Cella F. & Marsella E. (2000) – Rifted margin formation in the south Tyrrhenian Sea: a high resolution seismic profile across the north Sicily passive continental margin. Tectonics 19 (2): 241-257.

- Piangiamore G.L., Faggioni O. & Barbano M.S. (2004). Anomalie geomagnetiche in strutture di apertura di bacino: l'esempio del mar tirreno. GNGTS – Atti del 23° Convegno Nazionale / 15.13.

- Rehault J.P., Moussar, E. and Fabbri, A. (1987) - Structural evolution of the Tyrrhenian back-arc basin. Mar. Geol., 74, 1:123-150.

- Rehault, J. P., Boillot, G., and Mauffret, A., (1985) - The western Mediterranean Basin. In Stanley, D. J., Wezel, F. C. (Eds.), Geological evolution of the Mediterranean Basin. New York (Springer-Verlag), 101-129.

- Ridente, D., Trincardi, F., (2002) - Eustatic and tectonic control on deposition and lateral variability of Quaternary regressive sequences in the Adriatic basin (Italy). Marine Geology 184, 273–293.

- Robin, C., Colantoni, P., Genessaux, M., Rehault, J.P., (1987) - Vavilov seamount: a midly alkaline Quaternary volcano in the Tyrrhenian basin. Marine Geology 78, 125–136.

- Sartori R (2003) - The Tyrrhenian back-arc basin and subduction of the Ionian lithosphere. Episodes 26(3):217–221.

- Sartori R. (1989) - Evoluzione neogenico-recente del bacino tirrenico e suoi rapporti con la geologia delle aree circostanti. Giornale di Geologia, 51, 1-39.

- Sartori R. (1990) - The main results of ODP Leg 107 in the frame of Neogene to Recent geology of peri-Tyrrhenian areas. In: KASTENS K.A., MASCLE J. (Eds.): "Proceedings of the ODP". Scientific Results, 107: 715-730.

- Sartori, R., (1986). - Notes on geology of the acoustic basament in the Tyrrhenian sea. Mem. Soc.Geol. It. 36: 99-108.

- Sartori, R., Torelli, L., Zitellini, N., Carrara, G., Matteo, M., and Mussoni, P., (2004) - Crustal features along a W-E Tyrrhenian transect from Sardinia to Campania margins (Central Mediterranean), Tectonophysics, 383, 3-4, 171-192.

- Savelli C. (1988) - Late Oligocene to recent episodes of magmatism in and around the Tyrrhenian Sea: implications for the processes of opening in a young inter-arc basin of intra-orogenic (Mediterranean) type. Tectonophysics, 146: 163-181.

- Savelli, C. (2002) - Time-space distribution of magmatic activity in the western Mediterranean and peripheral orogens during the past 30 Ma (a stimulus to geodynamic considerations), J. Geodyn., 34, 99–126.

- Savelli, C., (1984) - Eta` K/Ar delle principali manifestazioni riolitiche dell'isola di Ponza. Rend. Soc. Geol. Ital. 6, 39–42.

- Savelli, C., (1987) K/Ar ages and chemical data of volcanism in the western Pontine Islands (Tyrrhenian Sea). Boll. Soc. Ital. 106, 356–546.

- Schnyder J., Cardello G. L. and Hirt A. M. (2012) - A structural and Anisotropy of Magnetic Susceptibility study from the Paleozoic basement, the Mesozoic-Tertiary sedimentary cover and the Pleistocene lavas from the Island of Zannone (Tyrrhenian Sea, Italy). Vol. 14, EGU2012-8981, 2012

- Scrocca D., Carminati E., Doglioni C. & Marcantoni D. (2007) - Slab retreat and active shortening along the central-northern Apennines. In: Thrust belts and Foreland Basins: From Fold Kinematics to Hydrocarbon Systems, O. Lacombe, J. Lavé, F. Roure and J. Verges (Eds.), Frontiers in Earth Sciences, Springer, 471-487.

- Scrocca D., Doglioni C. & Innocenti F. (2003) - Constraints for an interpretation of the Italian geodynamics: a review. In: Scrocca D., Doglioni C., Innocenti F., Manetti P., Mazzotti A., Bertelli L. Burbi L., D'Offizi S. (Eds.): "CROP Atlas: seismic reflection profiles of the Italian crust". Mem. Descr. Carta Geol. It., 62, 15-46.

- Scutter, C.R., Cas, R.A.F., Moore, C.L., (1998) - Facies architecture and origin of a submarine rhyolitic lava flow-dome complex, Ponza, Italy. J. Geophys. Res. 103, 27551– 27566.

- Segre A. (1954) - Morfologia e geologia. In: E. Zavattini, "Biogeografia dell'Isola di Zannone". Acc. Naz., XL (IV)

- Segre A.G. (1958) - Neue geologische und morphologische Untersuchungen im tyrrenischen Gebiet. Geol. Rundschau, 47, 196-207

- Selli R. (1974) - Appunti sulla geologia del mar Tirreno. In paleogeografia del Terziario sardo nell'ambito del Mediterraneo Occidentale. Rend. Semin. Fac. Sc. Univ. Cagliari Supll., 327-351.

- Selli R. (1981) - Thoughts on the geology of the Mediterranean Region. In: Wezel F.C. (Ed): "Sedimentary basins of Mediterranean margins", Tecnoprint, Bologna 489-501.

- Selli R. and Fabbri, A (1971) - Tyrrhenian: a Pliocene deep-sea. Rend. Atti accad. Naz.Lincei, 50,5:580-592.

- Selli R., Lucchini F., Rossi P.L., Savelli C., Del Monte M. (1977) - Dati geologici, petrochimici e radiometrici sui vulcani centro-tirrenici. Gionale di Geologia, XLII, 221-246.

- Selvaggi G. and Chiarabba C. (1995) - Seismicity and P-wave velocity image of the Southern Tyrrhenian subduction zone. Geophys. J. Int. 121, 818-826.

- Serri, G., (1990) - Neogene–Quaternary magmatism of the Tyrrhenian region: characterization of the magma sources and geodynamic implication. Mem. Soc. Geol. It. 41, 219–242.

- Spadini, G. and Wezel, F.C. (1994) - Structural evolution of the "41st parallel zone": Tyrrhenian Sea. Terra Nova, 6, 552-562.

- Stein, S. & Wysession, M. (2003) - An Introduction to Seismology, Earthquakes, and Earth Structure: 498 pp. Oxford: Blackwell Science.

- Trincardi, F. and N. Zitellini (1987) - The rifting of the Tyrrhenian basin. Geomar. Lett., 7, 1-6.

- Turco, E., Schettino A., Pierantoni P.P. and Santarelli G. (2006) - The Pleistocene extension of the Campania Plain in the framework of the Southern Tyrrhenian tectonic evolution: morphotectonic analysis, kinematic model and implications for volcanism, In: Volcanism in the Campania Plain – Vesuvius, Campi Flegrei and Ignimbrites, edited by B. De Vivo, Dev. Volcano., 9, 27-51.

- Valensise G. & Pantosti D. (2001) – Database of Potential Sources for Earthquakes Larger than 5.5 in Italy. Ann. Geof., Suppl. to vol. 44 (4): pp. 180, with CD-ROM, INGV.

- Vezzoli, L., (1999) - Geologia ed evoluzione Plio-Quaternaria dell'Isola di Palmarola (Arcipelago Pontino). In: Orombelli, G. (Ed.), Studi geografici e geologici in onore di Severino Belloni. Universita` degli Studi di Milano, Milano, pp. 645– 656.

- ViDEPI, 2009. Progetto Visibilità Dati Esplorazione Petrolifera in Italia. Ministero dello Sviluppo Economico UNMIG, Società Geologica Italiana, Assomineraria.

- Walsh J.J., C. Childsa, J. Imbera, T. Manzocchia, J. Wattersonb, P.A.R. (2003) - Strain localization and population changes during fault system growth within the Inner Moray Firth, Northern North Sea Journal of Structural Geology Volume 25, Issue 2, 307–315.

- Wang, C.Y., Hwang, W.T., Shi, Y., (1989) - Thermal evolution of a Rift Basin: The Tyrrhenian Sea. Journal of Geophysical Research, Vol. 94, No. B4, 3991-4006.

- Wernicke, B., (1985) - Uniform-sense normal simple shear of the continental lithosphere, Can. J. Earth Sci., 22, 108-125.

- Whitmarsh, R.B., Manatschal, G., Minshull, T.A. (2001) - Evolution of magma-poor continental margins from rifting to seafloor spreading. Nature 413, 150-154.

- Yilmaz, O. (2001) - Seismic data analysis: processing, inversion and interpretation of seismic data. Society of Exploration Geophysicists. Series: Investigation in Geophysics 10, Tulsa, OK.

- Zitellini N., Trincardi F., Marani M., Fabbri A., (1986) - Neogene tectonics of the northern Tyrrhenian Sea. Giorn.Geol., 48: 1/2, 25-40.

- Zitellini, L., Marani, M., Borsetti, A.M., (1984) - Post-orogenic tectonic evolution of Palmarola and Ventotene basins (Pontine archipelago). Mem. Soc. Geol. It. p. 27: 121-131.

- Zito G., Mongelli F., De Lorenzo S. and Doglioni C., (2003) - Heat flow and geodynamics in the Tyrrhenian Sea. Terra Nova, 15, (6), 425–432.

- Report TIR 10 cruise available at http://www.ismar.cnr.it/prodotti/reports-campagne/2010-2019.